# Roles of Toll-like receptors and NKT cells in gene/environment interactions in a mouse model of Multiple Sclerosis

**Thesis submitted by**

**Socorro Miranda-Hernandez**

**Bachelor in Veterinary**

**Autonomous University of State of Mexico, Mexico**

**In August 2013**

**for the degree of Doctor of Philosophy**

**in the School of Pharmacy and Molecular Sciences,**

**Comparative Genomics Centre,**

**James Cook University**

# STATEMENT OF ACCESS

I, the undersigned, author of this work, understand that James Cook University will make this thesis available for use within the University Library and, via the Australian Digital Theses network, for use elsewhere.

I understand that, as an unpublished work, a thesis has significant protection under the Copyright Act and; I do not wish to place any further restriction on access to this work.

_____ _____

Signature Date

_____

Name

# STATEMENT ON SOURCES

I declare that this thesis is my own work and has not been submitted in any form for another degree or diploma at any university or other institution of tertiary education. Collaborations and information derived from the published or unpublished work of others has been acknowledged in the text and a list of references is given.

_____ _____

Signature Date

_____

Name

# ELECTRONIC COPY

I, the undersigned, author of this work, declare that the electronic copy of this thesis provided to James Cook University library is an accurate copy of the print thesis submitted, within the limits of technology available.

_____ _____

Signature Date

_____

Name

# CONTRIBUTIONS OF OTHERS

| Contribution | Names or Affiliations |
|---|---|
| Financial support | Universidad Autonoma del Estado de Mexico (Autonomous University of the State of Mexico)<br>Mexican Consejo Nacional de Ciencia y Tecnologia (CONACYT)<br>James Cook University |
| Editorial Assistance | Kellie Johns<br>Elizabeth Tynan<br>Rosemary Dunn<br>Kasturi-Reddy Lopata<br>Paul Wayne Marsh<br>Michell Tirell |

# APPROVAL OF ETHICS

This research presented and reported in this thesis was conducted in compliance with the National Health and Medical Research Council (NHMRC) Australian Code of Practice for the Care and Use of Animals for Scientific Purposes, 7th Edition, 2004 and the Qld Animal Care and Protection Act, 2001.

The proposed research study received animal ethics approval from the JCU Animal Ethics Committee Approval Numbers #A1163 and #A1518.

# ACKNOWLEDGEMENTS

I am thankful to the Universidad Autonoma del Estado de Mexico (Autonomous University of the State of Mexico), to the Mexican Consejo Nacional de Ciencia y Tecnologia (CONACYT) and to James Cook University for their financial support during my doctoral studies.

I am very grateful to my supervisor, Dr. Alan G Baxter for his interest, support and guidance in my PhD studies at James Cook University.

I sincerely appreciate the participation of the staff of the Immunogenetics Research Facility at James Cook University: Nicole Fraser, Kylie Robertson, Jo-Anne Diaz, Rohan Henderson, Shevourne O'Reilly, Kirilly O'Reilly, Samuel Page, Liam Finn, Lisa Brown and Nicole Smith. Their expertise in the animal management and their support were invaluable for the development of this project.

Special thanks to Klaus Griewank and Albert Bendelac for their dedicated work in generating the construct for TCR V alpha14 transgenic mice.

I appreciate the help of Erik Biros and Shahead Chowdhury in the genotyping of the different TLR knockout mice.

I acknowledge Sue Reilly for her teachings in histology techniques and tolerance.

I appreciate the help of Latifa Atagazli and Jaime Neal in the process of histopathological samples.

I am very grateful to Kellie Johns, Elizabeth Tynan, Kasturi-Reddy Lopata Rosemary Dunn, Paul Marsh and Michell Tirell for their editorial support.

Thanks to Julie M. Fletcher and Nicole Gerlach for her support.

To Miguel *in Memoriam.*

# ABSTRACT

Multiple Sclerosis (MS) is a degenerative disease affecting the central nervous system. The molecular mechanisms and the development of therapies for MS are mainly studied in the animal model Experimental Autoimmune Encephalomyelitis (EAE), which is an induced demyelinating paralysis model, resembling some aspects of MS. Although significant advances have been achieved in MS and EAE, the genetic and environmental factors underlying the initiation and progression of MS are unclear and no curative or preventive therapies are known.

Toll-like receptors (TLRs) mediate the effects of some environmental factors in the immune system and initiate inflammatory responses against pathogen associated molecular patterns (PAMP) and danger associated molecular patterns (DAMP). Although studies show that TLR expression increases during MS and EAE in the CNS, the role of TLRs remains unclear in both diseases. In this study, it was examined the development of $MOG_{35-55}$/CFA + PTX–induced EAE in the absence of MyD88 and TLR1, TLR2, TLR4, TLR6, TLR9, TLR2/9 and TLR4/9. On the other hand regulatory cells such as NKT cells have been associated with inflammation in MS; nevertheless, the role of NKT cells in the disease is indistinct. In this study,

it was examined the genetic control of NKT cell numbers in the severity of $MOG_{35-55}$/CFA + PTX–induced EAE.

C57BL/6 mice developed a chronic form of $MOG_{35-55}$/CFA + PTX–induced EAE. The absence of TLR1, TLR4, TLR6 and TLR4/9 did not affect the severity of chronic active $MOG_{35-55}$/CFA + PTX–induced EAE in C57BL/6 mice; however, C57BL/6.*Myd88*$^{-/-}$ mice were completely protected from the disease. Female C57BL/6.*Tlr2*$^{-/-}$ and C57BL/6.*Tlr9*$^{-/-}$ mice showed less severe clinical signs of $MOG_{35-55}$/CFA + PTX–induced EAE compared with wild type (WT) B6 mice. C57BL/6.*Tlr2*$^{-/-}$*9*$^{-/-}$ male and females mice also decreased the severity of $MOG_{35-55}$/CFA + PTX–induced EAE compared with WT B6 mice but the disease was not less severe that that seen in single deficient female mice in TLR2 or TLR9.

The passive form of chronic $MOG_{35-55}$/CFA + PTX–induced EAE confirmed protection from disease in the absence of TLR2 and TLR9. Passive $MOG_{35-55}$/CFA + PTX–induced EAE was ameliorated in C57BL/6.*Tlr9*$^{-/-}$ female mice but the clinical signs of disease were similar to those seen in active $MOG_{35-55}$/CFA + PTX–induced EAE. However, both male and female C57BL/6.*Tlr2*$^{-/-}$ mice were completely protected. Protection of disease in the absence of TLR2 was associated with fewer CNS-infiltrating $CD4^+$ T cells, fewer CNS-infiltrating $CD4^+$ T cells secreting IL17, increasing proportions of central ($CD62L^+$)

$CD4^+CD25^+Foxp3^+$ regulatory T cells and reduced prevalence of detectable circulating levels of IL6.

As type 1 diabetes (T1D)-prone NOD mice are susceptible to $MOG_{35-55}$/CFA + PTX–induced EAE, we used the same approach to study $MOG_{35-55}$/CFA + PTX–induced EAE in this strain in order to dissect the interrelationships between organ-specific autoimmune diseases. NOD mice showed a mild form of relapsing-remitting $MOG_{35-55}$/CFA + PTX–induced EAE. The absence of TLR1, TLR2, TLR4, TLR6 and TLR9 did not affect the clinical course of relapsing remitting $MOG_{35-55}$/CFA + PTX–induced EAE in both males and female mice compared to the WT NOD/Lt controls. As the absence of TLR2 did not decrease the severity of $MOG_{35-55}$/CFA + PTX–induced EAE in NOD mice, it was hypothesized that insulitis associated with T1D development in some way compensated for the lack of TLR2 signalling in NOD mice. To test this hypothesis, NOD/Lt mice carrying the MHC haplotype $H2^b$ from C57BL/6 mice (NOD.$H2^b$) were crossed onto the NOD.$Tlr2^{-/-}$ strain. NOD.$H2^b$ mice were completely protected from T1D and insulitis but showed more severe relapsing-remitting $MOG_{35-55}$/CFA + PTX–induced EAE than NOD/Lt mice. In contrast, the severity of relapsing remitting $MOG_{35-55}$/CFA + PTX–induced EAE decreased in NOD.$H2^b$.$Tlr2^{-/-}$ mice. Moreover, NOD.$H2^b$.$Tlr2^{-/-}$ mice were protected from relapses of $MOG_{35-55}$/CFA + PTX–induced EAE. This data suggest that both TLR2 signalling and immunological events

associated with autoimmunity at distant site can mediate relapses in CNS autoimmunity.

Because mice with increased numbers of NKT cells are protected from T1D and NKT cells have been associated with both increase severity and decrease severity of MS. In this study, it was hypothesized that genetic control of NKT cells numbers affects the severity of $MOG_{35-55}$/CFA + PTX–induced EAE. The clinical course of active $MOG_{35-55}$/CFA + PTX–induced EAE was not affected in NOD/Lt congenic mice for *Nkrp1b, NKT1, NKT2a, NKT2b* and *NKT2e*. The absence of *Cd1d* did not affect the severity of $MOG_{35-55}$/CFA + PTX–induced EAE neither in C57BL/6 mice nor in NOD/Lt mice. NOD.*Idd13* mice showed an increased severity of $MOG_{35-55}$/CFA + PTX–induced EAE. Transgenic C57BL/6.Tg(mCD4-V$\alpha$14)6 female mice but not male mice ameliorated the severity of $MOG_{35-55}$/CFA + PTX–induced EAE. Both male and female C57BL/6.Tg(mCD4-V$\alpha$14)5 decreased the severity of $MOG_{35-55}$/CFA + PTX–induced EAE. C57BL/6.Tg(mCD4-V$\alpha$14)2 female were completely protected but not males. These data indicate that increased numbers of NKT cells play a role in CNS autoimmune inflammation.

In conclusion, these results indicate that signalling provided by TLR9 play a partial role in the severity of CNS autoimmunity. The effector phase of autoimmune inflammation in the CNS is dependent of TLR2 signalling.

Genetic control of NKT numbers is associated with the severity of autoimmune CNS inflammation.

# TABLE OF CONTENT

**STATEMENT OF ACCESS** ..... **ii**

**STATEMENT ON SOURCES** ..... **iii**

**ELECTRONIC COPY** ..... **iv**

**CONTRIBUTIONS OF OTHERS** ..... **v**

**APPROVAL OF ETHICS** ..... **vi**

**ACKNOWLEDGEMENTS** ..... **vii**

**ABSTRACT** ..... **ix**

**TABLE OF CONTENT** ..... **xiv**

**LIST OF TABLES** ..... **xxiii**

**LIST OF FIGURES** ..... **xxiv**

**PREFACE** ..... **xxxi**

**ACHIEVEMENTS** ..... **xxxiii**

**ABBREVIATIONS** ..... **xxxvii**

**CHAPTER 1** ..... **1**

**INTRODUCTION** ..... **1**

**1.1 Autoimmunity** ..... **1**

**1.2 Multiple Sclerosis** ..... **3**

1.2.1 Genetic and environmental factors in MS ..... 5

**1.3 Toll-like receptors** ..... **7**

**1.4 Toll-like receptors in Multiple Sclerosis ..... 8**

1.4.1 Toll-like Receptor One in Multiple Sclerosis ..... 9

1.4.2 Toll-like Receptor Two in Multiple Sclerosis ..... 10

1.4.3 Toll-like Receptor Three in Multiple Sclerosis ..... 12

1.4.4 Toll-like Receptor Four in Multiple Sclerosis ..... 13

1.4.5 Toll-like Receptor Five in Multiple Sclerosis ..... 13

1.4.6 Toll-like Receptor Six in Multiple Sclerosis ..... 14

1.4.7 Toll-like Receptor Seven in Multiple Sclerosis ..... 14

1.4.8 Toll-like Receptor Eight in Multiple Sclerosis ..... 16

1.4.9 Toll-like Receptor Nine in Multiple Sclerosis ..... 16

1.4.10 Toll-like Receptor Ten in Multiple Sclerosis ..... 17

1.4.11 Toll-like Receptor Eleven in Multiple Sclerosis ..... 17

**1.5 Animal Models of Multiple Sclerosis ..... 18**

1.5.1 Experimental Autoimmune Encephalomyelitis ..... 19

**1.6 MyD88 in Animal Models of Multiple Sclerosis ..... 22**

1.6.1 Toll-like Receptor One in Animal Models of Multiple Sclerosis ..... 23

1.6.2 Toll-like Receptor Two in Animal Models of Multiple Sclerosis ..... 24

1.6.3 Toll-like Receptor Three in Animal Models of Multiple Sclerosis ..... 26

1.6.4 Toll-like Receptor Four in Animal Models of Multiple Sclerosis ..... 27

1.6.5 Toll-like Receptor Five in Animal Models of Multiple Sclerosis ..... 29
1.6.6 Toll-like Receptor Six in Animal Models of Multiple Sclerosis 29
1.6.7 Toll-like Receptor Seven in Animal Models of Multiple Sclerosis ..... 30
1.6.8 Toll-like Receptor Eight in Animal Models of Multiple Sclerosis ..... 31
1.6.9 Toll-like Receptor Nine in Animal Models of Multiple Sclerosis ..... 31
1.6.10 Toll-like Receptors Eleven, Twelve and Thirteen in Animal Models of Multiple Sclerosis..... 33
**1.7 Natural Killer T cells in Multiple Sclerosis and Experimental Autoimmune Encephalomyelitis ..... 34**
1.7.1 NKT cells classification..... 35
1.7.2 NKT cells in Multiple Sclerosis ..... 36
1.7.3 NKT cells in Experimental Autoimmune Encephalomyelitis .... 38
**1.8 Summary and project aims..... 39**
**CHAPTER 2..... 46**
**MATERIALS AND METHODS..... 46**
**2.1 Mice..... 46**
2.1.1 Sources of C57BL/6 and NOD/Lt mice ..... 46
2.1.2 Sources and generation of knockout, congenic and transgenic mice ..... 46
2.1.2.1 Knockout mice..... 46

2.1.2.2 Congenic and transgenic mice ..... 48

**2.2 Mouse identification and housing ..... 49**

**2.3 Genotyping ..... 49**

2.3.1 DNA extraction..... 49

2.3.2 Polymerase chain reaction (PCR) and polyacrylamide gel electrophoresis (PAGE) ..... 50

2.3.3 Processing and staining of cells from blood for Flow Cytometry ..... 51

**2.4 Induction of EAE ..... 51**

2.4.1 Mouse immunisation for active $MOG_{35-55}$-induced EAE..... 51

2.4.2 Mouse immunisation for passive $MOG_{35-55}$-induced EAE..... 52

2.4.2.1 Donor immunisation and organ collection ..... 52

2.4.2.2 Single cell suspension and cell culture ..... 53

2.4.2.3 Adoptive transfer of EAE to recipients ..... 54

**2.5 Clinical scoring of active and passive EAE ..... 54**

**2.6 Diabetes incidence..... 55**

**2.7 Histopathology ..... 56**

2.7.1 Organ removal and fixation ..... 56

2.7.1.1 Central Nervous System (CNS)..... 56

2.7.2 Parafination, section, de-waxing and hydratation..... 56

2.7.3 Staining ..... 57

2.7.3.1 Hematoxilin and Eosin Staining ..... 57

2.7.3.2 Luxol fast blue ..... 58

2.7.3.3 Bielschowsky's Silver ..... 58

**2.8 Histological evaluation ..... 59**

2.8.1 Spinal cord ..... 59

**2.9 Flow Cytometry ..... 60**

2.9.1 Organ removal ..... 60

2.9.2 Preparation of single cell suspensions ..... 60

2.9.2.1 Spleen ..... 60

2.9.2.2 Lymph nodes ..... 61

2.9.2.3 Central Nervous System ..... 61

**2.9.3 FACs staining and analysis ..... 62**

2.9.3.1 Blocking FcR binding ..... 62

2.9.3.2 Cell surface staining ..... 62

2.9.3.3 Intracellular staining ..... 64

2.9.3.3.1 Tregs staining ..... 64

2.9.3.3.2 IL17 in spleen ..... 64

2.9.3.3.3 IL17 Secretion Assay ..... 64

**2.10 Cytokines assays ..... 66**

2.10.1 Plasma collection and storage ..... 66

2.10.2 Th1/Th2/Th17 cytokine assays ..... 67

2.10.2.1 IFNβ ELISA ..... 68

**2.11 Intraperitoneal injections of IL6 ..... 68**

**2.12 Mice treated with antibiotics ..... 68**

**2.13 Statistical analysis ..... 69**

**CHAPTER 3 ..... 70**

**ROLES FOR TLR2, TLR9 AND MyD88 BUT NOT TLR1, TLR4 AND TLR6 IN ACTIVE $MOG_{35-55}$/CFA + PTX–INDUCED EAE ..... 70**

**3.1 Introduction ..... 70**

**3.2 Results ..... 71**

3.2.1 Toll-like receptors and MyD88 in active $MOG_{35-55}$/CFA + PTX–induced EAE ..... 71

3.2.2 Histopathology of damage to the spinal cord in the absence of TLRs and MyD88 ..... 82

3.2.3 Leukocyte infiltration in the CNS at the peak of active $MOG_{35-55}$/CFA + PTX-induced EAE ..... 88

3.2.4 Plasma cytokines in active $MOG_{35-55}$/CFA + PTX-induced EAE ..... 94

**3.3 Discussion ..... 97**

**CHAPTER 4 ..... 100**

**ROLE FOR TLR2 AND TLR9 IN PASSIVE EAE ..... 100**

**4.1 Introduction ..... 100**

**4.2 Results ..... 102**

4.2.1 Absence of PTX and irradiation in passive EAE ..... 102

4.2.2 The absence of TLR4 in the severity of passive EAE ..... 105

4.2.3 TLR9 and TLR2 in passive EAE ..... 108

4.2.4 $CD4^+$ T cells in the CNS in passive EAE ..... 117

4.2.5 $CD4^+$ T cells secreting IL17 in the absence of TLR2 in the CNS ..... 120

4.2.6 Absolute numbers of CD62L-expressing Tregs in the absence of TLR2 ..... 122

4.2.7 Microflora in passive EAE ..... 128

**4.3 Discussion ..... 131**

**CHAPTER 5 ..... 135**

**THE ROLE OF TLR2 IN ACTIVE $MOG_{35-55}$/CFA + PTX-INDUCED RELAPSING-REMITTING EAE ..... 135**

**5.1 Introduction ..... 135**

**5.2 Results ..... 136**

5.2.1 Active $MOG_{35-55}$/CFA + PTX–induced relapsing-remitting EAE in NOD/Lt deficient mice in TLR1, TLR2, TLR4, TLR6 and TLR9 136

5.2.2 Active $MOG_{35-55}$/CFA + PTX–induced relapsing-remitting EAE in NOD.$H2^b$ and NOD.$H2^d$ mice ..... 143

5.2.3 Active $MOG_{35-55}$/CFA + PTX–induced relapsing-remitting EAE in NOD.$H2^b$.$Tlr2^{-/-}$ ..... 148

5.2.4 IL6 in active $MOG_{35-55}$/CFA + PTX–induced relapsing-remitting EAE in the absence of TLR2 ..... 155

5.2.5 Circulating levels of cytokines in active $MOG_{35-55}$/CFA + PTX–induced relapsing-remitting EAE in NOD.$H2^b$.$Tlr2^{-/-}$ and NOD.$Tlr2^{-/-}$ mice ..... 159

**5.3 Discussion ..... 162**

**CHAPTER 6 ..... 164**

**NKT CELLS IN THE INTERACTION BETWEEN ENVIRONMENTAL AND GENETIC RISK FACTORS FOR EAE 164**

**6.1 Introduction ..... 164**

**6.2 Results ..... 166**

6.2.1 Active $MOG_{35-55}$/CFA + PTX-induced EAE in NOD/Lt mice and NOD.*Nkrp1b* mice ..... 166

6.2.2. *Cd1d* in active $MOG_{35-55}$/CFA + PTX-induced EAE ..... 169

6.2.3. The *Idd13* locus in active $MOG_{35-55}$/CFA + PTX-induced EAE ..... 173

6.2.4 Active $MOG_{35-55}$/CFA + PTX-induced EAE in *NOD.Nkrp1b* mice congenic for *Nkt1*, *Nkt2a*, *Nkt2b*, *Nkt2e* ..... 177

6.2.5 Active $MOG_{35-55}$/CFA + PTX-induced EAE in TCR CD4-Vα14 transgenic mice ..... 180

6.2.5.1 C57BL/6.Tg(mCD4-Vα14)6 mice ..... 180

6.2.5.2 C57BL/6.Tg(mCD4-Vα14)5 mice ..... 181

6.2.5.3 C57BL/6.Tg(mCD4-Vα14)2 mice ..... 183

**6.3 Discussion ..... 187**

**CHAPTER 7 ..... 191**

**GENERAL DISCUSSION AND CONCLUSIONS ..... 191**

**REFERENCES ..... 200**

**Appendix 1 ..... 261**

**LOCALIZATION OF TOLL-LIKE RECEPTORS ..... 261**

**APPENDIX 2 ..... 262**

**PRODUCTION OF C57BL/6.*Cd1d*$^{-/-}$ MICE ..... 262**

**APPENDIX 3..... 263**

**PRODUCTION OF NOD.*H2*$^{b}$.*Tlr2*$^{-/-}$ MICE..... 263**

**APPENDIX 4..... 264**

**MOUSE IDENTIFICATION ..... 264**

**APPENDIX 5 SEQUENCES OF PRIMERS ..... 265**

**APPENDIX 6..... 266**

**POLYMERASE CHAIN REACTION (PCR) ..... 266**

**APPENDIX 7 TERMOCYCLING PROTOCOLS FOR PCR..... 267**

**APPENDIX 8 ANTIBODIES FOR FLOW CYTOMETRY ANALYSIS ..... 268**

**APPENDIX 9 PREPARATION OF SOLUTIONS AND BUFFERS . 271**

# LIST OF TABLES

Table 1.1 Toll-like receptors in EAE..... 42

Table 3.1 Characteristics of active $MOG_{35-55}$/CFA + PTX–induced EAE in male and female C57BL/6 and C57BL/6 mice deficient in TLR1, TLR2, TLR4, TLR6, TLR9, TLR2/9, TLR4/9 and MyD88 ..... 77

Table 3.2 Active $MOG_{35-55}$/CFA + PTX –induced EAE in C57BL/6 female mice deficient in TLR2 and TLR9 ..... 81

Table 4.1 Passive EAE in C57BL/6 mice treated with or without PTX and irradiation..... 104

Table 4.2 Passive EAE in TLR-deficient C57BL/6 mice and C57BL/6 WT control mice ..... 110

Table 6.1. Active $MOG_{35-55}$/CFA + PTX –induced EAE in NOD/Lt and NOD.*Idd13* female mice..... 174

# LIST OF FIGURES

Figure 3.1 Representative clinical course of active $MOG_{35-55}$/CFA + PTX–induced EAE in individual mice ..... 75

Figure 3.2 Clinical course of active $MOG_{35-55}$/CFA + PTX–induced EAE in male and female mice ..... 76

Figure 3.3 Scoring system of spinal cord histopathology after 40 days of active $MOG_{35-55}$/CFA + PTX –induced EAE ..... 85

Figure 3.4 Representative transverse histopathological sections of spinal cords taken 40 days after active $MOG_{35-55}$/CFA + PTX-induced EAE..... 86

Figure 3.5 Histopathological analysis of damage in spinal cords of mice with 40 days of active $MOG_{35-55}$/CFA + PTX -induced EAE ..... 87

Figure 3.6 Representative gating of FACS analysis showing the proportions of leukocytes from CNS of male and female C57BL/6 (positive and negative control groups), C57BL/6.*Tlr2*$^{-/-}$, C57BL/6.*Tlr9*$^{-/-}$ and C57BL/6.*Tlr2*$^{-/-}$*9*$^{-/-}$ mice 21 days after $MOG_{35-55}$/CFA/PTX immunisation. 92

Figure 3.7 CNS-infiltrating leucocytes of C57BL/6 positive control group (*closed circles*), C57BL/6 negative control group (*closed diamonds*), C57BL/6.*Tlr2*$^{-/-}$ (*closed squares*), C57BL/6.*Tlr9*$^{-/-}$ (*closed downward triangles*), C57BL/6.*Tlr2*$^{-/-}$*9*$^{-/-}$ (*closed upward triangles*) and C57BL/6.*Myd88*$^{-/-}$ (*open diamonds*) male and female mice..... 93

Figure 3.8 Cytokine levels in the plasma of C57BL/6 and C57BL/6.*Tlr*$^{-/-}$ male mice, 21 days after $MOG_{35-55}$/CFA + PTX immunisation..... 96

Figure 4.1 Analysis of the clinical course of passive EAE in female C57BL/6 (*closed circles*) and C57BL/6.*Tlr4*$^{-/-}$ (*open circles*) mice..... 107

Figure 4.2 Analysis of the clinical course of passive EAE in female C57BL/6 (closed circles) and C57BL/6.*Tlr9*$^{-/-}$ (open circles) mice ..... 111

Figure 4.3 Analysis of the clinical course of passive EAE in male C57BL/6 (*closed circles*) and C57BL/6.*Tlr2*$^{-/-}$ (*open circles*) mice..... 112

Figure 4.4 Analysis of the clinical course of passive EAE in female C57BL/6 (*closed circles*) and C57BL/6.*Tlr2*$^{-/-}$ (*open circles*) mice..... 113

Figure 4.5 Analysis of the clinical course of passive EAE in female mice. ..... 116

Figure 4.6 Representative FACS analysis showing the proportions of brain and spinal cord leukocytes from female C57BL/6, C57BL/6 (PBS), C57BL/6.*Tlr2*$^{-/-}$ and C57BL/6.*Tlr9*$^{-/-}$, 34 days after adoptive transfer of EAE ..... 118

Figure 4.7 Total numbers of $CD4^+$ T cells, $CD8^+$ T cells, inflammatory macrophages and, myeloid dendritic cells (MFI- mean fluorescence intensity) in the CNS of C57BL/6 (*closed cicles*), C57BL/6.*Tlr2*$^{-/-}$ (*closed squares*), C57BL/6.*Tlr9*$^{-/-}$ (*downward closed triangles*), C57BL/6 (PBS) (*closed diamonds*) female mice ..... 119

Figure 4.8 Representative experiments of IL17 secretion of Central Nervous System leukocytes and splenocytes from naive mice, and mice with passive EAE. Cells were stimulated with PMA and controls were not stimulated 121

Figure 4.9 Representative flow cytometry gating of $CD4^+$ T cells and Tregs: $CD3^+CD4^+CD25^+FoxP3^+$ and $CD3^+CD4^+CD25^+FoxP3^+CD62L^+$. ..... 124

Figure 4.10 Total numbers of $CD4^+$ T cells and Tregs from spleen of male and female C57BL/6.*Tlr2*$^{-/-}$, C57BL/6.*Tlr9*$^{-/-}$ and C57BL/6 WT control mice. ..... 125

Figure 4.11 IL6 levels in plasma after 10 days of passive EAE induction 126

Figure 4.12 IL6 levels in plasma after 34 days of passive EAE induction 127

Figure 4.13 Analysis of the clinical course of passive $MOG_{35-55}$/CFA + PTX -induced EAE in female C57BL/6 (*closed circles*), C57BL/6.*Tlr2*$^{-/-}$, (*closed downward triangles*) and C57BL/6.*Tlr9*$^{-/-}$ (*closed diamonds*) mice fed with normal diet and; female C57BL/6 (*open circles*), C57BL/6.*Tlr2*$^{-/-}$, (*open downward triangles*) and C57BL/6.*Tlr9*$^{-/-}$ (*open diamonds*) mice fed with medicated diet. ..... 130

Figure 5.1. Representative clinical course of active $MOG_{35-55}$/CFA + PTX–induced relapsing-remitting EAE in individual NOD/Lt control WT (*closed circles*) and NOD.*Tlr1*$^{-/-}$, NOD.*Tlr2*$^{-/-}$, NOD.*Tlr4*$^{-/-}$, NOD.*Tlr6*$^{-/-}$ and NOD.*Tlr9*$^{-/-}$ (*open circles*) male and female mice ..... 140

Figure 5.2 Clinical course of active $MOG_{35-55}$/CFA + PTX–induced relapsing-remitting EAE in NOD/Lt WT control (*closed circles*) and NOD.*Tlr1*$^{-/-}$, NOD.*Tlr2*$^{-/-}$, NOD.*Tlr4*$^{-/-}$, NOD.*Tlr6*$^{-/-}$ and NOD.*Tlr9*$^{-/-}$ (*open circles*) female and male mice ..... 141

Figure 5.3. Analysis of the clinical course of active $MOG_{35-55}$/CFA + PTX-induced relapsing-remitting EAE in NOD/Lt (*closed cicles*), NOD.*Tlr1*$^{-/-}$ (*open squares*), NOD.*Tlr2*$^{-/-}$ (*open cicles*), NOD.*Tlr4*$^{-/-}$ (*open downward triangles*), NOD.*Tlr6*$^{-/-}$ (*open upward triangles*) and NOD.*Tlr9*$^{-/-}$ (*open diamonds*) male and female mice ..... 142

Figure 5.4. Cumulative diabetes incidence in NOD/Lt (*closed cicles*), NOD.*H2*$^{b}$ (*open cicles*) and NOD.*H2*$^{d}$ (*open circles*) female mice ..... 145

Figure 5.5. Representative clinical course of active $MOG_{35-55}$/CFA + PTX-induced relapsing-remitting EAE in individual female NOD/Lt (*closed circles*), NOD.*H2*$^{b}$ (*open circles*) and NOD.*H2*$^{d}$ (*open forwards triangles*) mice. ..... 146

Figure 5.6. Analysis of the clinical course of active $MOG_{35-55}$/CFA + PTX-induced relapsing-remitting EAE in NOD/Lt (*closed circles*), NOD.*H2*$^{b}$ (*open circles*) and NOD.*H2*$^{d}$ (*open forwards triangles*) female mice..... 147

Figure 5.7 Clinical course of active $MOG_{35-55}$/CFA + PTX–induced EAE in NOD.*H2*$^{b}$ control mice (WT) (*closed circles*), NOD.*H2*$^{b}$.*Tlr2*$^{-/-}$ (*open circles*) and; NOD/Lt control mice (WT) (*closed downward triangles*) and NOD.*Tlr2*$^{-/-}$ (*open upwards triangles*)..... 153

Figure 5.8. Analysis of the clinical course of active $MOG_{35-55}$/CFA + PTX-induced relapsing-remitting EAE in NOD.*H2*$^{b}$ (*close circles*) and NOD.*H2*$^{b}$.*Tlr2*$^{-/-}$ (*open circles*); and NOD/Lt (*closed downwards triangles*) and NOD.*H2*$^{b}$.*Tlr2*$^{-/-}$ (*open upwards triangles*) in males and female mice.. ..... 154

Figure 5.9 Analysis of the clinical course of active $MOG_{35-55}$/CFA + PTX–induced EAE in NOD.*H2*$^{b}$ control mice (WT) (*closed circles*), NOD.*H2*$^{b}$.*Tlr2*$^{-/-}$ mice treated with PBS (*open circles*) and NOD.*H2*$^{b}$.*Tlr2*$^{-/-}$ mice treated with IL6 (*open downward triangles*) ..... 158

Figure 5.10 Circulating levels of IL6 and IL22 in NOD.*H2*$^{b}$ (*close cicles*), NOD.*H2*$^{b}$.*Tlr2*$^{-/-}$ treated with PBS (*open cicles*), NOD.*H2*$^{b}$.*Tlr2*$^{-/-}$ treated with IL6 (*open downward triangles*), naive NOD.*H2*$^{b}$ (*closed squares*), naive NOD.*H2*$^{b}$.*Tlr2*$^{-/-}$ (*open squares*), naive NOD/Lt (*open diamonds*), naive NOD.*Tlr2*$^{-/-}$ (*closed diamonds*) ..... 161

Figure 6.1 Analysis of the clinical course of active $MOG_{35-55}$/CFA + PTX - induced EAE in female NOD/Lt (*closed circles*) and NOD.*Nkrp1b* (*open circles*) mice ..... 168

Figure 6.2. Analysis of the clinical course of active $MOG_{35-55}$/CFA + PTX - induced EAE in female C57BL/6 (*closed circles*) and C57BL/6.*Cd1d*$^{-/-}$ (*open circles*) mice ..... 171

Figure 6.3 Analysis of the clinical course of active $MOG_{35-55}$/CFA + PTX - induced EAE in female NOD/Lt (*closed circles*) and NOD.*Cd1d*$^{-/-}$ (*open circles*) mice. ..... 172

Figure 6.4 Analysis of the clinical course of active $MOG_{35-55}$/CFA + PTX - induced EAE in male NOD/Lt (*closed circles*) and NOD.*Idd13* (*open circles*) mice.. ..... 175

Figure 6.5 Representative analysis of clinical course of active $MOG_{35-55}$/CFA + PTX -induced EAE in female NOD/Lt (*closed circles*) and NOD.*Idd13* (*open circles*) mice from two independent experiments ..... 176

Figure 6.6 Analysis of the clinical course of active $MOG_{35-55}$/CFA + PTX - induced EAE in female NOD.*Nkrp1b* (*closed circles*), NOD.*Nkt1* (*open circles*), NOD.*Nkt2a* (*open upward triangles*), NOD.*Nkt2b* (*open downward triangles*) and NOD.*Nkt2e* (*open diamonds*) mice ..... 179

Figure 6.7 Analysis of the clinical course of active $MOG_{35-55}$/CFA + PTX - induced EAE in male C57BL/6 (*closed circles*), C57BL/6.Tg(mCD4-Va14)6 (*upward triangles*), C57BL/6.Tg(mCD4-Va14)5 (*open squares*) mice ..... 184

Figure 6.8 Analysis of the clinical course of active $MOG_{35-55}$/CFA + PTX - induced EAE in male C57BL/6 (*closed circles*), C57BL/6.Tg(mCD4-Va14)2 (*open cicles*) mice ..... 185

Figure 6.9 Analysis of the clinical course of active $MOG_{35-55}$/CFA + PTX - induced EAE in female C57BL/6 (*closed circles*), C57BL/6.Tg(mCD4-Va14)2 (*upward triangles*), C57BL/6.Tg(mCD4-Va14)5 (*open square*) and C57BL/6.Tg(mCD4-Va14)2 (*open circles*) mice..... 186

# PREFACE

The studies shown in this thesis describe the importance of Toll-like receptors (TLRs) and Natural Killer T cells (NKT cells) in the best characterised animal model of Multiple Sclerosis (MS), Experimental Autoimmune Encephalomyelitis (EAE).

Chapter 1 presents an analysis of literature about TLRs and NKT cells in MS and EAE. This is followed by the materials and methods used in the experimental work. A study of the role of TLRs in active $MOG_{35-55}$/CFA + PTX-induced EAE in C57BL/6 mice and C57BL/6 mice deficient in TLR1, TLR2, TLR4, TLR6, TLR9, TLR2/9, TLR4/9 and MyD88 is described in the Chapter 3. The Chapter 4 describes studies in the passive model of EAE in C57BL/6 mice and mice deficient in TLR2 and TLR9.

In Chapter 5 is presented a study of TLR2 in $MOG_{35-55}$/CFA + PTX-induced relapsing-remitting EAE and the role of NKT cells in active EAE is described in the Chapter 6. Chapter 7 presents a general discussion of the involvement of TLRs and NKT cells in EAE and their implications in MS as a possible way in the improvement of therapies for patients with the disease.

To GOD with love, thanks for giving me the opportunity to live and for teaching me to love and to forgive.

To my family gratefully, thank you for believing in me, for your unconditional support and for their worthy examples of improvement and delivery.

To Paul Wayne Marsh with love, thanks for your continued support and unconditional love and for being a friend and constant companion, a source of wisdom, calm and advice at all times.

To my friends fondly, thanks for your friendship and support.

To Connor and Nicola who are in my heart forever.

# ACHIEVEMENTS

This work has been published and presented in national and international conferences. It has also been awarded several times.

Published papers

- Miranda-Hernandez S, Gerlach N, Fletcher JM, Biros E, Mack M, Körner H, Baxter AG. Role for MyD88, TLR2 and TLR9 but not TLR1, TLR4 or TLR6 in experimental autoimmune encephalomyelitis. *The Journal of Immunology*. 2011; 187(2): 791-804.

- Miranda-Hernandez S and Baxter AG. Role of toll-like receptors in multiple sclerosis. *American Journal of Clinical and Experimental Immunology*. 2013; 2(1): 75-93.

Published abstracts

- Miranda-Hernandez S, Fletcher JM, Gerlach N, Erik B, Chowdhury S, Heinrich K, Baxter AG. Toll-like receptors signalling in Experimental Autoimmune Encephalomyelitis. Progress in MS

Research Conference, Melbourne, Australia, 2011: Conference Abstracts. Multiple Sclerosis, May 2012, 18: 697-703.

Oral presentations

- Australasian Association for Immunology 2009. ASI Infection and Immunity workshop.
- My research in 3 minutes 2010 at James Cook University.
- "so you think you can research" North Queensland Festival of Life Sciences 2012.
- Three minutes poster oral session. Australasian Association for Immunology 2012.

Poster presentations

- Brisbane Immunology group Annual Retreat 2007 and 2011.
- North Queensland Festival of Sciences 2007, 2010, 2011 and 2012.
- Australasian Association for Immunology 2009, 2010, 2012.
- Neuroimmunology Australia 2010.
- 14$^{th}$ International Congress of Immunology, Kansai, Japan 2010.
- Multiple Sclerosis Australia 2011.

- TLROZ 2012. 3rd National Conference of the Australian Toll-like Receptors Research Network.

Other participations

- Microscopy image competition 2011, James Cook University. Queensland, Australia.

Awards

- Best PhD student oral presentation. ASI Infection and Immunity Workshop. Australasian Society for Immunology Meeting 6th – 10th December 2009 (ASI Gold Cost 2009). Conrad Jupiters, Broadbeach, Queensland, Australia.
- Poster Presentation award at North Queensland Festival of Sciences 2010, James Cook University, Townsville, Queensland, Australia.
- Poster presentation award at the TLROZ 2012 Meeting 3rd National Conference of Australian Toll-Like Receptors Research Network. Melbourne, Australia.
- Winner of oral presentation of "so you think you can research" North Queensland Festival of Life Sciences 2012.

Future presentations

- Progress on MS Research Conference November 2013.

# ABBREVIATIONS

| | | |
|---|---|---|
| **°C** | | Degrees Celsius |
| **15-HC** | - | 15-a-hydroxicholestene |
| **2-ME** | - | 2-Mercaptoethanol |
| **APC** | - | Antigen presenting cell(s) |
| **BAFF** | - | B-cell activating factor |
| **bp** | | Base pair |
| **BSA** | | Bovine serum albumin |
| **C57BL/6** | - | C57 black 6 mouse |
| **C57BL/6.*Cd1d*$^{-/-}$** | - | C57 black 6 mouse deficient in *CD1d* |
| **C57BL/6.*Myd88*$^{-/-}$** | - | C57 black 6 mouse deficient in Myeloid differentiation primary response gene (88) |
| **C57BL/6.Tg(mCD4-Vα14)** | - | C57 black 6 mouse transgenic for CD4-Vα14 |
| **C57BL/6.*Tlr*** | - | C57 black 6 mouse –Toll like receptor |
| **C57BL/6.*Tlr*$^{-/-}$** | - | C57 black 6 mouse –Toll like receptor knockout |
| **C57BL/6.*Tlr1*$^{-/-}$** | - | C57 black 6 mouse deficient in Toll like receptor one |

| | | |
|---|---|---|
| **C57BL/6.*Tlr2*$^{-/-}$** | - | C57 black 6 mouse deficient in Toll like receptor two |
| **C57BL/6.*Tlr2*$^{-/-}$*9*$^{-/-}$** | - | C57 black 6 mouse deficient in Toll like receptor two and nine |
| **C57BL/6.*Tlr4*$^{-/-}$** | - | C57 black 6 mouse deficient in Toll like receptor four |
| **C57BL/6.*Tlr4*$^{-/-}$*9*$^{-/-}$** | - | C57 black 6 mouse deficient in Toll like receptor two and nine |
| **C57BL/6.*Tlr6*$^{-/-}$** | - | C57 black 6 mouse deficient in Toll like receptor six |
| **C57BL/6.*Tlr9*$^{-/-}$** | - | C57 black 6 mouse deficient in Toll like receptor nine |
| **$CaCl_2$** | - | Calcium chloride |
| **CCL2** | - | Chemokine (C-C motif) ligand 2 |
| **CCR2** | - | Chemokine (C-C motif) receptor 2 |
| **CD** | - | Cluster of differentiation |
| **CD62L** | - | L-selectin |
| **CDI** | - | Clinical disease index |
| **cDNA** | - | Complementary deoxyribonucleic acid |
| **CFA** | - | Complete Freund's Adjuvant |
| **CNS** | - | Central Nervous System |

| | | |
|---|---|---|
| **$CO_2$** | - | Carbon dioxide |
| **CpG** | - | -cytosine-phosphate-guanine- |
| **CpG-ODN** | - | CpG Oligodeoxynucleotide |
| **CSF** | - | Cerebrospinal fluid |
| **CXCL** | - | Chemokine (C-X-C motif) |
| **DAMP** | - | Damage associated molecular pattern (s) |
| **DC** | - | Dendritic cell(s) |
| **dd$H_2O$** | - | Double distilled water |
| **d$H_2O$** | - | Distilled water |
| **DNA** | - | Deoxyribonucleic acid |
| **DNase** | - | Deoxyribonuclease |
| **DPBS** | - | Dulbecco's Phosphate Buffered Saline |
| **DPX** | - | Mixture of distyrene, plasticizer and xylene |
| **Dr** | - | Doctor |
| **dsRNA** | - | Double stranded ribonucleic acid |

| | | |
|---|---|---|
| **DW** | - | Distillated water |
| **e.g.** | - | For exmple |
| **EAE** | - | Experimental Autoimmune Encephalomyelitis |
| **EDTA** | - | Ethylenediaminetetraacetic acid |
| **ELISA** | - | Enzyme-linked immunosorbent assay |
| **F1** | - | *Filial 1* |
| **F3** | - | *Filial 3* |
| **FCS** | - | Fetal calf serum |
| **Foxp3** | - | Forkhead box P3 |
| ***g*** | | Gravitational |
| **GalC** | - | Galactocerebrocide |
| **GM-CSF** | - | Granulocyte macrophage colony-stimulating factor |
| **GWAS** | - | Genome-wide association studies |
| **Gy** | - | Gray |
| ***H pylori*** | - | *Helicobacter pylori* |

| | | |
|---|---|---|
| **HBSS** | - | Hank’s Balanced Salt Solution |
| **HI** | - | High |
| **HLA** | - | Human Leukocyte Antigen |
| **HMGB1** | - | High-mobility group protein B1 |
| **HSP70** | - | Heat shock protein seventy |
| **HSP90** | - | Heat shock protein ninety |
| **i.p.** | - | Intraperitoneal |
| **IF1H1** | - | Interferon Induced with Helicase C domain 1 |
| **IFA** | - | Incomplete Freund’s Adjuvant |
| **iGb3** | - | Isoglobotrihexosylceramide |
| **IL10** | - | Interleukin ten |
| **IL12** | - | Interleukin twelve |
| **IL13** | - | Interleukin thirteen |
| **IL17** | - | Interleukin seventeen |
| **IL18** | - | Interleukin eighteen |

| | | |
|---|---|---|
| **IL1R** | - | Interleukin-1 receptor |
| **IL1α** | - | Interleukin one alpha |
| **IL1β** | - | Interleukin one beta |
| **IL2** | - | Interleukin two |
| **IL21** | - | Interleukin twenty one |
| **IL22** | - | Interleukin twenty-two |
| **IL23** | - | Interleukin twenty-three |
| **IL27** | - | Interleukin twenty-seven |
| **IL3** | - | Interleukin three |
| **IL4** | - | Interleukin four |
| **IL5** | - | Interleukin five |
| **IL6** | - | Interleukin six |
| **IL7** | - | Interleukin seven |
| **IFN** | - | Interferon(s) |
| **IFNβ** | - | Interferon beta |

| | | |
|---|---|---|
| **IFNγ** | - | Interferon gamma |
| **iNKT cells** | - | Invariant Natural Killer T cells |
| **iNOS** | - | Inducible nitric oxide synthase |
| **IRAK** | - | Interleukin-1 receptor-associated kinase 1 |
| **ISGF3** | - | IFN-stimulated gene factor 3 |
| **KCl** | - | Potassium chloride |
| **KO** | - | Knockout |
| **LFB** | - | Luxol fast blue |
| **LPS** | - | Lipopolysaccharides |
| **LT** | - | Lymphotoxin |
| ***M. tuberculosis*** | | *Mycobacterium tuberculosis* |
| **MBP** | - | Myelin basic protein |
| **MFI** | - | Mean fluorescence intensity |
| **Mg** | | Miligrams |
| **$MgCl_2$** | - | Magnesium chloride |

| | | |
|---|---|---|
| **MHC** | - | Major histocompatibility complex |
| **MIP-1β** | - | Macrophage inflammatory protein beta |
| **Ml** | - | Milliliters |
| **mM** | | Millimolar |
| **MOG** | - | Myelin Oligodendrocyte Glycoprotein |
| **$MOG_{35-55}$** | - | Myelin Oligodendrocyte Glycoprotein 35-55 |
| **mRNA** | - | Messenger RNA |
| **MS** | - | Multiple Sclerosis |
| **MyD88** | - | Myeloid differentiation primary response gene (88) |
| **NaCl** | - | Sodium chloride |
| **NFκ-β** | - | Nuclear factor kappa-light-chain |
| **Ng** | | Nanograms |
| **NK cells** | - | Natural Killer cells |
| **NKT cells** | - | Natural Killer T cells |
| **NOD** | - | Non-obese diabetic mouse |

| | | |
|---|---|---|
| **NOD. *Tlr*$^{-/-}$** | - | Non-obese diabetic mouse – Toll-like receptor knockout |
| **NOD.Tlr** | - | Non-obese diabetic mouse – Toll-like receptor |
| **NOD1** | - | Nucleotide-binding oligomerization domain-containing protein 1 |
| **NOD2** | - | Nucleotide-binding oligomerization domain-containing protein 2 |
| **OPC** | - | Oligodendrocyte precursor cell(s) |
| **PAGE** | - | Polyacrylamide gel electrophoresis |
| **PAMP** | - | Pathogen Associated Molecular Pattern(s) |
| **PBMC** | - | Peripheral blood mononuclear cell (s) |
| **PBS** | - | Dulbecco's Phosphate Buffered Saline |
| **PCR** | - | Polymerase chain reaction |
| **PE** | - | Phycoerythrin |
| **PerCp-Cy5.5** | | Peridinin-chlorophyII Protein Complex with cyanine dye (Cy5.5) |
| **PGN** | - | Peptidoglycans |
| **PI** | - | Propidium Iodide |
| **PIM** | - | Phospatidylinositol mannosedes |

| | | |
|---|---|---|
| **PLP** | - | Proteolipid protein |
| **PMA** | - | Phorbol 12-myristate 13-acetate |
| **Poly I:C** | - | Polyinosinic:polycytidylic |
| **PPMS** | - | Primary Progressive Multiple Sclerosis |
| **PRR** | - | Pattern-recognition receptors |
| **PTX** | - | Pertussis toxin |
| **QIMR** | - | Queensland Institute of Medical Research |
| **Rag** | - | Recombination activating genes |
| **RBC** | - | Red blood cell |
| **Rcf** | | Compute relative centrifugal force |
| **RIG-I** | - | Retinoic acid-inducible gene 1 |
| **RIPK2** | - | Receptor-interacting serine/threonine-protein kinase 2 |
| **RNA** | - | Ribonucleic acid |
| ***RORC*** | - | Retinoic acid-related orphan nuclear hormone receptor C |
| **RPMS** | - | Relapsing Progressive Multiple Sclerosis |

| | | |
|---|---|---|
| **RRMS** | - | Relapsing-Remitting Multiple Sclerosis |
| **RT-PCR** | - | Reverse transcription polymerase chain reaction |
| **SD** | | Standard deviation |
| **SEM** | | Standard error of mean |
| **SFB** | - | Segmented filamentous bacteria |
| **siRNA** | - | Small interfering RNA |
| **SNP** | - | Single-nucleotide polymorphism |
| **SPMS** | - | Secondary Progressive Multiple Sclerosis |
| **ssRNA** | - | Single stranded ribonucleic acid |
| **STAT1** | - | Signal Transducer and Activator of Transcription one |
| **STAT2** | - | Signal Transducer and Activator of Transcription two |
| **T1D** | - | Type one diabetes |
| **T1R** | - | Toll/interleukin-1 receptor |
| **TAE** | - | Tris base, acetic acid and Ethylenediaminetetraacetic acid |
| **TCR** | - | T cell receptor |

| | | |
|---|---|---|
| **TCR V** | - | T cell receptor V |
| **TCRβ** | - | T cell receptor beta |
| **TGF-β1** | - | Transforming grown factor beta 1 |
| **TGFβ** | - | Transforming grown factor beta |
| **Th1/Th2** | - | T helper 1/T helper 2 |
| **Th17** | - | T helper 17 |
| **Th2** | - | T helper 2 |
| **TIR** | - | Toll/interleukin-1 receptor |
| **TLR** | - | Toll-like receptor (s) |
| **Tlr$^{-/-}$** | - | Toll-like receptor knockout |
| **TLR1** | - | Toll-like receptor one |
| **TLR10** | - | Toll-like receptor ten |
| **TLR11** | - | Toll-like receptor eleven |
| **TLR13** | - | Toll-like receptor thirteen |
| **TLR2** | - | Toll-like receptor two |

| | | |
|---|---|---|
| **Tlr2$^{-/-}$Tlr9$^{-/-}$** | - | Absence of Toll-like receptor two and nine |
| **TLR2/9** | - | Toll-like receptor two and nine |
| **TLR3** | - | Toll-like receptor three |
| **TLR4** | - | Toll-like receptor four |
| **Tlr4$^{-/-}$ Tlr9$^{-/-}$** | - | Absence of Toll-like receptor four and nine |
| **TLR4/9** | - | Toll-like receptor four and nine |
| **TLR5** | - | Toll-like receptor five |
| **TLR6** | - | Toll-like receptor six |
| **TLR7** | - | Toll-like receptor seven |
| **TLR8** | - | Toll-like receptor eight |
| **TLR9** | - | Toll-like receptor nine |
| **TMEV** | - | Theiler's Murine Encephalomyelitis Virus |
| **TNF** | - | Tumor necrosis factor |
| **TRAF** | - | TNF receptor associated factor |
| **Tregs** | - | Regulatory T cells |

| | | |
|---|---|---|
| **TRIF** | - | TIR-domain-containing adapter-inducing interferon-β |
| **U** | | Units |
| **VLA-4** | - | Very-late activation antigen-4 |
| **WT** | - | Wild type |
| **α-GalCer** | - | Alpha-galatosylceramide |
| **αTCR** | - | Alpha T cell receptor |
| **β** | - | Beta |
| **μg** | | Micrograms |
| **μL** | | Microliters |
| **μm** | | Micrometers |

# CHAPTER 1

# CHAPTER 1

# INTRODUCTION

## 1.1 Autoimmunity

The body responds to invading pathogens and damaged tissues by producing pro-inflammatory molecules such as cytokines and chemokines, generating an inflammatory response. Immune cells such as antigen presenting cells (APC) and lymphocytes are recruited during inflammation into the affected area(s). The cessation of the stimulus stops the production of inflammatory mediators leading to resolution of the response (Janssen et al., 2012).

The 1908 Nobel Laureate in Medicine, Paul Ehrlich, called autoimmunity "horror autotoxicus" and was the first scientist to mentioned its effects (http://www.nature.com/nature/journal/v435/n7042/pdf/435583a.pdf).

Autoimmunity is characterised by the presence of autoreactive lymphocytes and autoantibodies and the main cause of autoimmunity is the breakdown of self-tolerance (Silverstein, 2001; Rioux et al., 2005).

The approximate prevalence of autoimmune diseases in the world is about 6-9.4% and at least 65% of affected people are women (Cooper et al., 2003; Cooper et al., 2009; Agmon-Levin et al., 2011). Western societies have the highest number of people with autoimmune diseases: about 5 to 6% of their populations (Moroni et al., 2012). The number of autoimmune diseases increases as well as its prevalence and incidence (review in Cooper GS et al., 2003). In response to the global increase in autoimmune diseases, a number of synthetic drugs (e.g. anti-inflammatory, immunosuppressive and disease modified drugs) have been developed (Schütz et al., 2010). However, many of these therapies treat the clinical signs and symptoms but do not prevent the disease or act on the underlying cause. Many of these drugs produce side effects and adverse symptoms affecting organs and tissues such as liver, stomach, heart, blood vessels and kidneys (Lindberg 2013). Limits in our understanding of the etiology and biology of autoimmunity have restricted preventive therapies, and suitable diagnostic and therapeutic options.

To date environmental and genetic factors have been associated with the failure of self-tolerance that triggers an autoimmune disease (McGonagle et al., 2006; Sirota et al., 2009). Genetic factors in autoimmune diseases are strong; however, their participation needs to be demonstrated, since monozygotic twins do not develop autoimmunity to 100% (Gregersen, 1993; Barcellos et al., 2003; Anaya et al., 2006), suggesting that environmental factors must be required for the initiation of autoimmunity.

Moreover, it is important to note that the presentation of autoimmunity differs among affected individuals who apparently suffer the same autoimmune disease, supporting the hypothesis that genetics together with environmental factors are critical for the initiation and development of autoimmune diseases (Agmon-Levin, et al., 2011).

Despite the great efforts made and progress achieved in the study of autoimmune diseases, many knowledge gaps remain. In particular, research is under way to clarify how environmental factors interact with genetic factors to initiate and maintain an autoimmune response. One potential link between environmental factors and genetic susceptibility to autoimmune diseases such as Multiple Sclerosis (MS) is the class of cellular environmental sensors, Toll-like receptors (TLRs). Another potential link in the development of MS is the deficiency and dysfunction of regulatory cells such as Natural Killer T cells (NKTs). This literature review will focus on the role of TLRs and NKT cells in the interaction between genetics and environmental factors in MS and its animal model Experimental Autoimmune Encephalomyelitis (EAE).

## 1.2 Multiple Sclerosis

MS is an autoimmune disease that damages the myelin sheaths in the central nervous system (CNS) leading to demyelination, severely affecting the

patient's quality of life. Signs and symptoms related to the disease including bladder dysfunction, bowel dysfunction, cognitive problems, depression, difficulty walking, fatigue, headache, heat temperature sensitivity, numbness, spasticity, difficulty swallowing, tremors and problems with memory and vision (http://www.msaustralia.org.au). In general, MS has four patterns: 1) relapsing-remitting (RRMS), characterised by unpredictable relapses with partial or complete periods of recovery; 2) secondary progressive (SPMS) that develops in patients who initially have RRMS but progress to greater disability later; 3) primary progressive (PPMS), characterised by slow onset and progressively worsening symptoms; and 4) relapsing progressive (RPMS), characterised by gradual worsening of disability together with relapses from the onset of disease (http://www.msaustralia.org.au).

MS mainly affect young adults and is more common in women than in men, but more severe in men than in women (Wynn et al., 1990; Duquette et al., 1992; Moldovan et al., 2008). Sexual dimorphism is also seen in some MS therapies, such as interferon-β, which is more beneficial in women (Sena et al., 2008).

Approximately $2.5 \times 10^6$ people live with MS and there is a higher prevalence of patients in temperate areas such as the United States, Canada, North Europe, New Zealand and Australia (Melcon et al., 2013; Aguirre-

Cruz et al., 2011; Grzesiuk 2011; Marrie et al., 2010; Milo et al., 2010; Poppe et al., 2008; Bhigjee et al., 2007; Flachenecker et al., 2006). Currently, approximately 21,200 Australian suffer MS and the prevalence of the disease increases 4% every year (http://www.msaustralia.org.au). Although advances in treatment are developing rapidly, no preventive or curative therapies are known and the aetiology and pathogenic mechanisms underlying the onset and development of the disease remain unclear.

### 1.2.1 Genetic and environmental factors in MS

Epidemiological, genetic and immunological studies of MS suggest that the disease results from an interaction between genetic and environmental factors. The evidence of a genetic basis for MS includes racial prevalence and ethnic differences, familial aggregation, increased concordance in monozygotic twins than dizygotic twins, HLA associations, linkage association studies, genome-wide association studies (GWAS) and epistasis studies (Bertrams et al., 1976; Ebers et al., 1993; Ebers et al., 1995; Haines et al., 1998; Giordano et al., 2002; Harbo 2004; Hansen et al., 2005; Hemminki et al., 2009; Ramagopalan et al., 2009; Lincoln et al., 2009; Kemppinen et al., 2011). Environmental contributions to MS include viral and bacterial infection, reduced ultraviolet light exposure, migration and cigarette consumption (McLeod et al., 2012; Djelilovic-Vranic et al., 2012; McLeod et al., 2011; Pekmezovic et al., 2006; Geier et al., 2005; Contini et al., 2004; Munger et al., 2004; Rosati 2001; Elian et al., 1990; Visscher et

al., 1981). In summary, MS is a complex genetic disease with multiple genetic and environmental factors contributing to risk.

The molecular and cellular mechanisms of MS are also not yet fully clarified, other than the involvement of the immune system in the development of disease. Examples of immune system involvement include: 1) increased numbers of myelin reactive T cells in MS patients (Venken et al., 2010; Raddassi et al., 2011); 2) accumulation of B cells in cerebrospinal fluid (CSF) of MS patients (Colombo et al., 2000); 3) dysfunction of Tregs in MS patients (Viglietta et al., 2004; Fransson et al., 2010; Venken et al., 2008); 4) increased activity of monocytes in peripheral blood of MS patients (Kouwenhoven 2001); 5) decrease activity of NK cells in MS patients (Lünemann et al., 2011); 6) activation of microglia in cortical lesions of MS (Kastrukoff et al., 1998); 7) high numbers of monocytes in acute MS lesions (Hammann et al., 1986); 8) high proportion of Ig-containing cells in MS plaques (Esiri 1980); 9) association of single nucleotide polimorphisms in IL2 and IL7 cytokine receptors with MS and; 10) increased expression of BAFF and CXCL13 chemokines during MS relapses in CSF (Ragheb et al., 2011; Dalla Libera et al., 2011; Wootla et al., 2011). All together, resident and infiltrating APC and lymphocytes generate a chronic inflammatory response against unclear antigens in MS.

# 1.3 Toll-like receptors

Toll-like receptors (TLRs) are part of the family of Pattern-recognition receptors (PRR) (Table 1.1) that identify Pathogen Associated Molecular Patterns (PAMP) or damage associated molecular patterns (DAMP) and trigger an immune response against invaders and/or self components (Akira et al., 2006; Sutmuller et al., 2006; Kaisho et al., 2006). Thirteen members of the TLR family have been identified. Humans express 11 members (from TLR1 to TLR11) and mice express 12 members of the TLR family (from TLR1 to TLR9 and from TLR11 to TLR13) (Takeuchi et al., 1999; Tabeta et al., 2004; Kaisho et al., 2006; Kawai et al., 2007). TLRs have been classified according their localization in two groups (Appendix 1): 1) Extracellular, which include TLR1, TLR2, TLR4, TLR5, TLR6, TLR10 and; 2) Intracellular, which contain TLR3, TLR7, TLR8, TLR9, TLR11, TLR13 (Akira et al., 2006; Kaisho et al., 2006; Govindaraj et al., 2010; Pifer et al., 2011; Oldenburg et al., 2012). The genes *Tlr7* and *Tlr8* are localized in chromosome X (Du X, et al., 2000).

TLRs respond to different components of microorganisms. For example, TLR1, TLR2 and TLR6 respond to lipopeptides; TLR4 identifies lipoglycans; TLR5, TLR11 sense proteins; and TLR3, TLR7, TLR8, TLR9 and TLR13 react against nucleic acids (Roach et al., 2005). TLRs also form heterodimers. For example, TLR2 can heterodimerize with TLR1 and TLR6 and TLR10; TLR10 can also heterodimerize with TLR1 (Takeda et al.,

2002; Quesniaux et al., 2004; Hasan et al., 2005; Matsumoto et al., 2012). Activation of TLRs leads to the production of Type I interferon and pro-inflammatory cytokines (Akira et al., 2006). Interestingly, TLRs are expressed in almost every tissue of the body, including the immune cells and CNS cells (Takeda et al. 2002; Bsibsi et al., 2002).

To summarize, TLRs respond to extracellular and intracellular stimuli from the main components of microorganisms and signal of damage, indicating that they are a key component in the generation of immune responses against invaders. Moreover, TLRs are expressed in most cells of the body, suggesting that this family of receptors can promptly initiate an immune response in every bodily tissue. The failure of tolerance that leads to autoimmunity in MS may be related to immune responses triggered by TLRs, as TLRs are expressed in resident and infiltrating cells in the CNS and trigger the activity of other genes involved in the pathogenesis of MS.

## 1.4 Toll-like receptors in Multiple Sclerosis

The immune system responds to environmental factor stimuli by the maturation of antigen presenting cells (APCs) and lymphocytes via cellular receptors such as TLRs (TLR; Weber et al., 2004; Visser, et al., 2005). TLR mediate responses to self components called DAMPs; e.g. high mobility group Figure 1.1 (HMGB1), heat shock protein 70 (HSP70), heat

shock protein 90 (HSP90), and cellular RNA), and components of microorganisms termed PAMPs; e.g., lipoproteins or lipopeptides, peptidoglycans, lipopolysaccharides (LPS), single stranded ribonucleic acid (ssRNA), double stranded ribonucleic acid (dsRNA) and CpG-DNA). TLR ligation can trigger an inflammatory immune response and cell migration (Taukeuchi et al., 1999; Hemmi et al., 2000; Alexopoulou et al., 2001; Wang et al. 2004; Takeuchi et al., 2010).

In MS, leucocytes such as monocytes, dendritic cells (DCs), NK cells, $CD4^+$ and $CD8^+$ T cells and B cells, migrate and accumulate in the central nervous system (CNS) mediating myelin destruction and neuronal cell death (Toneatto et al., 1999; Deng et al., 2003; Walder et al., 2004). Both infiltrating and resident cells of the CNS express TLRs and their expression increases in MS (Zekki et al., 2002; Lafon et al., 2006; Zhou et al., 2009). Augmentation of TLR expression in the CNS has been also associated with degenerative, neuro-protective and restorative functions (Bsibsi et al., 2006; O'Brien et al., 2008, Enevold et al., 2010).

### 1.4.1 Toll-like Receptor One in Multiple Sclerosis

TLR1 is expressed as a heterodimer with TLR2, and binds bacterial triacyl lipopeptides. It is widely expressed on APC monocytes, macrophages, DC and B cells. It is also expressed on Human NT2-N and CHP-212 neuronal

cell lines (Prehaud et al., 2005, Lafon et al., 2006, Zhou et al., 2009) and has been identified by RT PCR on microglia (Bsibsi et al., 2002). TLR1 is down regulated in peripheral blood mononuclear cells (PBMC) of MS patients and up regulated in patients treated with IFNβ (Fernald et al., 2007, Singh et al., 2007).

### 1.4.2 Toll-like Receptor Two in Multiple Sclerosis

TLR2 is expressed as both a homodimer and as a heterodimer, partnered with either TLR1 or TLR6. It is expressed on monocytes, macrophages and myeloid DC, and can bind a wide range of ligands, including lipoteichoic acid from Gram-positive bacteria, bacterial lipopeptides and glycolipids, fungal beta glucan (zymosan) and endogenous DAMPs Hyaluronan, HSP70 and HMGB1. TLR2 has been identified on CNS endothelial cells, microglia, astrocytes and oligodendrocytes (Bsibsi et al., 2002, Nagyoszi et al., 2010) and on infiltrating cells in MS. It is up regulated on PBMCs, cerebrospinal fluid (CSF) mononuclear cells and in demyelinating lesions of MS patients (Bsibsi et al., 2002, Prehaud et al., 2005, Lafon et al., 2006, Zhou et al., 2009, Sloane et al., 2010).

MS relapses have been reported during bacterial infections (Correale et al., 2006). Monocyte-derived dendritic cells from MS patients with bacterial infections express higher levels of HLA-DR and costimulators than those

from uninfected patients and drive higher production of IL12, IL17 and IFNγ (Correale and Farez, 2007). Several TLR2 ligands have been identified in the brains and CSF of MS patients. For example, the TLR2 ligand peptidoglycan, a major component of the Gram-positive bacterial cell walls, has been reported as present in the brains of MS patients within macrophage/DC-like APC that express costimulatory molecules (CD80, CD86 and CD40) and proinflammatory cytokines (IL1α, IL6, IL12, TNF and IFNγ; (Schrijver et al., 2001). High numbers of macrophages and microglia expressing the endogenous TLR2 ligand HMGB1 are also found in acute and RRMS (Andersson et al., 2008). The migration and differentiation of oligodendrocyte precursor cells (OPC) play important roles in myelin repair after inflammatory damage. MS lesions contain hyaluronan deposits that, once fragmented by the hyaluronidases expressed by OPCs, inhibit the maturation of OPC and remyelination via TLR2 ligation (Sloane et al., 2010, Back et al., 2005, Visser et al., 2005).

The TLR2 ligand zymosan can modulate the severity of MS by inducing peripheral blood DC from MS patients treated with IFNβ to secrete IL10, which suppresses IL23 and IL1β production (Sweeney et al., 2011). Similarly, surface expression of TLR2 on B cells and DC was significantly higher in helminth-infected MS patients, who had better clinical and radiological outcomes than uninfected patients. Protection was associated with regulatory T cell induction and increased TGFβ and IL10 levels. In

contrast, immunisation with *S. pneumoniae* exacerbates MS (de la Monte et al., 1986).

### 1.4.3 Toll-like Receptor Three in Multiple Sclerosis

TLR3 is expressed in DC and B cells and binds double-stranded (viral) RNA and the endogenous microtubule regulator stathmin. TLR3 ligation induces the activation of NF-κB via the adaptor TRIF to increase production of type I interferons. Cerebral endothelial cells (Nagyoszi et al., 2010), neurons, microglia, astrocytes and oligodendrocytes express TLR3 (Bsibsi et al., 2002, Farina et al., 2005, Jack et al., 2005, Lafon et al., 2006). Adult normal human astrocytes increase the production of anti-inflammatory cytokines such as IL10 and downregulate proinflammatory cytokines such as IL12 (p40) and IL23 in response to TLR3 ligation (Bsibsi et al., 2002). The endogenous TLR3 ligand stathmin was identified in astrocytes, microglia, and neurons of MS-affected human brain, and was shown by cDNA arrays to initiate the same set of neuroprotective factors as the synthetic TLR3 agonist polyinosinic:polycytidylic (poly I:C) acid (Bsibsi et al., 2010).

Association studies of *TLR3* sequence variants have failed to identify any significant association with MS (Szvetko et al., 2009, Szvetko et al., 2010).

## 1.4.4 Toll-like Receptor Four in Multiple Sclerosis

TLR4 is expressed on monocytes and macrophages, myeloid DC and T and B lymphocytes, as well as intestinal epithelium. It can bind LPS from Gram-negative bacteria, bacterial and endogenous HSP, as well as the endogenous ligands HMGB1, fibrinogen, heparan sulphate and hyaluronic acid.

TLR4 expression has been identified in cerebral endothelial cells (Nagyoszi et al., 2010) and microglia by RT-PCR (Bsibsi et al., 2002). Both TLR4 and its endogenous ligand HMGB1 are increased in expression in the CSF mononuclear cells of MS patients compared to healthy controls (Andersson et al., 2008). Association studies of functional (missense) mutations in *TLR4* (Asp299Gly and Thr399Ile) failed to identify any association with MS (Kroner et al., 2005, Reindl et al., 2003). A subsequent study of nine *TLR4* single nucleotide polymorphisms (SNP) tested for association with MS in 362 MS patients and 467 healthy controls also failed to identify any significantly associated loci (Urcelay et al., 2007).

## 1.4.5 Toll-like Receptor Five in Multiple Sclerosis

TLR5 binds bacterial flagellin and is expressed on monocytes and macrophages, some DC and intestinal epithelium; its expression has been

identified in microglia by RT-PCR (Bsibsi et al., 2002). Little has been published on any role it may play in MS.

## 1.4.6 Toll-like Receptor Six in Multiple Sclerosis

TLR6 is expressed on monocytes and macrophages, B cells and mast cells and it binds to diacyl lipopeptides from Mycoplasma. It has been identified in cerebral endothelial cells and microglia by RT-PCR (Bsibsi et al., 2002). The *TLR6* SNP *rs5743810* was associated with the development of IFNβ-specific neutralizing antibodies in men but not in women after 24 months of treatment with IFNβ (Enevold et al., 2010).

## 1.4.7 Toll-like Receptor Seven in Multiple Sclerosis

TLR7 is expressed in monocytes and macrophages, plasmacytoid DC and B cells, and binds to single-stranded (viral) RNA. TLR7 expression has been identified in microglia by RT-PCR (Bsibsi et al., 2002).

The pro-inflammatory cytokine IL17 plays a critical role in the immunopathogenesis of MS and EAE (Matusevicius et al., 1999, Lock et al., 2002, Hofstetter et al., 2005, Chen et al., 2006, Hecker et al., 2011) and its production is downregulated by type I IFNs (Guo et al., 2008; Kürtüncü

et al., 2012). *In vitro* treatment of human monocyte-derived DCs with IFNβ1a induced the expression of TLR7 and, in a TLR7-dependent fashion, the members of its downstream signalling pathway (MyD88, IRAK4, and TRAF6), but inhibited the expression of IL1R. TLR7 expression was also necessary for IFNβ1a-induced secretion of IL27 by DCs and the inhibition of IL1β and IL23. Supernatants from IFNβ1a-treated DCs inhibited Th17 differentiation of CD4 T cells, with down regulation of retinoic acid-related orphan nuclear hormone receptor C (*RORC*) and *IL17A* gene expression and IL17A secretion. Again, inhibition of IL17A was TLR7 dependent and could be blocked by TLR7 siRNA silencing (Zhang et al., 2009).

At the onset of MS, a subset of patients (11 of 61) expressed elevated mRNA levels of TLR7, together with RIG-1 and IFIH1 – an IFN expression signature potentially attributable to an overactivity of IFN-stimulated gene factor 3 (ISGF3, a complex formed by STAT1, STAT2 and IFN regulatory factor 9). This phenotype was shared by a subset of healthy control subjects (Hundeshagen et al., 2012). Patients with a relatively high IFN expression signature at baseline showed no significant modulation in the expression of the genes involved in IFN -related pathways during IFNβ therapy. In contrast, patients with a low endogenous IFN gene signature showed strong gene induction after 1 month of treatment (Hundeshagen et al., 2012).

## 1.4.8 Toll-like Receptor Eight in Multiple Sclerosis

TLR8 is expressed on monocytes and macrophages, a subset of DC and mast cells; it binds to single stranded (viral) RNA. TLR8 expression has also been identified in microglia by RT-PCR (Bsibsi et al., 2002). As is the case for TLR7, at the onset of MS, a subset of patients and healthy controls express elevated mRNA levels of TLR8, as part of an endogenous IFN gene signature (Hundeshagen et al., 2012).

## 1.4.9 Toll-like Receptor Nine in Multiple Sclerosis

TLR9 is expressed in monocytes and macrophages, plasmacytoid DC and B cells; it binds to unmethylated CpG DNA, which is present in bacteria and DNA viruses. TLR9-expressing plasmacytoid DC are present in the leptomeninges and demyelinating lesions of patients with MS. Plasmacytoid DC are a major source of type I IFN, and secrete IFNα in response to TLR9 ligation within the early endosomes (Liu, 2005) and this response is enhanced in untreated patients with MS (Balashov et al., 2010). IFNβ treatment down regulates the expression of TLR9 in MS patients with a low endogenous IFN gene signature (Hundeshagen et al., 2012) and inhibits TLR9 processing (activation) and TLR9 ligation-induced secretion of IFNα by plasmacytoid DC in all treated patients (Aung et al., 2010, Balashov et al., 2010).

Following stimulation of TLR9 by CpG-DNA (with or without stimulation via the B cell receptor and CD40), the B cells of MS patients secrete more lymphotoxin (LT), TNF and IL12, and less IL10, than those of healthy controls (Bar-Or et al., 2010, Hirotani et al., 2010). The TLR9-stimulated production of IL10 correlates with TLR9 expression levels in $CD27^+$ (memory) B cells, which is significantly reduced in MS patients (Hirotani et al., 2010).

## 1.4.10 Toll-like Receptor Ten in Multiple Sclerosis

Little is known about TLR10, its tissue distribution, its specificity or any possible role in MS.

## 1.4.11 Toll-like Receptor Eleven in Multiple Sclerosis

TLR11 is expressed on monocytes and macrophages, as well as in the liver and in kidney and urinary bladder epithelial cells. It binds profilin from the parasite *Toxoplasma gondii* and an unidentified ligand from uropathogenic *Escherichia coli* (Zhang et al., 2004; Yarovinsky et al., 2005). Little has been published on any role TLR11 may play in MS.

# 1.5 Animal Models of Multiple Sclerosis

Clinical research on MS is supported by animal models of the pathogenesis and immunoregulation of CNS autoimmunity. Commonly used models in the research of MS include:

1) Cuprizone

Cuprizone is a copper chealator that induces oligodendrocyte cell death, reversible demyelination, axonal injury and microglial activation (Kipp et al., 2009, Werner et al., 2010). It is used to model aspects of demyelination, OPG migration and activation, and remyelination.

2) Theiler's murine encephalomyelitis virus

Theiler's murine encephalomyelitis virus (TMEV) is a single stranded RNA murine cardiovirus used to infect genetically susceptible mice (e.g. SJL strain) intra-cerebrally, resulting in persistent infection and chronic demyelinating disease (Turrin, 2008). The TMEV DA strain infects astrocytes, microglia and macrophages, resulting in chronic encephalomeyelits that resembles the chronic and progressive forms of MS (Theiler, 1937, Dal Canto and Lipton 1977). The disease can also be induced in resistant mouse strains (e.g. C57BL/6 strain) by activating innate immunity with two LPS injections after TMEV infection (Turrin, 2008).

3) Experimental autoimmune encephalomyelitis

Experimental autoimmune encephalomyelitis (EAE) is a family of models of autoimmune CNS damage induced by the immunisation of experimental animals with CNS components (either an extract, purified protein or a peptide), usually in the presence of an adjuvant (Baxter, 2007).

## 1.5.1 Experimental Autoimmune Encephalomyelitis

The pathogenesis of CNS damage caused by EAE, and the specific CNS components targeted, are affected by strain and species of animal, choice of antigen (e.g. myelin oligodendrocyte glycoprotein (MOG), proteolipid protein (PLP) or myelin basic protein (MBP)) and adjuvant (e.g. Complete Freund's Adjuvant (CFA), CpG, LPS or Pertussis toxin (PTX)), and whether the disease studied is active (i.e. that occurring in the immunised individual) or passive (i.e. that occurring in the recipient of adoptively transferred T cells from the immunised individual). Various combinations can result in monophasic, relapsing–remitting or chronic EAE (Bettelli et al., 2003, Stromnes and Goverman, 2006).

As a generalization, EAE in mice is associated with an autoimmune CD4 T cell response dominated by the production of IFNγ and IL6, IL23 and IL17;

features it shares with MS (Gijbels et al., 1990; Jewtoukoff et al., 1992; Kuchroo et al., 1993; Stromnes and Goverman; 2006, Holmoy, 2007; Aranami and Yamamura, 2008; Miljković et al., 2011; Komiyama et al., 2006). Damage to the blood-brain barrier permits the influx of monocytes and macrophages, DCs, NK cells, $CD4^+$ and $CD8^+$ T cells, NKT cells and B-lymphocytes. CNS resident cells respond with astrocytic hypertrophy, microglial activation and OPG migration and activation (Sriram et al., 1982; Zamvil and Steinman, 1990; Jaskiewicz, 2004; Jack et al., 2005; von Budingen et al., 2006). The model is characterised by autoantibody production and inflammation, demyelination, axon damage and atrophy of the CNS (Karlsson et al., 2003; Bö et al., 2006; Hafler et al., 2005; Sospedra and Martin, 2005). CNS inflammation in the mouse model is predominately restricted to the spinal cord, causing an ascending flaccid paralysis that starts in the tail and progresses to the hind limbs and then the forelimbs (Stromnes and Goverman, 2006).

Responses to the antigens administered are associated with the generation of autoreactive T cells and the induction of autoantibodies (Stefferl et al., 1999). While disease can occur in the absence of adjuvant, the rate of onset, incidence and severity of disease are all enhanced by the administration of adjuvant at the time of immunisation (Baxter, 2007). CFA is the most commonly used (Billiau and Matthys, 2001). PTX is believed to facilitate leucocyte infiltration into the CNS (Linthicum et al., 1982), increase secretion of IL12 and IL6 (Hofstetter et al., 2002; Racke et al., 2005),

decrease production of IL10 and decrease differentiation of regulatory $CD4^{+}CD25^{+}$ T cells (Tregs) (Pasare and Medzhitov, 2003).

This system has significant limitations in modeling some aspects of MS, but these limitations are generally well characterised: i) The initiation is unlikely to reflect a natural correlate in MS; ii) Where a single protein or peptide has been introduced, the diversity of antigenic targets seen in MS is not reflected; iii) As disease is induced by introduction of an extrinsic antigen, the roles of MHC class I presentation and CD8 T cells in induction are completely absent, and in pathogenesis are imperfectly modelled; and iv) Not all molecular and cellular components of the immune system have identical functions in non human species.

These limitations have resulted in failure of some therapies identified in preclinical studies to exhibit significant activity in clinical trials. In particular, therapies targeted at specific HLA/peptide/TCR interactions resulting from EAE studies using defined induction antigens have performed poorly (Baxter, 2007). Nevertheless, EAE has been, and remains, a critically important model system for studying many aspects of CNS autoimmunity, such as: immune cell trafficking, CNS entry and apoptosis; roles of endogenous and infiltrating cells in CNS damage and repair; interactive cellular and cytokine networks; and the immunoregulation of

remission and relapse. To date, every effective therapy for MS has been successfully trialed in EAE.

The mouse model of EAE has a particular advantage in studying the roles of TLR in CNS autoimmunity, because it provides a well-validated platform for specific gene deletion.

## 1.6 MyD88 in Animal Models of Multiple Sclerosis

There is a consensus that EAE is dependent on MyD88 (Prinz et al., 2006; Marta et al., 2008), an adaptor protein for both TLR and cytokine signalling (Adachi et al., 1998; Zhang et al., 1999). The cytoplasmic portions of TLR receptors include a conserved motif, termed the toll/interleukin-1 receptor (TIR) domain. The TIR domains of TLRs are homologous with the respective domain of the interleukin 1 receptor (IL1R) and the cytoplasmic adaptor protein family. The TIR domains of the adaptor proteins interact with those of TLRs or IL1R and trigger the activation of downstream protein kinases and multiple transcription factors, including the NFκB family. All TLR except TLR3 signal through the adaptor protein MyD88; TLR3 signals through a MyD88-independent, TRIF-dependent pathway and

TLR4 uses both MyD88-dependent and -independent pathways (Kumar et al., 2009).

Increased expression of MyD88 mRNA was found in the $MOG_{35-55}$/CFA+PTX induced model of EAE in C57BL/6 mice (Prinz et al., 2006) and targeted gene deletion of *Myd88* reduced expression of several key inflammatory cytokines, including IL6, IL23 and IL17, and prevented EAE (Prinz et al., 2006; Marta et al., 2008). Paradoxically, MyD88-signalling in B cells induced IL10, which inhibited secretion of IL-6, IL-12, IL-23, and TNF by CpG-activated DC, suppressing inflammatory T cell responses in EAE and aiding recovery from disease (Lampropoulou et al., 2008).

### 1.6.1 Toll-like Receptor One in Animal Models of Multiple Sclerosis

Although *Tlr1* mRNA expression is increased in the $MOG_{35-55}$/CFA+PTX induced (active) model of EAE, the clinical course of the disease in the absence of TLR1 has not been studied (Prinz et al., 2006); Table 1.1).

## 1.6.2 Toll-like Receptor Two in Animal Models of Multiple Sclerosis

Increased expression of TLR2 mRNA was found in the $MOG_{35-55}$/CFA+PTX induced model of EAE in C57BL/6 mice (Prinz et al., 2006), as well as in the EAE model induced in rats immunized with recombinant rat MOG in IFA (Andersson et al., 2008) and in mice after TMEV infection (Turrin, 2008).

The effects of *Tlr2* targeted deletion on active EAE appear to be operator dependent. While Prinz et al (2006) and Hermann et al (2006) reported mice deficient of TLR2 developing a normal clinical course of active EAE, Shaw et al (2011) reported a mild decrease in the clinical scores in female mice, and Reynolds et al (2010) described a similar result in adoptive transfer recipients of $Tlr2^{-/-}$ bone marrow.

Cells differentiated in the presence of the TLR2 ligand Pam3Cys showed a ~50% increase in the proportion expressing IL17, while $Tlr2^{-/-}$ T cells did not exhibit obvious differences in Th17 polarization in the absence of exogenous TLR2 ligands compared to WT controls; the number of IL-17-producing $Tlr2^{-/-}$ cells was also unaffected when stimulated with Pam3Cys (Reynolds et al., 2010).

Exacerbation of MS after active immunisation with a pneumococcal vaccine has been reported by de la Monte et al., (1986) and Herrmann et al., (2006) confirmed a similar effect of *Streptococcus pneumonie* infection on EAE; this effect was TLR2 dependent. Similarly, phosphorylated dihydroceramides from the common human oral bacterium *Porphyromonas gingivalis* induced dendritic cell IL6 production, decreased spinal cord $Foxp3^+$ T cells and enhanced EAE in a TLR2-dependent manner (Nichols et al., 2009; Nichols et al., 2011).

Visser et al (Visser et al., 2005; Visser et al., 2006) hypothesized that peptidoglycan can contribute to disease development and progression in MS and EAE in the absence of infection or bacterial replication. They found that bacterial peptidoglycan was able to be substituted for heat killed Mycobacteria tuberculosis in CFA in the induction of active EAE (Visser et al., 2005). They subsequently reported persistence of TLR ligands in the CNS in MS patients as well as in two nonhuman primate models of EAE, associated with reduced local expression of two major PGN-degrading enzymes, lysozyme and N-acetylmuramyl-l-alanine amidase (Visser et al., 2006). As peptidoglycan can be sensed by cytoplasmic PAMP receptors (NOD1 and NOD2) in addition to TLR2, Shaw et al (2011) compared induction of $MOG_{35-55}$/CFA+PTX EAE in female *Tlr2*$^{-/-}$, *Nod1*$^{-/-}$, *Nod2*$^{-/-}$, and *Ripk2*$^{-/-}$ mice. *Tlr2*$^{-/-}$ mice decrease the severity of EAE while *Nod1*$^{-/-}$,

*Nod2*$^{-/-}$, and *Ripk2*$^{-/-}$ mice showed arguably greater protection (Shaw et al., 2011). The authors make a good case for RIP2 at least contributing to activation of CNS-infiltrating dendritic cells, and thereby EAE, in WT/*Ripk2*$^{-/-}$ bone marrow chimeric mice (Shaw et al., 2011).

As for MS, DAMPs that are TLR2 ligands have also been associated with EAE. For example, HMGB1 has been identified in active EAE lesions and its levels correlate with active inflammation (Andersson et al., 2008). Increased serum concentrations of 15-a-hydroxicholestene (15-HC) have also been identified in mice with secondary progressive EAE and 15-HC activated microglia, macrophages and astrocytes, and enhanced expression of TNF, iNOS and CCL2 mRNA in CNS-infiltrating monocytes/macrophages, through a pathway involving TLR2 (Farez et al., 2009).

### 1.6.3 Toll-like Receptor Three in Animal Models of Multiple Sclerosis

Although increased expression of TLR3 was not found in the $MOG_{35-55}$/CFA+PTX induced model of EAE in C57BL/6 mice (Prinz et al., 2006), it was upregulated in mice susceptible to demyelinating disease (SJL strain) after TMEV infection, but not in resistant mice (Turrin, 2008).

Repeated i.p. injections of the TLR3 ligand poly I:C (a double-stranded RNA analog) induced expression of endogenous IFNβ and the peripheral induction of the CC chemokine CCL2, and strongly inhibited EAE induced in SJL/J mice by immunisation of PLP peptide 139-151 in CFA (Touil et al., 2006).

### 1.6.4 Toll-like Receptor Four in Animal Models of Multiple Sclerosis

Increased expression of *Tlr4* mRNA was found in the $MOG_{35-55}$/CFA+PTX induced model of EAE in C57BL/6 mice (Prinz et al., 2006), as well as in the Dark Agouti rat EAE model with MOG emulsified in incomplete Freund's adjuvant (Andersson et al., 2008).

Conflicting outcomes have been published in studies of EAE susceptibility in mice deficient in TLR4. C57BL/6.*Tlr4* deficient mice showed increased *Il6* and *Il23* mRNA expression by myeloid DC, an increased proportion of T cells producing IL17 and increased EAE clinical scores following immunisation with recombinant rat MOG (Marta et al., 2008). In contrast, in the $MOG_{35-55}$ peptide-induced model, the severity of disease was unaffected by targeted deletion of *Tlr4* (Kerfoot et al., 2004), unless a

marginal dose of *M. tuberculosis* was used in the inoculum, in which case the severity of disease was sometimes reduced compared to C57BL/6 in a mechanism that appeared to involve pertussis toxin (PTX) signalling through TLR4 (Kerfoot et al., 2004). In a model of active EAE induced in C57BL/6. *Rag1*$^{-/-}$ hosts reconstituted by CD4 T cell adoptive transfer from either WT or *Tlr4*$^{-/-}$ mice, the prevalence of EAE induced by $MOG_{35-55}$/CFA+PTX was halved in the recipients of *Tlr4*$^{-/-}$ T cells (Reynolds et al., 2012). The protected mice had reduced numbers of infiltrating cells and consequently reductions in *Il17*, *Ifng*, *Ccr6* and *Ccl2* transcripts in total CNS mRNA analyses.

The TLR4 ligand poly-g-glutamic acid from *Bacillus subtilis* signals naive $CD4^+$ T cells via TLR4 and MyD88 to induce TGFβ and upregulate FoxP3 expression, suppressing EAE in the C57BL/6 $MOG_{35-55}$/CFA+PTX model (Lee et al., 2012).

Complement C5a synergizes with TLR4 ligation by LPS to induce APC to produce serum factors, including IL6, that drive Th17-cell differentiation (Fang et al., 2009). In the passive (adoptive transfer) model of $MOG_{38-50}$/CFA, if the T cells to be adoptively transferred were first re-stimulated *in vitro* in the presence of serum from mice treated with C5a in addition to LPS, a greater severity of EAE resulted (Fang et al., 2009).

Different models of EAE reproduce various aspects of EAE but no single model replicates MS. The review of literature about the role of TLR4 in EAE is difficult to interpret because EAE is influenced by auto-antigens, adjuvants, doses and genetic background. However, it is possible to deduce that T cells require of TLR4 signalling to promote or regulate EAE.

### 1.6.5 Toll-like Receptor Five in Animal Models of Multiple Sclerosis

Little is known about the role of TLR5 in animal models of MS. TLR5 was not increased in expression in the $MOG_{35-55}$/CFA+PTX induced model of EAE in C57BL/6 mice (Prinz et al., 2006).

### 1.6.6 Toll-like Receptor Six in Animal Models of Multiple Sclerosis

Increased expression of *Tlr6* mRNA was found in the $MOG_{35-55}$/CFA+PTX induced model of EAE in C57BL/6 mice (Prinz et al., 2006), as well as in mice susceptible to demyelinating disease (SJL strain) after TMEV infection, but not in resistant mice (Turrin, 2008). Targeted deletion of *Tlr6* did not affect the severity of EAE in C57BL/6 mice (Prinz et al., 2006; Marta et al., 2008).

### 1.6.7 Toll-like Receptor Seven in Animal Models of Multiple Sclerosis

Increased expression of *Tlr7* mRNA was found in the $MOG_{35-55}$/CFA+PTX induced model of EAE in C57BL/6 mice (Prinz et al., 2006) as well as in mice after TMEV infection (Turrin, 2008).

Repeated low dose administration of the synthetic TLR7 agonist 9-benzyl-8-hydroxy-2-(2-methoxyethoxy) adenine upregulated expression of the TLR signal inhibitors IRAK-M, and SHIP-1, and induced hyporesponsiveness to TLR2, -7 and -9, resulting in reduced EAE clinical scores in the $MOG_{35-55}$/CFA+PTX induced model (Hayashi et al., 2009). The TLR7 agonist Imiquimod, administered on days one, three and five post administration of $MOG_{35-55}$/CFA+PTX also delayed disease onset and reduced EAE clinical scores; the treatment was associated with the endogenous production of IFNβ (O'Brien et al., 2010).

## 1.6.8 Toll-like Receptor Eight in Animal Models of Multiple Sclerosis

Increased expression of *Tlr8* mRNA was found in the $MOG_{35-55}$/CFA+PTX induced model of EAE in C57BL/6 mice (Prinz et al., 2006) as well as in mice susceptible to demyelinating disease (SJL strain) after TMEV infection, but not in resistant mice (Turrin, 2008). Intra-axonal accumulations of TLR8 protein were confirmed for the $MOG_{35-55}$/CFA+PTX model (Soulika et al., 2009). Little else is known about the potential role of TLR8 in animal models of MS.

## 1.6.9 Toll-like Receptor Nine in Animal Models of Multiple Sclerosis

Increased expression of *Tlr9* mRNA was found in the $MOG_{35-55}$/CFA+PTX induced model of EAE in C57BL/6 mice (Prinz et al., 2006), as well as in mice after TMEV infection (Turrin, 2008).

Whereas C57BL/6.*Tlr9*$^{-/-}$ mice showed a decreased severity of disease following EAE induction with $MOG_{35-55}$ (Prinz et al., 2006), disease was exacerbated in TLR9-deficient mice treated with recombinant rat MOG (Marta et al., 2008). Lampropoulou et al., (2008) examined EAE susceptibility of mice bearing TLR9-deficiency on only B cells by using a

mixed bone marrow chimeric system with μMT mice (carrying a gene deletion of the μ heavy chain) and *Tlr9*$^{-/-}$*Cd40*$^{-/-}$ mice as donors and WT mice as recipients. The onset and recovery from EAE was indistinguishable from that of control mice (Lampropoulou et al., 2008).

Consistent with TLR9 playing a role in EAE pathogenesis, TLR9 ligation with CpG DNA was able to induce EAE. Mice that expressed the transgenic TCR 5B6, which is specific for the PLP peptide 139-151, on the EAE-resistant (EAE-resistant) B10.S background rarely developed spontaneous EAE, in contrast to 5B6 transgenic mice on the EAE-susceptible SJL background. The relative resistance to spontaneous EAE in transgenic B10.S mice appeared to be due to a lower activation state of the APCs. When APCs in 5B6 transgenic B10.S mice were activated by TLR9 ligation with CpG DNA, T cell tolerance was broken, resulting in encephalomyelitis (Walder et al., 2004). Similar results were obtained in an analogous, but non-transgenic system: Adult SJL mice injected i.p. with a PLP peptide emulsified in IFA fail to mount proliferative or cytokine responses and are protected from EAE upon subsequent challenge with the PLP/CFA. Again, the tolerized PLP-specific lymph node cells regained the ability to transfer EAE once reactivated *in vitro* in the presence of CpG oligonucleotides (Ichikawa et al., 2002). Finally, a combination of TLR4 and TLR9 agonists (CpG-ODN and LPS) was able to replace mycobacteria in Freund's

adjuvant to induce EAE in Lewis rats immunized with MBP peptide 68-86 (Wolf et al., 2007).

### 1.6.10 Toll-like Receptors Eleven, Twelve and Thirteen in Animal Models of Multiple Sclerosis

Nothing has been published on the potential roles of these TLR in animal models of MS.

To summarize, TLRs play an important role in CNS autoimmune inflammation; however, research about the role of TLRs has been done using different protocols for EAE induction and different environments, which seem to lead to conflicting results and unclear interpretation. It is necessary to clarify confronting data by using a single protocol in the same environment. Moreover, it is also important to know the phenotype of EAE in the absence of TLRs in both male and females in order to establish clearer data for the development of more specific therapies.

## 1.7 Natural Killer T cells in Multiple Sclerosis and Experimental Autoimmune Encephalomyelitis

Natural Killer T cells (NKT cells) are a heterogeneous group of T cells identified in 1987 that originate in the thymus (Fowlkes et al., 1987; Pellicci et al., 2002). NKT cells express common markers from both T cells and NK cells such as CD161 (NK1.1), CD122 (IL-2Rβ) and αβTCR (Godfrey et al., 2000; MacDonald HR. 2002).

Recognition of antigens by NKT cells is restricted by the CD1d molecule (Godfrey et al., 2000; MacDonald 2002). NKT cells are activated by exogenous and endogenous ligands such as α-galatosylceramide (α-GalCer), α-glycuronsyl ceramides, α-galactosyl diacylglycerol, phospatidylinositol mannosedes (PIM), lipophosphoglycans and isoglobotrihexosylceramide (iGb3) (Kinjo et al., 2005; Speak et al., 2008; and Muindi et al., 2010).

## 1.7.1 NKT cells classification

In general two different classification systems group NKT cells:

1) According to the NKT cells' surface expression and function, humans have 3 subsets of NKT cells: a) $CD4^{+}CD8^{-}$, b) $CD4^{-}CD8^{-}$ and c) $CD4^{-}CD8^{+}$) and mice have 2 subsets of NKT cells: a) $CD4^{+}CD8^{-}$ and b) $CD4^{-}CD8^{-}$) (review in Berzins et al., 2011).

2) According to the NKT cells' reactivity to the Glycolipid α-GalCer, the CD1d-dependent and the αTCR chains, NKT cells have 2 subsets: a) Type I NKT cells or iNKT cells (invariant $V\alpha24^{+}J\alpha18$ in humans and $V\alpha14^{+}J\alpha18$ in mice) which react to α-GalCer in a CD1d dependent manner and are limited to αTCR. This group includes a $CD4^{+}$ and a $CD4^{-}CD8^{-}$ populations; b) Type II NKT cells which do not react to α-GalCer, are CD1d dependent and have diverse αTCR (Seino et al., 2005).

NKT cells produce large amounts of IL4 after activation (Bendelac et al., 1997). Different subsets of NKT cells secrete IL2, IL3, IL5, IL13, IL17, IL21, GM-CSF and/or osteopontin after activation and have cytotoxic activity (Godfrey et al., 2004; Coquet et al., 2008; Coquet et al., 2007; Jiang et al 2005; review in Berzins et al., 2011). Cytokines production by NKT cells plays a key role in autoimmunity. IL4 drives the differentiation and

growth of Th2 cells and regulates autoimmunity and; IL17 drives the differenciation and growth of Th17 cells, which are associated with autoimmunity damage.

Because NKT cells are active cells in autoimmunity, recognize exogenous and endogenous ligands and secrete the pro-inflammatory cytokines found in MS and EAE, it is possible that NKT cells play a role in CNS autoimmunity in both diseases.

## 1.7.2 NKT cells in Multiple Sclerosis

Altered numbers of NKT cells are seen in MS patients. For example, the number and diversity of NKT cells expressing the Vα24 marker is reduced in blood of MS patients including patients in remission (Illés et al. 2000; Démoulins et al. 2003; Araki et al. 2003). Opposing these findings, studies have reported that NKT cells expressing the invariant Vα24-Jα18$^{+}$ T-cell receptor are increased in peripheral blood of MS patients (O'Keeffe et al., 2008). These studies indicate that NKT cell numbers may correlate with the immunopathology of MS; however, the precise role of NKT cells in the disease remains unclear.

Cytokine production by NKT cells is also altered in MS patients, for example $CD4^-CD8^-V\alpha24J\alpha Q$ T cells from peripheral blood of patients with RR-MS produce less IL4 but not IFNγ compared with $CD4^-CD8^-V\alpha24J\alpha Q$ T cells from patients with progressive MS or healthy controls (Gigli et al., 2007). Moreover, analysis of blood of MS patients indicates that MS treatment affects NKT cell numbers and function. For example, type 1 interferon beta therapy increased the percentage of $Valpha24^+$ NKT cells through myeloid dendritic cell maturation (Gigli et al., 2007). After type IFNβ therapy, NKT cells increased the secretion of IL4 (Gigli et al., 2007). Natalizumab, a monoclonal antibody therapy for RRMS that blocks the entry of leucocytes into the CNS by binding to the $\alpha_4$ subunit of a very-late activation antigen-4 (VLA-4), has a higher binding to NKT cells and NK cells than to $CD3^+$ T cells. In addition, natalizumab, decreases levels of beta 1 integrin surface expression on NKT cells and T cells, B cells and NK cells (Harrer et al., 2011; Harrer 2012). These studies indicate that NKT cells migrate into the CNS and play an important role in cell signalling, regulation of cell cycle and regulation of inflammation in MS.

Ligands for NKT cells are extensively found in myelin. The dry weight of myelin comprises approximately 73-81% lipids and 20-25% protein (Deber et al., 1991; Aggarwal et al., 2011). The most abundant lipids in myelin are glycolipids such as galactocerebrocide (GalC) and its sulfated version sulfatide and phospholipids (Aggarwal et al., 2011). This suggests that

APCs can present glycolipids from the myelin to NKT cells during local inflammation in the CNS.

### 1.7.3 NKT cells in Experimental Autoimmune Encephalomyelitis

Stimulation of NKT cells decreases the severity of EAE by the production of pathogenic or protective cytokines. For example, the severity of EAE is increased in IL4 knockout mice and decreased in IFN-γ knockout mice when stimulated by alpha-GC (Pál et al., 2001). However, controversial results have been found during immunisation with NKT cells ligands such as sulfatide and alpha-GC. Immunisation with sulfatide at the same time as EAE induction protects mice from developing EAE (Jahng et al., 2004). Pre-immunisation of mice with α-Galcer protects C57BL/6 and B10PL mice against EAE (Furlan et al., 2003; Jahng et al., 2001); however, immunisation with α-Galcer at the same time as EAE induction protects C57BL/6 mice, while in B10PL mice the disease is exacerbated (Jahng et al., 2001). Other studies have found no effect or a minimal effect in the development of EAE when mice are immunized with α-Galcer (Pál et al., 2001).

A potential association has been found recently between NKT cells and vitamin D, which could be related to the initiation and progression of both MS and EAE. NKT cells require vitamin D for development and function, and vitamin D is associated with the onset and development of EAE and MS (Cantorna et al 2012).

Overall, the role of NKT cells in the development of both EAE and MS needs to be clarified. The reduced number of NKT cells in MS patients could explain the lack of antinflammatory properties by regulatory cytokines such as IL4 and IL10 produced by NKT cells. However, NKT cells also produced IFNγ and IL17, which increase the severity of EAE. Whether NKT cells are associated with MS and EAE is being debated.

## 1.8 Summary and project aims

Although research into MS has been accelerating, particularly in recent years due to the constant increase in the incidence and prevalence of the disease, the interaction between genetics and environmental factors remain undiscovered. The deeper understanding of the interactions of these factors is required for better diagnostics, and improvement of therapies for the prevention and cure of MS.

In this study, Toll-like receptors and NKT cells were proposed as potential mechanisms for the development of CNS-autoimmune inflammation seen in MS. The roles of TLRs and NKT cells in gene/environment interactions can be studied in the EAE model because it provides a well-validated platform for specific gene and environmental manipulation. The mouse model of MS used in these studies was $MOG_{35-55}$/CFA+PTX induced EAE.

As mentioned before and summarized in Table 1.1, the absence of TLR2, TLR4 and TLR9 in EAE has generated controversial results. The lack of TLR1, TLR3, TLR5, TLR7, TLR8 and TLR10-TLR13 has not been studied in EAE. TLR6 has been ruled out to contribute to EAE. The previous studies that contributed to find the role of TLRs in EAE used different protocols for EAE induction, different environments and the sex of the animals is not declare in some findings (Table 1.1). It is unclear whether the conflicts in results stem from variation in the sex, methods of induction or environment. The first hypothesis of this study is that discrepancies in the studies of the role of TLRs in EAE can be partially solved by comparing the disease in male and female mice using a single model of EAE and the same environment. To test this hypothesis, the roles of TLR1, TLR2, TLR4, TLR6, TLR9, TLR2/9, TLR4/9 and MyD88 were examined in the mouse model $MOG_{35-55}$/CFA+PTX induced EAE at the Comparative Genomics Centre.

As NOD/Lt mice, the most common animal model of T1D, are also susceptible to EAE, $MOG_{35-55}$/CFA+PTX induced EAE was used to study the roles of TLR1, TLR2, TLR4, TLR6 and TLR9 in this strain in order to dissect the inter-relationships between organ-specific autoimmune diseases. Unlike C57BL/6.*Tlr2*$^{-/-}$ mice, NOD.*Tlr2*$^{-/-}$ mice did not decrease the severity of EAE. To test the hypothesis that insulitis associated with T1D development in some way compensated for the lack of TLR2 signalling in NOD mice, the role of TLR2 was examined in NOD.*H2*$^{b}$ and NOD.*H2*$^{b}$.*Tlr2*$^{-/-}$ mice.

Finally, most of the previous studies on the role of NKT cells in EAE have been performed using NKT cell ligands and little is know about the contribution of NKT cell numbers to EAE. It was hypothesized that different numbers of NKT cells alter the phenotype of EAE. To test this hypothesis the clinical course of $MOG_{35-55}$/CFA+PTX induced EAE was examined in mice with different numbers of NKT cells.

Table 1.1 Toll-like receptors in EAE.

| Mutation | Strain mouse | Sex | Auto antigen | Adjuvant | Enhacement | Age of induction | *Result | Reference |
|---|---|---|---|---|---|---|---|---|
| TLR1 | Non known | Non known | Non known | Non known | Non known | Non known | Non known | Non known |
| TLR2 | C57BL/6 | Female | $MOG_{35–55}$ | CFA | PTX | 6-12 weeks | Susceptible | Prinz et al., 2006 |
| | C57BL/6 | Female | $MOG_{35–55}$ | CFA | PTX | 6-8 weeks | Susceptible | Hermann et al., 2006 |
| | C57BL/6 | No specified | $MOG_{35–55}$ | CFA | PTX | 6-8 weeks | No mentioned | Chen et al., 2009 |
| | C57BL/6 | Female | $MOG_{35–55}$ | CFA | PTX | 7-7 weeks | Resistant | Shaw et al., 2011 |
| TLR3 | Non known | Non known | Non known | Non known | Non known | Non known | Non known | Non known |
| TLR4 | C57BL/6 | Female | Recombinant rat $MOG_{190-250}$ protein | CFA | PTX | 8-12 weeks<br>9 weeks | Exacerbates | Marta et al., 2008 |
| | C57BL/10ScCr | No specified | $MOG_{35–55}$ | CFA | PTX | 9 weeks | Susceptible | Kerfoot et al., 2004 |
| | C57BL/10ScCr | No specified | $MOG_{35–55}$ | CFA | PTX | | Resistant | Kerfoot et al., 2004 |
| | C57BL/10ScCr | No specified | $MOG_{35–55}$ | CFA | No enhacement | 9 weeks | Resistant | Kerfoot et al., 2004 |

Continue **Table 1.1** Toll-like receptors in EAE

| Mutation | Strain mouse | Sex | Autoantigen | Adjuvant | Enhacement | Age of induction | *Result | Reference |
|---|---|---|---|---|---|---|---|---|
| TLR5 | Non known | Non known | Non known | Non known | Non known | Non known | Non known | Non known |
| TLR6 | C57BL/6 | Female | Recombinant rat $MOG_{190-250}$ protein | CFA | PTX | 8-12 weeks | Susceptible | Marta et al., 2008 |
| TLR7 | Non known | Non known | Non known | Non known | Non known | Non known | Non known | Non known |
| TLR8 | Non known | Non known | Non known | Non known | Non known | Non known | Non known | Non known |
| TLR9 | C57BL/6<br>C57BL/6 | Female<br>Female | Recombinant rat $MOG_{190-250}$ protein<br>$MOG_{35–55}$ | CFA<br>CFA | PTX<br>PTX | 8-12 weeks<br>6-12 weeks | Exacerbates<br>Resistant | Marta , et al., 2008<br>Prinz et al., 2006 |
| TLR10-TLR13 | Non known | Non known | Non known | Non known | Non known | Non known | Non known | Non known |

Continue **Table 1.1** Toll-like receptors in EAE

| Mutation | Strain mouse | Sex | Autoantigen | Adjuvant | Enhacement | Age of induction | *Result | Reference |
|---|---|---|---|---|---|---|---|---|
| MyD88 | C57BL/6 | Female | $MOG_{35–55}$ | CFA | PTX | 6-12 weeks | Complete resistant | Prinz et al., 2006 |
| MyD88 | C57BL/6<br>C57BL/6 | Female<br>No specified | Recombinant rat $MOG_{190-250}$ protein<br>$MOG_{35–55}$ | CFA<br>CFA | PTX<br>PTX | 8-12 weeks<br>No specified | Complete resistant<br>Complete resistant | Marta et al., 2008<br>Lampropoulou et al., 2008 |
| TLR2/4 | C57BL/6 | No specified | $MOG_{35–55}$ | CFA | PTX | No specified | Susceptible | Lampropoulou et al., 2008 |
| IRAK1 | C57BL/6 | No specified | $MOG_{35–55}$ | CFA | PTX | No specified | Susceptible | Deng et al., 2003 |
| IRAK1 | C57BL/6 | No specified | MBP Ac1-11 | CFA | No enhacement | 7-10 weeks | Complete resistant (A-EAE)<br>Susceptible (P-EAE) | Hansen et al., 2006 |

Continue **Table 1.1** Toll-like receptors in EAE

| Mutation | Strain mouse | Sex | Autoantigen | Adjuvant | Enhacement | Age of induction | *Result | Reference |
|---|---|---|---|---|---|---|---|---|
| TRIFLps2/Lps2 | C57BL/6 | No specified | $MOG_{35–55}$ | CFA | PTX | No specified | Exacerbates | Guo et al., 2008 |
| | | | | | | | | |
| NF-kappa B1 | C57BL/6 | No specified | $MOG_{38–50}$ | CFA | PTX | 4-6 weeks | Resistant | Hilliard et al., 1999 |

*Susceptible means that there is not difference between knockout mice and the control group.

*Exacerbates means that knockout mice are more susceptible than the control group.

*Resistant means that knockout mice decrease significantly the disease when compared with the control group.

*Complete resistant means that knockout mice do not develop clinical signs of EAE.

# CHAPTER 2

# CHAPTER 2

# MATERIALS AND METHODS

## 2.1 Mice

### 2.1.1 Sources of C57BL/6 and NOD/Lt mice

C57BL/6 and NOD/Lt mice were bought from The Jackson Laboratory (Bau Harbor, Maine, USA) and were bred and housed at The Immunogenetics Research Facility, James Cook University.

### 2.1.2 Sources and generation of knockout, congenic and transgenic mice

#### 2.1.2.1 Knockout mice

Dr Shizuo Akira from Osaka University (Osaka, Japan) kindly provided the C57BL/6-*Tlr* knockout mice (Takeuchi et al., 1999; Hemmi et al., 2000; Adachi et al., 1998; Hoshino et al., 1999; Takeuchi et al., 2001; Takeuchi et al., 2002). C57BL/6.*Tlr*$^{-/-}$ mice were originally generated on the 129/SvJ background and backcrossed to B6. Erick Biros and Shahead Chowdly helped to found the C57BL/6.*Tlr*$^{-/-}$ and NOD.*Tlr*$^{-/-}$ mice by backcrossing and genotyping the mice in the Comparative Genomics Centre. C57BL/6.*Tlr1*$^{-/-}$

and C57BL/6.*Tlr6*$^{-/-}$ mice had been backcrossed to C57BL/6 for six generations on arrival. They were subsequently further backcrossed to C57BL/6 mice for a total of 10 generations before intercrossing to generate homozygous knockout mice. C57BL/6.*Tlr2*$^{-/-}$, C57BL/6.*Tlr4*$^{-/-}$, C57BL/6.*Tlr9*$^{-/-}$ and C57BL/6.*MyD88*$^{-/}$ mice had been backcrossed to C57BL/6 mice for 10 generations before intercrossing to generate homozygous mutants. Double-knockout mice (C57BL/6.*Tlr2*$^{-/-}$*Tlr9*$^{-/-}$ and C57BL/6.*Tlr4*$^{-/-}$*Tlr9*$^{-/-}$) were generated by crossing single knockout mice, intercrossing the F1 progenies and genotyping a selection of homozygous mutants as founders for the new line (Adachi et al., 1998; Hoshino et al., 1999; Takeuchi et al., 1999; Hemmi et al., 2000; Takeuchi et al., 2001; Takeuchi et al., 2002).

NOD/Lt mice were crossed to C57BL/6.*Tlr1*$^{-/-}$, C57BL/6.*Tlr2*$^{-/-}$, C57BL/6.*Tlr4*$^{-/-}$, C57BL/6.*Tlr6*$^{-/-}$, C57BL/6.*Tlr9*$^{-/-}$ and C57BL/6.*MyD88*$^{-/-}$ mice and the progeny backcrossed to NOD/Lt mice for 10 more generations. At each generation, pups were genotyped by PCR tail DNA to select heterozygous mutants. The inbred lines were founded by intercrossing the F1 progenies and genotyping for selection of homozygous mutants.

The Queensland Institute of Medical Research (QIMR) (Brisbane QLD, Australia) provided C57BL/6.*Cd1d*$^{-/-}$ mice. C57BL/6.*Cd1d*$^{-/-}$ mice were backcrossed to C57BL/6 (Appendix 2). Blood samples from the F1

progenies were analyzed by Flow Cytometry to find the homozygous knockout (KO) mice using anti-mouse CD1d PE antibody (clone 1B1) (Appendix 8) and anti-mouse TCRβ PerCP-Cy5.5 (clone H57-597) (Appendix 8).

NOD.*Cd1d*$^{-/-}$ mice were bought from The Jackson Laboratory.

### 2.1.2.2 Congenic and transgenic mice

Alan G Baxter established the NOD.*Nkrp1b* mice (Poulton, et al., 2001). Julie M Fletcher crossed NOD.*Nkrp1b* mice with NOD.*Cd1d*$^{-/-}$ mice in order to establish NOD.*Nkrp1b*.*Cd1d*$^{-/-}$ mice in the Comparative Genomics Centre. Margaret Jordan and Christine Hawke established the NOD.*H2*$^{d}$ mice in the Comparative Genomics Centre. NOD.*Idd13* were bought from The Jackson Laboratory. Tim Butler and Tatiana Tsoutsman established the NOD.*Nkt1*, NOD.*Nkt2a*, NOD.*Nkt2b* and NOD.*Nkt2e* mice in the Comparative Genomics Centre. Klaus Griewank generated the construct for TCR V alpha14 transgenic mice in the Albert Bendelac' Laboratory at Howard Hughes Medical Institute, Committee on Immunology, Deparment of Pathology, University of Chicago, USA.

NOD.*H2*$^{b}$ mice were crossed to NOD.*Tlr2*$^{-/-}$ mice. The F1 progeny were intercrossed and genotyped by PCR tail DNA to generate NOD.*H2*$^{b}$.*Tlr2*$^{-/-}$ homozygous mice (Appendix 3).

## 2.2 Mouse identification and housing

Mice aged 7-14 weeks were used in the research studies. Every mouse was ear-clipped for identification (Appendix 4). Mice were kept under specific pathogen-free conditions in the Immunogenetics Research Facility at James Cook University. The studies were reviewed and approved by the James Cook University Animal Care and Ethics Committee.

## 2.3 Genotyping

### 2.3.1 DNA extraction

Mouse-tail tips at around 8 millimeters were cut to extract DNA. Every tail tip was digested in 420μL of Tissue digest (QIAGEN Sciences, Maryland, USA) and 10μL of Digest enzyme (QIAGEN Sciences, Maryland, USA) overnight at 56°C. Samples were vortexed and then centrifuged for 5 minutes at 2500 rcf. The amount of 220μL of the digested tails was transferred to 96 well storage plates.

DNA extraction was done on a CAS-1810 X-TractorGene (Corbett Robotics) using the DX Reagent Pack (QIAGEN Sciences) and following a method developed in the Baxter laboratory at the Comparative Genomics Centre. After extraction, 2μL of extracted DNA were used to measure the DNA concentration in a nonodrop.

### 2.3.2 Polymerase chain reaction (PCR) and polyacrylamide gel electrophoresis (PAGE)

PCR and PAGE were used to identify the targeting constructs. PCR was done in 20μL to 25μL volume containing $H_2O$, GoTaq Green Master mix (Promega, Wisconsin, USA) (2x buffer), the specific primers (Appendix 5 and 6) and DNA. Samples were run in the Thermal cycler following the thermocycling protocols shown in Appendix 7. Samples were stored at 4°C until PAGE was performed.

The amount of 5μL to 10μL per sample was analyzed by PAGE run for 30 minutes to distinguish amplified DNA fragments. Fragment sizes were determined by separation of a 100 bp ladder (Invitrogen; Victoria, Australia) run in parallel.

### 2.3.3 Processing and staining of cells from blood for Flow Cytometry

The amount of 100μL of mouse blood was collected by retro-orbital venipuncture with plastic clad micro hematocrit tubes (Becton Dickinson; Pennsylvania, USA). Peripheral blood was stained with anti-CD1d (clone IB1, eBiosciences, California, USA) and anti-TCRβ (clone H57-597, BD Biosciences, California, USA) (Appendix 8) antibodies for 30 minutes at room temperature in the dark. After incubation, red cells were lysed with 2mL 1x RBC Lysis Buffer (Sigma, Ayrshire, UK) and washed with 2 ml of MACS buffer (Appendix 9) and resuspended in MACS buffer (Appendix 9) to be analyzed by Flow Cytometry.

## 2.4 Induction of EAE

### 2.4.1 Mouse immunisation for active $MOG_{35-55}$-induced EAE

Mice were injected subcutaneously (s.c.) at day 0 and day 7 in the inguinal and flank regions with 200 μg of $MOG_{35-55}$ peptide (Auspep; Victoria, Australia) in PBS (Invitrogen; Victoria, Australia) emulsified in an equal volume (1:1) of Complete Freud's Adjuvant (CFA, containing 5mg/ml of heat-killed *Mycobacteria tuberculosis* (Difco laboratories; Michigan and

Missouri, USA). Each mouse also received an intra-peritoneal (i.p.) injection containing 250ng of PTX (List biological laboratories; California, USA) at days 0 and 2 (Prinz et al., 2006).

## 2.4.2 Mouse immunisation for passive $MOG_{35-55}$-induced EAE

### 2.4.2.1 Donor immunisation and organ collection

Donor mice were injected subcutaneously at day 0 in the inguinal regions and flanks with 200 μg of $MOG_{35-55}$ peptide (Auspep; Victoria, Australia) in PBS (Invitrogen; Victoria, Australia) emulsified in an equal volume (1:1) of Complete Freund's Adjuvant (CFA; containing 5mg/ml of heat-killed *Mycobacteria tuberculosis* (Difco laboratories; Michigan and Missouri, USA). An intra-peritoneal injection of 250ng of PTX (List biological laboratories; California, USA) was also administrated at days 0 and 2.

Mice were euthanized by $CO_2$ asphyxiation at day 10 to 11 after immunisation. The spleens and inguinal and axillary lymph nodes from donor mice were collected in HBSS (Invitrogen; Victoria, Australia) containing 100U/ml of penicillin/streptomycin (Invitrogen; Victoria, Australia) to prevent bacteria growth.

### 2.4.2.2 Single cell suspension and cell culture

Spleen and lymph nodes were placed in a petri dish and mashed between two microscope slides with HBSS (Invitrogen; Victoria, Australia) containing 100U/ml of penicillin/streptomycin (Invitrogen; Victoria, Australia). Red cells from the spleens were lysed with Red Blood Cell lysing buffer (Sigma-Aldrich; Ayrshire, UK). Cells were washed and resuspended in a culture medium (Invitrogen; Victoria, Australia) supplemented with 10% (v/v) FCS, 2 mM L-glutamine, 100 U/ml penicillin, 100 μg/ml streptomycin sulfate, 1 mM sodium pyruvate, and 2 μM 2-ME (Invitrogen; Victoria, Australia) at a concentration of 5 X $10^6$ cells/ml.

Cells were stimulated with 50μg/ml $MOG_{35-55}$ peptide (Auspep; Victoria, Australia), 10ng/ml IL23 (eBioscience; California, USA), 10ng/ml IL6 (Sigma; Missouri, USA) and 5ng/ml TGF-β (eBioscience; California, USA) and cultured at 37°C and 5% $CO_2$ in culture medium (Appendix 9). Cells were harvested at day 3 after cell culture. Cells adhering at the bottom of the flask were removed with a cell scraper. Dead cells were removed using Histopaque 1083 (Sigma; Missouri, USA) and centrifuged for 5 minutes with the centrifuge brake turned off.

### 2.4.2.3 Adoptive transfer of EAE to recipients

Recipient mice were irradiated with 3 Gray and 5 X $10^7$ cells were injected i.p. per mouse at day 0. Every mouse received an i.p. injection of 350ng of PTX (List biological laboratories; California, USA) at day 0 and 2.

## 2.5 Clinical scoring of active and passive EAE

Mice were scored daily over 30 days for clinical signs of active and passive EAE using the A scale in chronic EAE (Chapter 3 and Chapter 4). The B scale was used in subsequent chapters as NOD mice showed a marked weakness in the tail and hind-limp weakness with or without tail paralysis (Chapter 5 and Chapter 6).

**- A scale:**

0-no detectable signs of EAE; 0.5-hunching; 1-slight tail weakness; 1.5-distal limp tail or hind-limb weakness; 2-total tail paralysis; 2.5-hind leg totally paralyzed; 3-both hind legs totally paralyzed; 3.5-bilateral hind-limb paralysis in combination with unilateral fore-limb paralysis or weakness of forelimbs; 4-bilateral hind-limb and forelimb paralysis; 5-moribund state or death (modified from Becher et al., 2001 and Prinz et al, 2006). Mice were euthanized when the clinical score was 3.5 or higher.

**- B scale:**

0-no detectable signs of EAE; 0.5-hunching; 1-slight tail weakness; 1.5-distal limp tail or marked weakness in the tail; 2-total tail paralysis; 2.5-hind-limb weakness with or without tail paralysis; 3.0-hind leg totally paralyzed; 3.5-both hind legs totally paralyzed; 4.0-bilateral hind-limb paralysis in combination with unilateral fore-limb paralysis or weakness of forelimbs; 4.5-bilateral hind-limb and forelimb paralysis; 5-moribund state or death (modified from Becher et al., 2001 and Prinz et al, 2006). Mice were euthanized when the clinical score was 4.0 or higher.

## 2.6 Diabetes incidence

A drop of blood obtained by a tail venepucture was used to measure glucose with a CareSens Blood Glucose Meter (Life Biosciences) and a blood glucose test strip (Medical Technology Promedt Consulting GmbH; Ingbert, Germany). Every mouse was bled fortnightly during 250 days. Mice were considered diabetic after two consecutive glucose readings of at least 14.0 mM or a single glucose reading of “HI” (modified from Fletcher JM, et al., 2008). Diabetic mice were euthanized by $CO_2$ asphyxiation and their pancreata were collected in 10% formalin (Sigma; Missouri, USA) for histological analysis.

# 2.7 Histopathology

## 2.7.1 Organ removal and fixation

### 2.7.1.1 Central Nervous System (CNS)

Mice were euthanized by $CO_2$ asphyxiation. The right atrium was snipped and the left ventricle was perfused with 24 ml of PBS (Invitrogen; Victoria, Australia). The skin on the top of the mouse head was incised and the skull was opened to collect the brain. A middle skin incision along the dorsum was made and the spinal vertebrae were cut to collect the spinal cord. Both the brain and the spinal cord were fixed in 10% formalin (Sigma; Missouri, USA).

## 2.7.2 Parafination, section, de-waxing and hydratation

Fixed CNS in 10% formalin were put in ethanol overnight and embedded in paraffin (Leica Microsystems; New South Wales, Australia) to be sectioned in a Cryotomo (R. Jung Heidelberg). CNS was sectioned at 4μm for Hematoxilin and Eosin (provided by the Department of Marine and Tropical Biology, James Cook University), 5μm for Luxol Fast Blue (Sigma; New South Wales, Australia), 10μm for Bielschowsky's Silver (UNILAB;

Sydney, Australia). Sectioned tissues were de-waxed in Xylene (Merk; Victoria, Australia), and later put in absolute alcohol (Merk; Victoria, Australia) and 70% alcohol. Later, slides were washed in $dH_2O$.

## 2.7.3 Staining

### 2.7.3.1 Hematoxilin and Eosin Staining

Brains and spinal cords were stained with Mayer's Haemalum (1% concentration in destilled water) (provided by the Department of Marine and Tropical Biology, James Cook University) for 8 minutes and washed in $dH_2O$ two times at 20 dips each. They were then kept in blueing solution containing sodium bicarbonate, magnesium sulphate and distillated water (provided by the Department of Marine and Tropical Biology, James Cook University) for 30 seconds and washed as before, and stained with eosin (provided by the Department of Marine and Tropical Biology, James Cook University) for 3 minutes. Later, slides were dehydrated and cleared in 70% alcohol, absolute alcohol (Merk; Australia) and xylene (Merk; Victoria, Australia) and mounted with DPX (BDH; Poole, UK), which is a mixture of distyrene, plasticizer, and xylene (Protocols were adapted from Humason GH, 1972).

### 2.7.3.2 Luxol fast blue

Spinal cords were placed in 1% Luxol fast blue solution (Appendix 9) and left overnight at 56 °C. Slides were rinsed of excess staining with 95% ethyl alcohol (provided by the Department of Marine and Tropical Biology, James Cook University) and then rinsed with distilled water. Spinal cord sections were put in the lithium carbonate solution (Acros Biochemicals) (Appendix 9) for 30 seconds and 70% ethyl alcohol for 30 seconds. Sections were then rinsed in distilled water and checked microscopically to see if grey matter was clear and white matter was defined. After clear differentiation between grey and white matter, sections were put in distilled water, counterstained in 0.1% cresyl fast violet (The British Drug Houses; Poole, England) or 0.1% cresyl violet acetate (Sigma; New South Wales, Australia) (Appendix 9) solution for 30-40 seconds and rinsed in distilled water. Sections were then passed through 95% ethyl alcohol (provided by the Department of Marine and Tropical Biology, James Cook University) for 5 minutes, 100% alcohol (10 dips) (Merk; Australia) and xylene (10 dips) (Merk; Victoria, Australia) and mounted on DPX (BDH; Poole, UK) (method adapted from IHCWORLD, Life Science Information Network).

### 2.7.3.3 Bielschowsky's Silver

Spinal cords sections were placed in 10% silver nitrate solution (UNILAB; Sydney, Australia) (Appendix 9) at 40ºC for 20 minutes and washed by

distilled water. While the slides were in distilled water, concentrated ammonium hydroxide 28% (UNIVAR, New South Wales, Australia) was added to the 10% silver nitrate solution (Appendix 9) and the slides were then placed back into the ammonium silver solution (Appendix 9) for 60 minutes at 40 ºC. The slides were placed in 1% ammonium hydroxide (Appendix 9) solution for 3 minutes and then into developer working solution (Appendix 9) for 4 minutes. Later, the slides were placed in 1% ammonium hydroxide solution (Appendix 9) for 3 minutes to stop the silver reaction. The slides were placed in 5% sodium thiosulfate solution (Appendix 9) for 5 minutes and washed in distilled water, dehydrated and cleared through 95% ethyl alcohol and absolute ethyl alcohol and xylene (Merk; Victoria, Australia). The slides were then mounted with DPX (BDH; Poole, England) (method modified from IHCWORLD, Life Science Information Network).

## 2.8 Histological evaluation

### 2.8.1 Spinal cord

Cell infiltration and demyelination (loss of myelin) of spinal cords was assessed using the following semi-quantitative scoring system: 0 = no lesions, no cell infiltration and no reduction in LFB and Bielschowsky's silver staining; 1 = solitary lesions with cell infiltration of low cellular density with or without mildly reduced LFB and Bielschowsky's silver

staining; 2 = two to three lesions level with moderate cell infiltration associated with reduced LFB staining and Bielschowsky's silver; 3 = many lesions in almost all fields with extensive cell infiltration associated with severe reduction in LFB and Bielschowsky's silver staining (modified from Hempel et al., 1985).

# 2.9 Flow Cytometry

## 2.9.1 Organ removal

Mice were euthanized by $CO_2$ asphyxiation. Spleens and superficial and deep cervical lymph nodes were removed and placed in PBS (Invitrogen Victoria, Australia). CNS was removed after snipping the right atrium and perfusion via the left ventricle with 24 ml of PBS (Invitrogen Victoria, Australia). All samples were kept at 4°C.

## 2.9.2 Preparation of single cell suspensions

### 2.9.2.1 Spleen

Each spleen was placed in a petri dish with MACS buffer (Appendix 9) and mashed between two microscope slides and centrifuged. The pellet obtained after centrifugation was resuspended in red blood cell lysing buffer (Sigma; Ayrshire, UK) and incubated for 8 minutes in ice to destroy the red cells.

After incubation, the cells were washed with MACS buffer (Appendix 9) and resuspended in 1ml of MACS buffer (Appendix 9) and counted using a cell counter (Beckman Coulter, Instance Number 898673; California, USA).

### 2.9.2.2 Lymph nodes

Lymph nodes from every mouse were mashed between two microscope slides in MACS buffer (Appendix 9), centrifuged and resuspended in 1ml of MACS buffer (Appendix 9). Cells were counted with a Beckman Coulter (Instance Number 898673; California, USA).

### 2.9.2.3 Central Nervous System

Every CNS was minced through a wire mesh sieve and centrifuged for 15 minutes at 4°C. Pellets were resuspended in enzyme/ collagenase buffer containing 0.5ml/mg of Collagenase Type II (Sigma; NSW, Australia) and 500U/ml of DNase I (Sigma; NSW, Australia) and incubated at 37°C for 60 minutes. Samples were topped up to 50 ml with PBS (Invitrogen Victoria, Australia) after incubation and centrifuged for 15 minutes at 400 X *g*. Pellets were resuspended in 20 ml of 30% v/v isotonic percoll (GE Healthcare Bio-Sciences; New South Wales, Australia), underlayed with 7.5ml of 70% v/v isotonic percoll (GE Healthcare Bio-Sciences; New

South Wales, Australia), topped with 7.5ml of PBS (Invitrogen Victoria, Australia) and centrifuged for 25 minutes at 25°C, 600 X *g*. Cells between 30% and 70% density were collected and washed in 50ml of PBS (Invitrogen Victoria, Australia). The pellet was resuspended in MACS buffer (Apendix 9) and counted with a cell counter (Beckman Coulter, Instance Number 898673; California, USA).

## 2.9.3 FACs staining and analysis

### 2.9.3.1 Blocking FcR binding

Leucocytes from CNS, spleens and lymph nodes were plated out in 96-well U-bottom plates at 1-2 million cells per well. Cells were incubated with Biotin-CD16/32 antibody (BD biosciences; California, USA) containing 10% mouse serum for 15 minutes to prevent non-specific antibodies bindings. Cell pellets were re-suspended for cell surface staining.

### 2.9.3.2 Cell surface staining

Each leukocyte sample from the CNS, spleens and lymph nodes were incubated with a cocktail of antibodies (Appendix 8) for 25 minutes after blocking FcR binding (BD biosciences; California, USA). Cells were washed with MACS buffer and centrifuged for 2 minutes at 4°C. A

secondary staining was done with streptavidin when biotinylated antibodies were used (Appendix 8). After cell surface staining, the pellet was re-suspended in 300μL of MACS buffer (Appendix 9) and filtered through 70μm nylon mesh (Clear Edge Filtration; Victoria, Australia) into Falcons tubes (BD biosciences; California, Australia). Propidium iodide (PI) (2ng/ml) (Invitrogen; Victoria, Australia) was added before cell analysis to detect dead cells. Data analysis was performed on a CyAn$^{TM}$ ADP Flow Cytomer (Beckman Coulter) and LSR Fortessa (BD Biosciences).

For CCR2 staining, cells were incubated with 50% mouse serum for 15 minutes at room temperature and centrifuged at 4°C for 3 minutes. Cells were incubated with CCR2 mAb biotinylated (Appendix 8) for 25 minutes and washed. Cells were then incubated with streptavidin-Dylight 649 (Appendix 8) for 25 minutes. Cells were washed in 200μL of Macs buffer (Appendix 9) and centrifuged at 4°C for 3 minutes. Later, cells were incubated with 10% rat serum for 30 minutes at 4°C, centrifuged and resuspended in MACS buffer (Appendix 9).

## 2.9.3.3 Intracellular staining

### 2.9.3.3.1 Tregs staining

Cell surface staining was done with anti TCR, CD4, CD25 and CD62L antibodies (Appendix 8) as described previously. Cells were fixed with 100µl of 1X FoxP3 Fix/Perm solution (BioLegend; California, USA) for 20 minutes. Cells were washed with Perm buffer twice (BioLegend; California, USA). Cells were stained with anti-FoxP3 antibody (BioLegend; California, USA) for 30 minutes, washed twice with FoxP3 Perm buffer (BioLegend; California, USA) and re-suspended in MACS buffer (Appendix 9).

### 2.9.3.3.2 IL17 in spleen

Cells were stimulated with Ionomycin (1µg/ml) (Invitrogen; Victoria, Australia) and PMA (10ng/ml) (Sigma-Aldrich; Missouri, United Kingdom) and incubated for 4 hours at 37°C. Samples were analyzed following the BD Cytofix/Cytoperm$^{TM}$ Plus Fixation/Permeabilization Kit with BD GolgiPlus$^{TM}$ protocol (BD biosciences; California, USA).

### 2.9.3.3.3 IL17 Secretion Assay

Leukocytes from CNS and spleen were washed with HBSS (Invitrogen; Victoria, Australia), centrifuged at 4°C for 10 minutes and then the

supernatant was aspirated. Each CNS pellet was re-suspended in RPMI medium (Invitrogen; Victoria, Australia) containing 5% of mouse serum and the spleens were re-suspended at $1X10^7$ cells/ml. CNS cells and spleen cells were placed in a 96 or 24 well cell culture plate respectively, stimulated with Ionomycin (1μg/ml) (Invitrogen; Victoria, Australia) and PMA (10ng/ml) (Sigma; Missouri, UK) and incubated for 3 hours at 37°C. Negative controls were not stimulated.

Cells were washed twice with cold buffer (PBS (Invitrogen; Victoria, Australia) containing 0.4% EDTA (AMRESCO; Ohio, USA) and 5 ml of 5% bovine serum albumin (BSA) (Invitrogen; Victoria, Australia) after 3 hours of stimulation and centrifuged. The pellet of leucocytes from the CNS was re-suspended in 90μL of cold buffer and the pellet of leucocytes from the spleen was re-suspended in 900μL of cold buffer. 10μL and 100μL of mouse IL17 Catch Reagent were added to the CNS and the spleen cells, respectively, and incubated for 5 minutes on ice. Buffers and Catch reagent were bought from Miltenyi Biotec (New South Wales, Australia).

Cells were topped up to 10ml of cell culture medium (Appendix 9) and incubated for 45 minutes at 37°C (the tubes were rotated every 5 minutes to re-suspend settled cells). Cells were then put on ice and washed with cold buffer. The pellet from the CNS cells was re-suspended in 100μL of cold

buffer and the pellet from the spleen cells was re-suspended in 900 µl of cold buffer. 10µL and 100µL of Mouse IL17 Detection Antibody were added to the CNS and the spleen cells, respectively, and incubated for 10 minutes on ice. Buffers were bought from Miltenyi Biotec; New South Wales, Australia).

Cells were then washed in 10 ml of cold buffer. The pellet from the CNS cells was re-suspended in 100µL cold buffer and the pellet from the spleen cells was re-suspended in 900 µL of cold buffer. 10µL and 100µL of streptavidin PE were added to the CNS and the spleen cells, respectively, and incubated for 10 minutes on ice. Cells were washed and stained with CD45.2, βTCR, CD4 and CD8 (Appendix 8) as described in cell surface staining cells before. Buffers were bought from Miltenyi Biotec (New South Wales, Australia).

## 2.10 Cytokines assays

### 2.10.1 Plasma collection and storage

Blood was collected by retro-orbital venipuncture with plastic clad micro hematocrit tubes (Becton Dickinson and Company; Pennsylvania, USA) at 21 days after active EAE induction, at 10 and 34 days after passive EAE and at 40 days in relapsing-remitting EAE. Blood was centrifuged at 4°C

and 6000 X *g* for 8 minutes. Plasma was collected and stored at -80°C until assayed.

## 2.10.2 Th1/Th2/Th17 cytokine assays

Plasma from C57BL/6, C57BL/6.*Tlr2*$^{-/-}$, C57BL/6.*Tlr9*$^{-/-}$, C57BL/6.*Tlr2*$^{-/-}$/9$^{-/-}$, C57BL/6.*MyD88*$^{-/-}$ male and female mice with active EAE and plasma from C57BL/6, C57BL/6.*Tlr2*$^{-/-}$ with passive EAE was analyzed to detect GM-CSF, IFNγ, IL-1α, IL-2, IL-4, IL-5, IL-6, IL-10, IL-17, TNF, IL-23 and/or IL-18, CXCL1/KC, and MIP-1β. Plasma from NOD.*H2*$^{b}$ and NOD.*H2*$^{b}$.*Tlr2*$^{-/-}$ was analyzed to detect IL13, IL1, IL22, IL5, IL21, IL6, IL10, IL27, IL23, IFNγ, TNF, IL4 and IL17 (eBiosciences). Samples were process following the Bender MedSystems protocols.

Samples were acquired on either a CyAn ADP (Beckman Counter) or an LSR Fortessa (BD Biosciences) Flow Cytometers. Data were analyzed with a multiparameter logistic nonlinear regression model using Flow Cytomix Pro 2.2.1 (Bender Medsystems) and Graph Pad Prism version 5.00 (Graph Pad for Mac, Software, San Diego, California, USA).

### 2.10.2.1 IFNβ ELISA

Plasma from C57BL/6, C57BL/6.*Tlr2*$^{-/-}$, C57BL/6.*Tlr9*$^{-/-}$, C57BL/6.*Tlr2*$^{-/-}$/9$^{-/-}$, C57BL/6.*MyD88*$^{-/-}$ male and female mice with active EAE was analyzed to detect IFNβ protein using enzyme-linked immunosorbent assay (ELISA) (plb interferon source; New Jersey, USA). ELISA was performed following the protocol of plb Biomedical Laboratories. Data analysis was performed on a micro-plate reader at an absorbance of 450nm (Versamax Microplate reader). The detection range was 15.6-1000 pg/ml.

## 2.11 Intraperitoneal injections of IL6

C57BL/6, C57BL/6.*Tlr2*$^{-/-}$, NOD.*H2*$^{b}$ and NOD.*H2*$^{b}$.*Tlr2*$^{-/-}$ mice received daily intraperitoneal injection of IL6 (Shenandoah Biotechnology, Pennsylvania, USA) (2μg in 200μl of PBS (Invitrogen; Victoria, Australia)) for 20 days during the induction of the disease.

## 2.12 Mice treated with antibiotics

Mice were fed with pellets of medicated food with 600mg of amoxicillin, 100mg clarithromycin, 200mg metronidazole and 4mg ameprazole per kilogram. Control mice were fed with normal food (no medicated food). All

medicated and non-medicated food was bought from Specialty Feeds, Glen Forrest, Western, Australia.

## 2.13 Statistical analysis

Mice from the control group were compared with knockout, congenic or transgenic mice of the same sex. Statistical calculations were performed using Microsoft Excel 2008, Graph Pad Prism version 5.00 (Graph Pad for Mac, Software, San Diego, California, USA www.graphpad.com), Graph Pad Prism version 4.0c (1994-2005) or InStat 3.0b (1992-2003). Data were statistically significant at $p < 0.05$ (Mann-Whitney U test or Kruskal-Wallis test with Dunn's multiple-comparison post-test unless otherwise stated).

# CHAPTER 3

# CHAPTER 3

# ROLES FOR TLR2, TLR9 AND MYD88 BUT NOT TLR1, TLR4 AND TLR6 IN ACTIVE $MOG_{35-55}$/CFA + PTX–INDUCED EAE

## 3.1 Introduction

MS is a chronic immune-mediated inflammatory/demyelinating disease of the CNS that occurs in young adulthood and is more common in women but more severe in men (Hsueh et al., 2013). The molecular mechanisms of MS and the development of therapies to treat it have been successfully studied in animal models such as EAE (Furlan et al., 2009). EAE causes a demyelinating paralysis resembling the common forms of MS and almost every therapy for MS has been developed in this animal model (Lindsey et al., 1996). Despite advances in the treatment of signs and symptoms of MS, the factors underlying its initiation and progression are unclear and no cure or preventive therapies are known.

Multiple genetic and environmental factors contribute to MS and EAE as discussed in Chapter 1. One potential mechanism by which environmental factors could regulate autoimmune responses is via the TLR system and

associated pathways. TLRs mediate inflammatory responses to environmental factors known as PAMP, and to endogenous molecules known as DAMP (Akira et al., 2006; Kaisho et al., 2006). Although TLR expression increases in CNS autoimmune inflammation, the role of TLRs remains controversial in MS and EAE (Bsibsi et al., 2002; Kerfoot, et al., 2004; Prinz et al., 2006; Marta et al., 2008; Reynolds et al., 2010). In this chapter, it is hypothesized that TLR ligation regulates CNS autoimmune inflammation in EAE. To test this hypothesis, the roles of TLR1, TLR2, TLR4, TLR6, TLR9, TLR2/9, TLR4/9 or MyD88 in active $MOG_{35-55}$/CFA + PTX–induced EAE are examined.

# 3.2 Results

## 3.2.1 Toll-like receptors and MyD88 in active $MOG_{35-55}$/CFA + PTX–induced EAE

Previous studies found that MyD88 is required for the development of EAE (Prinz et al., 2006). MyD88 is the adaptor molecule for almost all TLRs, except TLR3; TLR3 signals via the TRIF pathway, and TLR4 uses both the MyD88 pathway and the TRIF pathway (Uematsu et al., 2006). To determine whether signalling through TLRs play a role in the induction and/or effector phase of active $MOG_{35-55}$/CFA + PTX–induced EAE, the disease was induced in male and female C57BL/6 (WT, positive control

group) and C57BL/6 mice deficient in TLR1, TLR2, TLR4, TLR6, TLR9, TLR2/9, TLR4/9 or MyD88 (5-12 mice per group); with s.c. administration of $MOG_{35-55}$ peptide and CFA and i.p. administration of PTX. Negative control male and female C57BL/6 mice were treated with Phosphate Buffered Saline (PBS) (1 mouse), or PTX and an emulsion of CFA and PBS (CFA/PTX) (1 mouse).

Clinical signs of active $MOG_{35-55}$/CFA + PTX–induced EAE were examined over 40 days. Neither male nor female mice from the negative control groups showed clinical signs of EAE, while male and female C57BL/6 mice from the positive control group and C57BL/6 mice deficient in TLR1, TLR2, TLR4, TLR6, TLR9, TLR2/9, TLR4/9 immunized with $MOG_{35-55}$/CFA + PTX showed clinical signs of EAE (Figure 3.1 and Figure 3.2). PTX and CFA were unable to induce clinical signs of active EAE without $MOG_{35-55}$ peptide.

Clinical signs of active $MOG_{35-55}$/CFA + PTX–induced EAE appeared within 13-17 days in C57BL/6 (WT) male mice, and within 13-19 days in C57BL/6 (WT) female mice after the induction of EAE. Both male and female C57BL/6 mice developed a chronic form of EAE. The peak of active $MOG_{35-55}$/CFA + PTX–induced EAE was observed at 21 days after EAE induction, followed by a slight drop to a plateau disability in both sexes (Figure 3).

The clinical course of active $MOG_{35-55}$/CFA + PTX–induced EAE was compared between C57BL/6 mice (positive control group) and C57BL/6.Tlr-knockout mice. Both male and female mice deficient in TLR1 showed similar course of active $MOG_{35-55}$/CFA + PTX–induced EAE compared with C57BL/6 male or female mice respectively (Figure 3.2 and Table 3.1).

Male mice deficient in TLR4 showed a mild exacerbation of active $MOG_{35-55}$/CFA + PTX–induced EAE for four days (days 16, 17, 20, 21) and, TLR4/9 doubly deficient male mice had a mildly decreased severity of disease for eight days (days 20-24 and 30-32) compared with C57BL/6 male mice. However, in the absence of TLR4 or TLR4/9, mice showed similar clinical course of active $MOG_{35-55}$/CFA + PTX–induced EAE in female mice compared with C57BL/6 female mice. Also, no differences were seen in the daily clinical scores of active $MOG_{35-55}$/CFA + PTX–induced EAE in the absence of TLR6 compared with the positive control groups in both male and female mice (Figure 3.2 and Table 3.1).

The day of onset of active $MOG_{35-55}$/CFA + PTX–induced EAE, the maximum score of disease and the CDI were also similar between C57BL/6 and C57BL/6 mice deficient in TLR1, TLR4 TLR6 and TLR4/9 in both

male and female mice (Figure 3.2 and Table 3.1). These results indicate that signalling from TLR1, TLR4, TLR6 and TLR4/9 do not play a major role in active $MOG_{35-55}$/CFA + PTX–induced EAE.

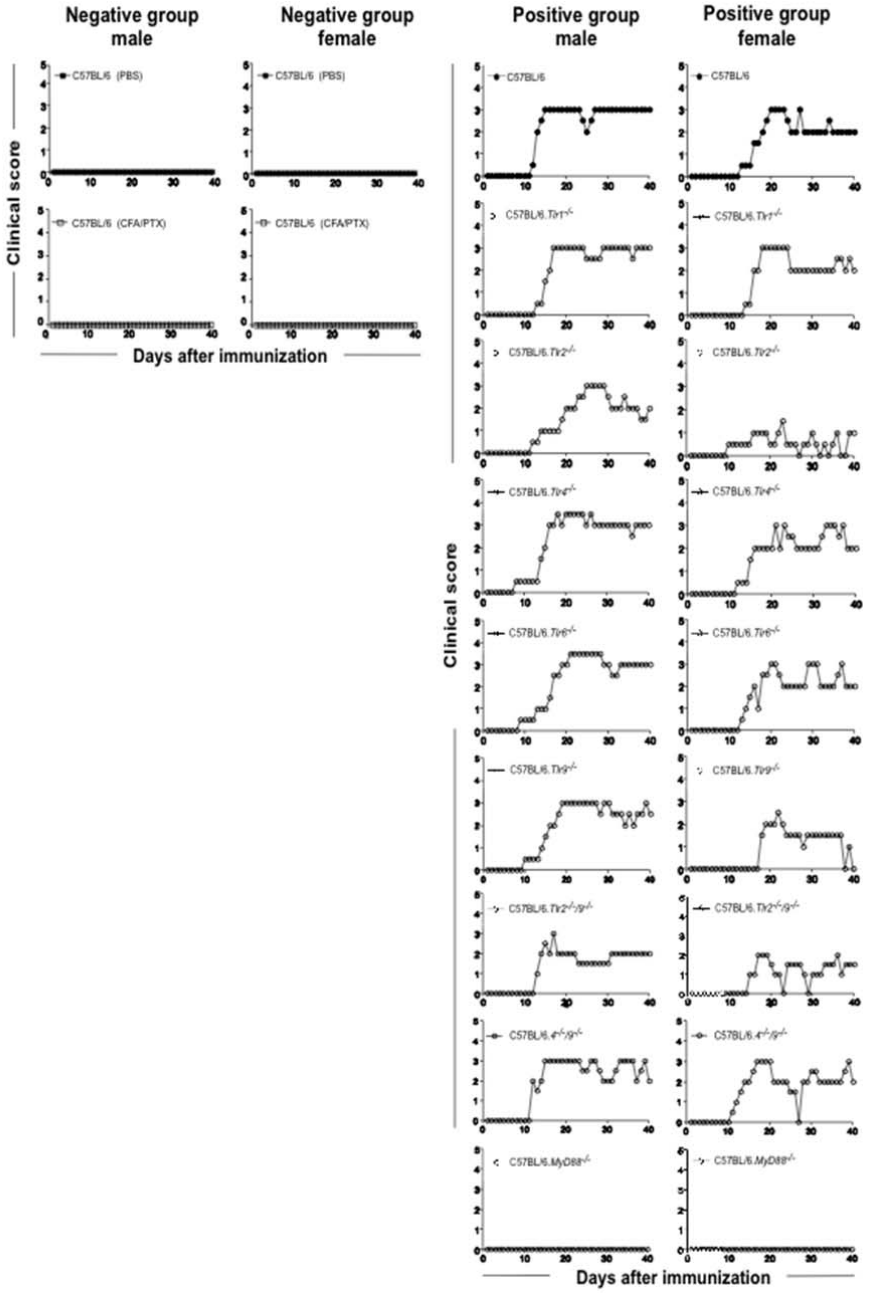


Figure 3.1 Representative clinical course of active $MOG_{35-55}$/CFA + PTX–induced EAE in individual mice. The two columns in the left side are the negative control C57BL/6 male and female mice immunized with PBS (*closed squares*) or CFA/PTX (*open squares*). The two columns in the right side are the positive control C57BL/6 and C57BL/6.*Tlr-knockout* male and female mice immunized with $MOG_{35-55}$/CFA/PTX. C*losed circles* correspond to C57BL/6 WT positive control mice and *open circles* correspond to C57BL/6.*Tlr1*$^{-/-}$, C57BL/6.*Tlr2*$^{-/-}$, C57BL/6.*Tlr4*$^{-/-}$, C57BL/6.*Tlr6*$^{-/-}$, C57BL/6.*Tlr9*$^{-/-}$, C57BL/6.*Tlr2*$^{-/-}$*9*$^{-/-}$, C57BL/6.*Tlr4*$^{-/-}$*9*$^{-/-}$ and C57BL/6.*Myd88*$^{-/-}$ male and female mice.

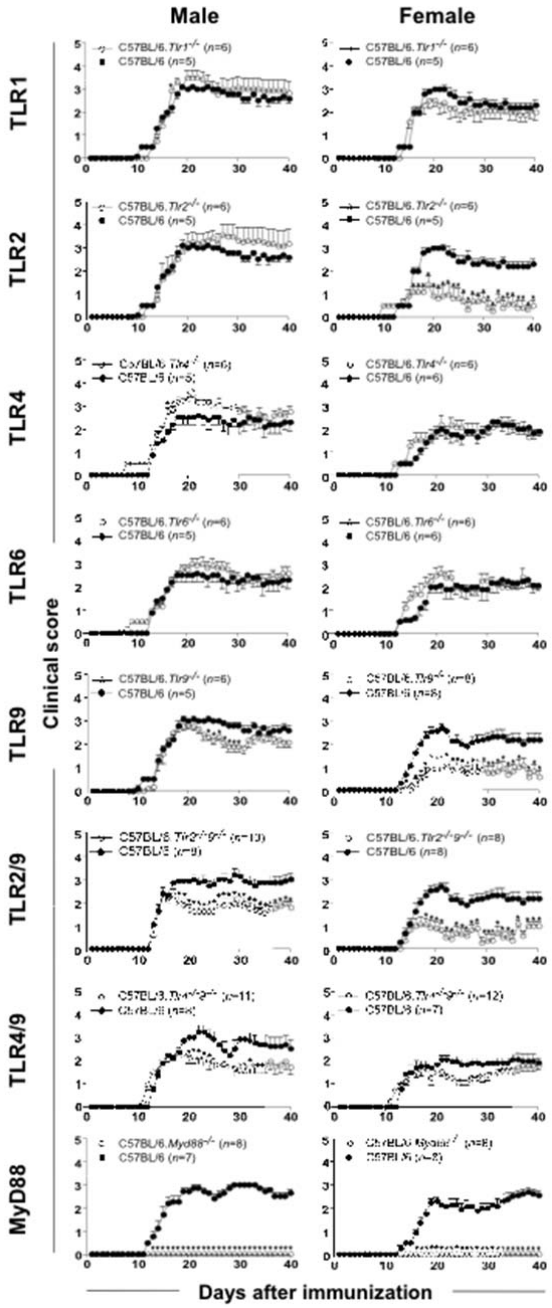


Figure 3.2 Clinical course of active $MOG_{35-55}$/CFA + PTX–induced EAE in male and female mice. *Close circles* represent to C57BL/6 (WT) mice and *open circles* represent C57BL/6.*Tlr1*$^{-/-}$, C57BL/6.*Tlr2*$^{-/-}$, C57BL/6.*Tlr4*$^{-/-}$, C57BL/6.*Tlr6*$^{-/-}$, C57BL/6.*Tlr9*$^{-/-}$, C57BL/6.*Tlr2*$^{-/-}$/*9*$^{-/-}$, C57BL/6.*Tlr4*$^{-/-}$/*9*$^{-/-}$ and C57BL/6.*Myd88*$^{-/-}$ mice. Each data point and error bar represents the mean per day ± SEM from five to twelve mice. Statically significant data between C57BL/6 and C57BL/6.*Tlr*$^{-/-}$ are indicated (*$p < 0.5$, uncorrected Mann Whitney-test).

Table 3.1 Characteristics of active $MOG_{35-55}$/CFA + PTX–induced EAE in male and female C57BL/6 and C57BL/6 mice deficient in TLR1, TLR2, TLR4, TLR6, TLR9, TLR2/9, TLR4/9 and MyD88.

| Experiment | Strain | *n* | Incidence (%) | Onset (days) | Maximum Disease Score | Cumulative Disease Index (CDI) |
|---|---|---|---|---|---|---|
| Male | | | | | | |
| Exp 1 | C57BL/6 | 5 | 100 | 14.2±0.2 | 3.1±0.1 | 71.8±2.9 |
| | C57BL/6.*Tlr1*$^{-/-}$ | 6 | 100 | 14.7±0.2 | 3.7±0.3 | 77.3±8.7 |
| | C57BL/6.*Tlr2*$^{-/-}$ | 6 | 100 | 14.5±0.2 | 3.8±0.4 | 80.2±12.1 |
| | C57BL/6.*Tlr9*$^{-/-}$ | 6 | 100 | 14.5±0.4 | 3.2±0.2 | 60.2±4.3 |
| Exp 2 | C57BL/6 | 5 | 100 | 13.2±0.2 | 2.9±0.2 | 62.1±8.3 |
| | C57BL/6.*Tlr4*$^{-/-}$ | 6 | 100 | 13.2±0.2 | 3.5±0.0* | 76.7±2.0 |
| | C57BL/6.*Tlr6*$^{-/-}$ | 6 | 100 | 13.0±0.0 | 3.3±0.2 | 67.3±4.3 |
| Exp 3 | C57BL/6 | 6 | 100 | 15.2±0.5 | 3.0±0.0 | 64.9±5.2 |
| | C57BL/6.*Tlr9*$^{-/-}$ | 6 | 100 | 15.3±0.2 | 2.8±0.2 | 60.5±3.7 |
| Exp 4 | C57BL/6 | 7 | 100 | 13.4±0.2 | 3.4±0.1 | 80.9±7.0 |
| | C57BL/6.*Tlr2*$^{-/-}$ | 8 | 100 | 13.8±0.3 | 3.8±0.2 | 74.5±8.3 |
| | C57BL/6.*Tlr2/9*$^{-/-}$ | 10 | 100 | 13.8±0.2 | 2.8±0.1** | 49.4±5.4*** |
| Exp 5 | C57BL/6 | 7 | 100 | 14.3±0.4 | 3.0±0.0 | 70.3±2.9 |
| | C57BL/6.*Myd88*$^{-/-}$ | 8 | 0 | Na | 0.0±0.0*** | 0.0±0.0*** |
| Exp 6 | C57BL/6 | 8 | 100 | 13.7±0.2 | 3.25±0.2 | 71.9±6.7 |
| | C57BL/6.*Tlr4/9*$^{-/-}$ | 11 | 100 | 12.4±0.3* | 2.4±0.2 | 54.6±8.0 |
| Female | | | | | | |
| Exp 1 | C57BL/6 | 5 | 100 | 16.0±0.0 | 3.1±0.1 | 61.1±3.8 |
| | C57BL/6.*Tlr1*$^{-/-}$ | 6 | 100 | 15.2±0.2** | 2.7±0.3 | 53.6±9.7 |
| | C57BL/6.*Tlr2*$^{-/-}$ | 6 | 100 | 15.7±0.8 | 1.6±0.3** | 14.2±8.8* |
| | C57BL/6.*Tlr4*$^{-/-}$ | 6 | 100 | 15.7±1.6 | 3.2±0.4 | 64.0±19.2 |
| | C57BL/6.*Tlr6*$^{-/-}$ | 6 | 100 | 15.5±1.6 | 3.1±0.5 | 65.1±19.8 |
| | C57BL/6.*Tlr9*$^{-/-}$ | 6 | 33.3 | 17.0±1.2* | 0.8±0.5** | 8.5±7.8** |
| Exp 2 | C57BL/6 | 6 | 100 | 13.7±0.3 | 2.9±0.3 | 57.7±10.3 |
| | C57BL/6.*Tlr9*$^{-/-}$ | 6 | 100 | 17±0.0** | 2.2±0.2* | 32.0±5.5* |
| | C57BL/6.*Myd88*$^{-/-}$ | 5 | 40 | 22.0±2.6** | 1.1±0.4** | 8.8±7.3** |

| | | | | | | |
|---|---|---|---|---|---|---|
| Exp 3 | C57BL/6 | 5 | 100 | 15.8±0.6 | 2.6±0.2 | 48.4±2.8 |
| | C57BL/6.*Tlr2*$^{-/-}$ | 5 | 100 | 22.8±3.1 | 1.4±0.3* | 14.0±9.0 |
| Exp 4 | C57BL/6 | 6 | 100 | 16.2±0.3 | 2.4±0.2 | 46.9±4.3 |
| | C57BL/6.*Tlr2*$^{-/-}$ | 5 | 100 | 19.6±2.5 | 1.5±0.4 | 16.2±10.0 |
| Exp 5 | C57BL/6 | 8 | 100 | 15.9±0.5 | 2.9±0.1 | 53.3±3.7 |
| | C57BL/6.*Tlr2*$^{-/-}$ | 8 | 100 | 15.4±0.2 | 2.6±0.2 | 44.9±3.5 |
| | C57BL/6.*Myd88*$^{-/-}$ | 8 | 0 | Na | 0.0±0.0*** | 0.0±0.0*** |
| Exp 6 | C57BL/6 | 6 | 100 | 17.3±0.8 | 2.7±0.2 | 45.5±5.5 |
| | C57BL/6.*Tlr4*$^{-/-}$ | 6 | 100 | 17±1.5 | 2.4±0.3 | 47.7±7.6 |
| Exp 7 | C57BL/6 | 6 | 100 | 17.0±0.8 | 2.6±0.3 | 48.0±8.0 |
| | C57BL/6.*Tlr6*$^{-/-}$ | 5 | 100 | 14.8±0.8 | 2.9±0.2 | 54.8±4.2 |
| Exp 8 | C57BL/6 | 8 | 100 | 15.4±0.2 | 2.9±0.1 | 56.0±5.0 |
| | C57BL/6.*Tlr9*$^{-/-}$ | 8 | 100 | 21.6±2.5*** | 1.6±0.2*** | 19.9±6.7*** |
| | C57BL/6.*Tlr2/9*$^{-/-}$ | 8 | 100 | 16.2±0.8 | 1.6±0.2*** | 19.1±4.9*** |
| Exp 9 | C57BL/6 | 5 | 100 | 14.8±1.1 | 2.7±0.3 | 53.1±9.9 |
| | C57BL/6.*Tlr2/9*$^{-/-}$ | 8 | 100 | 15.4±0.6 | 2.3±0.2 | 44.8±7.3 |
| Exp 10 | C57BL/6 | 7 | 100 | 13.8±0.2 | 2.4±0.2 | 51.9±4.06 |
| | C57BL/6.*Tlr4/9*$^{-/-}$ | 12 | 100 | 13.01±0.6* | 2.6±0.2 | 42.1±4.8 |

Mean ± SEM of the clinical score of EAE. Statistically significant data between C57BL/6 mice (WT, positive control group) and C57BL/6.*Tlr-knockout* mice are indicated (*$p < 0.05$, **$p < 0.01$, ***$p < 0.01$, uncorrected Mann Whitney-test *U* test).

The absence of MyD88 protected mice from active $MOG_{35-55}$/CFA + PTX–induced EAE. Neither male nor female mice deficient in MyD88 showed clinical signs of EAE (Figure 3.2 and Table 3.1), confirming that MyD88 plays a definitive role in the development of EAE as reported by Marta et al., (2008) and Prinz et al., (2006).

Less severe clinical signs of EAE occurred in the absence of TLR9. The clinical course of EAE was decreased in the absence of TLR9 in female mice during 26 days (days 14-36 and 38-40) compared to C57BL/6 female mice. Female mice deficient in TLR9 had less severe clinical signs of EAE (mean maximum score ± SEM = 0.8 ± 0.5, $p < 0.01$ and; mean CDI ± SEM = 8.5 ± 7.8, $p < 0.01$) compared with C57BL/6 female mice (mean maximum score ± SEM = 3.1 ± 0.1 and CDI ± SEM = 61.1 ± 3.8). The onset of the disease was also delayed in C57BL/6 female mice deficient in TLR9 (19.3 ± 1.2 days, $p < 0.001$) when compared with C57BL/6 female mice (15.0 ± 0.2 days) (Figure 3.2 and Table 3.1). A pool analysis of three cohorts of C57BL/6.*Tlr9*$^{-/-}$ female mice and their respective controls exhibited a milder mean maximum score ($p < 0.001$) and a decreased CDI ($p < 0.001$) compared with C57BL/6 mice (Figure 3.2 and Table 3.2). Although the course of active $MOG_{35-55}$/CFA + PTX –induced EAE was decreased in the absence of TLR9 in male mice for 7 days (days 24-30), no differences were seen in the day of onset of disease, maximum clinical score

and CDI when compared with C57BL/6 male mice (Figure 3.2 and Table 3.2).

Less severe clinical signs of EAE occurred in the absence of TLR2. Female mice deficient in TLR2 showed a decreased severity of EAE during 25 days (days 16-40) compared to C57BL/6 female mice. The severity of EAE was also decreased in the absence of TLR2 (mean of maximum score ± SEM = 1.6 ± 0.3, $p < 0.01$) and mean of CDI ± SEM = 14.2 ± 8.8, $p < 0.05$) compared with C57BL/6 female mice (mean maximum score ± SEM of 3.1 ± 0.1 and CDI ± SEM of 61.1 ± 3.8) (Figure 3.2 and Table 3.1). A pooled analysis of four cohorts of C57BL/6.*Tlr2*$^{-/-}$ female mice and their respective control showed highly significant differences in mean maximum score ($p < 0.001$) and CDI ($p < 0.001$) (Figure 3.2 and Table 3.2). In contrast, no differences were seen in the clinical course of EAE, onset day of disease, maximum score of disease and CDI in the absence of TLR2 in male mice compared with C57BL/6 male mice (Figure 3.2 and Table 3.1). These results showed that sexual dimorphism is present in the severity of active $MOG_{35-55}$/CFA + PTX –induced EAE in the absence of TLR2 and TLR9.

Table 3.2 Active $MOG_{35-55}$/CFA + PTX –induced EAE in C57BL/6 female mice deficient in TLR2 and TLR9.

| Experiment | Strain | *n* | Incidence (%) | Onset (days) | Mean Maximum Disease Score | Cumulative Disease Index (CDI) |
|---|---|---|---|---|---|---|
| Female | | | | | | |
| TLR2 | C57BL/6 | 24 | 100 | 15.9±0.2 | 2.7±0.0 | 52.2±2.0 |
| | C57BL/6.*Tlr2*$^{-/-}$ | 24 | 100 | 17.8±0.9 | 1.8±0.1*** | 24.8±4.5*** |
| TLR9 | C57BL/6 | 19 | 100 | 15±0.2 | 2.9±0.1 | 57.8±3.8 |
| | C57BL/6.*Tlr9*$^{-/-}$ | 20 | 80 | 19.3±1.2*** | 1.5±0.2*** | 20.1±4.2*** |

Mean ± SEM of the clinical score of EAE. Statistically significant data between C57BL/6 mice (WT, positive control group) and C57BL/6.*Tlr2*$^{-/-}$ and C57BL/6.*Tlr9*$^{-/-}$ female mice are indicated (*p < 0.05, **p < 0.01, ***p < 0.01, uncorrected Mann Whitney-test *U* test).

As active $MOG_{35-55}$/CFA + PTX–induced EAE appeared to be partially dependent on TLR2 and TLR9 signalling in female mice but not in male mice, the disease was analyzed in female and male C57BL/6 (WT) and C57BL/6.*Tlr2*$^{-/-}$*Tlr9*$^{-/-}$ mice. C57BL/6.*Tlr2*$^{-/-}$*Tlr9*$^{-/-}$ female mice showed significantly less severe disease, with a mean maximum disease score ± SEM of 1.6 ± 0.2 ($p<0.001$) and a mean CDI ± SEM of 19.1 ± 4.9 ($p<0.001$) compared with the WT control group (2.9 ± 0.01 and 56.0 ± 5.0, respectively). Less severe disease was also observed in C57BL/6.*Tlr2*$^{-/-}$*Tlr9*$^{-/-}$ male mice, with a mean maximum score ± SEM of 2.8 ± 0.1 ($p<0.01$) and a mean CDI ± SEM of 49.4 ± 5.4 ($p<0.001$) compared with the WT control group (3.4 ± 0.1 and 80.9 ± 7.0, respectively) (Figure 3.2, Table 3.1). Even though the severity of EAE was decreased in C57BL/6.*Tlr2*$^{-/-}$*Tlr9*$^{-/-}$ male mice, the severity of disease in C57BL/6.*Tlr2*$^{-/-}$*Tlr9*$^{-/-}$ female mice was not

lower than that seen in single deficient mice in TLR2 or TLR9 (Figure 3.2 and Table 3.1).

All together, these results show that C57BL/6.*Tlr2*$^{-/-}$ and C57BL/6.*Tlr9*$^{-/-}$ mice as well as male and female C57BL/6.*Tlr2*$^{-/-}$*Tlr9*$^{-/-}$ showed less severe EAE, whereas female and male C57BL/6.*Myd88*$^{-/-}$ are resistant to EAE. Given the strong suppression of EAE in the absence of MyD88, these results also indicates that MyD88 plays a role in the pathogenesis of EAE in addition to its role as the adaptor molecule for TLR2 and TLR9.

## 3.2.2 Histopathology of damage to the spinal cord in the absence of TLRs and MyD88

Spinal cords from male and female C57BL/6 (WT) mice (positive and negative controls) and C57BL/6.*Tlr1*$^{-/-}$, C57BL/6.*Tlr2*$^{-/-}$, C57BL/6.*Tlr4*$^{-/-}$, C57BL/6.*Tlr6*$^{-/-}$, C57BL/6.*Tlr9*$^{-/-}$, C57BL/6.*Tlr2*$^{-/-}$*9*$^{-/-}$ and C57BL/6.*Myd88*$^{-/-}$ mice (5-20 mice per group) were assessed 40 days post EAE induction for cell infiltration, loss of myelin and axonal injury. Transversal sections from the spinal cords were scored using a semi-quantitative scoring system, as shown in the Figure 3.3 and described in Material and Methods.

The spinal cords from C57BL/6 male and female mice showed cell infiltration, loss of myelin and axonal damage. In contrast, the spinal cords from male and female negative controls mice did not show evidence of EAE. Neither cell infiltration nor defects in LFB and Bielschowsky's silver stain were observed in C57BL/6.*Myd88*$^{-/-}$ male or female mice (score mean ± SEM = 0.0 ± 0.0, $p<0.001$ in both male and female) compared with WT mice (score mean in male ± SEM = 2.82 ± 0.03 and score mean in female ± SEM = 2.59 ± 0.09) (Figure 3.4 and Figure 3.5). These results confirm that, in the absence of MyD88, the CNS is completely resistant to active EAE.

Spinal cords from C57BL/6.*Tlr9*$^{-/-}$ and C57BL/6.*Tlr2*$^{-/-}$ female mice had significantly decreased infiltration and demyelinating lesions (score mean ± SEM = 1.28 ± 0.13 ($p<0.001$) and 0.80 ± 0.41 ($p<0.01$), respectively) compared with WT mice (score mean ± SEM = 2.59 ± 0.09). In contrast, spinal cords from C57BL/6.*Tlr9*$^{-/-}$ and C57BL/6.*Tlr2*$^{-/-}$ male mice did not differ to those of the positive control group. Both C57BL/6.*Tlr2*$^{-/-}$*Tlr9*$^{-/-}$ male and female mice had significantly fewer lesions and less infiltration (score mean ± SEM = 1.74 ± 0.15, $p<0.001$, and 1.42 ± 0.28, $p<0.01$, respectively) compared with WT mice (score mean ± SEM = 2.82 ± 0.03 and 2.59 ± 0.1, respectively) (Figure 3.4 and 3.5).

Histopathological analysis confirmed that the severity of disease was reduced in the absence of TLR2 and TLR9 in female mice, but not in male mice, and in the absence of TLR2/9 in both male and female mice, whereas the lack of MyD88 completely protected mice from EAE.

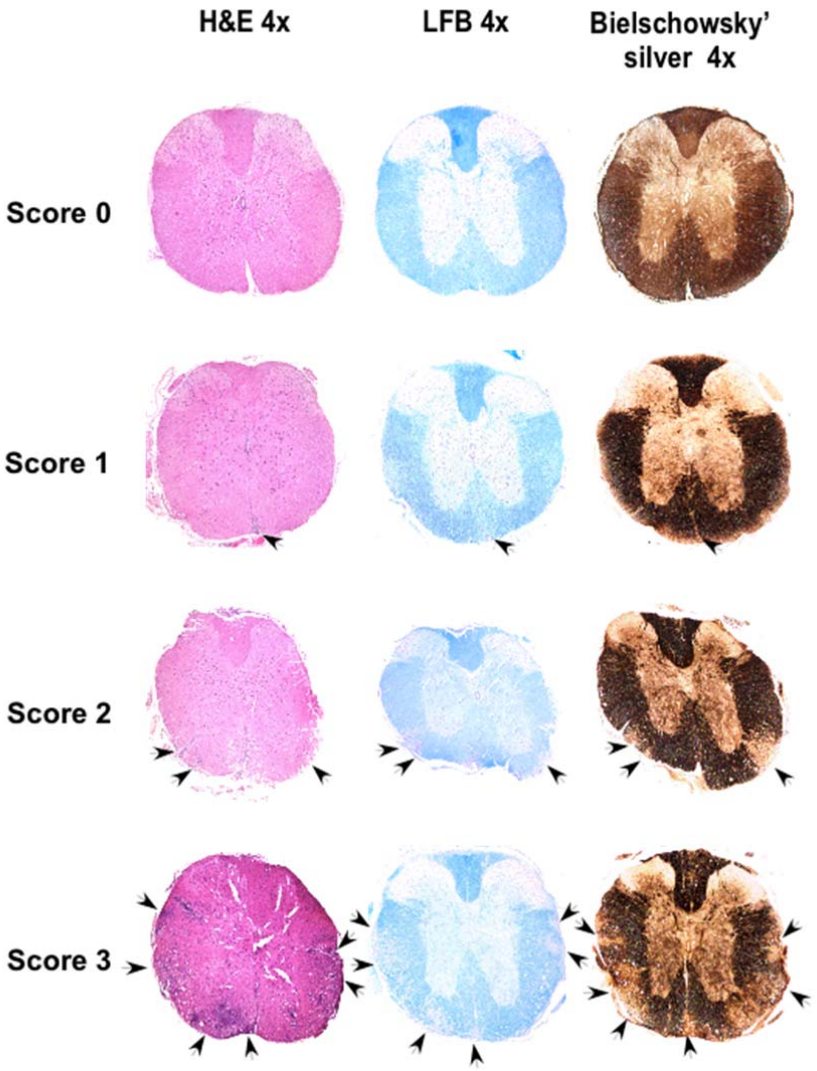


Figure 3.3 Scoring system of spinal cord histopathology after 40 days of active $MOG_{35-55}$/CFA + PTX –induced EAE. Spinal cord was stained with Hematoxylin and Eosin (H&E) *(column on left side)*, Luxol fast Blue *(middle column)* and Bielschowsky's *(column on right side)*. Representative pictures show four different grades of lesions in the spinal cord numbered from 0 to 3: score 0 = no lesions, no cell infiltration and no reduction in LFB and Bielschowsky's silver staining (*first row*); 1 = solitary lesions with cell infiltration of low cellular density with or without mildly reduced LFB and Bielschowsky's silver staining (*second row*); 2 = two to three lesions level with moderate cell infiltration associated with reduced LFB staining and Bielschowsky's silver (*third row*); 3 = many lesions in almost all fields with extensive cell infiltration associated with severe reduction in LFB and Bielschowsky's silver staining (*fourth row*). The objective magnification used is 4x. Lesions, cell infiltration and reduction of LFB and Bielschowsky's silver are indicated with arrows (scoring system was modified from Hempel *et al*., 1985).

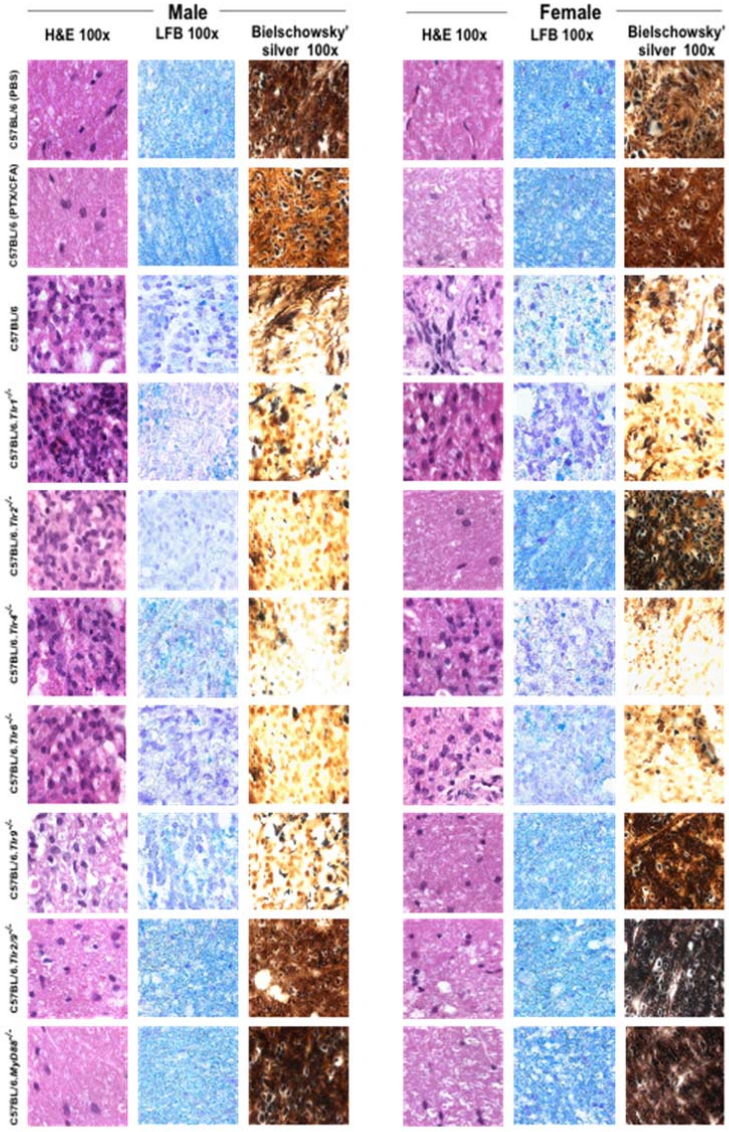


Figure 3.4 Representative transverse histopathological sections of spinal cords taken 40 days after active $MOG_{35-55}$/CFA + PTX-induced EAE. Males are shown on the left side and female are shown on the right side. At the top of every column is indicated the staining (H&E, LFB and Bielschowsky's silver) and magnification (100x): Fist row and second row show C57BL/6 negative control *(mice treated with PBS or PTX/CFA respectively)*, followed by positive controls (mice treated with $MOG_{35-55}$/CFA + PTX) and C57BL/6.*Tlr*$^{-/-}$ mice.

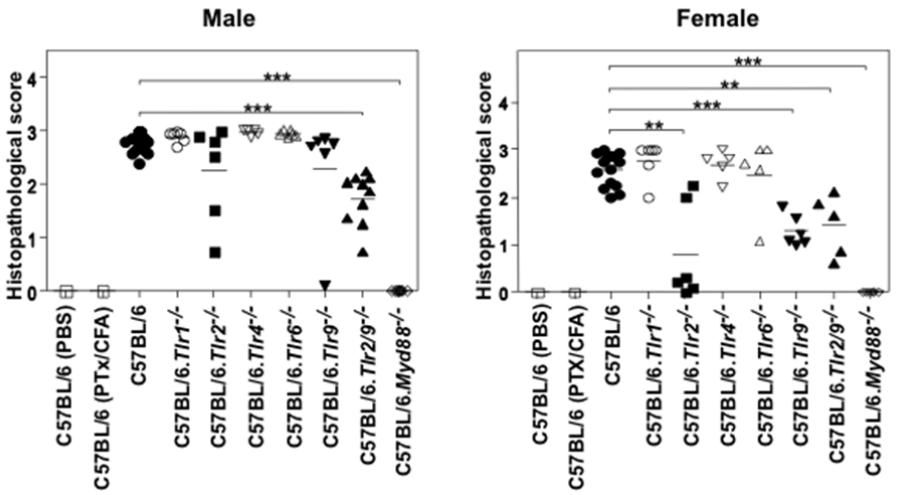


Figure 3.5 Histopathological analysis of damage in spinal cords of mice with 40 days of active $MOG_{35-55}$/CFA + PTX -induced EAE. C57BL/6 negative control groups treated with PBS or PTX/CFA *(open squares)*, C57BL/6 positive control groups immunized with $MOG_{35-55}$/CFA + PTX *(closed cicles)* and C57BL/6.*Tlr1*$^{-/-}$ *(open circles)*, C57BL/6.*Tlr2*$^{-/-}$ *(closed squares)*, C57BL/6.*Tlr4*$^{-/-}$ *(downward open triangles)*, C57BL/6.*Tlr6*$^{-/-}$ *(open upward triangles)*, C57BL/6.*Tlr9*$^{-/-}$ *(closed downward triangles)*, C57BL/6.*Tlr2*$^{-/-}$*Tlr9*$^{-/-}$, *(closed upwards triangles)* and C57BL/6.*Myd88*$^{-/-}$ *(open diamonds)*. Statistically significant differences between C57BL/6 and C57BL/6.*Tlr*$^{-/-}$ mice are indicated (*$p < 0.05$, **$p < 0.01$, ***$p <$ 0.001 uncorrected Mann-Whitney *U* test; $n$ = 1-20).

## 3.2.3 Leukocyte infiltration in the CNS at the peak of active $MOG_{35-55}$/CFA + PTX-induced EAE

TLR ligation triggers an inflammatory immune response and cell migration (Taukeuchi et al., 1999; Hemmi et al., 2000; Alexopoulou et al., 2001; Wang et al., 2004). CNS damage in EAE is characterised by the presence of inflammatory cells that migrate from the periphery into the CNS (Smorodchenko et al., 2007; Furtado et al., 2008). Potential explanations for the relative resistance of C57BL/6.*Tlr2*$^{-/-}$, C57BL/6.*Tlr9*$^{-/-}$, C57BL/6.*Tlr2*$^{-/-}$ *Tlr9*$^{-/-}$ and C57BL/6.*Myd88*$^{-/-}$ mice to active EAE induced with $MOG_{35-55}$/CFA + PTX include effects on recruitment of inflammatory cells to the CNS and differences in subsets recruited. To determine the nature of cells infiltrating the CNS of TLR-deficient C57BL/6 mice, CNS infiltrating leukocytes of female and male C57BL/6, C57BL/6.*Tlr2*$^{-/-}$, C57BL/6.*Tlr9*$^{-/-}$, C57BL/6.*Tlr2*$^{-/-}$*Tlr9*$^{-/-}$ and C57BL/6.*Myd88*$^{-/-}$ mice were compared by flow cytometric analysis 21 days after immunisation with $MOG_{35-55}$/CFA +PTX (Figure 3.6).

A significant decrease was observed in the total number of $CD4^+$ and $CD8^+$ T cells infiltrating the CNS of female C57BL/6.*Myd88*$^{-/-}$ mice compared to C57BL/6 mice ($p < 0.001$ and $p < 0.01$ respectively, Kruskal-Wallis Test with Dunn's multiple comparison post-test; Figure 3.7) and a significant reduction in $CD8^+$ T cells in female C57BL/6.*Tlr9*$^{-/-}$ mice ($p < 0.05$). As

TLR2- and TLR9- deficient mice showed a trend to lower T cell numbers, an additional cohort of C57BL/6, C57BL/6.*Tlr2*$^{-/-}$ and C57BL/6.*Tlr9*$^{-/-}$ mice was assessed and the data combined. Numbers of CD4$^{+}$ T cells infiltrating the CNS of female C57BL/6.*Tlr2*$^{-/-}$ and C57BL/6.*Tlr9*$^{-/-}$ mice of the combined experiment were significantly decreased ($p < 0.05$ and $p < 0.01$ respectively, Kruskal-Wallis Test with Dunn's multiple comparison post-test; $n$ = 11-13), as were the numbers of CD8$^{+}$ T cells infiltrating the CNS of C57BL/6.*Tlr9*$^{-/-}$ mice ($p < 0.01$).

Whereas male C57BL/6.*Myd88*$^{-/-}$ mice showed a statistically significant decrease in only the total number of infiltrating CD4$^{+}$ T cells ($p < 0.01$; Kruskal-Wallis Test with Dunn's multiple comparison post-test; $n$ = 7-8/group; Figure 3.7), neither the C57BL/6.*Tlr2*$^{-/-}$ nor C57BL/6.*Tlr9*$^{-/-}$ male mice showed any significant difference in CNS infiltration, consistent with the clinical data. As the C57BL/6.*Tlr2*$^{-/-}$*Tlr9*$^{-/-}$ double mutant and C57BL/6.*Myd88*$^{-/-}$ male mice showed some trends from the control mice in terms of some infiltrating cell subsets, an additional cohort of C57BL/6, C57BL/6.*Tlr2*$^{-/-}$*Tlr9*$^{-/-}$ and C57BL/6.*Myd88*$^{-/-}$ male mice was assessed and the data combined. Numbers of CD4$^{+}$ and CD8$^{+}$ T cells infiltrating the CNS of male C57BL/6.*Myd88*$^{-/-}$ mice of the combined experiment were significantly decreased ($p < 0.001$ and $p < 0.05$ respectively, Kruskal-Wallis Test with Dunn's multiple comparison post-test; $n$ = 13/group).

CD45 staining in combination with CD11b and/or CD11c was used to distinguish between dendritic cells (DCs) ($CD45^{int}SS^{hi}CD11c^{+}$), macrophages/monocytes ($CD45^{hi}SS^{hi}CD11b^{+}$) and inflammatory monocytes ($CD45^{hi}SS^{hi}CD11c^{+}CD11b^{+}$) (Figure 3.6). In contrast to female C57BL/6 mice, which develop severe EAE with high numbers of infiltrating cells, female C57BL/6.*Myd88*$^{-/-}$ mice had statistically significantly fewer infiltrating DCs, macrophages and inflammatory monocytes ($p < 0.05$, $p < 0.01$ and $p < 0.001$ respectively, Kruskal-Wallis Test with Dunn's multiple comparison post-test; n = 4-6/group). Analysis of the combined experiment also found a significant reduction in CNS infiltrating macrophages in both C57BL/6.*Tlr2*$^{-/-}$ and C57BL/6.*Tlr9*$^{-/-}$ female mice ($p < 0.05$ in both cases) and a significant reduction in inflammatory monocytes in female C57BL/6.*Tlr2*$^{-/-}$ mice ($p < 0.01$).

As for the T cells, male mutant mice tended to a phenotype more similar to that of WT mice in terms of macrophage/monocyte infiltration. Only male C57BL/6.*Myd88*$^{-/-}$ mice showed statistically significant decreases in numbers of CNS infiltrating DCs and macrophages ($p < 0.05$ and $p < 0.01$ respectively; Kruskal-Wallis Test with Dunn's multiple comparison post-test; $n$ = 7-8/group; Figure 3.7). Analysis of the combined experiment confirmed reduction of DCs, macrophages and inflammatory monocytes in only the male C57BL/6.*Myd88*$^{-/-}$ mice ($p < 0.05$, $p < 0.01$ and $p < 0.05$ respectively; Kruskal-Wallis Test with Dunn's multiple comparison post-test; $n$ = 13/group).

Thus, the milder clinical disease and resistance to EAE seen in female C57BL/6.*Tlr2*$^{-/-}$, C57BL/6.*Tlr9*$^{-/-}$, C57BL/6.*Tlr2*$^{-/-}$*Tlr9*$^{-/-}$ and C57BL/6.*Myd88*$^{-/-}$ mice and male C57BL/6.*Myd88*$^{-/-}$ mice is associated with decreased numbers of CNS infiltrating cells compared to C57BL/6 WT mice.

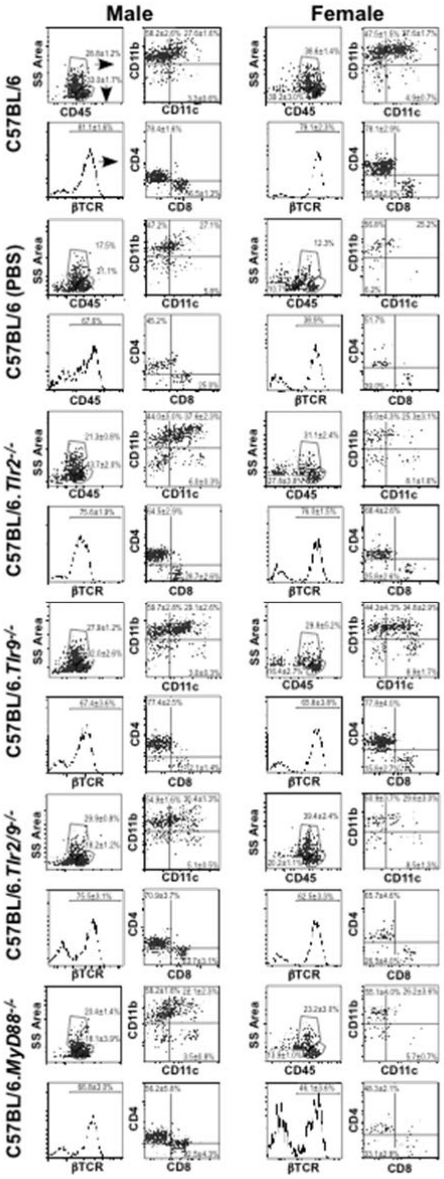


Figure 3.6 Representative gating of FACS analysis showing the proportions of leukocytes from CNS of male and female C57BL/6 (positive and negative control groups), C57BL/6.*Tlr2*$^{-/-}$, C57BL/6.*Tlr9*$^{-/-}$ and C57BL/6.*Tlr2*$^{-/-}$*Tlr9*$^{-/-}$ mice 21 days after $MOG_{35-55}$/CFA/PTX immunisation. Lymphocytes and APCs were detected using side scatter area (SSA) vs CD45. Other cell populations were identified are the following: $CD45^{hi}TCR^{+}CD4^{+}$ were $CD4^{+}$ T cells; $CD45^{hi}TCR^{+}CD8^{+}$ were $CD8^{+}$ T cells; $CD45^{int}SS^{hi}CD11b^{+}CD11c^{-}$ were macrophages/monocytes; $CD45^{int}SS^{hi}CD11b^{+}CD11c^{+}$ were inflammatory monocytes; $CD45^{int}SS^{hi}CD11b^{-}CD11c^{+}$ were dendritic cells (DCs). The mean ± SD of four to six mice per group, except the negative control group that is represented by a single mouse, is indicated in every plot.

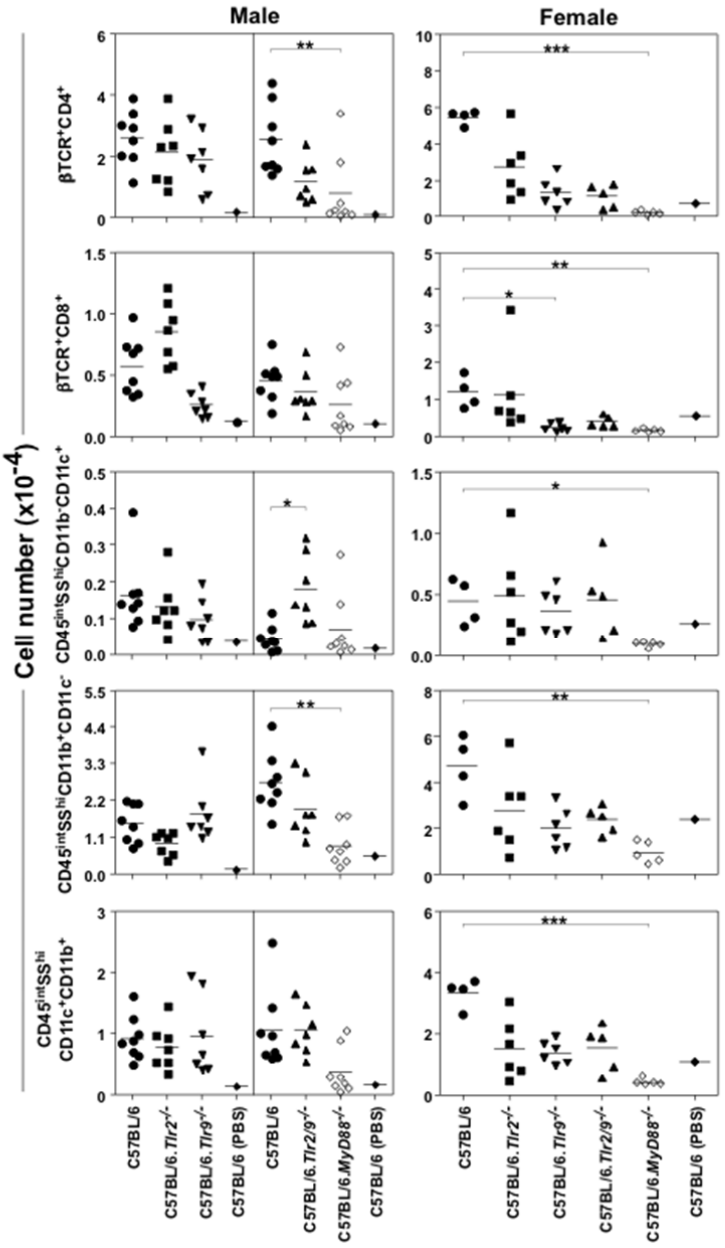


Figure 3.7 CNS-infiltrating leucocytes of C57BL/6 positive control group (closed circles), C57BL/6 negative control group (*closed diamonds*), C57BL/6.*Tlr2*$^{-/-}$ (*closed squares*), C57BL/6.*Tlr9*$^{-/-}$ (*closed downward triangles*), C57BL/6.*Tlr2*$^{-/-}$*Tlr 9*$^{-/-}$ (*closed upward triangles*) and C57BL/6.*Myd88*$^{-/-}$ (*open diamonds*) male and female mice. The left column shows two separated experiments in male mice devided by a vertical line, and the right column shows a single experiment in female mice. Significant differences are indicated (*$p < 0.05$, **$p < 0.01$, ***$p < 0.01$, Kruskal-Wallis test with Dunn's multiple-comparison post-test).

## 3.2.4 Plasma cytokines in active $MOG_{35-55}$/CFA + PTX-induced EAE

TLR ligation triggers the production of inflammatory cytokines in autoimmunity including EAE (Mills et al., 2011). To determine whether target deletion of TLRs affect the development of active $MOG_{35-55}$/CFA + PTX-induced EAE, plasma from C57BL/6 mice and C57BL/6 mice deficient in TLR2, TLR9, TLR2/9 and MyD88 was analyzed at 21 days post-immunisation for IFNβ, GM-CSF, IL-1α, IL-2, IL-4, IL-5, IL-6, IL-10, IL-17, IL-18, IL-23, IFNγ, TNF, CXCL1/KC, and MIP-1β.

Plasma levels of IFN-β (4 to 10 mice per group) were examined using an enzyme-linked immunosorbent assay (ELISA) (PBL Biomedical Laboratories; Piscataway, NJ, USA). IFNß was undetectable in all lines of mice. Plasma levels of GM-CSF, IL-1α, IFNγ, IL-2, IL-4, IL-5, IL-6, IL-10, IL-17, IL-18, IL-23, TNF, CXCL1/KC, and MIP-1β were examined by cytometric bead arrays using Bender Medsystems (Viena, Austria) (4-8 mice per group). Plasma levels of IL5, IL6 and IL18 were significantly increased in male mice deficient in MyD88 ($p < 0.01$, $p < 0.05$, $p < 0.01$ respectively), but not in female mice deficient in MyD88, when compared with C57BL/6 mice (Figure 9). Increased levels of IL18 might be due to an infection, although mice did not show evidence of infection. Plasma levels of IL17 were significantly decreased in female mice deficient in TLR2/9 (*p*

< 0.05) but not in TLR2/9 deficient male mice (Figure 8). No significant differences were observed in the levels of GM-CSF, IL-1α, IFNγ, IL-2, IL-4, IL-10, IL-23, TNF, CXCL1/KC, and MIP-1β. These results discard an association between TLR2, TLR9, TLR2/9 and MyD88 and circulating cytokines in the development of clinical signs of EAE at the peak of the disease, suggesting that circulating cytokines play a role during the induction of EAE not at the peak of disease.

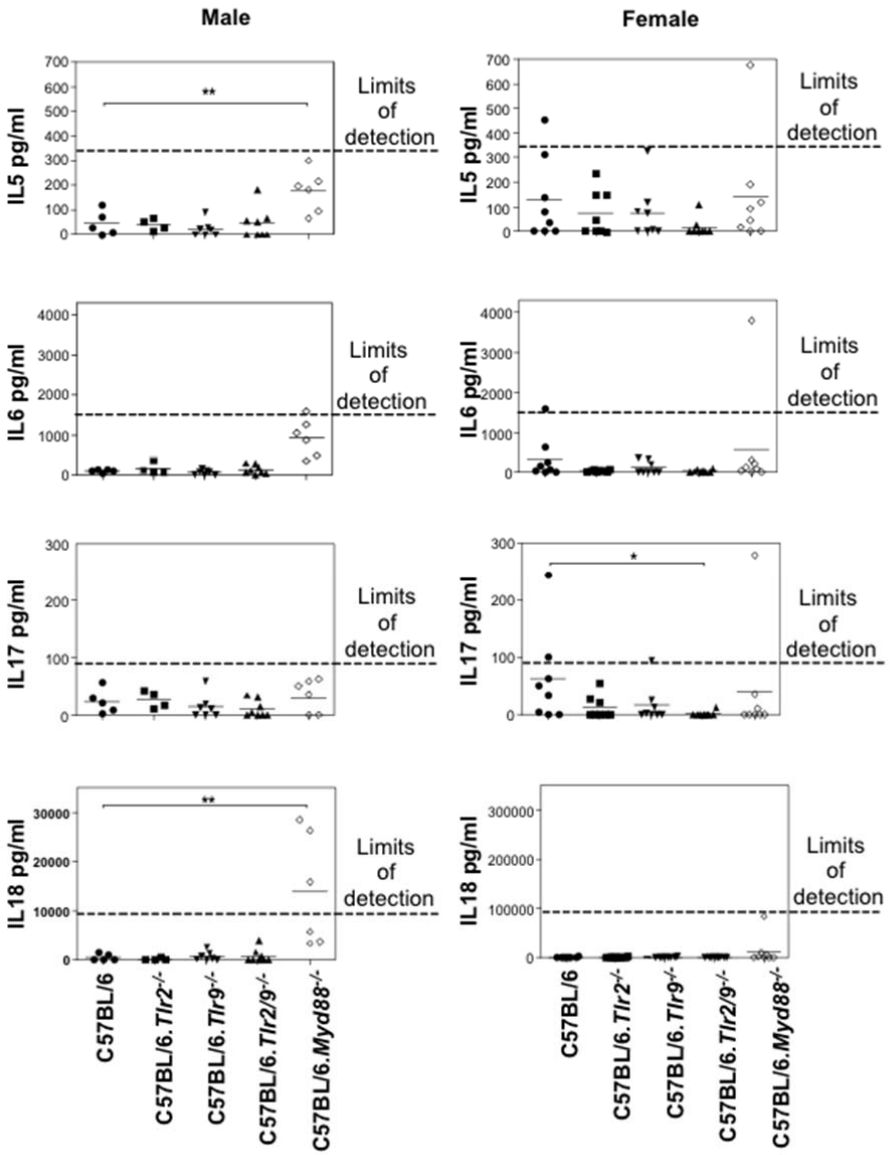


Figure 3.8 Cytokine levels in the plasma of C57BL/6 and C57BL/6.*Tlr*$^{-/-}$ male mice, 21 days after $MOG_{35-55}$/CFA + PTX immunisation. WT mice were compared to C57BL/6 mice deficient in TLR2, TLR9, TLR2/9 and MyD88. Data were considered statically significant when *$p < 0.05$, **$p < 0.01$ (uncorrected Mann Whitney-test *U* test).

## 3.3 Discussion

As previously reviewed in Baxter 2007, the use of CFA and Pertussis toxin were indispensable in this study to induce active EAE suggesting that components of microorganisms are involved in the induction of disease. TLRs recognize PAMP and DAMP and trigger immune responses (Taukeuchi et al., 1999; Hemmi et al., 2000; Alexopoulou et al., 2001; Wang et al., 2004). TLR ligands such as CpG ODN (Segal et al., 2000), LPS (Reynolds et al., 2010; Hansen et al., 2006; Wolf et al., 2007) and zymosan (Hansen et al., 2006) have been successfully used as adjuvants in the induction of EAE, or have been used to modulate the severity of disease, indicating the capacity of TLR signalling to promote the disease.

Consistent with previous studies (Prinz M, et al., 2006; Marta et al., 2008; Lampropoulou et al., 2008), MyD88 signalling was essential for the development of clinical signs and lesions in the CNS in this study. MyD88 is the adaptor molecule for signalling induced by IL1, IL18 and all TLRs, except TLR3 (Adachi et al., 1998; Kumar et al., 2009). Activation of MyD88 by IL1/1L18 promotes the production of IL17 (Kumar et al., 2009; Lalor SJ, et al., 2011). Absences of both IL1 and IL18 have been studied in EAE. $IL1^{-/-}$ mice were reported to show a decrease in the clinical signs of EAE (Sutton C, et al., 2006) while the course of EAE in $IL18^{-/-}$ mice was controversial (Shi FD, et al 2000; Gutcher I, et al., 2006) suggesting that in addition to the role of IL1/1L18 in the phenotype of MyD88 in EAE, TLRs

also participate in the activation of MyD88 to promote or to regulate the production of IL17 in EAE.

TLR1, TLR4 and TLR6 did not contribute to the severity of active $MOG_{35-55}$/CFA + PTX-induced EAE in this study. To my knowledge, this study is the first in discarding a role of TLR1 in EAE. The role of TLR6 was previously reported by Prinz et al., (2006) and confirmed in this study as not necessary to the development of EAE. Whereas TLR1 and TLR6 did not affect the severity of EAE, the contribution of TLR2, TLR4 and TLR9 to EAE is controversial. Mice deficient in TLR4 have been reported to increased severity (Marta et al., 2008), decreased severity and unaffected EAE (Kerfoot et al., 2004). In this study, the absence of TLR4 did not affect the phenotype of active EAE. Differences in the results must be associated to the differences protocols used to induce EAE. TLR9 and TLR2 played a partial role in active EAE in this study. However, previous studies have reported that active EAE is exacerbated (Marta et al., 2008) or decreased in the absence of TLR9 (Prinz et al., 2006); and TLR2 do not affect (Prinz et al., 2006) the severity of EAE (Shaw PJ et al., 2011).

TLR2 can signal as homodimer or else as heterodimer with TLR1 or TLR6; however, neither TLR6 nor TLR1 appear to play a role in active EAE. So in this study TLR2 must be act as a homodimer. The combination of deficiency of TLR2 and TLR9 did not affect the severity of EAE more than

the deficiency of either TLR2 or TLR9 indicating that the role of each receptor is independent of each other. Discrepancies of previous studies in the role of TLR2 and TLR9 could be because of sex susceptibility to EAE as showed in this study.

All together, while male and female mice deficient in MyD88 were completely protected from active EAE, no TLR knockout mice was totally protected from the disease. As the absence of IL1 showed less severe EAE and the absence of IL18 is indistinct in the disease (Shi FD, et al 2000; Gutcher I, et al., 2006; Sutton C, et al., 2006), MyD88 play a definitive role in the pathogenesis of EAE in addition to its role as the adaptor molecule of IL1/1L18/TLRs. EAE is dependent of the activation of MyD88 by IL1, TLR2 and TLR9.

# CHAPTER 4

# CHAPTER 4

# ROLE FOR TLR2 AND TLR9 IN PASSIVE EAE

## 4.1 Introduction

The most common animal model to study Multiple Sclerosis is EAE. The two main types of EAE are: 1) active EAE, induced with autoantigen, such as MOG, adjuvants, for example CFA, and PTX, and 2) passive EAE which is induced by adoptive cell transfer from donors to recipients (Stromnes et al., 2006; Miller et al., 2007).

The active form of EAE involves the use of killed *M. tuberculosis* as a component of the adjuvant. *M. tuberculosis* possess agonists for TLR2 (Brightbill et al., 1999; Jones et al., 2001; Means et al., 1999; Thoma-Uszynski et al., 2000), TLR4 (Means et al., 1999; Thoma-Uszynski et al., 2000; Abel et al., 2002; Brian et al., 2002) and TLR9 (Bafica et al., 2005). In the previous chapter we found that the severity of active $MOG_{35-55}$/CFA + PTX–induced EAE decreased in the absence of TLR2 and TLR9. An explanation for the relative resistance of C57BL/6.*Tlr2*$^{-/-}$ and C57BL/6.*Tlr9*$^{-/-}$ to $MOG_{35-55}$/CFA + PTX–induced EAE is that the suppression of TLR2 and TLR9 signalling inhibited the adjuvant activity of CFA. To determine

whether the adjuvant activity of CFA is inhibited in the absence of TLR2 and TLR9, the passive form of EAE was examined in C57BL/6, C57BL/6.*Tlr2*$^{-/-}$ and C57BL/6.*Tlr9*$^{-/-}$ mice.

In addition to the action of CFA in EAE, a question remains, what could trigger TLR2 and TLR9 signalling? Recently evidence implicates microbiota in autoimmune diseases including MS and EAE (Fung et al., 2012). For example: Li et al., (2007) reported that *H. pylori* is associated with protection against MS in the Japanese population. Berer et al., (2011) reported that commensal gut flora is essential to trigger myelin specific $CD4^+$ T cells in relapsing-remitting EAE. Lee et al., (2011) found that germ-free mice decreased the severity of EAE compared with mice colonized with normal flora; and colonization with segmented filamentous bacteria (SFB) induces $CD4^+$ T cells, which produce IL17 in CNS. Decrease of clinical signs of EAE was associated with lower levels of IFNγ and IL17, and increase numbers of Tregs. In addition, Lee et al., (2011) showed that mice infected with SFB are able to restore the severity of EAE (Lee et al., 2011). Thus, a possible explanation that trigger TLR2 and TLR9 signalling is microflora, which could partially regulate autoimmune responses via these TLRs. To determine whether microflora could be responsible for TLR dependent EAE, the clinical course of passive EAE was analysed in C57BL/6.*Tlr9*$^{-/-}$ and C57BL/6.*Tlr2*$^{-/-}$ female mice treated with amoxocilin, clarithromycin, metronidazole and omeprazole.

# 4.2 Results

## 4.2.1 Absence of PTX and irradiation in passive EAE

The passive EAE mouse model used in this study have a number of refinements in order to increase the severity of disease. In this model, cells adoptively transfer the disease from active immunized donors after reactivation *in vitro* into preconditioned mice by irradiation and immunized with PTX, as described in chapter 2. To determine the importance of PTX and irradiation in passive EAE, we characterised the effect of PTX and irradiation in our mouse model by inducing the disease in three different forms: 1) passive EAE with both PTX and gamma irradiation (control group); 2) passive EAE with PTX in the absence of gamma irradiation; 3) passive EAE with gamma irradiation in the absence of PTX.

Mice treated with PTX together with irradiation, as well as those only immunized with PTX, showed clinical signs of disease (Table 4.1). Five mice from a group of six mice treated with irradiation in the absence of PTX showed clinical signs of disease (Table 4.1). Mice treated with both irradiation and PTX showed more severe maximum clinical score ± SEM (3.00 ± 0.00) and CDI ± SEM (41.33 ± 5.51) compared to mice treated only with irradiation (maximum clinical score ± SEM = 1.58 ± 0.32, $p < 0.01$ and

CDI ± SEM = 11.75 ± 3.29, $p < 0.01$) or mice treated only with PTX (maximum clinical score ± SEM = 2.41 ± 0.20, $p < 0.05$ and CDI ± SEM = 24.92 ± 4.30, $p < 0.05$) (Table 4.1). Because the use of PTX and irradiation in the passive EAE mouse model showed 100% incidence of EAE and developed more severe disease, the mouse model was used in subsequent experiments.

Table 4.1 Passive EAE in C57BL/6 mice treated with or without PTX and irradiation.

| Strain | *n* | Irradiation | Pertussis Toxin | Incidence (%) | Mean Maximum Score | Cumulative Disease Index (CDI) |
|---|---|---|---|---|---|---|
| [a] C57BL/6 | 6 | Yes | Yes | 100 | 3.00±0.00 | 41.33±5.51 |
| [b] C57BL/6 | 6 | No | Yes | 100 | 2.41±0.2* | 24.92±4.30* |
| [c] C57BL/6 | 6 | Yes | No | 83.3 | 1.58±0.32** | 11.75±3.29** |

Leukocytes from spleen and lymph nodes from donor mice immunized with CFA, PTX and $MOG_{35-55}$ were reactivated *in vitro* and transferred into recipient mice with different treatments. [a] Irradiated C57BL/6 mice plus PTX, [b] no irradiated C57BL/6 mice plus PTX, [c] irradiated C57BL/6 mice without PTX. Statistical differences comparing irradiated C57BL/6 mice plus PTX with no irradiated C57BL/6 mice plus PTX and irradiated C57BL/6 mice without PTX are indicated (*$p < 0.05$, **$p < 0.01$, ***$p < 0.001$; uncorrected Mann-Whitney U test).

## 4.2.2 The absence of TLR4 in the severity of passive EAE

It has been reported that PTX signal via TLR4 (Kerfoot et al., 2004; Nishida et al., 2010). Although the phenotype of active $MOG_{35-55}$/CFA+PTX–induced EAE was similar between C57BL/6.*Tlr4*$^{-/-}$ mice and C57BL/6 mice (WT-control group) (data showed in chapter 3), it remains possible that it did contribute to the activity of PTX in a passive model in either sex. Similarly, studies indicate that irradiation produces intrinsic TLR4 agonists (Apetoh et al., 2007), as well as the translocation of commensal gut microflora into mesenteric lymph nodes and elevation of circulating LPS (Paulos et al., 2007). To clarify the role of TLR4 in EAE, the passive form of EAE was induced in C57BL/6 (control group) and C57BL/6.*Tlr4*$^{-/-}$ female mice.

C57BL/6 mice deficient in TLR4 showed clinical signs of EAE (Figure 4.1). The clinical course of passive EAE in the absence of TLR4 decreased during six days (day 25 to day 30). The onset day of disease was delayed (20.17 ± 0.70 days, $p < 0.01$) and the CDI ± SEM was decreased (20.42 ± 5.15, $p < 0.05$) in C57BL/6.*Tlr4*$^{-/-}$ female mice compared with C57BL/6 female mice (13.33 ± 2.02 days and CDI ± SEM = 41.33 ± 5.51). However, no difference was seen in maximum score of disease between C57BL/6.*Tlr4*$^{-/-}$ and C57BL/6 mice (Figure 4.1).

Although clinical signs of EAE were decreased in the absence of TLR4 in passive EAE, the inhibition of disease was not as great as in the mice that lacked PTX, indicating that, if PTX does not act through TLR4, it is also likely to have activities mediated by other mechanisms in this model.

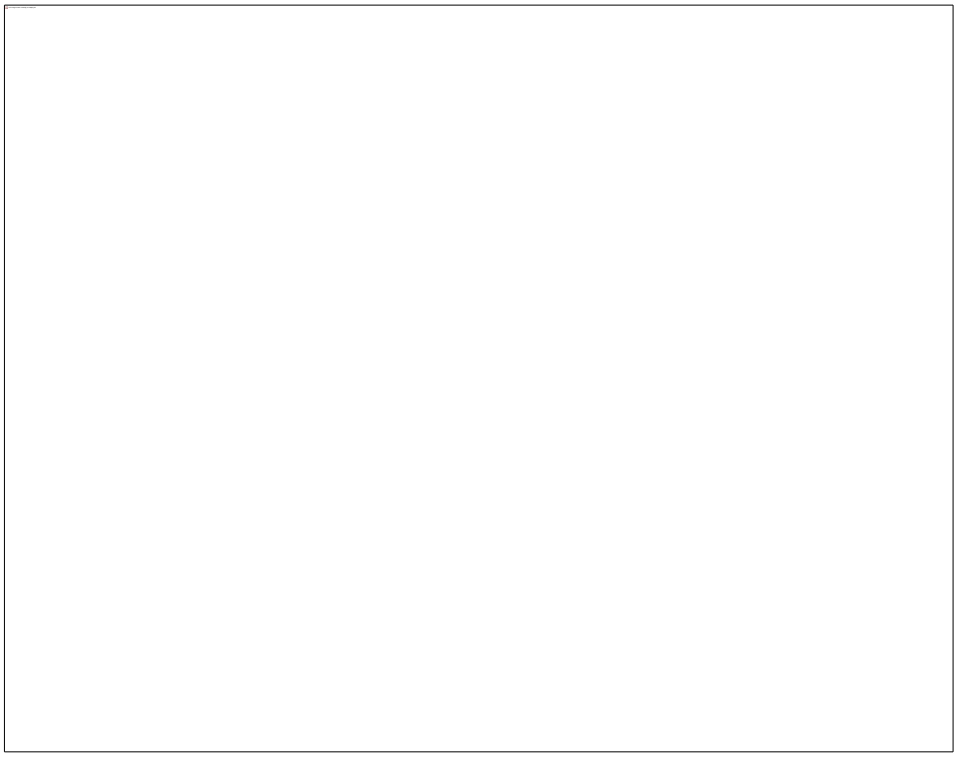

Figure 4.1 Analysis of the clinical course of passive EAE in female C57BL/6 (*closed circles*) and C57BL/6.*Tlr4*$^{-/-}$ (*open circles*) mice. Significant differences in the clinical score per day between C57BL/6 and C57BL/6.*Tlr4*$^{-/-}$ mice are indicated (*$p < 0.05$). Differences in the onset of disease, maximum clinical score and cumulative disease are shown (*$p < 0.05$, **$p < 0.01$, ***$p < 0.001$ uncorrected Mann-Whitney *U* test; $n = 6$).

## 4.2.3 TLR9 and TLR2 in passive EAE

CFA contains *M. tuberculosis* and TLR2, TLR4 and TLR9 are activated in response to *M. tuberculosis* (Brightbill et al., 1999; Means et al., 1999; Thoma-Uszynski et al., 2000; Jones et al., 2001; Abel et al., 2002; Bafica et al., 2005). Passive EAE is induced in the absence of CFA. Previously we found that TLR4 did not play a major role neither in active EAE nor passive EAE. However, it is possible that target deletion of *Tlr2* and *Tlr9* decreased the severity of active $MOG_{35-55}$/CFA+PTX–induced EAE because the lack of TLR2 and TLR9 signalling suppress the adjuvant action of CFA. To determine whether the components of killed *Mycobacteria tuberculosis* used as adjuvant in active $MOG_{35-55}$/CFA + PTX–induced EAE were responsible for TLR2 and TLR9 dependent disease; the passive form of EAE was examined in the absence of TLR2 and TLR9.

A pool analysis of three independent experiments in female mice showed that the clinical course of passive EAE decreased during 10 days (day 25 to day 34) in C57BL/6.*Tlr9*$^{-/-}$ mice compared to C57BL/6 ($p < 0.5$) (Figure 4.2). The clinical signs of disease were less severe in the absence of TLR9 (mean maximum score ± SEM = 1.6 ± 0.4, $p < 0.5$) compared to C57BL/6 mice (mean maximum score ± SEM = 2.8 ± 0.2) (Table 4.2 and Figure 4.2). The onset of disease was not affected in any of the three experiments or combined experiments. Although the CDI showed significant differences in one of three independent experiments between C57BL/6.*Tlr9*$^{-/-}$ (CDI ± SEM

= 4.4 ± 1.5, $p < 0.01$) and C57BL/6 (CDI ± SEM = 34.4 ± 4.7), the pool analysis of the three experiments did not show differences (Table 4.2 and Figure 4.2). In contrast, five independent experiments in both male and female showed that the absence of TLR2 completely protect mice from the passive form of EAE (Table 4.2, Figure 4.3 and figure 4.4).

Table 4.2 Passive EAE in TLR-deficient C57BL/6 mice and C57BL/6 WT control mice

| Experiment | Strain | *n* | Incidence (%) | Onset (days) | Mean Maximum Score | Cumulative Disease Index (CDI) |
|---|---|---|---|---|---|---|
| Female | | | | | | |
| Exp 1 | C57BL/6 | 5 | 100 | 17.0±2.3 | 2.8±0.2 | 34.4±4.7 |
| | C57BL/6.*Tlr2*$^{-/-}$ | 3 | 0 | Na | 0.0±0.0* | 0.0±0.0* |
| | C57BL/6.*Tlr9*$^{-/-}$ | 5 | 80 | 13.8±1.8 | 1.6±0.4* | 25.1±9.3 |
| Exp 2 | C57BL/6 | 6 | 100 | 23.8±0.5 | 2.7±0.2 | 21.8±2.1 |
| | C57BL/6.*Tlr2*$^{-/-}$ | 4 | 0 | Na | 0.0±0.0** | 0.0±0.0** |
| | C57BL/6.*Tlr9*$^{-/-}$ | 4 | 100 | 23.3±1.3 | 1.5±0.2** | 4.4±1.5** |
| Exp 3 | C57BL/6 | 4 | 100 | 19.5±1.8 | 2.5±0.5 | 33.4±7.9 |
| | C57BL/6.*Tlr2*$^{-/-}$ | 6 | 0 | Na | 0.0±0.0** | 0.0±0.0** |
| | C57BL/6.*Tlr9*$^{-/-}$ | 5 | 100 | 19.4±2.8 | 2.1±0.5 | 26.0±11.1 |
| Combined | C57BL/6 | 15 | 100 | 20.4±1.2 | 2.7±0.2 | 29.1±3.0 |
| | C57BL/6.*Tlr2*$^{-/-}$ | 13 | 0 | Na | 0.0±0.0*** | 0.0±0.0*** |
| | C57BL/6.*Tlr9*$^{-/-}$ | 14 | 92.8 | 18.8±0.5 | 1.8±0.2** | 19.5±5.5 |
| Male | | | | | | |
| Exp 1 | C57BL/6 | 4 | 100 | 23±1.0 | 2.6±0.4 | 16.9±3.2 |
| | C57BL/6.*Tlr2*$^{-/-}$ | 3 | 0 | Na | 0.0±0.0 | 0.0±0.0 |
| Exp 2 | C57BL/6 | 6 | 100 | 21±0.2 | 3.0±0.0 | 22.8±2.4 |
| | C57BL/6.*Tlr2*$^{-/-}$ | 6 | 0 | Na | 0.0±0.0** | 0.0±0.0** |
| Combined | C57BL/6 | 10 | 100 | 21.8±0.5 | 2.8±0.1 | 18.9±1.9 |
| | C57BL/6.*Tlr2*$^{-/-}$ | 9 | 0 | Na | 0.0±0.0*** | 0.0±0.0*** |

Passive EAE was induced by adoptive transfer of *in vitro* activated lymph nodes and splenocytes from $MOG_{35-55}$/CFA immunized C57BL/6 mice into C57BL/6.*Tlr2*$^{-/-}$, C57BL/6.*Tlr9*$^{-/-}$ and C57BL/6 (control WT mice). Mean ± SEM of the clinical scores of EAE. Statistical differences between B6 WT control mice and TLR-deficient mice for TLR2 and TLR9 are indicated (*$p < 0.05$, **$p < 0.01$, ***$p < 0.001$; uncorrected Mann-Whitney U test). na = not appropriate.

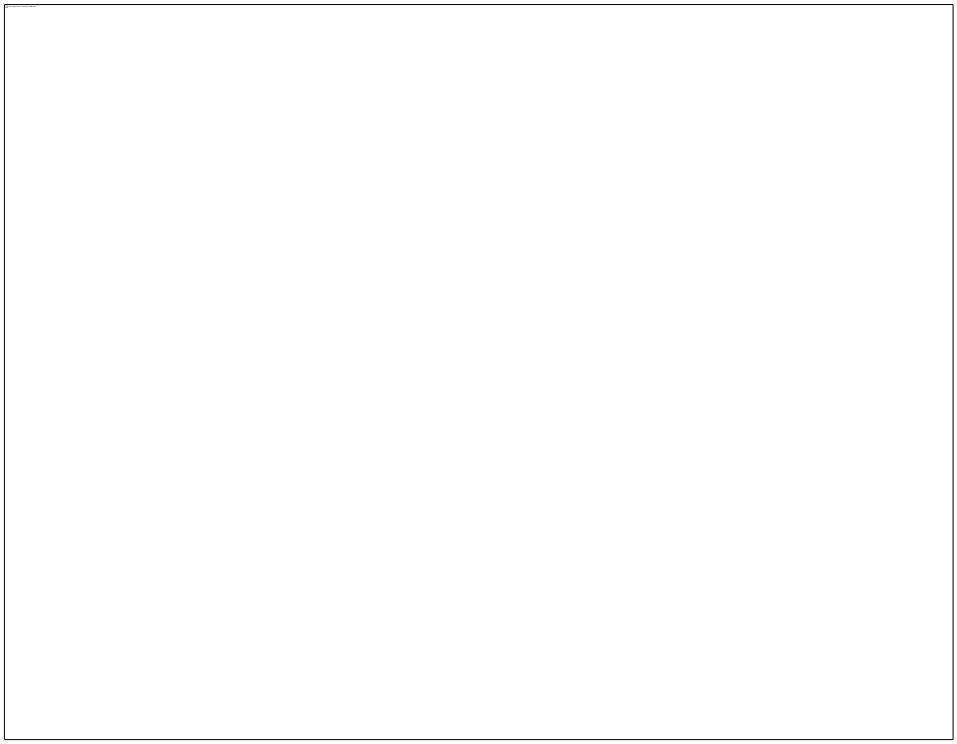

Figure 4.2 Analysis of the clinical course of passive EAE in female C57BL/6 (*closed circles*) and C57BL/6.*Tlr9*$^{-/-}$ (*open circles*) mice. Data pool from three experiments using female donors and recipients. Significant differences in the clinical score per day between C57BL/6 and C57BL/6.*Tlr9*$^{-/-}$ mice are indicated (*$p < 0.05$). Differences in the onset of disease, maximum clinical score and cumulative disease are shown (*$p < 0.05$, **$p < 0.01$, ***$p < 0.001$ uncorrected Mann-Whitney *U* test; $n = 6$).

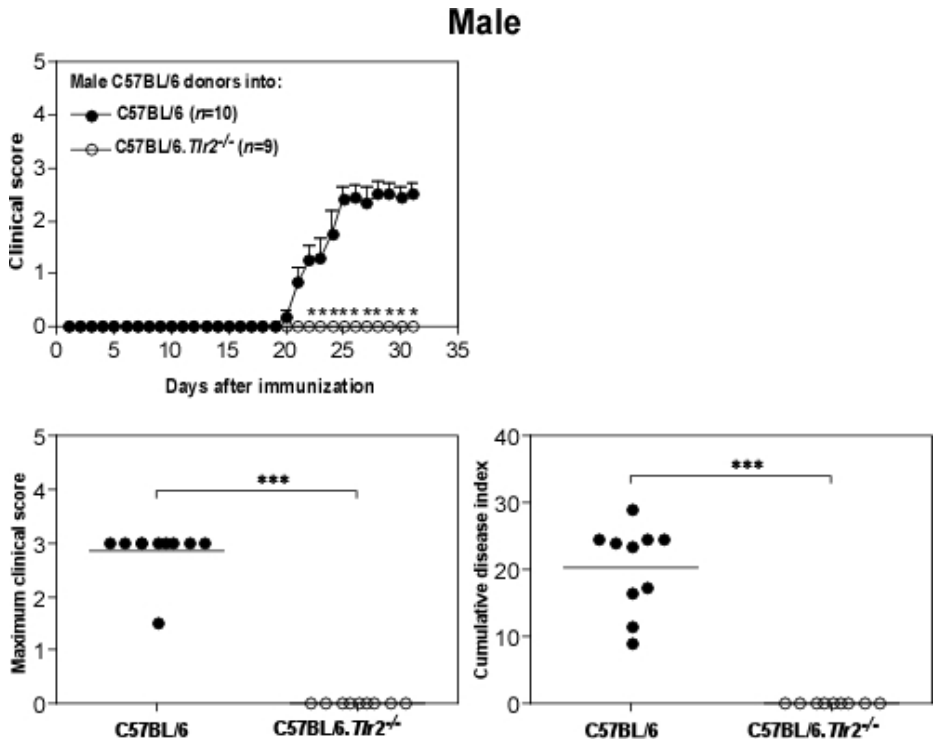


Figure 4.3 Analysis of the clinical course of passive EAE in male C57BL/6 (*closed circles*) and C57BL/6.*Tlr2*$^{-/-}$ (*open circles*) mice. Data pool from two experiments using male donors and recipients. Significant differences in the clinical score per day between C57BL/6 and C57BL/6.*Tlr2*$^{-/-}$ mice are indicated (*$p < 0.05$). Differences in the onset of disease, maximum clinical score and cumulative disease are shown (*$p < 0.05$, **$p < 0.01$, ***$p < 0.001$ uncorrected Mann-Whitney *U* test; $n = 9$-10).

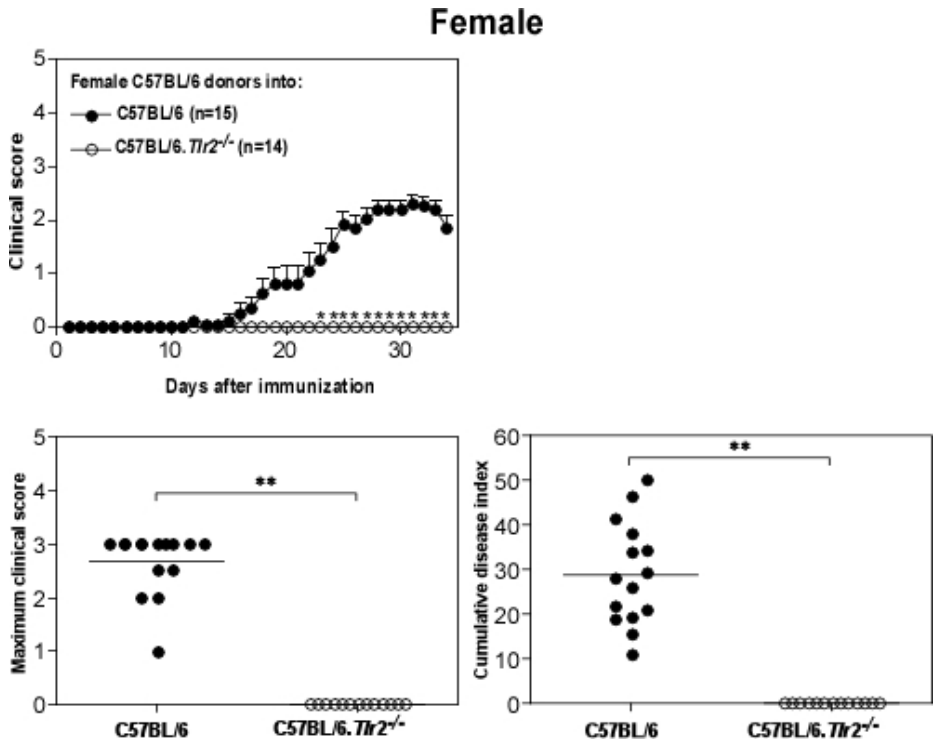


Figure 4.4 Analysis of the clinical course of passive EAE in female C57BL/6 (*closed circles*) and C57BL/6.*Tlr2*$^{-/-}$ (*open circles*) mice. Data pool from three experiments using female donors and recipients. Significant differences in the clinical score per day between C57BL/6 and C57BL/6.*Tlr2*$^{-/-}$ mice are indicated (*$p < 0.05$). Differences in the onset of disease, maximum clinical score and cumulative disease are shown (*$p < 0.05$, **$p < 0.01$, ***$p < 0.001$ uncorrected Mann-Whitney *U* test; $n = 6$).

Because mice deficient in TLR2 did not show clinical signs of passive EAE, a further examination of the role of TLR2 in passive EAE was done in female mice by adoptive transfers from: a) C57BL/6 into C57BL/6 (control group); b) C57BL6.*Tlr2*$^{-/-}$ into C57BL6.*Tlr2*$^{-/-}$; c) C57BL6.*Tlr2*$^{-/-}$ into C57BL/6; d) C57BL/6 into C57BL6.*Tlr2*$^{-/-}$.

Leucocytes transferred from C57BL/6 into C57BL/6 mice resulted in severe clinical course of passive EAE, while C57BL/6 leukocytes into C57BL/6.*Tlr2*$^{-/-}$ mice did not show clinical signs of disease (Figure 4.5) ($p < 0.05$). The adoptive transfer of leukocytes from C57BL/6.*Tlr2*$^{-/-}$ into C57BL/6, and C57BL/6.*Tlr2*$^{-/-}$ into C57BL/6.*Tlr2*$^{-/-}$ resulted in a lower clinical course of disease compared with leucocytes transferred from C57BL/6 into C57BL/6 mice ($p < 0.05$) (Figure 4.5).

The onset ± SEM of passive EAE was delayed when leukocytes were transferred from: C57BL6.*Tlr2*$^{-/-}$ into C57BL6.*Tlr2*$^{-/-}$ (26.6 ± 0.94 days, $p < 0.001$); C57BL6.*Tlr2*$^{-/-}$ into C57BL/6 (28.0 ± 1.15 days, $p < 0.001$) compared with leukocytes transferred from C57BL/6 into C57BL/6 (13.3 ± 0.28 days) (Figure 4.5).

The maximum clinical scores ± SEM were less severe when leukocytes were transferred from: C57BL6.*Tlr2*$^{-/-}$ into C57BL/6 (1.88 ± 0.30, $p < 0.05$)

compared with leukocytes transferred from C57BL/6 into C57BL/6 (3.0 ± 0.0). No differences in the maximum clinical score were seen when leukocytes were transferred from C57BL6.*Tlr2*$^{-/-}$ into C57BL6.*Tlr2*$^{-/-}$ compared with leukocytes transferred from C57BL/6 into C57BL/6 (Figure 4.5).

The CDI ± SEM was decreased when leukocytes were transferred from: C57BL6.*Tlr2*$^{-/-}$ into C57BL6.*Tlr2*$^{-/-}$ (8.95 ± 2.39, $p < 0.001$); C57BL6.*Tlr2*$^{-/-}$ into C57BL/6 (5.44 ± 2.34, $p < 0.01$) compared with leukocytes transferred from C57BL/6 into C57BL/6 (41.33 ± 5.51) (Figure 4.5).

These results confirm that TLR2 plays a role in exacerbating the severity of EAE. The prevention of clinical signs of EAE in TLR2-deficient recipients of WT cells suggests that the presence of receptor at induction of EAE creates a dependence on TLR2 signalling in the effector phase.

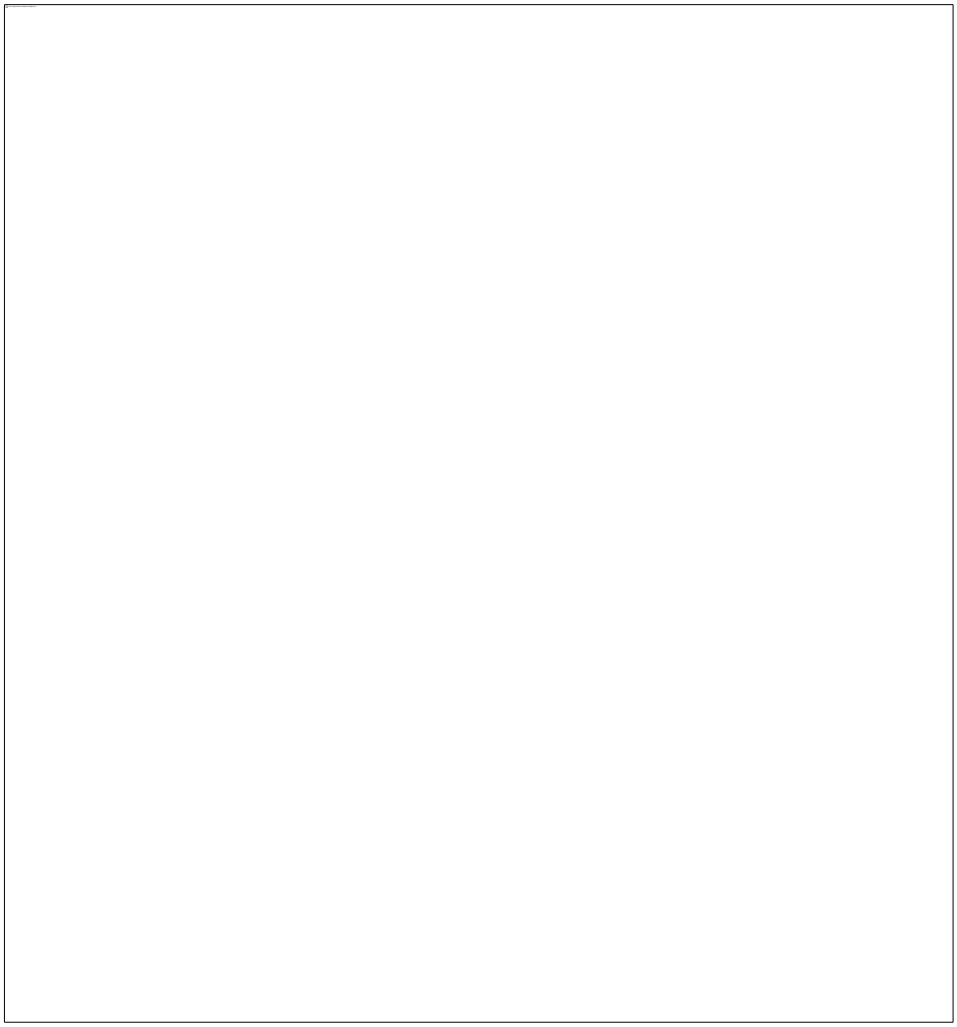

Figure 4.5 Analysis of the clinical course of passive EAE in female mice. Data pool from three experiments using female donors and recipients. Adoptive transfer from: C57BL/6 into C57BL/6 *(closed circles)*, C57Bl/6.*Tlr2*$^{-/-}$ into C57Bl/6.*Tlr2*$^{-/-}$ *(upward triangles)*, C57Bl/6.*Tlr2*$^{-/-}$ into C57BL/6 *(closed diamonds)*, C57BL/6 into C57Bl/6.*Tlr2*$^{-/-}$ *(closed squares)*. Significant differences in the clinical score per day are indicated (*$p < 0.05$). Differences in the onset of disease, maximum clinical score and cumulative disease are shown (*$p < 0.05$, **$p < 0.01$, ***$p < 0.001$ uncorrected Mann-Whitney *U* test; $n = 6$-10).

## 4.2.4 $CD4^+$ T cells in the CNS in passive EAE

Potential explanations for the relative resistance of C57BL6.*Tlr2*$^{-/-}$ and C57BL6.*Tlr9*$^{-/-}$ mice to passive EAE involve effects on recruitment of inflammatory cells to the CNS. To determine whether inflammatory cells could accumulate in CNS in the absence of TLR2 and TLR9 in passive EAE, leucocytes from brain and spinal cord were isolated and analysed by flow cytometry 34 days after passive transfer of leukocytes from female C57BL/6 donors into female C5BL6.*Tlr9*$^{-/-}$ and C5BL6.*Tlr2*$^{-/-}$ recipients (Figure 4.6).

Consistent with the clinical signs of passive EAE, C5BL6.*Tlr2*$^{-/-}$ mice had fewer total numbers of CNS-infiltrating $CD4^+$ T cells ± SEM (0.8 ± 0.01, $p < 0.01$; pair wise Mann Whitney U test) than C57BL/6 mice (0.64 ± 0.25) (Figure 4.7). C5BL6.*Tlr2*$^{-/-}$ mice also had less MFI ± SEM of CNS-infiltrating myeloid DCs (85.50 ± 1.26, $p < 0.05$) compared with C57BL/6 mice (108.3 ± 7.58) (Figure 4.8). No differences in total numbers of $TCR^+CD8^+$ T cells and $CD11b^+Ly6C^{hi}CCR2^{hi}$ (inflammatory macrophages) in the CNS were observed in C5BL6.*Tlr9*$^{-/-}$ and C5BL6.*Tlr2*$^{-/-}$ compared to C57BL/6 mice (Figure 4.7). Thus, the absence of TLR2 diminished the entry of inflammatory cells in the CNS.

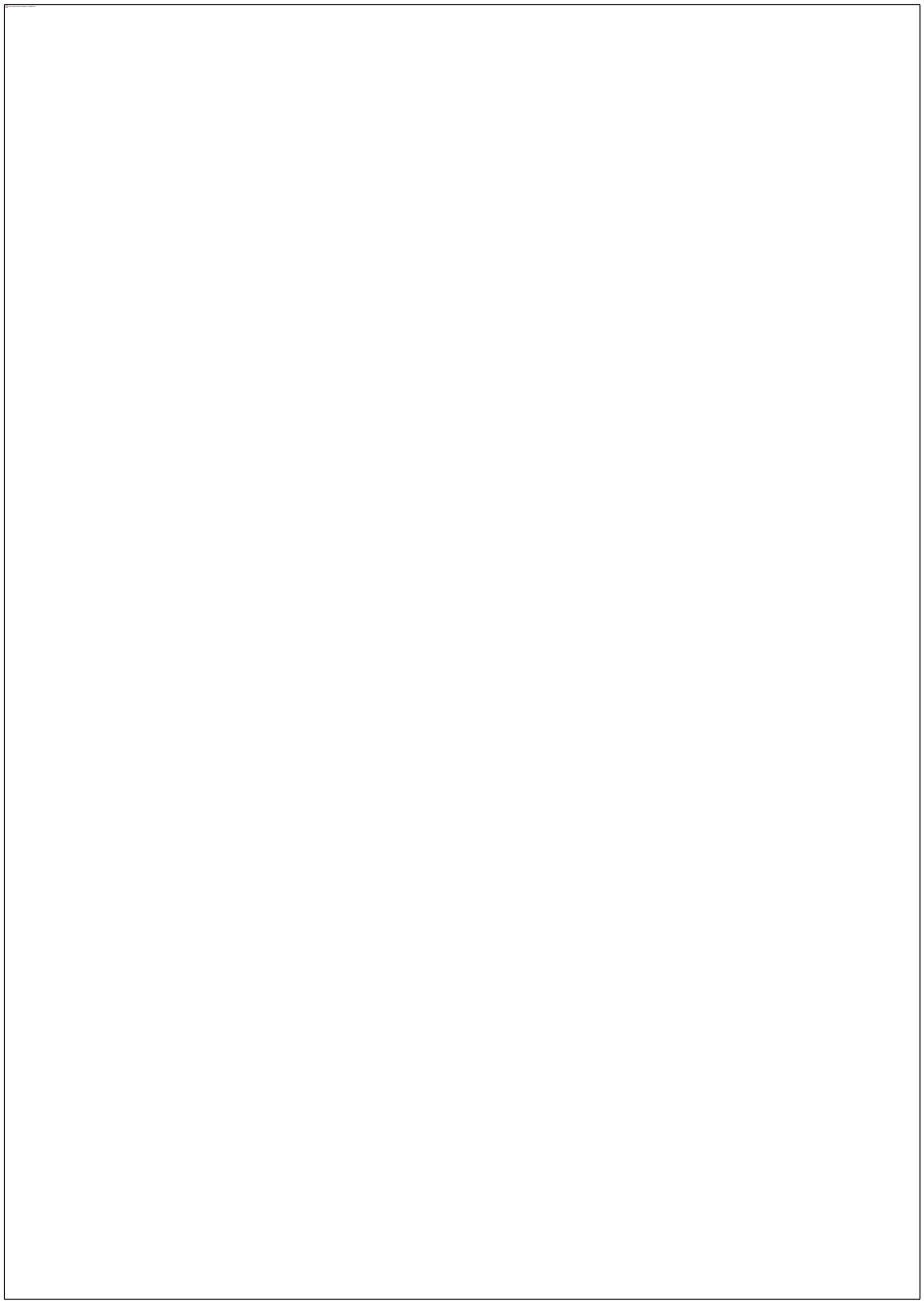

Figure 4.6 Representative FACS analysis showing the proportions of brain and spinal cord leukocytes from female C57BL/6, C57BL/6 (PBS), C57BL/6.*Tlr2*$^{-/-}$ and C57BL/6.*Tlr9*$^{-/-}$, 34 days after adoptive transfer of EAE. Lymphocytes were identified as CD45$^{hi}$ and SSA$^{low}$. βTCR in combination with CD4 or CD8 were used to detect CD4$^{+}$ and CD8$^{+}$ T cells respectively. Inflammatory macrophages were Ly6C$^{+}$CCR2$^{+}$ and myeloid DCs were CD11b$^{+}$CD11c$^{+}$.

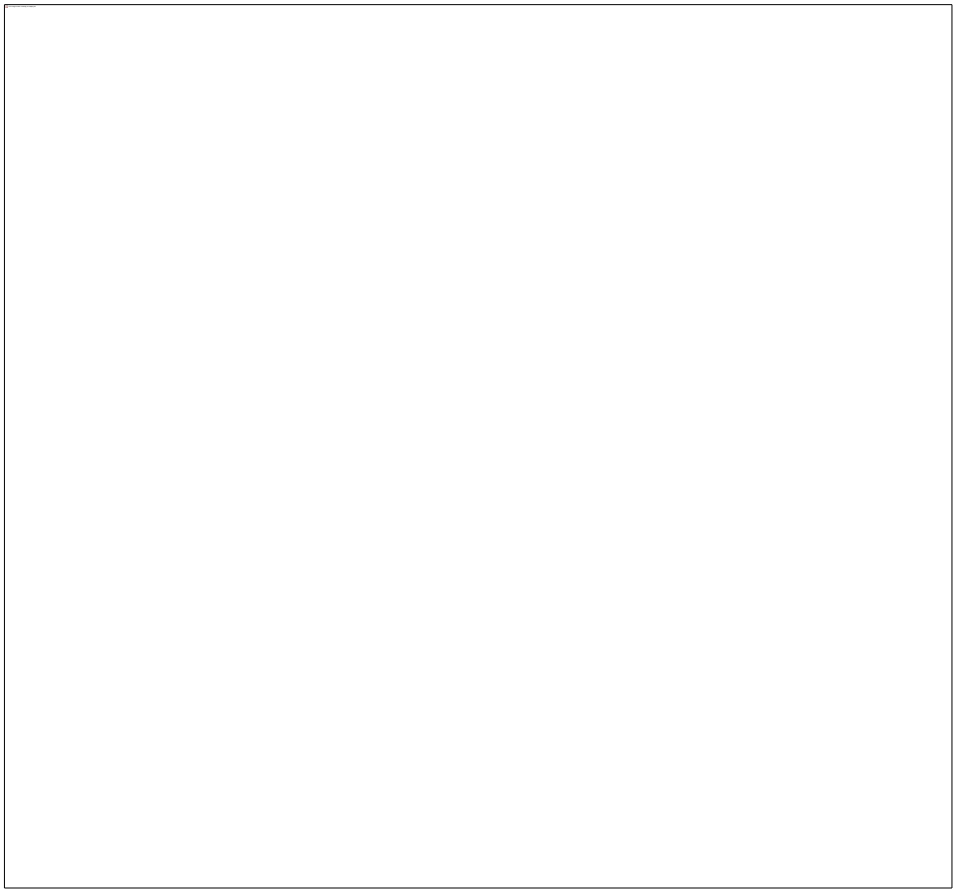

Figure 4.7 Absolute numbers of $CD4^+$ T cells, $CD8^+$ T cells, inflammatory macrophages and, myeloid dendritic cells (MFI- mean fluorescence intensity) in the CNS of C57BL/6 (*closed cicles*), C57BL/6.*Tlr2*$^{-/-}$ (*closed squares*), C57BL/6.*Tlr9*$^{-/-}$ (*downward closed triangles*), C57BL/6 (PBS) (*closed diamonds*) female mice. Statistical differences between the C57BL/6.*Tlr-deficient* mice and C57BL/6 control group are indicated (*$p < 0.05$, **$p < 0.01$, ***$p < 0.001$ uncorrected Mann-Whitney *U* test; $n$ = 1-6).

## 4.2.5 $CD4^+$ T cells secreting IL17 in the absence of TLR2 in the CNS

As $CD4^+$ T cells decreased in the absence of TLR2 in the CNS, and both $CD4^+$ T cells and IL17 play a crucial role in EAE (Harrington et al., 2005; Park et al., 2005), the secretion of IL17 by $CD4^+$ T cells were examined in the CNS and spleen in passive EAE. Leucocytes from mice with passive EAE were isolated from CNS and spleens 30 days after the induction of disease. CNS leukocytes and splenocytes were stimulated *in vitro* with PMA as described in the Chapter 2 and analyzed by flow cytometry (Figure 4.8).

Four independent experiments for both males ($n$ = 3-6 mice) and females (n = 5-6 mice) showed that the total numbers of $CD4^+$ T cells secreting IL17 ± SEM was reduced in the absence of TLR2 in the CNS of both sexes (males: 0.03 ± 0.00, $p < 0.05$; females: 0.00 ± 0.00, $p < 0.01$) compared with the C57BL/6 mice (males 0.15 ± 0.03, females 0.18 ± 0.04) (Figure 4.8). However, no differences were seen in the total numbers $CD4^+$ T cells secreting IL17 in spleens when compared with C57BL/6 mice (Figure 4.8). These results indicated that TLR2 signalling is required for the secretion of IL17 by $CD4^+$ T cells infiltrating the CNS.

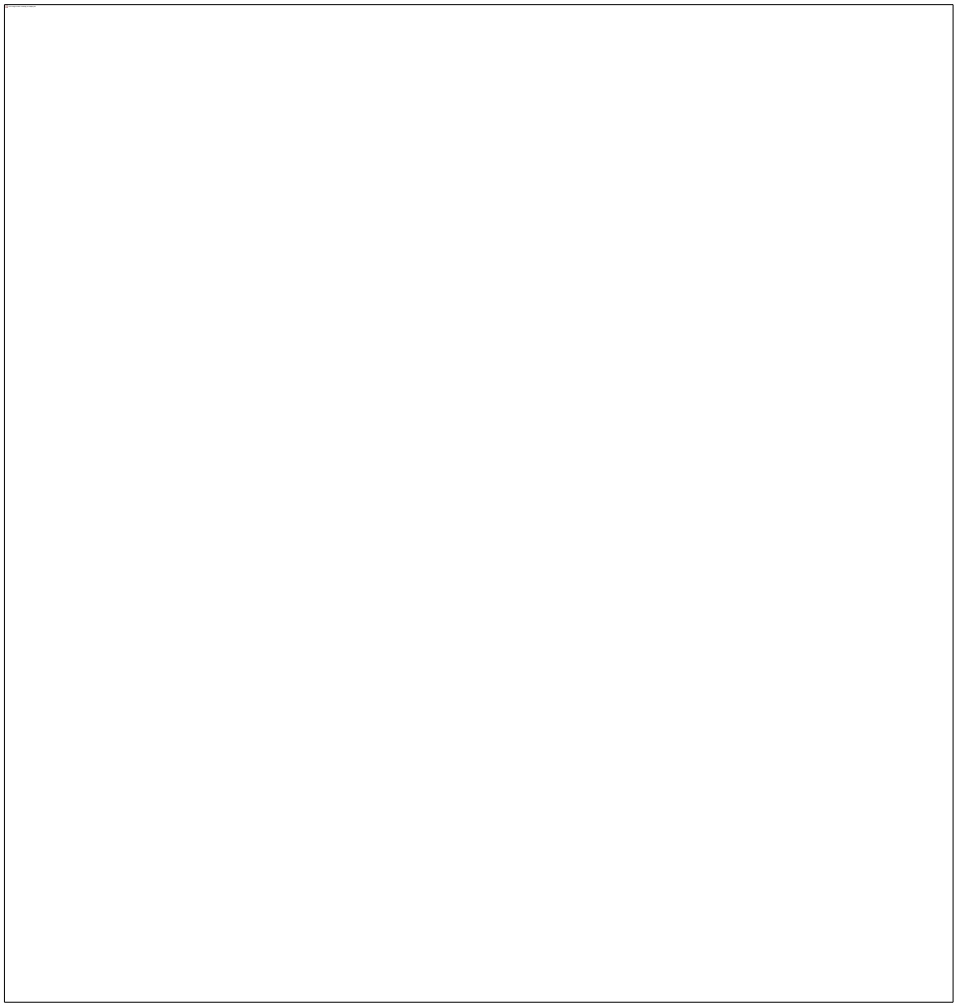

Figure 4.8 Representative experiments of IL17 secretion of Central Nervous System leukocytes and splenocytes from naive mice, and mice with passive EAE. Cells were stimulated with PMA and controls were not stimulated. Unstimulated naive C57BL/6 cells (*closed diamonds*), stimulate naive C57BL/6 cells (*open diamonds*), unstimulated C57BL/6 cell from mice with passive EAE (*closed squares*), stimulated C57BL/6 cells from mice with passive EAE (*closed cicles*), unstimulated C57BL/6.*Tlr2*$^{-/-}$ cells from mice with passive EAE (open squeare), stimulated C57BL/6.*Tlr2*$^{-/-}$ cells from mice with passive EAE (*open circles*). Significant data are indicated (*$p < 0.05$, **$p < 0.01$, ***$p < 0.001$ uncorrected Mann-Whitney *U* test; $n = 1$-6).

## 4.2.6 Absolute numbers of CD62L-expressing Tregs in the absence of TLR2

Tregs and Tregs subsets have been associated with the suppression of Th17 cells (Ichiyama et al., 2008). For example, activation of CD62L-expressing Tregs suppresses autoimmunity by the production of regulatory cytokines such as IL10 (Lau et al., 2008). It is possible that the reduced number of $CD4^+$ T cells and $CD4^+$ T cells secreting IL17 observed in the CNS in C57BL/6.*Tlr2*$^{-/-}$ mice is associated with the activity of regulatory Tregs or CD62L-expressing Tregs. To examine whether Tregs or CD62L-expressing subset of splenic Tregs is associated with the suppression of activation and expansion of autoreactive T cells in the absence of TLR2, splenic Tregs were analyzed by flow cytometry after the induction of passive EAE in C57BL/6 and C57BL/6.*Tlr2*$^{-/-}$ (Figure 4.9).

The total numbers of Tregs were similar between C57BL/6 and C57BL/6.*Tlr2*$^{-/-}$ in male and female mice. However, C57BL/6.*Tlr2*$^{-/-}$ male had more total numbers of Tregs expressing $CD62L^+$ in spleens (mean ± SEM = 22.69 ± 1.79, $p < 0.5$) than C57BL/6 male mice (mean ± SEM = 15.61 ± 1.61) (Figure 4.10). C57BL/6.*Tlr2*$^{-/-}$ female mice also had more total numbers of Tregs expressing $CD62L^+$ in spleens (mean ± SEM = 28.7 ± 2.0, $p < 0.01$) than C57BL/6 (20 ± 0.8) female mice. No differences were found between C57BL/6.*Tlr9*$^{-/-}$ and C57BL/6 female mice (Figure 4.10).

In an attempt to identify a molecular mechanism for the increase numbers of central ($CD62L^{+}$) Tregs in C57BL/6.*Tlr2*$^{-/-}$ passive EAE recipients, plasma from mice with passive EAE was analyzed for levels of IL1, IL2, IL4, IL5, IL6, IL10, IL17, INFγ, TNF, and GM-CSF at 10 and 34 days after adoptive transfer. Almost all cytokines were undetected in plasma except IL6, which was detected in 4 of 6 C57BL/6 recipient mice after 10 days of passive EAE (Figure 4.11); and 3 of 5 C57BL/6 recipient mice after 34 days of induction of passive EAE (Figure 4.12). In contrast, levels of IL6 were undetectable in the plasma in the absence of TLR2 (Figure 11 and 12) indicating that TLR2 is associated to central (CD62L-expressing) Tregs and IL6 in autoimmune inflammation.

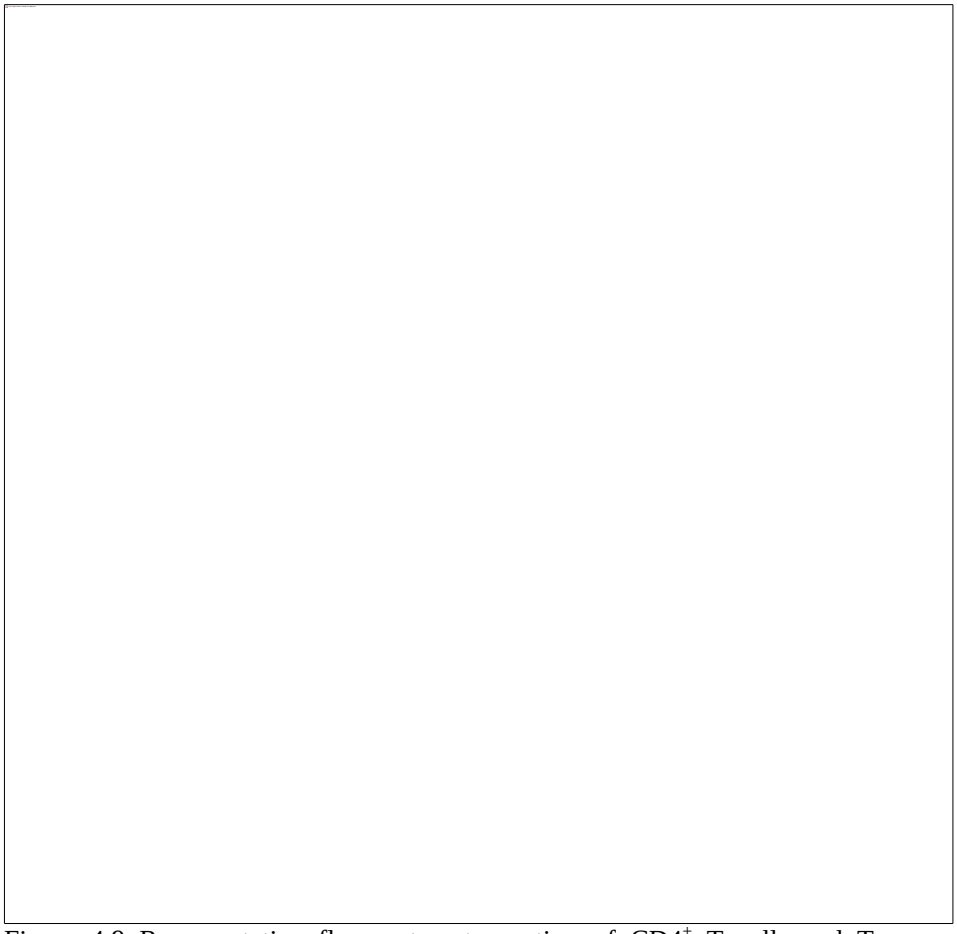

Figure 4.9 Representative flow cytometry gating of $CD4^+$ T cells and Tregs: $CD3^+CD4^+CD25^+FoxP3^+$ and $CD3^+CD4^+CD25^+FoxP3^+CD62L^+$.

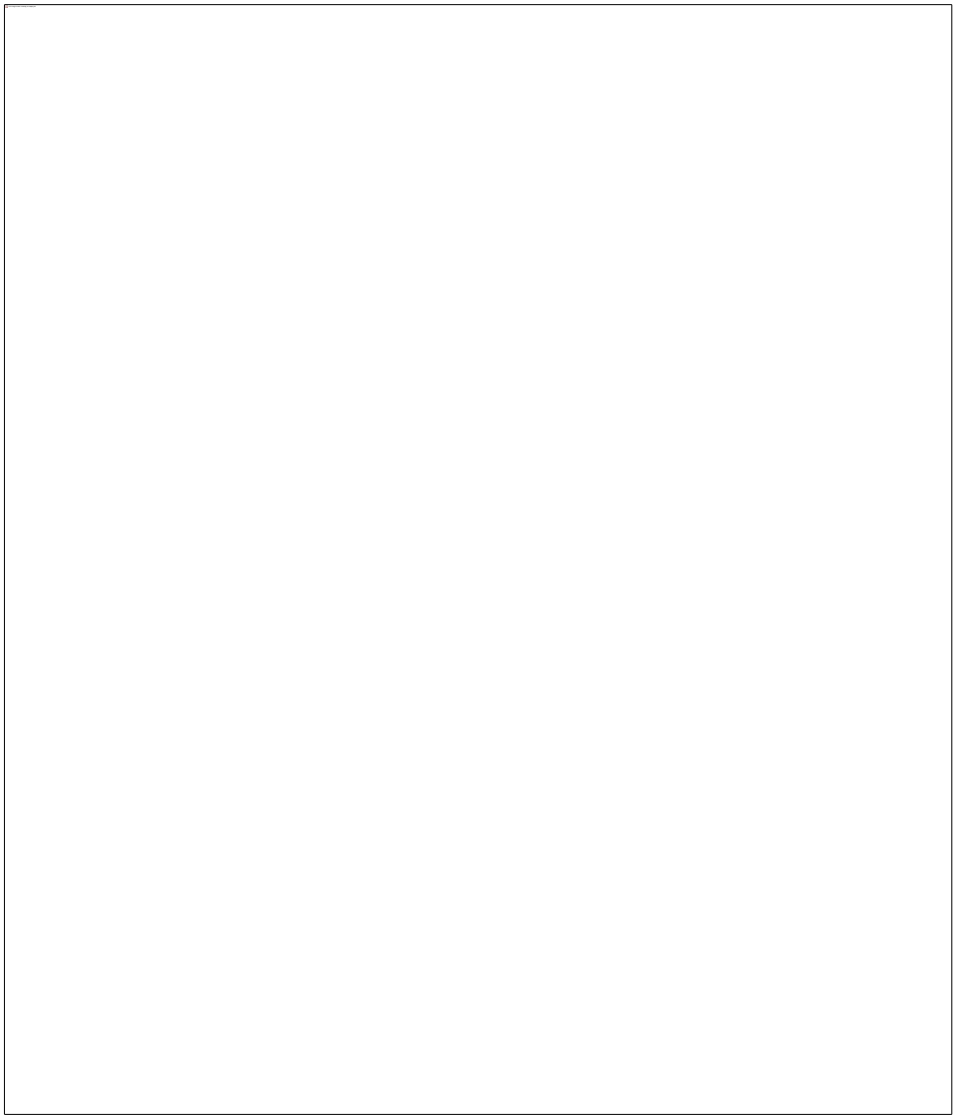

Figure 4.10 Total numbers of $CD4^+$ T cells and Tregs from spleen of male and female C57BL/6.*Tlr2*$^{-/-}$, C57BL/6.*Tlr9*$^{-/-}$ and C57BL/6 WT control mice. At least four mice per group were analyzed and the mean value of each group is indicated as a bar. Statistical differences between the C57BL/6 control group and C57BL/6.*Tlr2*$^{-/-}$ or C57BL/6.*Tlr9*$^{-/-}$ mice are indicated (*$p < 0.05$, **$p < 0.01$, ***$p < 0.001$ uncorrected Mann-Whitney U test; $n = 1$-6).

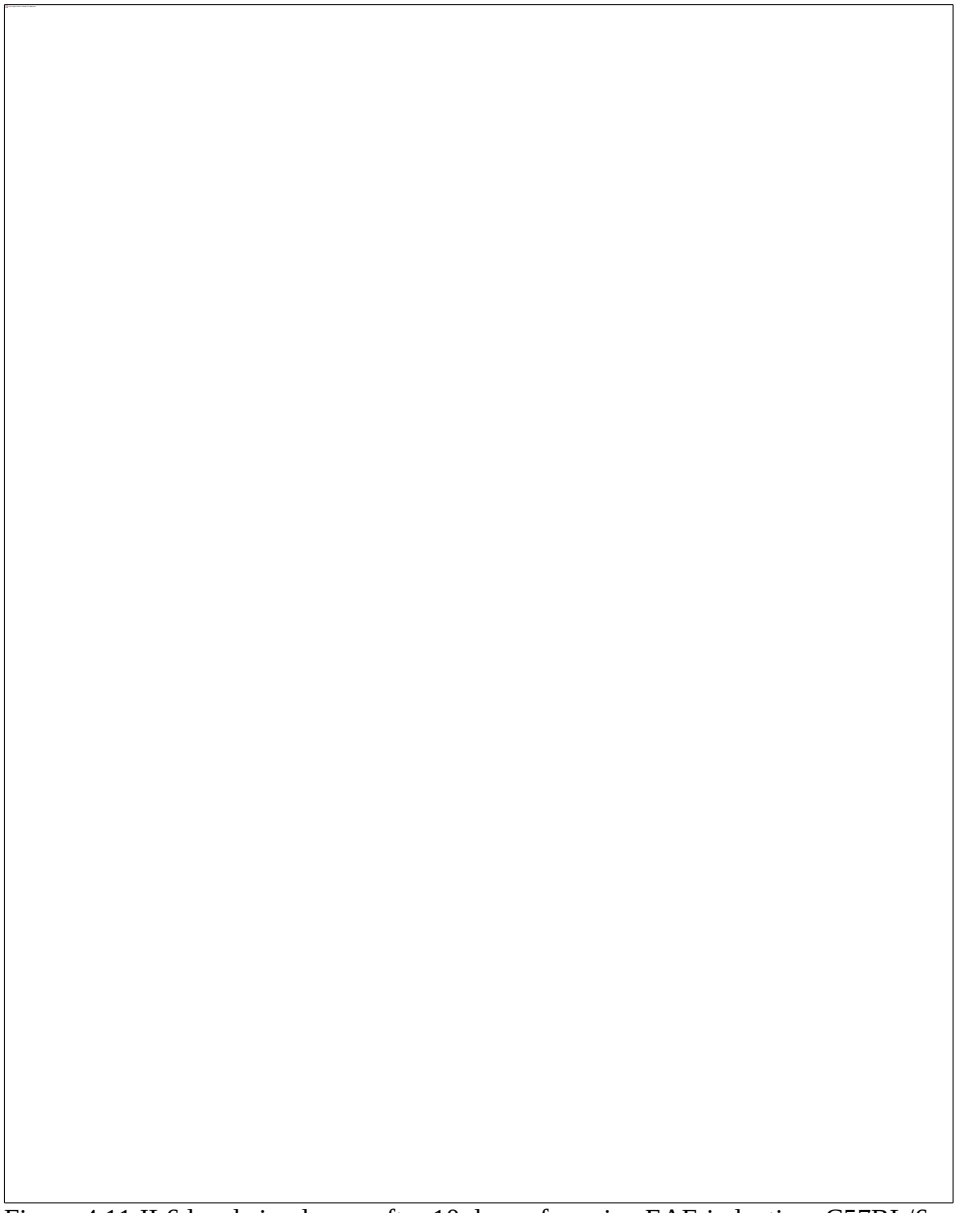

Figure 4.11 IL6 levels in plasma after 10 days of passive EAE induction. C57BL/6 *(closed cicles)* and C57BL/6.*Tlr2*$^{-/-}$ *(close squares)* (*$p < 0.05$, **$p < 0.01$, ***$p <$ 0.001 uncorrected Mann-Whitney *U* test; $n = 6$).

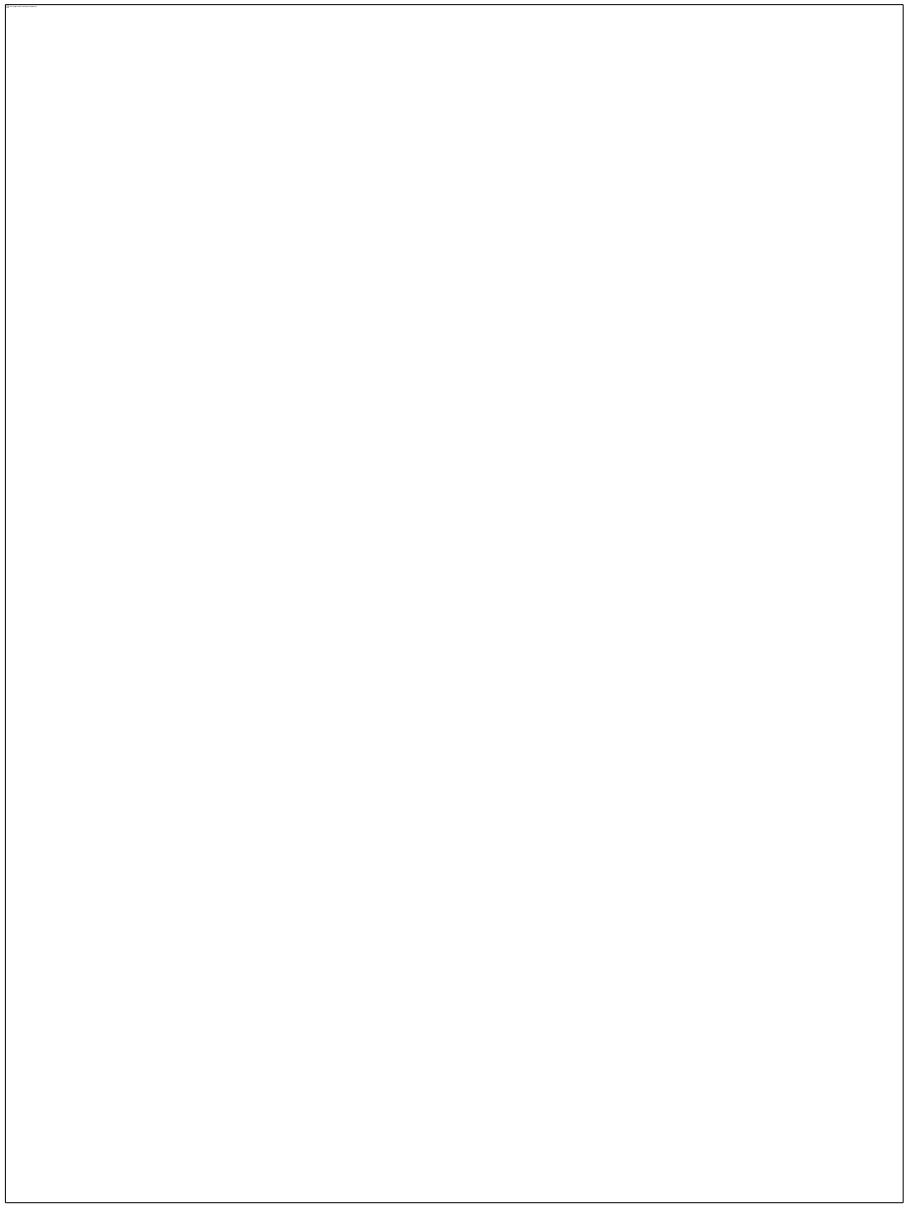

Figure 4.12 IL6 levels in plasma after 34 days of passive EAE induction. C57BL/6 *(closed cicles)* and C57BL/6.*Tlr2*$^{-/-}$ *(close squares)* (**p* < *0.05*, ***p* < *0.01*, ****p* < *0.001* uncorrected Mann-Whitney *U* test; *n* = 6).

## 4.2.7 Microflora in passive EAE

The passive form of EAE was dependent on TLR2 and partially dependent on TLR9. However, a question remained, what triggers TLR2 and TLR9 signalling. The activation of TLR2 and TLR9 signalling could occur via endogenous and/or exogenous ligands. An explanatory mechanism by which TLR2 and TLR9 could be activated is microflora. To determine whether microflora could be responsible for TLR dependent passive EAE, microflora from female mice were altered by the used of amoxocilin, clarithromycin, metronidazole and omeprazole and the clinical course of disease was analyzed in the absence of TLR2 and TLR9.

Mice were separated in two main groups and six subgroups. The first main group was fed with normal diet and the second main group was fed with diet treated with amoxocilin, clarithromycin, metronidazole and omeprazole for five weeks. Subgroups of mice with normal diet included: C57BL/6 (control group), C57BL/6.Tlr2$^{-/-}$ and C57BL/6.Tlr9$^{-/-}$. Subgroups of mice fed with treated diet with antibiotics included: C57BL/6 (control group), C57BL/6.Tlr2$^{-/-}$ and C57BL/6.Tlr9$^{-/-}$.

C57BL/6.*Tlr9*$^{-/-}$ mice fed with normal diet or medicated diet had less severe clinical course of passive EAE compared with C57BL/6 mice ($p < 0.05$). C57BL/6.*Tlr2*$^{-/-}$ mice fed with normal diet and treated diet did not show

clinical signs of disease (Figure 4.11). Clinical signs of disease were delayed in C57BL/6 mice with normal diet (onset of disease ± SEM = 23.83 ± 0.47) compared to C57BL/6 with treated diet (onset of disease ± SEM 18.8 ± 1.41, $p < 0.01$) (Figure 4.11). No significant differences were seen in the maximum clinical score and CDI between mice with normal diet and medicated diet (Figure 4.11). Data confirmed previous results showing that passive EAE is dependent of TLR2 and partially depend on TLR9. Manipulation of microflora with amoxocilin, clarithromycin, metronidazole and omeprazole delayed the clinical signs of passive EAE in C57BL/6 mice but not in mice deficient in TLR2 and TLR9, suggesting that while the antibiotics had an effect microflora might modulate CNS autoimmune inflammation via TLRs.

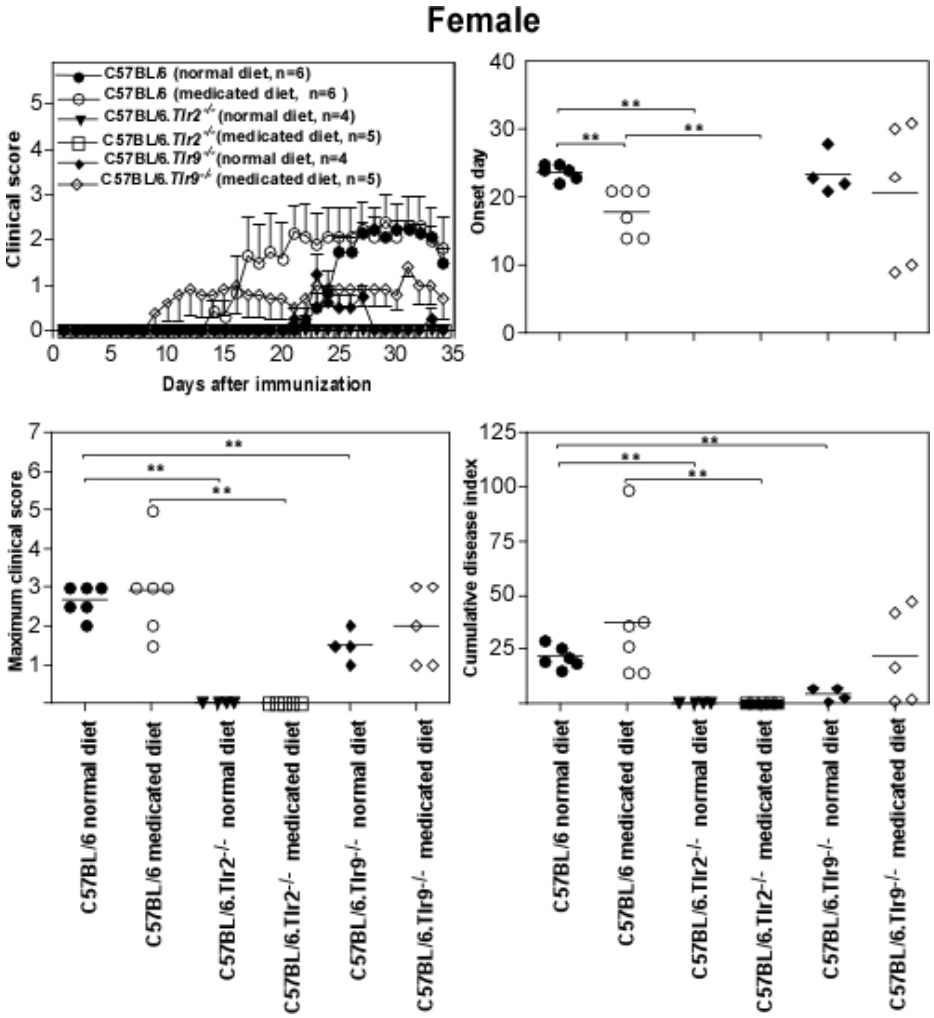


Figure 4.13 Analysis of the clinical course of passive $MOG_{35-55}$/CFA + PTX - induced EAE in female C57BL/6 (*closed circles*), C57BL/6.*Tlr2*$^{-/-}$, (*closed downward triangles*) and C57BL/6.*Tlr9*$^{-/-}$ (*closed diamonds*) mice fed with normal diet and; female C57BL/6 (*open circles*), C57BL/6.*Tlr2*$^{-/-}$, (*open squares*) and C57BL/6.*Tlr9*$^{-/-}$ (*open diamonds*) mice fed with medicated diet. Significant differences are indicated (*$p < 0.05$, **$p < 0.01$, ***p < 0.001 uncorrected Mann-Whitney *U* test; $n$ = 4-6).

## 4.3 Discussion

Encephalomyelitis can be experimentally induced in laboratory animals in the absence of adjuvant and the severity and incidence of EAE increases by its addition (review in Baxter 2007). The most common adjuvants in EAE are CFA, which contains *Mycobacteria tuberculosis*, and PTX. The adjuvant activity of *Mycobacteria tuberculosis* is mediated by NOD2 recognition of muramide peptide, and cell lines transfected with human TLR2 or TLR4 were responsive to *M. tuberculosis* (Ferwerda et al., 2005). Kerfoot et al., (2004) proposed that the action of PTX in active EAE is mediated by TLR4.

To date, there is no evidence of an adjuvant immunisation event in the initiation of MS. On the other side, the dependence of EAE on induction by CFA containing *M. tuberculosis* and PTX raise concern that TLR-dependencies identified in the active model of EAE represent limitations of this model, and not characteristics of MS. However, the use of CFA in active EAE can be avoided by using the passive form of EAE. Adoptive cell transfer from donors to recipients induces passive EAE. The passive model of EAE requires of a number of refinements to enhance the disease. The refinements include: mild (3Gy) gamma irradiation and pretreatment with PTX of the recipient.

In Chapter 3, it was found that TLR4 do not play a role in active EAE. In this Chapter, we showed that the C57BL/6.Tlr4$^{-/-}$ mice ameliorated the clinical signs of passive EAE but inhibition of disease was not as great as in the mice that did not receive PTX, indicating that PTX do not signal via TLR4. Apetoth (2007) proposed that irradiation trigger the release of intrinsic TLR ligands. However, we found that the absence of irradiation in C57BL6 mice did not affect the course of passive EAE. Thus, neither the absence of CFA nor the use of PTX and irradiation alter the development of passive EAE in the absence of TLR4 suggesting that TLR4 have activities mediated by other mechanisms, including microflora in this model.

Studies from Reynold et al., (2007), Lee et al., (2012) and Fang et al., (2009) indicate that T cells require of TLR4 signalling to promote or regulate EAE. In our studies the absence of TLR4 did not alter the course of EAE in active EAE (Chapter 3), opposing this results the absence of TLR4 decreased the severity of passive EAE. As active EAE has both priming and effector phases and passive EAE has only the effector phase, our results suggest that TLR4 signalling is potentially important in both phases of EAE. In the presence of TLR4 priming T cells increase but in the absence of TLR4 primed T cells from WT mice are unable to augment the number of T cells.

In Chapter 3 it was also found that the severity of active EAE is partially dependent on TLR2 and TLR9. This chapter examined EAE in the absence of CFA in mice deficient in TLR2 and TLR9. Results revealed that mice deficient in TLR9 are partially protected of passive EAE, while mice deficient in TLR2 are completely protected from passive EAE. Protection was associated with the lack of circulating levels of IL6, an increased numbers of central ($CD62L^{+}$) regulatory T cells, a reduced recruitment of activated CD4 T cells in CNS and a reduced numbers of CD4 T cells producing IL17 in CNS. Previously, Prinz et al., (2006) reported a partial dependency on TLR9 expression on the adoptive transfer recipients. Our findings of complete dependence of TLR2 expression in recipients of WT cells is novel but consistent with Reynolds et al., (2010), who reported that bone morrow chimeras reconstituted with TLR2-deficient marrow expressed ameliorated disease after induction of active EAE.

In our model the presence of TLR2 during priming appears to confer a dependency on TLR2 during the effector phase of EAE. Cells from WT mice priming *in vitro* must lead to increasing expression of TLR2, produce regulatory and pathogenic cytokines and stimulate the cell that produce those cytokines. Transference of those cells into mice in the absence of TLR2 might increase levels of cytokines but without augmenting the numbers of cells that produce the pathogenic cytokines and increasing the cells that produce regulatory cytokines.

In addition, the dependence of passive induction of EAE on TLR2 expression in the recipient indicates the presence of tonic signalling through the receptor. This could occur via endogenous or exogenous ligands. Although many putative endogenous ligands for TLR2 have been proposed, none of them meet the reasonable criteria of purity and validation required to demonstrate their ability to directly bind and signal through TLR2 (Erridge et al., 2010). In contrast, microbial products from intestinal microflora have been detected in blood of healthy humans (Erridge et al., 2007) and mice (Clarke et al., 2010). Although alteration of microflora with antibiotics in the absence of TLR2 did not affect the development of passive EAE, the disease was delayed in WT mice without any treatment, suggesting that TLR2 is required to protect mice of CNS autoimmune inflammation; however, further studies are required to clarify the activation of TLR2 by microflora. Moreover, considering that gender influence the immune response to infections (McClelland EE, et al., 2011; Roberts BJ, et al., 2013), it might be possible that specific immune responses from microflora or pathogen exposure in male and female mice contribute to the phenotype of EAE.

# CHAPTER 5

# CHAPTER 5

# THE ROLE OF TLR2 IN ACTIVE $MOG_{35-55}$/CFA + PTX-INDUCED RELAPSING-REMITTING EAE

## 5.1 Introduction

Studies in Chapter 3 of this work reported a partial role of TLR2 and TLR9 in active $MOG_{35-55}$/CFA + PTX–induced EAE, and studies in Chapter 4 of this work reported a partial role of TLR9 and a definitive role of TLR2 in passive $MOG_{35-55}$/CFA + PTX–induced EAE; indicating that TLR2 plays a key role in EAE. Additional evidence that support the role of TLR2 in EAE and MS include: 1) the presence of TLR2 ligands in the CNS in MS and EAE (Schrijver et al., 2001; Andersson et al., 2008; Farez et al., 2009); 2) the dependence of TLR2 in the exacerbation of MS and EAE during bacterial infections (de la Monte et al., 1986; Herrmann et al., 2006; Nichols et al., 2009; Nichols et al., 2011); 3) the association of TLR2 with the decrease of severity of MS in helminth-infected MS patients (Correale et al., 2009); 4) the successful use of TLR2 ligands as adjuvant in the induction of EAE (Visser et al., 2005); 5) the inhibition of remyelination via TLR2

(Visser et al., 2005; Sloane et al., 2010; Back et al., 2005); and 6) the modulation of MS by TLR2 ligands (Sweeney et al., 2011).

Because CNS autoimmune inflammation was associated to TLR2 and TLR9 in C57BL/6 mice, in this chapter we further analysed the development of EAE in NOD mice, the mouse model of type 1 diabetes (T1D), in order to dissect the interrelationship between organ-specific autoimmune diseases.

## 5.2 Results

### 5.2.1 Active $MOG_{35-55}$/CFA + PTX–induced relapsing-remitting EAE in NOD/Lt deficient mice in TLR1, TLR2, TLR4, TLR6 and TLR9

NOD/Lt mice are commonly used as a model of TID because they develop spontaneous insulitis associated with the disease (Makino et al., 1980; Kachapati et al., 2012). In addition, NOD/Lt mice develop a form of relapsing-remitting EAE (Amor et al., 1993; Slavin et al., 1998). Relapsing-remitting EAE is characterised by partial or complete recovery from the onset of clinical signs of disease, and then relapses and remissions (Slavin et al., 1998). To determine the role of TLRs in active $MOG_{35-55}$/CFA + PTX–

induced relapsing-remitting EAE, the disease was induced in NOD/Lt (WT control group), NOD.*Tlr1*$^{-/-}$, NOD.*Tlr2*$^{-/-}$, NOD.*Tlr4*$^{-/-}$, NOD.*Tlr6*$^{-/-}$ and NOD.*Tlr9*$^{-/-}$ male and female mice.

Mice were observed and scored each individual day for clinical signs of active $MOG_{35-55}$/CFA + PTX–induced relapsing-remitting EAE over 71 days post EAE induction. As previously reported by Slavin et al., (1998), NOD/Lt mice developed relapsing-remitting EAE (Figure 5.1). The day of onset of clinical signs of active $MOG_{35-55}$/CFA + PTX–induced relapsing-remitting EAE appeared within 13-31 days in male NOD/Lt mice, and 10-31 days in female NOD/Lt mice after the induction of EAE. The onset of clinical signs of disease was followed by relapses and remissions (Figure 5.1, Figure 5.2 and Figure 5.3).

The clinical course of active $MOG_{35-55}$/CFA + PTX–induced relapsing-remitting EAE, the day of onset of clinical signs of disease, the maximum score of clinical signs and the CDI were similar between NOD/Lt and NOD.*Tlr1*$^{-/-}$ mice in either sex ($n$ = 8-9 mice) (Figure 5.2 and Figure 5.3).

The clinical course of active $MOG_{35-55}$/CFA + PTX–induced relapsing-remitting EAE decreased in the absence of TLR2 only one day in male mice (day 28) and two days in female mice (days 16 and 17) compared with

NOD/Lt mice ($n$ = 8 male mice, $p < 0.05$ and $n$ = 8 female mice, $p < 0.05$) (Figure 5.2 and Figure 5.3). No differences were observed in the onset of clinical signs of disease between NOD.*Tlr2*$^{-/-}$ male mice and NOD/Lt male mice. The day of onset of clinical signs of EAE was delayed in the absence of TLR2 in female mice (mean day of onset ± SEM = 25.5 ± 2.58, $p < 0.01$) compared with NOD/Lt female mice (mean day of onset ± SEM = 14.87 ± 0.71), but no differences were observed in male mice. Neither male nor female mice showed significant differences in the maximum score of disease and CDI in the absence of TLR2 when compared with NOD/Lt mice (Figure 5.2 and Figure 5.3).

The clinical course of active $MOG_{35-55}$/CFA + PTX–induced relapsing-remitting EAE decreased in the absence of TLR4 two days in female mice (day 27 and 28) compared with NOD/Lt female mice ($n$ = 8 mice, $p < 0.05$); but no differences were seen in male mice (Figure 5.2 and Figure 5.3). No significant differences on the day of onset of clinical signs of disease, the maximum score of EAE and CDI were observed between NOD/Lt and NOD.*Tlr4*$^{-/-}$ female and male mice (Figure 5.2 and Figure 5.3).

The clinical course of active $MOG_{35-55}$/CFA + PTX–induced relapsing-remitting EAE decreased in the absence of TLR6 three days (day 35-37) in male mice compared with NOD/Lt male mice ($n$ = 8 mice, $p < 0.05$); but no

differences were observed in female mice (Figure 5.2 and Figure 5.3). No significant differences on the day of onset of clinical signs of disease, the maximum score of disease and CDI where observed between NOD/Lt and NOD.*Tlr6*$^{-/-}$ mice in male and female (Figure 5.2 and Figure 5.3).

The clinical course of active $MOG_{35-55}$/CFA + PTX–induced relapsing-remitting EAE decreased in the absence of TLR9 five days in male mice (days 30, 47, 66, 69 and 70) and five days in female mice (days 16, 17 and 50-52) compared with NOD/Lt mice ($n$ = 8 mice, $p < 0.05$) (Figure 5.2 and Figure 5.3). The day of onset of clinical signs was delayed in the absence of TLR9 in female mice (mean day of onset ± SEM = 26.00 ± 2.43, $p < 0.05$) compared with NOD/Lt female mice (mean day of onset ± SEM 14.87 ± 0.71); but no differences were observed in male mice. No significant differences were seen in the maximum score of disease and CDI between NOD/Lt and NOD.*Tlr9*$^{-/-}$ female and male mice (Figure 5.2 and Figure 5.3). These results showed that TLR2 and TLR9 play a role in the onset of $MOG_{35-55}$/CFA+PTX–induced relapsing-remitting EAE in NOD mice.

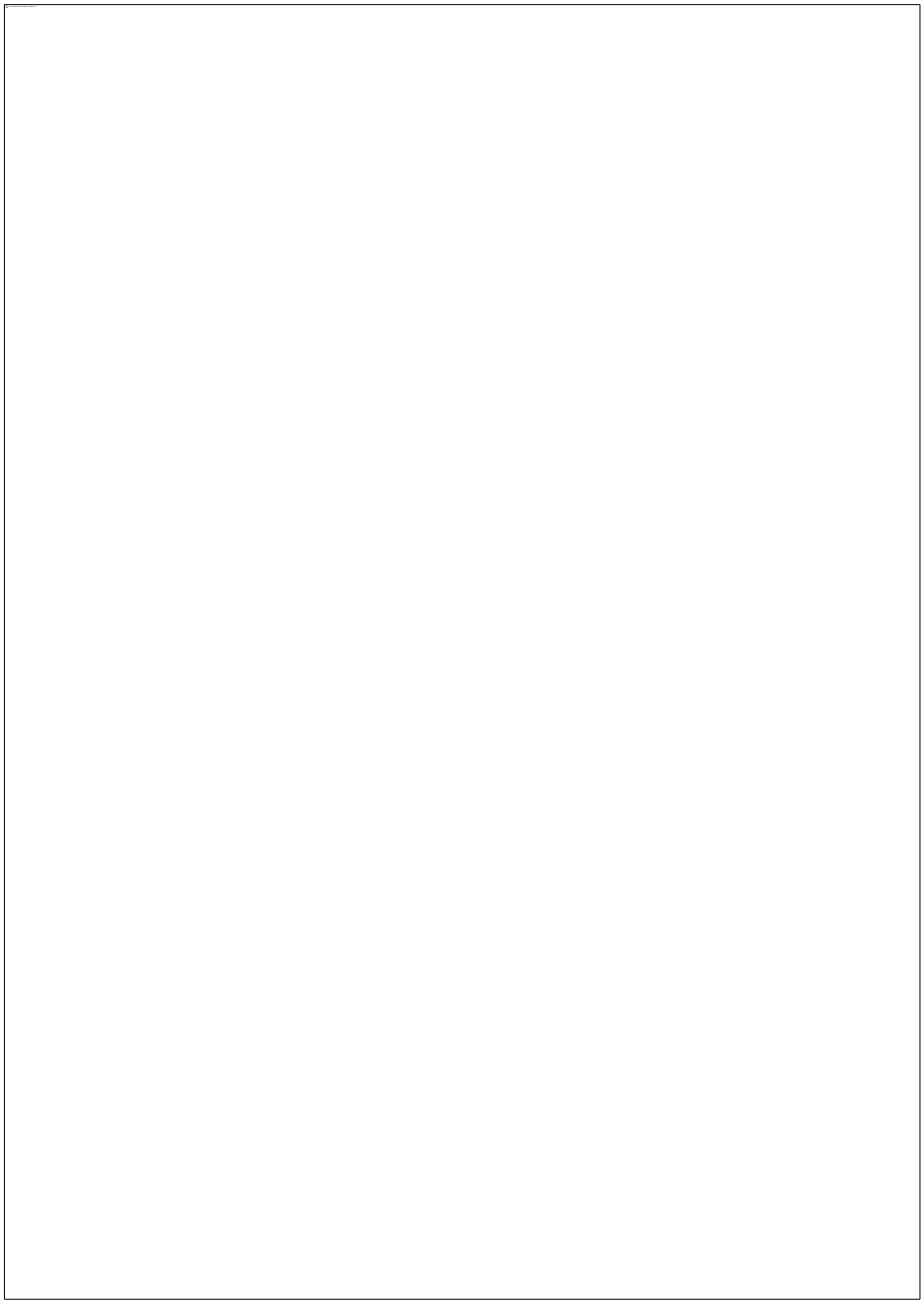

Figure 5.1. Representative clinical course of active $MOG_{35-55}$/CFA + PTX–induced relapsing-remitting EAE in individual NOD/Lt control WT (*closed circles*) and NOD.*Tlr1*$^{-/-}$, NOD.*Tlr2*$^{-/-}$, NOD.*Tlr4*$^{-/-}$, NOD.*Tlr6*$^{-/-}$ and NOD.*Tlr9*$^{-/-}$ (*open circles*) male and female mice. Clinical signs of EAE were monitored each day over 71 days ($n$ = 1).

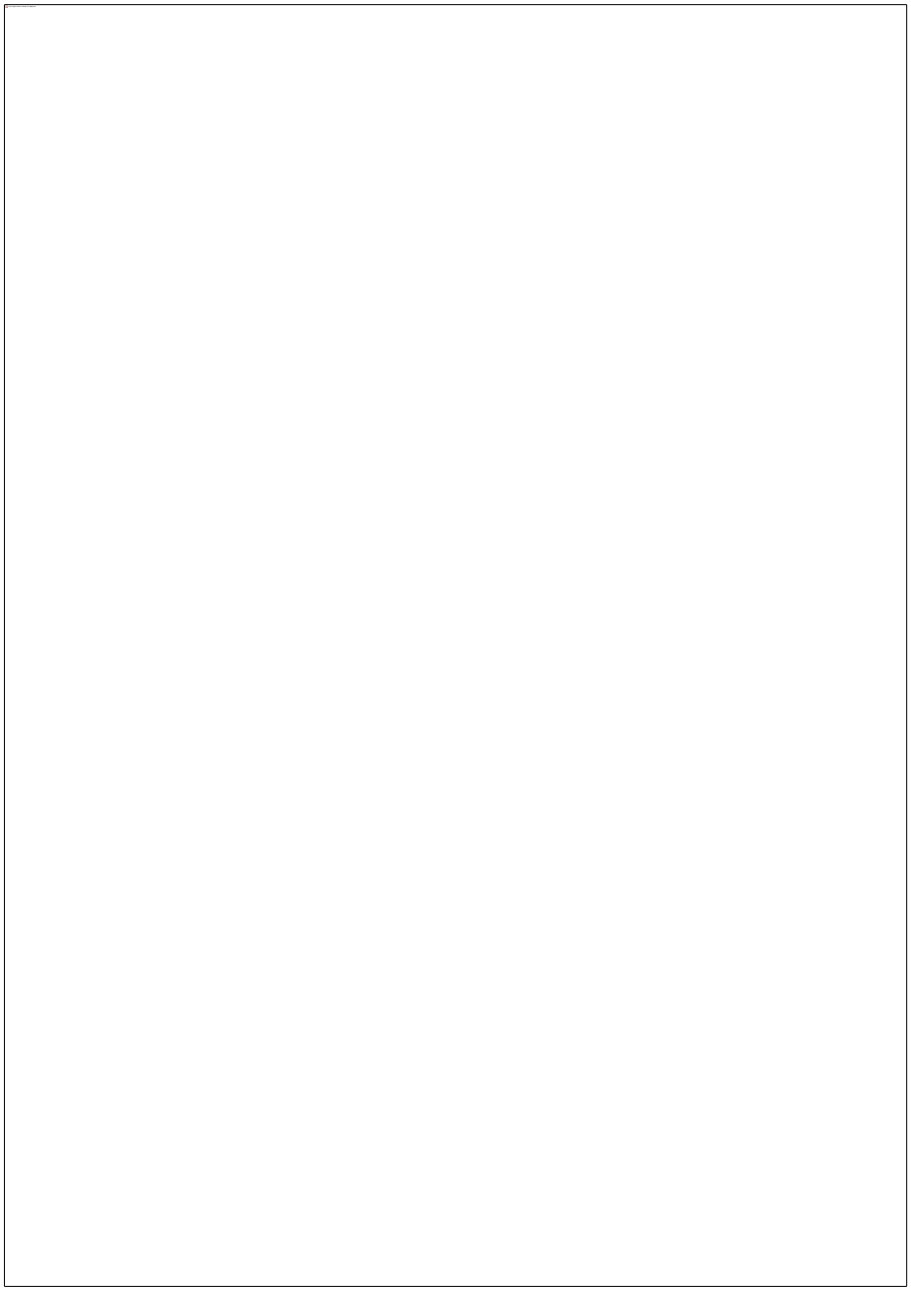

Figure 5.2 Clinical course of active $MOG_{35-55}$/CFA + PTX–induced relapsing-remitting EAE in NOD/Lt WT control (*closed circles*) and NOD.*Tlr1*$^{-/-}$, NOD.*Tlr2*$^{-/-}$, NOD.*Tlr4*$^{-/-}$, NOD.*Tlr6*$^{-/-}$ and NOD.*Tlr9*$^{-/-}$ (*open circles*) female and male mice. Male are in the left column. Female are in the right column. Each data point and error bar represents the mean ± SEM of the clinical score of each individual day. Significant data between NOD/Lt and NOD.*Tlr*$^{-/-}$ are indicated (*$p$ < 0.5, uncorrected Mann Whitney-test; $n$ = 5-12).

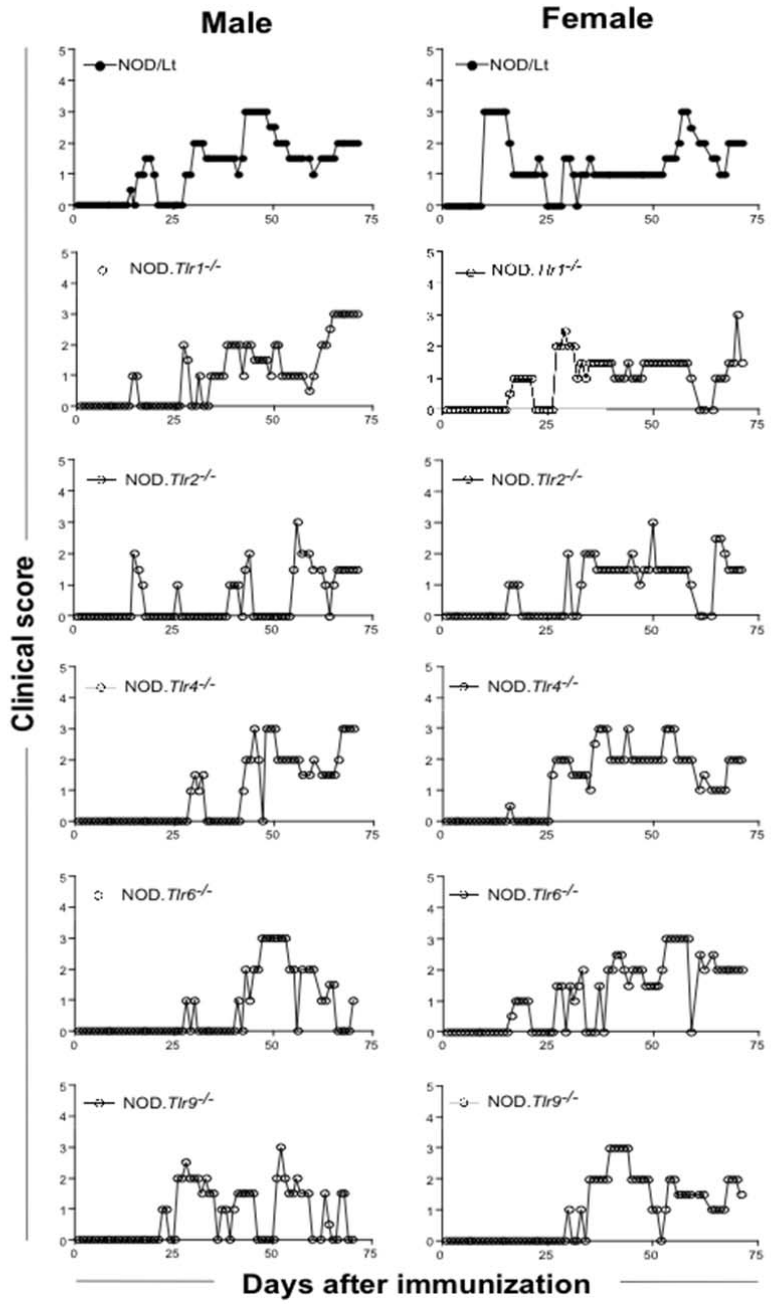


Figure 5.3. Analysis of the clinical course of active $MOG_{35-55}$/CFA + PTX- induced relapsing-remitting EAE in NOD/Lt (*closed cicles*), NOD.*Tlr1*$^{-/-}$ (*open squares*), NOD.*Tlr2*$^{-/-}$ (*open cicles*), NOD.*Tlr4*$^{-/-}$ (*open downward triangles*), NOD.*Tlr6*$^{-/-}$ (*open upward triangles*) and NOD.*Tlr9*$^{-/-}$ (*open diamonds*) male and female mice. Statistically significant differences between NOD/Lt and NOD.*Tlr*$^{-/-}$ mice are indicated (*$p < 0.05$, **$p < 0.01$, uncorrected Mann-Whitney *U* test; $n = 8$ or 9).

## 5.2.2 Active $MOG_{35-55}$/CFA + PTX–induced relapsing-remitting EAE in NOD.*H2*$^{b}$ and NOD.*H2*$^{d}$ mice

As the NOD mouse strain showed little influence of TLR2 on the onset of relapsing-remitting EAE but not in the severity of disease, we thought that might be due to ongoing autoimmune inflammation provided by inflammatory milieu, for example IL6 that we previously identified in an earlier chapter; otherwise being provided by the TLR2 signalling. To test the hypothesis that insulitis associated with T1D development in some way compensated for the lack of TLR2 signalling in NOD mice, we looked for a NOD mouse background but without the insulitis associated with T1D. We knew that NOD.*H2*$^{b}$ and NOD.*H2*$^{d}$ congenic mice were relatively free of T1D as declared by Pearson et al., (2003), Yoshida et al., (2008) and Jordan (2009) and showed in Figure 5.4. Thus, NOD.*H2*$^{b}$ and NOD.*H2*$^{d}$ female mice were immunized with $MOG_{35-55}$/CFA + PTX.

NOD.*H2*$^{d}$ female mice developed a relapsing-remitting form of EAE (Figure 5.5 and Figure 5.6). Clinical signs of EAE appeared earlier in NOD.*H2*$^{d}$ female mice (mean day of onset ± SEM = 12.14 ± 0.50, $p < 0.001$) than in NOD/Lt female mice (mean day of onset ± SEM = 15 ± 0.0) (Figure 5.6). However, no differences were observed in the maximum score

of clinical signs of EAE and CDI between NOD.*H2*$^{d}$ and NOD/Lt female mice (Figure 5.6).

NOD.*H2*$^{b}$ female mice also developed a form of relapsing-remitting EAE (Figure 5.5 and Figure 5.6). Clinical signs of EAE appeared earlier in NOD.*H2*$^{b}$ female mice (mean day of onset ± SEM = 13.12 ± 0.63, $p < 0.01$) than in NOD/Lt female mice (mean day of onset ± SEM = 15 ± 0.0) (Figure 5.6). Although no differences were seen in the maximum score of EAE, the cumulative disease index was clearly higher in NOD.*H2*$^{b}$ female mice compared with NOD/Lt female mice (CDI mean ± SEM = 57.93 ± 1.89 and CDI mean ± SEM = 38.42 ± 2.12 respectively; $p < 0.001$) (Figure 5.6).

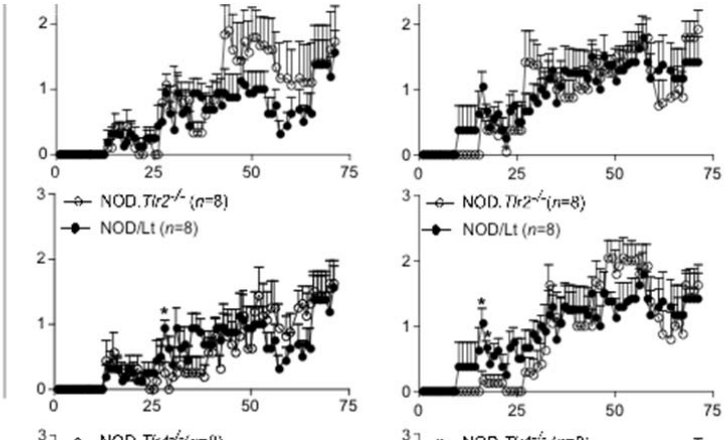


Figure 5.4. Cumulative diabetes incidence in NOD/Lt (*closed cicles*), NOD.$H2^b$ (*open cicles*) and NOD.$H2^d$ (*open cicles*) female mice. Mice were bled fortnightly for 36 weeks of age and random blood glucose levels determined. Significant data are indicated (*$p < 0.05$, **$p < 0.01$, ***$p < 0.001$ uncorrected Mann-Whitney *U* test; $n$ = 14-38).

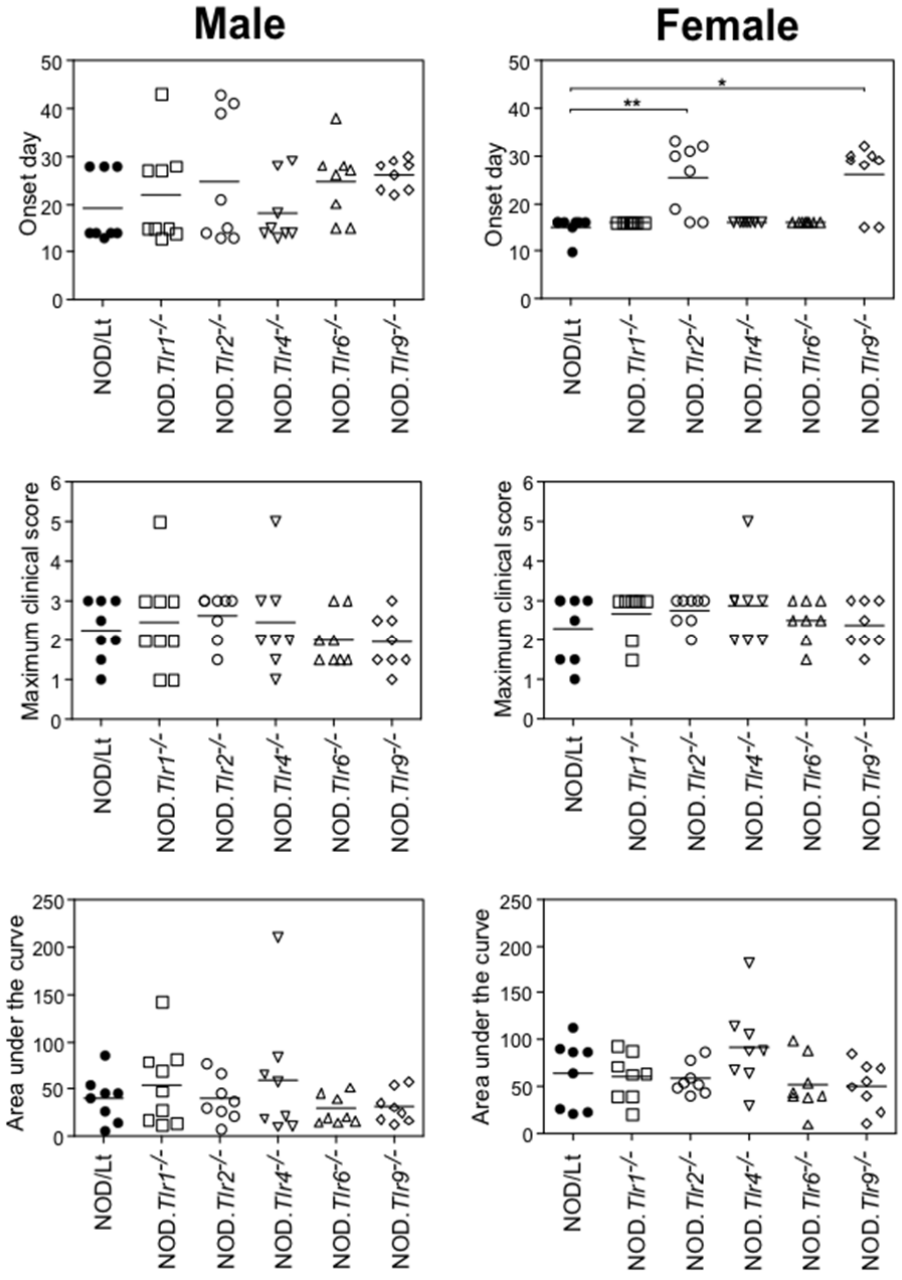


Figure 5.5. Representative clinical course of active $MOG_{35-55}$/CFA + PTX- induced relapsing-remitting EAE in individual female NOD/Lt (*closed circles*), NOD.$H2^b$ (*open circles*) and NOD.$H2^d$ (*open forwards triangles*) mice. Clinical signs of EAE were score each day over 40 days ($n$ = 1).

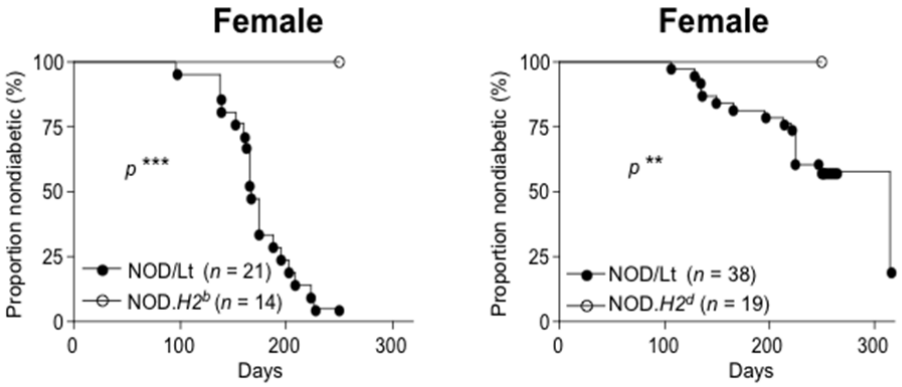


Figure 5.6. Analysis of the clinical course of active $MOG_{35-55}$/CFA + PTX- induced relapsing-remitting EAE in NOD/Lt (*closed circles*), NOD.$H2^b$ (*open circles*) and NOD.$H2^d$ (*open forwards triangles*) female mice. NOD.$H2^b$ mice showed a more severe form of relapsing-remitting EAE compared to NOD/Lt mice (WT). The appearance of clinical signs of disease was delayed in both NOD.$H2^b$ and NOD.$H2^d$ compared to WT. No differences were seen in maximum clinical score (*$p < 0.05$, **$p < 0.01$, ***$p < 0.001$ uncorrected Mann-Whitney *U* test; $n$ = 7-8).

## 5.2.3 Active $MOG_{35-55}$/CFA + PTX–induced relapsing-remitting EAE in NOD.*H2*$^{b}$.*Tlr2*$^{-/-}$

Because NOD.*H2*$^{b}$ mice developed significantly more severe form of relapsing-remitting EAE than NOD.*H2*$^{d}$, the phenotype of the disease was analyzed in NOD.*H2*$^{b}$, NOD.*H2*$^{b}$.*Tlr2*$^{-/-}$, NOD/Lt and NOD.*Tlr2*$^{-/-}$. The clinical course of active $MOG_{35-55}$/CFA + PTX–induced relapsing-remitting EAE decreased in NOD.*H2*$^{b}$.*Tlr2*$^{-/-}$ male mice over 19 days (day 11-13, 22-26, 28-30 and 33-40) compared with NOD.*H2*$^{b}$ male mice (Figure 5.7). The day of onset of disease was delayed in NOD.*H2*$^{b}$.*Tlr2*$^{-/-}$ male mice (mean of day of onset ± SEM = 14.3 ± 0.26, $p < 0.001$) compared with NOD.*H2*$^{b}$ male mice (mean of day of onset ± SEM = 11.33 ± 0.21). No differences were observed in the maximum score between NOD.*H2*$^{b}$ and NOD.*H2*$^{b}$.*Tlr2*$^{-/-}$ male mice. CDI decreased in NOD.*H2*$^{b}$.*Tlr2*$^{-/-}$ male mice (mean of the CDI ± SEM = 31.25 ± 3.39, $p < 0.001$) compared with NOD.*H2*$^{b}$ male mice (mean of the CDI ± SEM = 59.66 ± 4.56) (Figure 5.8).

The clinical course of active $MOG_{35-55}$/CFA + PTX–induced relapsing-remitting EAE decreased in NOD.*H2*$^{b}$.*Tlr2*$^{-/-}$ female mice over eight days (day 11-12, 22, 27-30 and 33) compared with NOD/Lt female mice (Figure 5.7). The day of onset of disease was delayed in NOD.*H2*$^{b}$.*Tlr2*$^{-/-}$ female mice (mean of day of onset ± SEM = 14.2 ± 0.24, $p < 0.05$) compared with

NOD.*H2*$^{b}$ male mice (mean of day of onset ± SEM = 11.11 ± 0.11). No differences were observed in the maximum score between NOD.*H2*$^{b}$ and NOD.*H2*$^{b}$.*Tlr2*$^{-/-}$ female mice. CDI decreased in NOD.*H2*$^{b}$.*Tlr2*$^{-/-}$ female mice (mean of the CDI ± SEM = 39.65 ± 3.70, $p < 0.01$) compared with NOD.*H2*$^{b}$ female mice (mean of the CDI ± SEM = 51.66 ± 1.35) (Figure 5.8).

The clinical course of active $MOG_{35-55}$/CFA + PTX–induced relapsing-remitting EAE decreased in NOD.*Tlr2*$^{-/-}$ male mice over 4 days (day 18, 21, 23 and 38) compared to NOD/Lt male mice (Figure 5.7). As seen before, no differences were observed on the day of onset of disease, the maximum score of disease and CDI between NOD/Lt male mice and NOD.*Tlr2*$^{-/-}$ male mice (Figure 5.8).

The clinical course of active $MOG_{35-55}$/CFA + PTX–induced relapsing-remitting EAE decreased only two days in NOD.*Tlr2*$^{-/-}$ female mice (day 37 and 39) compared with NOD/Lt female mice (Figure 5.7). Results confirmed a delayed on the day of onset of clinical signs of EAE in NOD.*Tlr2*$^{-/-}$ female mice (mean of day of onset ± SEM = 13.0 ± 0.0, $p < 0.05$) compared with NOD/Lt female mice (mean of day of onset ± SEM = 12.2 ± 5.45). No differences were observed in the maximum score of disease and CDI between NOD.*Tlr2*$^{-/-}$ and NOD/Lt female mice (Figure

5.8).

A further analysis of the clinical signs of active $MOG_{35-55}$/CFA + PTX–induced relapsing-remitting EAE showed that NOD.*H2*$^b$ male mice developed more severe relapsing-remitting EAE than NOD/Lt male mice (Figure 5.7). The mean ± SEM of maximum clinical score of EAE was 2.91 ± 0.20 ($p < 0.05$) in NOD.*H2*$^b$ male mice and 1.83 ± 0.21 in NOD/Lt male mice. The mean ± SEM of CDI was 59.66 ± 4.56 ($p < 0.001$) in NOD.*H2*$^b$ male mice and 19.66 ± 3.15 in NOD/Lt male mice. No differences were observed in the day of onset of disease between NOD.*H2*$^b$ male mice and NOD/Lt male mice (Figure 5.8).

Female NOD.*H2*$^b$ mice also developed more severe CDI than NOD/Lt male mice. The mean ± SEM of CDI was 51.66 ± 1.35 ($p < 0.001$) in NOD.*H2*$^b$ female mice and 28.8 ± 12.87 in NOD/Lt female mice. Moreover, the day of onset of clinical signs of EAE were delayed in NOD.*H2*$^b$ female mice. The mean ± SEM of the day of onset of disease was 11.11 ± 0.11 in NOD.H2$^b$ female mice and 12.2 ± 5.45 in NOD/Lt female mice. No differences were observed in the maximum score of EAE between NOD.*H2*$^b$ female mice and NOD/Lt female mice (Figure 5.8).

NOD.*H2*$^{b}$.*Tlr2*$^{-/-}$ male mice developed a later onset of active $MOG_{35-55}$/CFA + PTX–induced relapsing-remitting EAE and more severe disease than NOD.*Tlr2*$^{-/-}$ male mice (Figure 5.7). The day of onset of clinical signs of EAE ± SEM in NOD.*H2*$^{b}$.*Tlr2*$^{-/-}$ male mice was 14.3 ± 0.26 ($p < 0.01$) and 13.66 ± 0.71 in NOD.*Tlr2*$^{-/-}$ male mice. The maximum clinical score was 2.6 ± 0.1 ($p < 0.05$) in NOD.*H2*$^{b}$.*Tlr2*$^{-/-}$ male mice and 1.5 ± 0.0 in NOD.*Tlr2*$^{-/-}$ male mice. CDI was 31.25 ± 3.39 in NOD.*H2*$^{b}$.*Tlr2*$^{-/-}$ male mice and 17 ± 3.66 in NOD.*Tlr2*$^{-/-}$ male mice (Figure 5.8).

NOD.*H2*$^{b}$.*Tlr2*$^{-/-}$ female mice also developed a later onset of active $MOG_{35-55}$/CFA + PTX–induced relapsing-remitting EAE and more severe disease than NOD.*Tlr2*$^{-/-}$ female mice (Figure 5.7). The day of onset of clinical signs of EAE ± SEM in NOD.*H2*$^{b}$.*Tlr2*$^{-/-}$ female mice was 14.2 ± 0.24 ($p < 0.05$) and 13.0 ± 0.0 in NOD.*Tlr2*$^{-/-}$ female mice. The maximum clinical score ± SEM was 2.8 ± 0.16 ($p < 0.01$) in NOD.*H2*$^{b}$.*Tlr2*$^{-/-}$ female mice and 1.7 ± 0.2 in NOD.*Tlr2*$^{-/-}$ female mice. CDI ± SEM was 39.65 ± 7.70 (($p < 0.01$) in NOD.*H2*$^{b}$.*Tlr2*$^{-/-}$ female mice and 18.0 ± 4.08 in NOD.*Tlr2*$^{-/-}$ female mice (Figure 5.8).

All together, NOD.*H2*$^{b}$ mice, a resistant mouse strain to T1D, developed more severe active $MOG_{35-55}$/CFA + PTX–induced relapsing-remitting EAE and earlier onset of clinical signs of disease compared with NOD/Lt mice in

either sex. The severity of active $MOG_{35-55}$/CFA + PTX–induced relapsing-remitting EAE was lower in both male and females NOD.*H2*$^{b}$.*Tlr2*$^{-/-}$ mice compared with male and female NOD.*H2*$^{b}$ mice. Although relapses of EAE were observed in female and male NOD.*H2*$^{b}$ mice, NOD.*H2*$^{b}$.*Tlr2*$^{-/-}$ mice did not show relapses of disease after the initial peak of active $MOG_{35-55}$/CFA + PTX–induced relapsing-remitting EAE in either sex. These results suggest that both TLR2 signalling and immunological events associated with autoimmunity at distant site can mediate relapses in CNS autoimmunity.

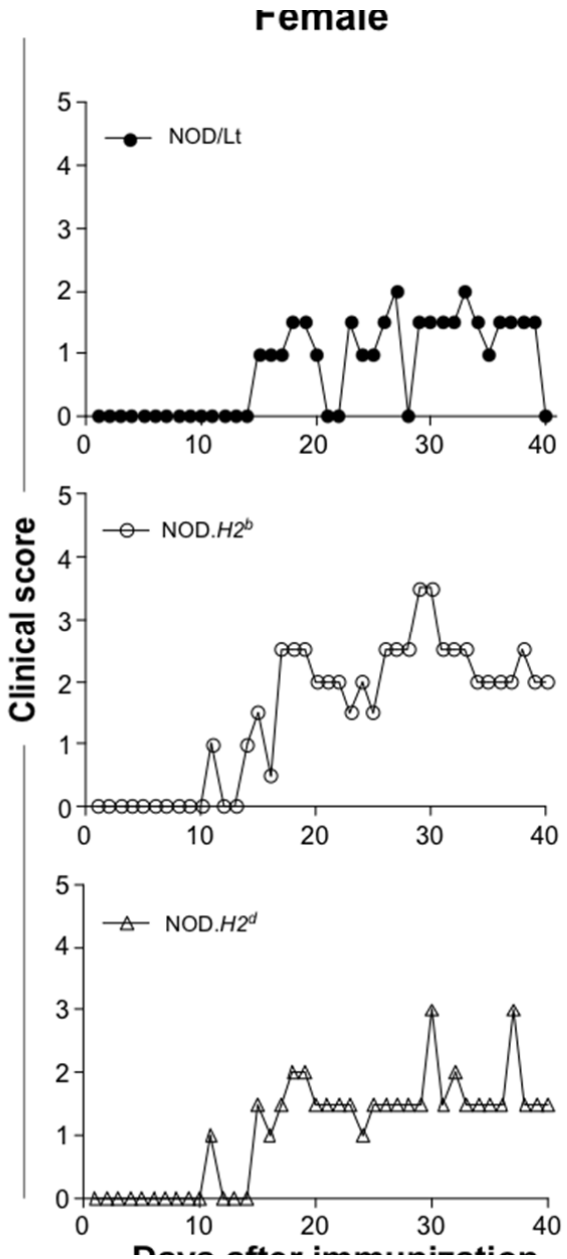


Figure 5.7 Clinical course of active $MOG_{35-55}$/CFA + PTX–induced EAE in NOD.*H2*$^{b}$ control mice (WT) (*closed circles*), NOD.*H2*$^{b}$.*Tlr2*$^{-/-}$ (*open circles*) and; NOD/Lt control mice (WT) (*closed downward triangles*) and NOD.*Tlr2*$^{-/-}$ (*open upwards triangles*). Each data point and error bar represents the mean ± SEM of the clinical score of each individual day from 6-10 mice. Statically significant data are indicated (*$p < 0.05$, uncorrected Mann Whitney-test; $n$ = 6-10).

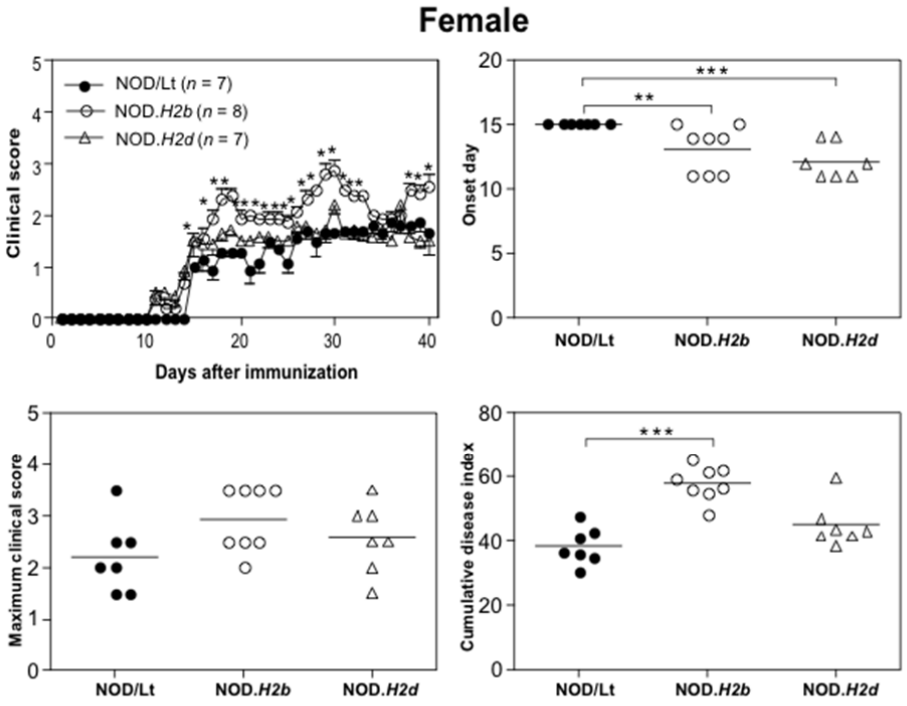


Figure 5.8. Analysis of the clinical course of active $MOG_{35-55}$/CFA + PTX- induced relapsing-remitting EAE in NOD.$H2^b$ (*close circles*) and NOD.$H2^b$.$Tlr2^{-/-}$ (*open circles*); and NOD/Lt (*closed downwards triangles*) and NOD.$H2^b$.$Tlr2^{-/-}$ (*open upwards triangles*) in males and female mice. Significant differences are indicated (*$p < 0.05$, **$p < 0.01$, ***$p < 0.001$ uncorrected Mann-Whitney *U* test; $n$ = 6-10).

## 5.2.4 IL6 in active $MOG_{35-55}$/CFA + PTX–induced relapsing-remitting EAE in the absence of TLR2

As previous studies showed that protection of chronic EAE in the absence of TLR2 was associated with detectable levels of circulating IL6 (Chapter 4), it remains possible that the severity of EAE decreased in NOD.*H2*$^{b}$.*Tlr2*$^{-/-}$ was due to circulating levels of IL6. To determine whether circulating levels of IL6 could influence the phenotype of active $MOG_{35-55}$/CFA + PTX–induced relapsing-remitting EAE in NOD.*H2*$^{b}$.*Tlr2*$^{-/-}$ mice, the disease was induced in NOD.*H2*$^{b}$ and NOD.*H2*$^{b}$.*Tlr2*$^{-/-}$ mice and; IL6 or PBS (control) was administrated i.p. in NOD.*H2*$^{b}$.*Tlr2*$^{-/-}$ mice during the induction of active $MOG_{35-55}$/CFA + PTX–induced EAE.

NOD.*H2*$^{b}$.*Tlr2*$^{-/-}$ male mice treated with PBS had less severe clinical course of relapsing-remitting EAE during nine days (day 22, 28, 30-33 and 35-37, $p < 0.05$) and NOD.*H2*$^{b}$.*Tlr2*$^{-/-}$ male mice treated with IL6 had less severe clinical course of relapsing-remitting EAE during four days (day 31-34, $p < 0.05$) compared with NOD.*H2*$^{b}$ male mice (Figure 5.9). CDI decreased in NOD.*H2*$^{b}$.*Tlr2*$^{-/-}$ male mice treated with PBS (CDI mean ± SEM = 36.25 ± 3.91, $p < 0.05$) compared with NOD.*H2*$^{b}$ male mice (CDI mean ± SEM = 61.0 ± 11.61); but no differences were observed between NOD.*H2*$^{b}$.*Tlr2*$^{-/-}$ male mice treated with IL6 and NOD.*H2*$^{b}$ male mice (Figure 5.9). ). No

differences were seen in the day of onset of disease and maximum clinical score in NOD.*H2*$^{b}$.*Tlr2*$^{-/-}$ male mice treated with IL6 or PBS compared with NOD.*H2*$^{b}$ male mice (Figure 5.9).

NOD.*H2b.Tlr2*$^{-/-}$ female mice treated with PBS had less severe clinical course of relapsing-remitting EAE during 12 days (26, 30-40, $p < 0.05$), and NOD.*H2*$^{b}$.*Tlr2*$^{-/-}$ female mice treated with IL6 had less severe clinical course of relapsing-remitting EAE during 19 days (21, and 23-40, $p < 0.05$) (Figure 5.9). CDI decreased in NOD.*H2*$^{b}$.*Tlr2*$^{-/-}$ female mice treated with PBS (CDI mean ± SEM = 38.42 ± 4.52, $p < 0.05$), and in NOD.*H2*$^{b}$.*Tlr2*$^{-/-}$ female mice treated with IL6 (CDI mean ± SEM = 30.93 ± 6.62, $p < 0.01$) compared with NOD.*H2*$^{b}$ female mice (CDI mean ± SEM = 67.37 ± 10.61). No differences were seen in the day of onset of disease and maximum clinical score in NOD.*H2*$^{b}$.*Tlr2*$^{-/-}$ female mice treated with IL6 or PBS compared with NOD.*H2*$^{b}$ female mice (Figure 5.9).

A further analysis of the clinical course of active $MOG_{35-55}$/CFA + PTX–induced relapsing-remitting EAE between NOD.*H2*$^{b}$.*Tlr2*$^{-/-}$ mice treated with IL6 and NOD.*H2*$^{b}$.*Tlr2*$^{-/-}$ mice treated with PBS showed no differences in the clinical course of active relapsing-remitting EAE, the day of onset of disease, the maximum clinical score and the CDI in either sex (Figure 5.9). These results suggest that circulating IL6 remained in plasma without

altering the severity of active $MOG_{35-55}$/CFA + PTX–induced relapsing-remitting EAE.

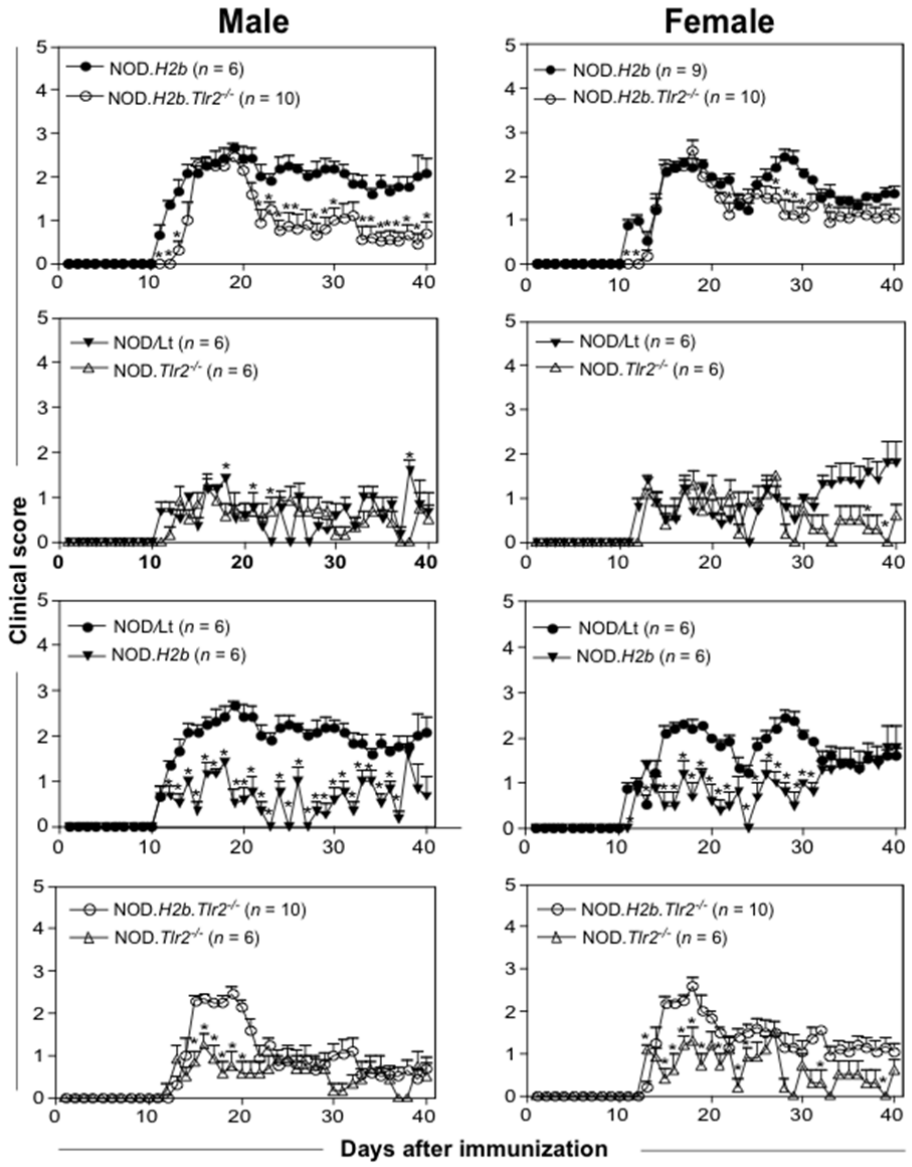


Figure 5.9 Analysis of the clinical course of active $MOG_{35-55}$/CFA + PTX–induced EAE in NOD.$H2^b$ control mice (WT) (*closed circles*), NOD.$H2^b$.$Tlr2^{-/-}$ mice treated with PBS (*open circles*) and NOD.$H2^b$.$Tlr2^{-/-}$ mice treated with IL6 (*open downward triangles*). Each data point and error bar represents the mean ± SEM of the clinical score. Statically significant data are indicated (*$p < 0.05$, **$p < 0.01$, ***$p < 0.01$, uncorrected Mann Whitney-test; $n = 8$).

## 5.2.5 Circulating levels of cytokines in active $MOG_{35-55}$/CFA + PTX–induced relapsing-remitting EAE in NOD.*H2*$^{b}$.*Tlr2*$^{-/-}$ and NOD.*Tlr2*$^{-/-}$ mice

In an attempt to find whether circulating cytokines influenced the development of $MOG_{35-55}$/CFA + PTX–induced relapsing-remitting EAE in *NOD.H2*$^{b}$ and NOD.*H2*$^{b}$.*Tlr2*$^{-/-}$ mice, plasma from NOD.*H2*$^{b}$ and NOD.*H2*$^{b}$.*Tlr2*$^{-/-}$ mice was analysed after 40 days of EAE induction.

Circulating levels of IL6 were detected in *NOD.H2*$^{b}$ and NOD.*H2*$^{b}$.*Tlr2*$^{-/-}$ mice treated with either IL6 or PBS. Circulating levels of IL6 decreased in NOD.*H2*$^{b}$.*Tlr2*$^{-/-}$ mice treated with IL6 (mean ± SEM = 254.1 ± 44.59) but not in NOD.*H2*$^{b}$.*Tlr2*$^{-/-}$ mice treated with PBS (mean ± SEM = 450.9 ± 117.5) compared with NOD.*H2*$^{b}$ mice (mean ± SEM = 481.7 ± 63.45). Surprisingly, IL22 levels increased in both NOD.*H2*$^{b}$.*Tlr2*$^{-/-}$ mice treated with IL6 (mean ± SEM = 145.5 ± 22.31) and in NOD.*H2*$^{b}$.*Tlr2*$^{-/-}$ mice treated with PBS (mean ± SEM = 271.2 ± 61.12) compared with NOD.*H2*$^{b}$ (mean ± SEM = 74.55 ± 10.49). No detectable levels of IL13, IL1, IL22, IL2, IL5, IL21, IL6, IL10, IL27, IL23, IFNγ, TNF, IL4 and IL17 were found neither in NOD.*H2*$^{b}$ nor NOD.*H2*$^{b}$.*Tlr2*$^{-/-}$ mice treated with either IL6 or

PBS. Data suggest that IL6 do not accumulate in the periphery when administrated i.p., and IL22 production is associated to TLR2 signalling.

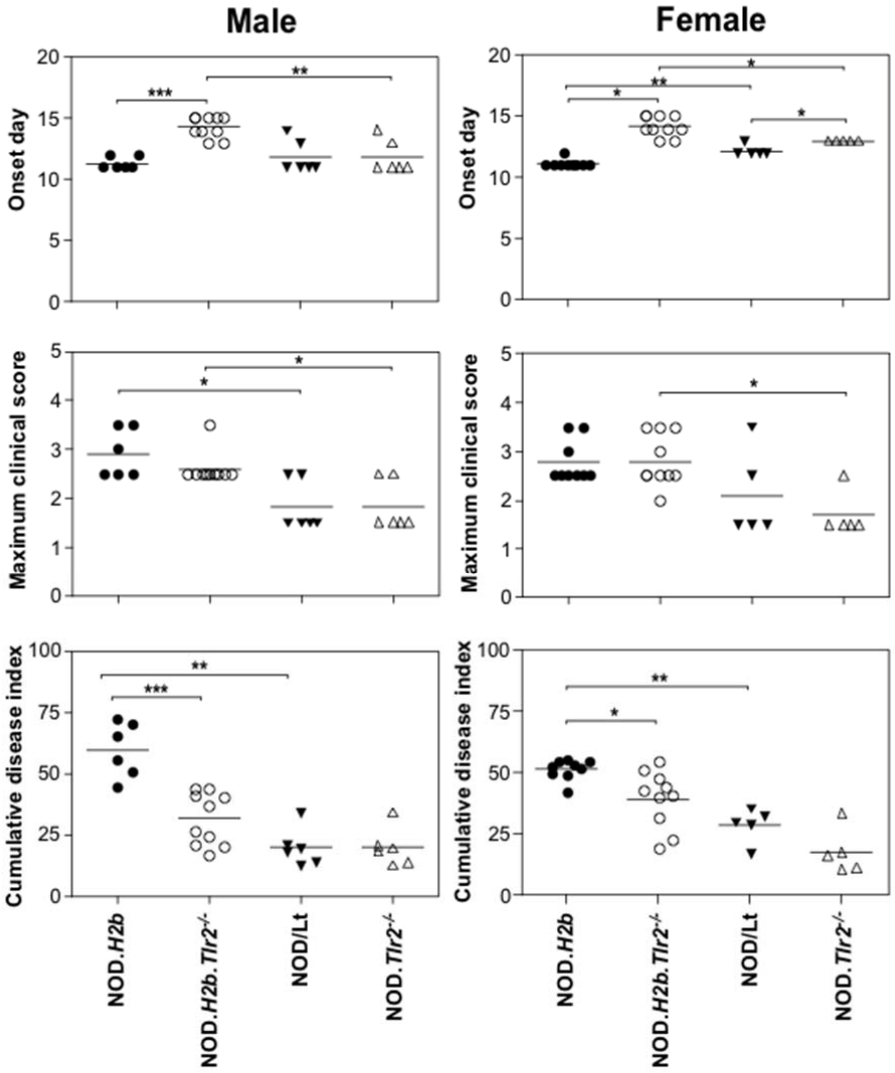


Figure 5.10 Circulating levels of IL6 and IL22 in NOD.$H2^b$ (*close cicles*), NOD.$H2^b$.$Tlr2^{-/-}$ treated with PBS (*open cicles*), NOD.$H2^b$.$Tlr2^{-/-}$ treated with IL6 (*open downward triangles*), naive NOD.$H2^b$ (closed squares), naive NOD.$H2^b$.$Tlr2^{-/-}$ (*open squares*), naive NOD/Lt (*open diamonds*), naive NOD.$Tlr2^{-/-}$ (*closed diamonds*). Limits of detention levels of cytokines are indicated with a horizontal line. Significant differences are shown (*$p < 0.05$, **$p < 0.01$, ***$p < 0.001$ uncorrected Mann-Whitney *U* test; $n$ = 6-10).

## 5.3 Discussion

In Chapter 3 we found that C57BL/6.*Tlr2*$^{-/-}$ mice show less severe clinical signs of EAE; and in Chapter 4 we found that adoptive transfer of EAE into C57BL/6.*Tlr2*$^{-/-}$ mice failed to transfer disease. This protection from EAE was associated with fewer infiltrating CD4$^{+}$ T cells in the CNS, reduced prevalence of detectable circulating IL6, and increased proportions of central (CD62L$^{+}$) Foxp3$^{+}$ Tregs. In this chapter, we studied the dependence of EAE on TLR2 in an autoimmune-prone genetic background. As NOD/Lt mice develop a mild form of relapsing/remitting EAE (Amor et al., 1993; Slavin et al., 1998), this strain of mice was used to study the role of TLRs in EAE in order to dissect the interrelationships between organ-specific autoimmune diseases.

In contrast to C56BL/6 mice, which developed a chronic form of EAE (Chapter 3 and Chapter 4) NOD/Lt mice developed a mild form of relapsing-remitting EAE. Furthermore, unlike to C57BL/6.*Tlr2*$^{-/-}$ mice, NOD.*Tlr2*$^{-/-}$ mice did not affect the severity of EAE. As NOD/Lt mice are susceptible to T1D (Kachapati et al., 2012), we tested whether insulitis associated with T1D development compensated for the lack of TLR2 signalling in these mice. Because our results confirmed that NOD.*H2*$^{b}$ and NOD.*H2*$^{d}$ mice did not develop insulitis or T1D as declared by Yoshida et al., (2008) and Pearson et al., 2003, active $MOG_{35-55}$/CFA + PTX was studied in these mice.

NOD.*H2*$^{b}$ mice showed increased severity of EAE compared to NOD/Lt mice, again in a relapsing/remitting pattern. To my knowledge this work show for first time that in the absence of insulitis, EAE is ameliorated in NOD.*H2*$^{b}$.*Tlr2*$^{-/-}$ mice and no relapses occurred after the initial peak of disease. These data suggest that both TLR2 signalling and immunological events associated with autoimmunity at a distant site can mediate relapses in CNS autoimmunity. As seen before circulating levels of IL6 did not affect the severity of active $MOG_{35-55}$/CFA + PTX –induced EAE after the induction of EAE in the absence of TLR2 confirming that circulating levels of IL6 increase before clinical signs of EAE appear. Although increased numbers of IL22 were found in the absence of TLR2, Kreymborg et al., (2007) reported that IL22 knockout mice are not protected from EAE. Further studies are required to find the mechanisms that influence the severity of EAE in NOD.*H2*$^{b}$ and NOD.*H2*$^{b}$.*Tlr2*$^{-/-}$ mice.

# CHAPTER 6

# CHAPTER 6

# NKT CELLS IN THE INTERACTION BETWEEN ENVIRONMENTAL AND GENETIC RISK FACTORS FOR EAE

## 6.1 Introduction

NKT cells are innate/memory T lymphocytes that recognize lipids and glycolipids presented by CD1d molecules (Godfrey et al., 2000; MacDonald 2002). NKT cells expressed the semi-invariant V$\alpha$24$^{+}$J$\alpha$18 in humans and V$\alpha$14$^{+}$J$\alpha$18 in mice (Budd et al., 1987; Fowlkes et al., 1987; review in MacDonald 2007). Activation of NKT cells releases the production of INF$\gamma$/IL4/IL17 cytokines (Godfrey et al., 2004; Coquet et al., 2008). The initiation and development of MS and EAE are also associated with the production of INF$\gamma$/IL4/IL17 cytokines (Lees et al., 2008; Stromnes IM, 2008). Despite knowing that different NKT cell subsets produced key cytokines involved in the phenotype of MS and EAE, the role of NKT cells in CNS-autoimmune inflammation remains far from clear.

The evidence that NKT cells contribute to EAE includes at least four mechanisms: 1) cytokine production by NKT cells ligation of lipids and

glycolipids (Hammond et al., 2002); 2) NKT cell cytokine production in response to specific NKT cell peptides (Liu et al., 2011; Fujita et al., 2009); 3) the activity of CD1d molecule in EAE (Jahng et al., 2001) and; 4) the NKT cell number in EAE (Miljković et al., 2011; Yokote et al., 2008).

Most studies indicate that increment of IL4 and IL10 and decrease of INFγ and IL17 by NKT cell ligation of α-GalCer, OCH and RCAI147/-160 protect mice from EAE (Miyamoto et al., 2001; Furlan et al., 2003; Oh et al., 2011; Shiozaki, et al., 2013). However, contradictory reports showed that α-GalCer treatment in EAE had no effect or is dependent of the time of EAE immunisation and route of administration (Furlan et al., 2003; Pál et al., 2001; Hammond et al., 2002). Other studies indicate that the expression of CD1d molecule is required for EAE protection (Singh et al., 2001; Mars et al., 2008). Few studies showed that NKT cell-enriched mice are protected against EAE (Mars et al., 2002; Mars et al., 2008).

At the time of writing most studies have been done by stimulation of NKT cells to produce INFγ/IL4/IL17 cytokines. Little research has been done in mice with different numbers of NKT cells. In this chapter, it was hypothesized that genetic control of NKT cells numbers alters the severity of EAE. To test this hypothesis, EAE was induced in genetically manipulated mice with different genes controlling NKT cell numbers.

# 6.2 Results

## 6.2.1 Active $MOG_{35-55}$/CFA + PTX-induced EAE in NOD/Lt mice and NOD.*Nkrp1b* mice

NOD/Lt mice are the most common animal models to study Type 1 diabetes (T1D) (Makino et al., 1980). NOD/Lt mice are also animal models to study systemic lupus erythematosus, Sojogren' syndrome and MS (Krause et al., 1999; Slavin et al., 1998; Robinson et al., 1997; Baker et al., 1995). NOD/Lt mice do not express the allelic marker NK1.1 while NOD.*Nkrp1b* mice express the allelic marker NK1.1 because NOD.*Nkrp1b* mice carry the B6-derived allele *Klrb1c*, a natural killer complex on chromosome 6 (from *D6mit105* to *D6mit135*) (Poulton et al., 2001).

Both NOD/Lt and NOD.*Nkrp1b* mice are characterised for having fewer NKT cell numbers than C57BL/6 mice (Jordan et al., 2009; Poulton et al., 2001). The difference of NKT cell numbers is associated with the resistance of C57BL/6 mice to T1D and the spontaneous development of T1D in NOD/Lt mice (Makino et al., 1980; Pearson et al., 2003). Although NOD.*Nkrp1b* carry the allele *Klrb1c* from C57BL/6 mice, NOD.*Nkrp1b* mice develop a similar pattern of T1D than NOD/Lt mice as the numbers of NKT cells between NOD/Lt and NOD.*Nkrp1b* is similar (Poulton et al., 2001; Fletcher et al., 2008). However, the development of EAE in C57BL/6

and NOD/Lt differs (Chapter 3, Chapter 4 and Chapter 5). NOD/Lt mice develop a mild form of relapsing-remitting EAE and C57BL/6 mice develop a chronic form of EAE (Slavin et al., 1998).

To determine the phenotype of EAE in mice with few NKT cell numbers that express the NK1.1 marker at the same time, NOD/Lt and NOD.*Nkrp1b* female mice were immunized for active $MOG_{35-55}$/CFA + PTX-induced EAE. As expected, all NOD/Lt and NOD.*Nkrp1b* mice developed clinical signs of disease and the clinical course of disease was similar in both groups (Figure 6.1). No differences were also observed in the onset of the disease, maximum clinical score and CDI (Figure 6.1), indicating that the population of NKT cells expressing the NK1.1 marker does not affect the severity of active $MOG_{35-55}$/CFA + PTX-induced EAE in NOD mice.

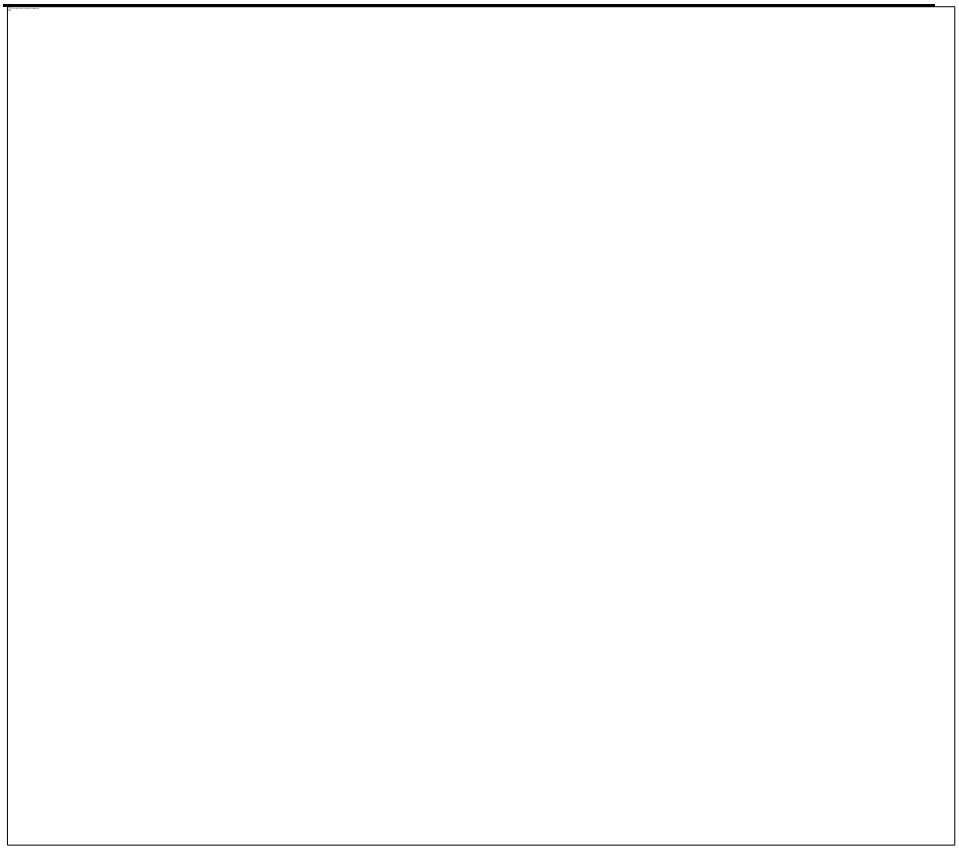

Figure 6.1 Analysis of the clinical course of active $MOG_{35-55}$/CFA + PTX -induced EAE in female NOD/Lt (*closed circles*) and NOD.*Nkrp1b* (*open circles*) mice. No significant differences were found between NOD/Lt and NOD.*Nkrp1b* (*$p < 0.05$, uncorrected Mann-Whitney *U* test; $n = 5$).

## 6.2.2. *Cd1d* in active $MOG_{35-55}$/CFA + PTX-induced EAE

CD1d molecules are cell surface glycoproteins expressed on APCs that present lipids and glycolipids to NKT cells (Porcelli et al., 1989). NKT cells are severely reduced in *Cd1d* knockout mice (Mendiratta et al., 1997). To determine whether targeted deletion of *Cd1d* affects the clinical course of active $MOG_{35-55}$/CFA + PTX-induced EAE, the disease was induced in NOD.*Cd1d*$^{-/-}$, C57BL/6.*Cd1d*$^{-/-}$, NOD/Lt and C57BL/6 mice.

Targeted deletion of *Cd1d* in C57BL/6 female mice did not influence the clinical course of active $MOG_{35-55}$/CFA + PTX-induced EAE, the onset day of disease, the maximum clinical score and the cumulative disease index ($p < 0.05$, uncorrected Mann Whitney-test *U* test) (Figure 6.2).

The clinical course of disease in the absence of *Cd1d* in NOD/Lt female mice increased only during three days (day 16, 40 and 39) and decreased for one day (day 18). No significant differences in the onset day of disease, the maximum clinical score and the cumulative disease index were observed in the absence of *Cd1d* in NOD/Lt female mice ($p < 0.05$, uncorrected Mann Whitney-test *U* test) (Figure 6.3).

These data discarded a role of CD1d in the severity of active $MOG_{35-55}$/CFA + PTX-induced EAE in NOD and C57BL/6 mice, suggesting that the course of disease is independent of CD1 molecule but it could be dependent of NKT cells after the antigen presentation by the CD1d molecule.

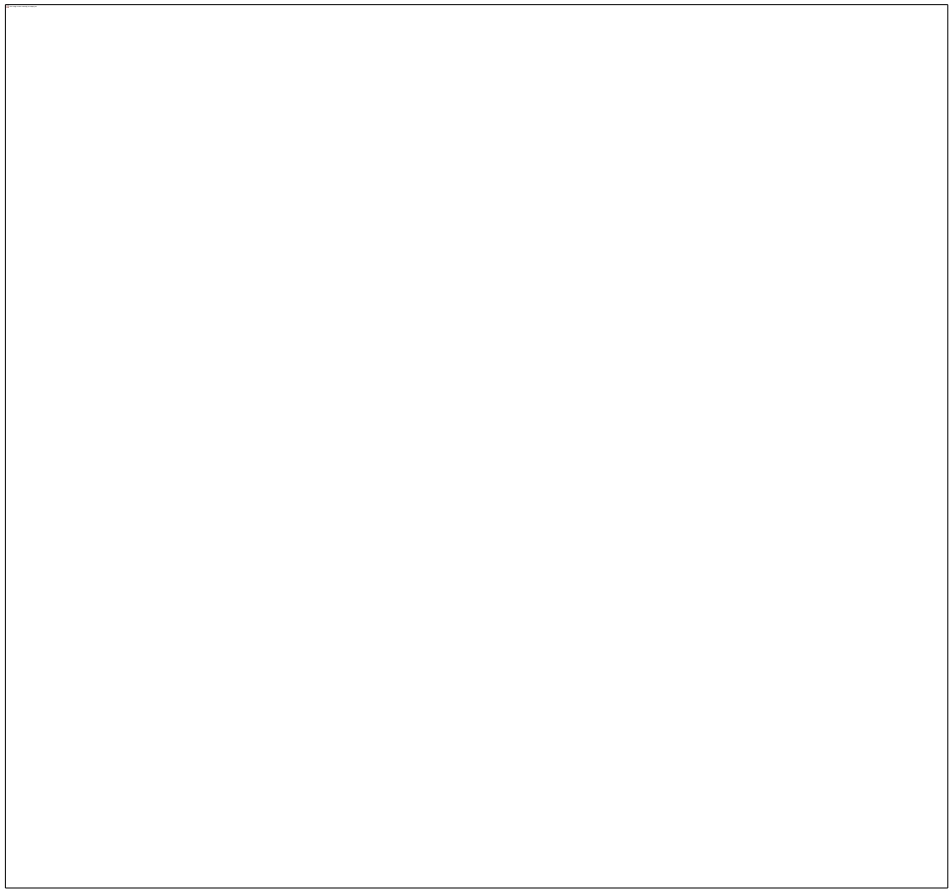

Figure 6.2. Analysis of the clinical course of active $MOG_{35-55}$/CFA + PTX -induced EAE in female C57BL/6 (*closed circles*) and C57BL/6.*Cd1d*$^{-/-}$ (*open circles*) mice. No significant differences were found between C57BL/6 and C57BL/6.*Cd1d*$^{-/-}$ (**p* < 0.05, uncorrected Mann-Whitney *U* test; *n* = 7-8).

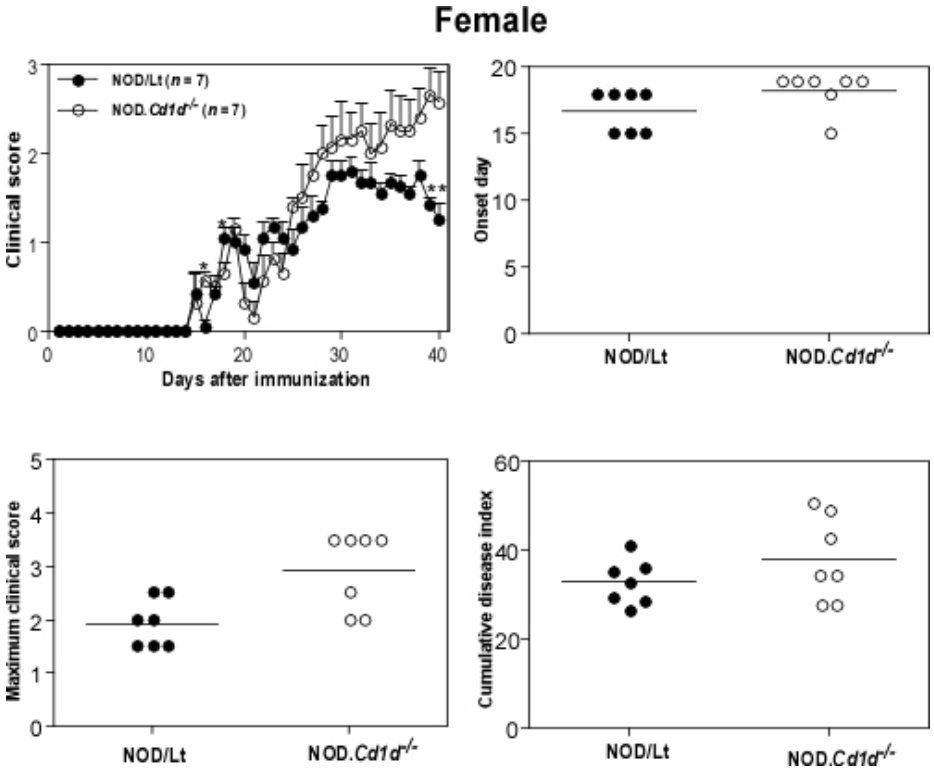


Figure 6.3 Analysis of the clinical course of active $MOG_{35-55}$/CFA + PTX -induced EAE in female NOD/Lt (*closed circles*) and NOD.*Cd1d*$^{-/-}$ (*open circles*) mice. NOD.*Cd1d*$^{-/-}$ mice showed an increase of clinical signs of disease only at days 16, 39 and 40 compared to NOD/Lt. No differences were seen in the onset of disease, maximum clinical score and cumulative disease index between NOD/Lt and NOD.*Cd1d*$^{-/-}$ (*$p < 0.05$, uncorrected Mann-Whitney *U* test; $n = 7$).

## 6.2.3. The *Idd13* locus in active $MOG_{35-55}$/CFA + PTX-induced EAE

*Idd13* locus regulates NKT cell numbers and NOD.*Idd13* mice increase NKT cell numbers compared to NOD/Lt mice (Esteban et al., 2003; Chen et al., 2007). To find out whether higher numbers of NKT cells participate in the development of EAE, males and females NOD/Lt and NOD.*Idd13* mice were immunized for $MOG_{35-55}$/CFA + PTX-induced EAE.

The clinical course of active $MOG_{35-55}$/CFA + PTX-induced EAE reached significant difference between NOD/Lt and NOD.*Idd13* only during three days in male mice (days 51, 54 and 55; $p < 0.05$, uncorrected Mann Whitney-test *U* test) (Figure 6.4). No significant differences between NOD/Lt and NOD.*Idd13* male mice were found in the onset day of disease, the maximum score and the clinical disease index (Figure 6.4).

The clinical course of disease increased in NOD.*Idd13* female mice for a period of 14 days (day 37, 40-47, 50, 54-55, 65-66; $p < 0.05$) compared to NOD/Lt female mice. No differences were observed on the onset day of disease between NOD/Lt and NOD.*Idd13* female mice. The maximum score of disease and CDI showed an increase in NOD.*Idd13* compared to NOD/Lt female mice (Table 1 and Figure 6.5).

An independent experiment in NOD.*Idd13* and NOD/Lt female mice showed more severe clinical course of the disease for 6 days (day 16, 32, 34-35, 39, 40: $p < 0.05$). Clinical signs of disease appeared earlier in NOD.*Idd13* ($p < 0.01$) compared to NOD/Lt female mice (Table 6.1). The clinical signs of disease and the CDI were more severe in NOD.*Idd13* ($p < 0.01$ and $p < 0.05$ respectively) than NOD/Lt female mice (Table 6.1). All together, these data suggest that increased numbers of NKT cells in NOD.*Idd13* mice is associated with more severe clinical signs of disease.

Table 6.1. Active $MOG_{35-55}$/CFA + PTX –induced EAE in NOD/Lt and NOD.*Idd13* female mice.

| Experiment | Strain | *N* | Incidence (%) | Onset (days) | Maximum Disease Score | Cumulative Disease Index (CDI) |
|---|---|---|---|---|---|---|
| Female | | | | | | |
| Exp 1 | NOD/Lt | 8 | 100 | 20.1±1.2 | 1.5±0.2 | 23.2±6.2 |
| | NOD.*Idd13* | 7 | 100 | 19.2±0.5 | 2.6±0.3* | 61.5±10.2** |
| Exp 2 | NOD/Lt | 7 | 100 | 16.7±0.6 | 1.9±0.1 | 32.9±1.9 |
| | NOD.*Idd13* | 7 | 100 | 13.7±0.5** | 2.8±0.2** | 42.7±2.8* |

Mean ± SEM of the clinical score of EAE. Statistically significant data between NOD/Lt mice and NOD.*Idd13* mice are indicated (*p < 0.05, **p < 0.01, ***p < 0.01, uncorrected Mann Whitney-test *U* test).

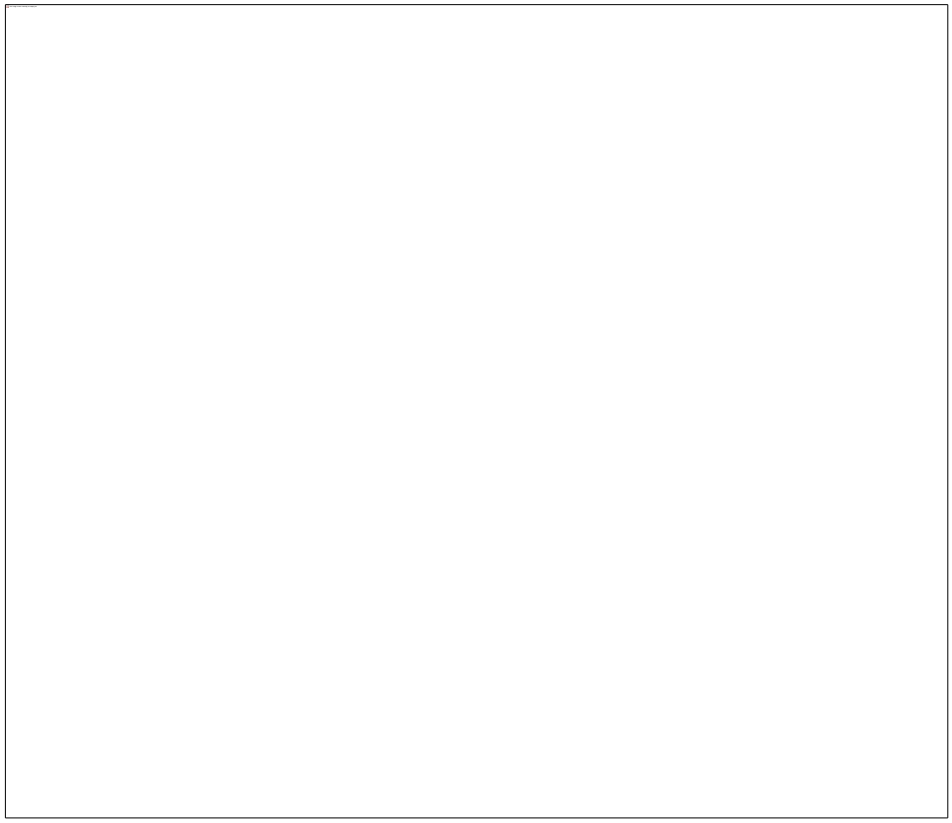

Figure 6.4 Analysis of the clinical course of active $MOG_{35-55}$/CFA + PTX -induced EAE in male NOD/Lt (*closed circles*) and NOD.*Idd13* (*open circles*) mice. NOD.*Idd13* mice showed an increase of clinical signs of disease during three days compared to NOD/Lt. However, no differences were seen in the onset of disease, maximum clinical score and cumulative disease index (*$p < 0.05$, uncorrected Mann-Whitney *U* test; $n = 7$-8).

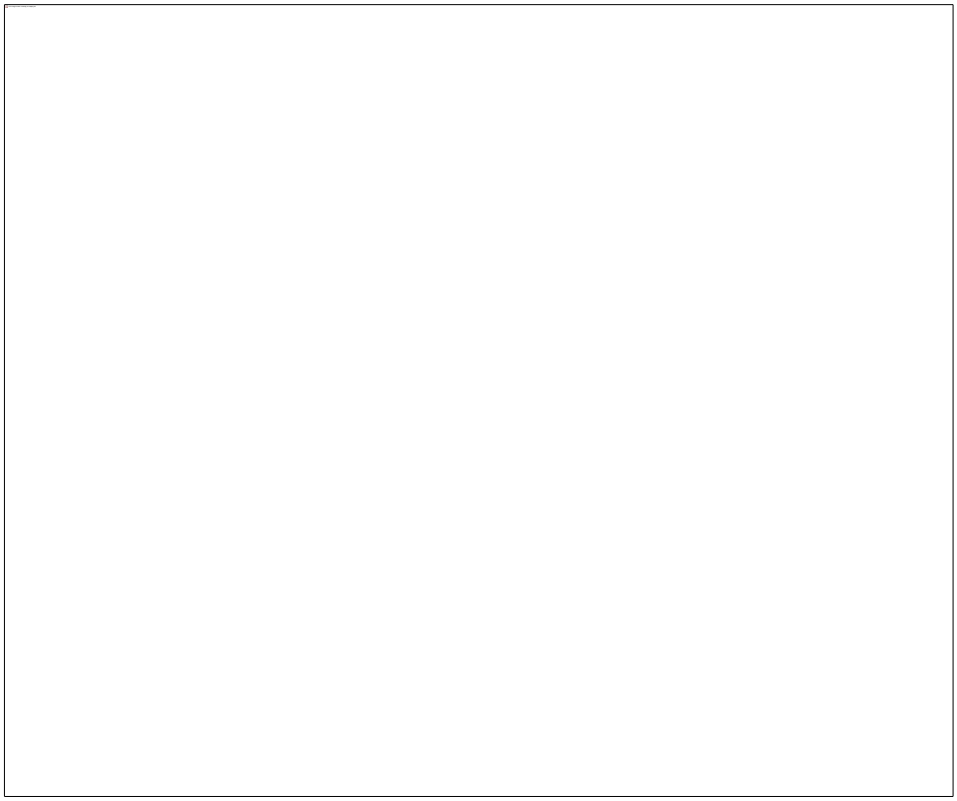

Figure 6.5 Representative analysis of clinical course of active $MOG_{35-55}$/CFA + PTX -induced EAE in female NOD/Lt (*closed circles*) and NOD.*Idd13* (*open circles*) mice from two independent experiments. Significant differences are indicated (*$p < 0.05$, **$p < 0.01$, ***$p < 0.001$ uncorrected Mann-Whitney *U* test; $n = 7$-8).

## 6.2.4 Active $MOG_{35-55}$/CFA + PTX-induced EAE in *NOD.Nkrp1b* mice congenic for *Nkt1, Nkt2a, Nkt2b, Nkt2e*

*Nkt1, Nkt2a, Nkt2b and Nkt2e* loci control NKT cell numbers and NOD.*Nkrp1b* mice congenic for the *Nkt1, Nkt2a, Nkt2b and Nkt2e* loci increase numbers of NKT cells (Esteban et al., 2003; Rocha-Campos et al., 2006; Fletcher et al., 2008). To determine whether increase numbers of NKT cells in the congenic segments *Nkt1, Nkt2a, Nkt2b and Nkt2e* affect the severity of EAE, NOD.*Nkrp1b.Nkt1*, NOD.*Nkrp1b.Nkt2a*, NOD.*Nkrp1b.Nkt2b*, NOD.*Nkrp1b.Nkt2e* and NOD.*Nkrp1b* (control group) were immunized for active $MOG_{35-55}$/CFA + PTX-induced EAE.

The clinical course of $MOG_{35-55}$/CFA + PTX-induced EAE between NOD.*Nkrp1b* (control group) and NOD.*Nkrp1b.Nkt1* showed significant difference only in two consecutive days (day 15-16: $p < 0.05$) (Figure 6.6). The control group increased the severity of disease on day 15 and the next the day NOD.*Nkrp1b.Nkt1* showed more severe disease (Figure 6.6). The maximum score decreased in NOD.*Nkrp1b.Nkt1* ($1.75 \pm 0.17$) compared with NOD.*Nkrp1b* ($2.92 \pm 0.3$). No differences where seen in the onset day of disease and CDI between NOD.*Nkrp1b* and NOD.*Nkrp1b.Nkt1* (Figure 6.6).

The clinical course of disease between NOD.*Nkrp1b* and NOD.*Nkrp1b.Nkt2a* differ significantly on days 14, 19, 23, 24, 26, 29 and 30 ($p < 0.05$): On days 14, 29 and 30 disease was more severe in NOD.*Nkrp1b.Nkt2a*; however, on days 23-24 and 26 the disease was more severe in NOD.*Nkrp1b*. No differences were seen in the day of onset of disease, in the maximum score and in the CDI (Figure 6.6).

The clinical course of disease was more severe only for one day in NOD.*Nkrp1b* compared with NOD.*Nkrp1b.Nkt2* and, in NOD.*Nkrp1b* compared with NOD.*Nkrp1b.Nkt2e*. No differences were seen in the day of onset of disease, maximum score and cumulative disease index between NOD.*Nkrp1b* and NOD.*Nkrp1b.Nkt2b* or between NOD.*Nkrp1b* compared with NOD.*Nkrp1b.Nkt2e* (Figure 6.6).

All together, these data showed that despite the *Nkt1, Nkt2a, Nkt2b and Nkt2e* loci increase numbers of NKT cells in NOD mice, this increase do not affect the severity of active $MOG_{35-55}$/CFA + PTX-induced EAE.

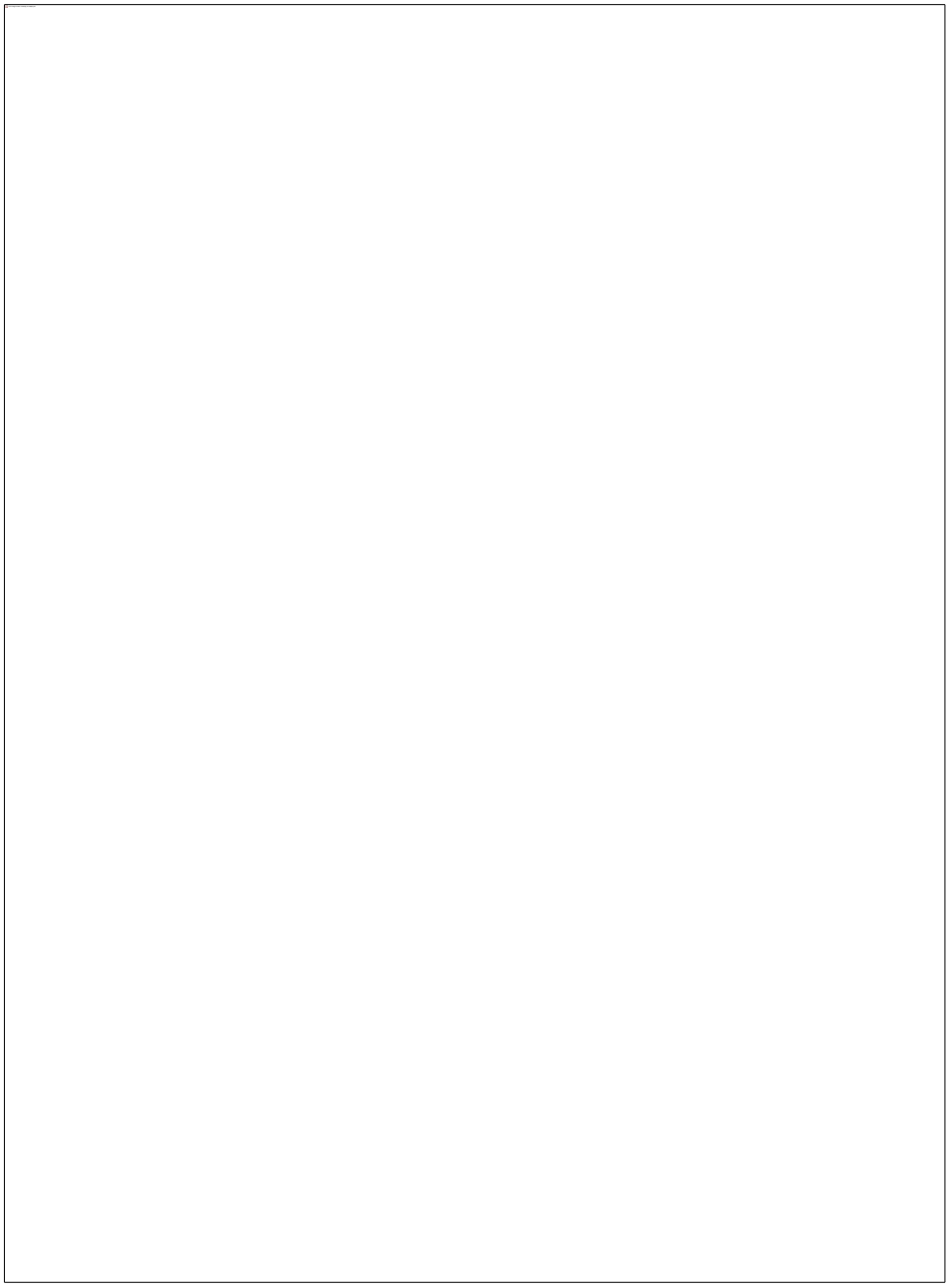

Figure 6.6 Analysis of the clinical course of active $MOG_{35-55}$/CFA + PTX -induced EAE in female NOD.*Nkrp1b* (*closed circles*), NOD.*Nkt1* (*open circles*), NOD.*Nkt2a* (*open upward triangles*), NOD.*Nkt2b* (open downward triangles) and NOD.*Nkt2e* (open diamonds) mice. Although differences in the clinical score were seen during few days between NOD.*Nkrp1b* compared to NOD.*Nkt1*, NOD.*Nkt2b* and NOD.*Nkt2e* no diferences were seen in the onset of disease, maximum clinical score and cumulative disease index in NOD.*Nkt1*, NOD.*Nkt2a*, NOD.*Nkt2b* and NOD.*Nkt2e* mice compared to NOD.*Nkrp1b* mice (*$p < 0.05$, uncorrected Mann-Whitney *U* test; $n = 6$-7).

## 6.2.5 Active $MOG_{35-55}$/CFA + PTX-induced EAE in TCR CD4-Vα14 transgenic mice

TCR CD4-Vα14 C57BL/6 transgenic mice are enriched in CD1-restricted NKT cells. The transgene was inserted in different places and every place was identified with the numbers 2, 5 and 6. A new line of mice were created from each insert. The three lines of mice were identified with the common names: C57BL/6.Tg(mCD4-Vα14)2, C57BL/6.Tg(mCD4-Vα14)5 and C57BL/6.Tg(mCD4-Vα14)6. To determine whether different inserts of the transgene TCR CD4-Vα14 C57BL/6 affect the severity of, active $MOG_{35-55}$/CFA + PTX-induced EAE, the disease was induced in female and male C57BL/6.Tg(mCD4-Vα14)2, C57BL/6.Tg(mCD4-Vα14)5 and C57BL/6.Tg(mCD4-Vα14)6 mice.

### 6.2.5.1 C57BL/6.Tg(mCD4-Vα14)6 mice

C57BL/6.Tg(mCD4-Vα14)6 male mice decreased the clinical course of disease during days 13, 14 and 15 ($p < 0.05$) compared to C57BL/6 male mice (Figure 6.7). The onset day of disease was delayed in C57BL/6.Tg(mCD4-Vα14)6 (15.4± 0.4) compared to C57BL/6 (13.17 ±

0.16) male mice (Figure 6.7). No differences in the maximum clinical score were seen between C57BL/6.Tg(mCD4-Vα14)6 and C57BL/6 male mice.

The clinical course of disease decreased in C57BL/6.Tg(mCD4-Vα14)6 female mice compared with C57BL/6 female mice (day 21-22, 24-27, 31, 33-35, 37-40: $p < 0.05$) (Figure 6.9). C57BL/6.Tg(mCD4-Vα14)6 female did not differ on the day of onset of disease compared with C57BL/6 female mice (Figure 6.9). The clinical signs of disease were less severe in female C57BL/6.Tg(mCD4-Vα14)6 mice (maximum clinical score ± SEM = 2.0 ± 0.44) compared with C57BL/6 female mice (maximum clinical score ± SEM = 3.5 ± 00). The CDI also decreased in C57BL/6.Tg(mCD4-Vα14)6 female mice (CDI ± SEM = 26.0 ± 14.78) compared with C57BL/6 female mice (CDI ± SEM = 73.83 ± 5.25). This data indicate that the TCR CD4-Vα14 transgene inserted in the place identify with the number six decrease the severity of active $MOG_{35-55}$/CFA + PTX-induced EAE.

### 6.2.5.2 C57BL/6.Tg(mCD4-Vα14)5 mice

C57BL/6.Tg(mCD4-Vα14)5 male mice show less severe clinical course of disease on days 13-23, 25-27, 31, 34-36 ($p < 0.05$) than C57BL/6 male mice (Figure 6.7). The day of onset of disease ± SEM was delayed in C57BL/6.Tg(mCD4-Vα14)5 (27.17 ± 4.88 days) compared to C57BL/6

(13.16 ± 0.16) male mice (Figure 6.7). The maximum clinical score and the cumulative disease index show no differences between C57BL/6.Tg(mCD4-Vα14)5 and C57BL/6 male mice (Figure 6.7).

C57BL/6.Tg(mCD4-Vα14)5 female mice showed lower clinical course of disease from day 17 to 40 compared to C57BL/6 ($p < 0.05$). The onset day of disease ± SEM was delayed in C57BL/6.Tg(mCD4-Vα14)5 female mice (31.8 ± 5.67 days) compared with C57BL/6 female mice (14.5 ± 0.76 days). The severity of clinical signs of disease decreased in C57BL/6.Tg(mCD4-Vα14)5 female mice (maximum clinical score ± SEM = 0.8 ± 0.49) than C57BL/6 female mice (maximum clinical score ± SEM = 3.5 ± 00). The cumulative disease index was lower in C57BL/6.Tg(mCD4-Vα14)5 female mice (CDI ± SEM = 11.2 ± 7.31) than C57BL/6 female mice (CDI ± SEM = 73.83 ± 5.25).

This data indicate that the TCR CD4-Vα14 transgene inserted in the place identify with the number five delayed the onset of clinical signs of disease and decrease the severity of active $MOG_{35-55}$/CFA + PTX-induced EAE.

### 6.2.5.3 C57BL/6.Tg(mCD4-Vα14)2 mice

C57BL/6.Tg(mCD4-Vα14)2 male mice show less severe clinical score on day 19, 25, 31 and 33-39 ($p < 0.05$) than C57BL/6 (Figure 6.8). The onset day of disease was delayed in C57BL/6.Tg(mCD4-Vα14)2 (16.0 ± 1.19) compared to C57BL/6 (13.5 ± 0.34) male mice (Figure 6.8). No differences were seen in the maximum clinical score. The cumulative disease index was lower in C57BL/6.Tg(mCD4-Vα14)2 (61.28 ± 9.78 than C57BL/6 male mice (88.5 ± 3.01) (Figure 6.8). C57BL/6.Tg(mCD4-Vα14)2 female were completely protected from EAE (Figure 6.9).

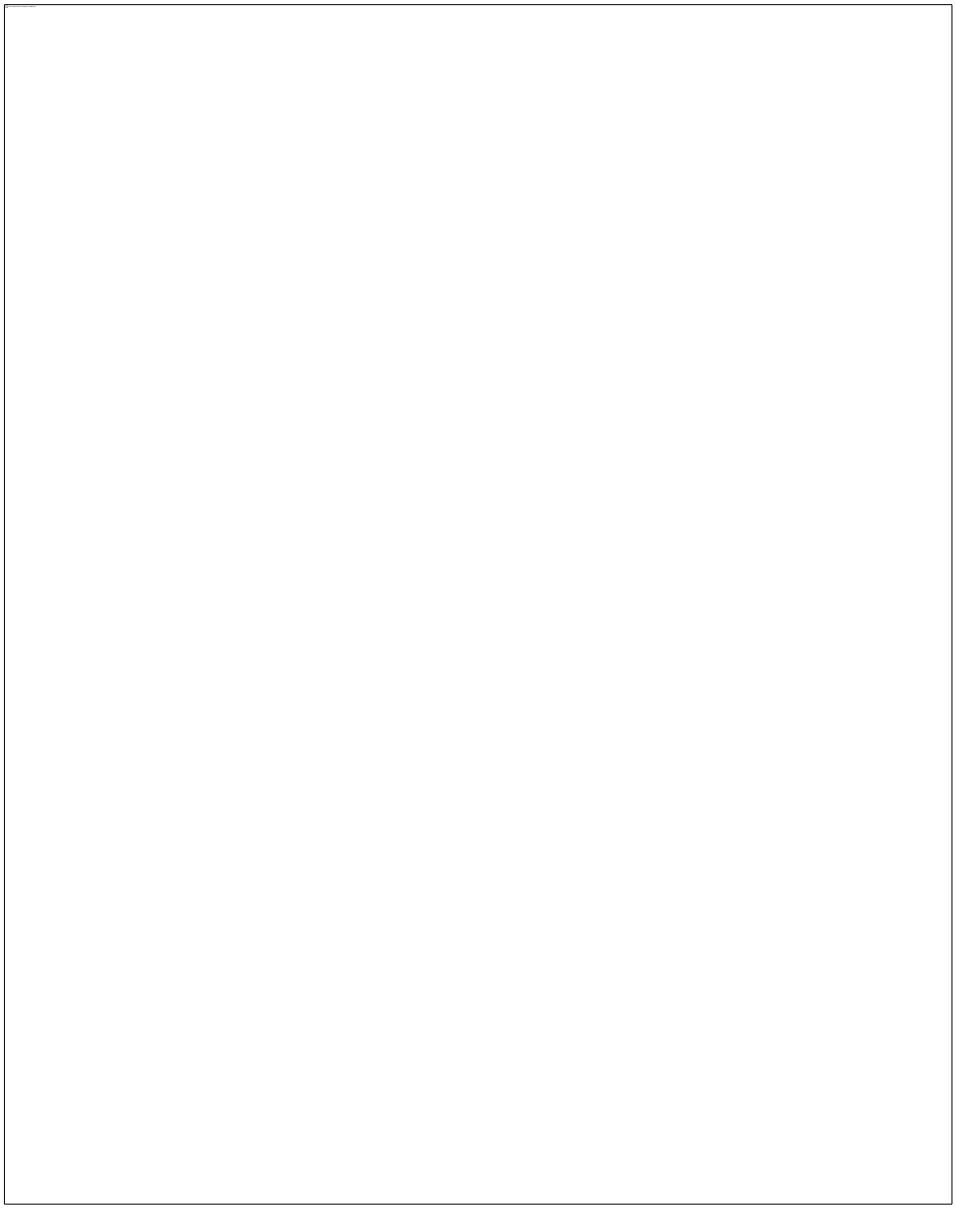

Figure 6.7 Analysis of the clinical course of active $MOG_{35-55}$/CFA + PTX -induced EAE in male C57BL/6 (*closed circles*), C57BL/6.Tg(mCD4-Va14)6 (*upward triangles*), C57BL/6.Tg(mCD4-Va14)5 (*open squares*) mice. Significant differences in clinical score per day between C57BL/6 and C57BL/6.Tg(mCD4-Va14) mice are indicated (*$p < 0.05$). Differences in the onset of disease, maximum clinical score and cumulative disease are indicated (*$p < 0.05$, **$p < 0.01$, ***$p < 0.001$ uncorrected Mann-Whitney $U$ test; $n$ = 5-6).

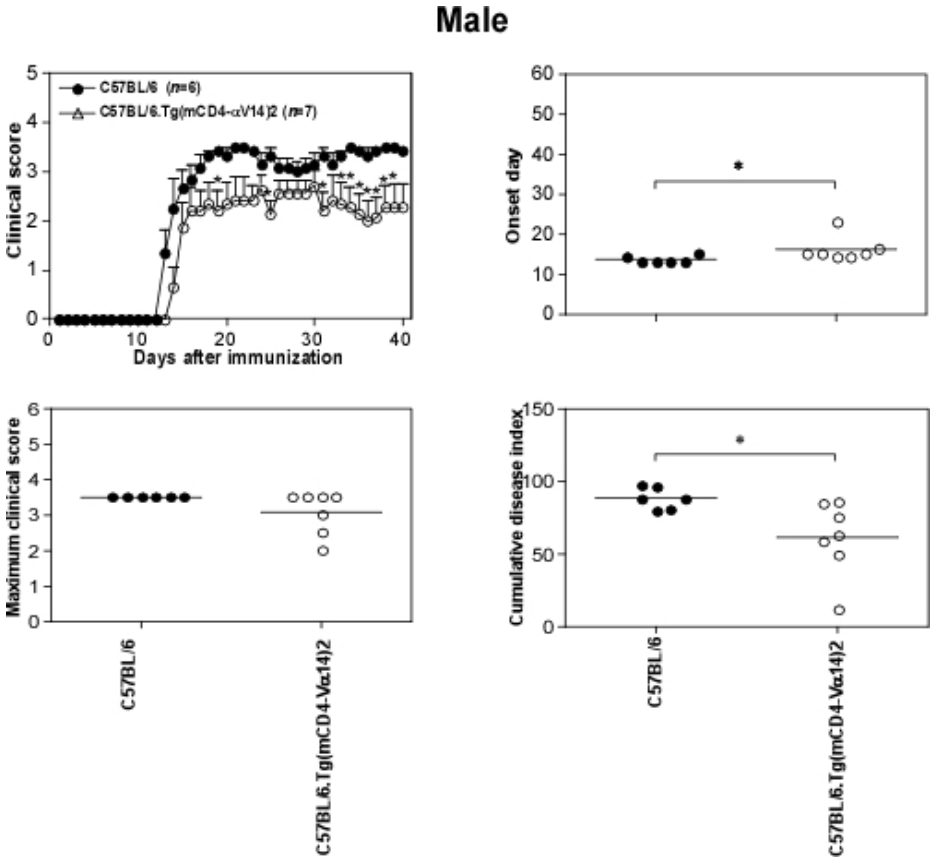


Figure 6.8 Analysis of the clinical course of active $MOG_{35-55}$/CFA + PTX -induced EAE in male C57BL/6 (*closed circles*), C57BL/6.Tg(mCD4-Va14)2 (*open cicles*) mice. Significant differences in clinical score per day between C57BL/6 and C57BL/6.Tg(mCD4-Va14) mice are indicated (*$p < 0.05$). Differences in the onset of disease, maximum clinical score and cumulative disease are indicated (*$p < 0.05$, **$p < 0.01$, ***$p < 0.001$ uncorrected Mann-Whitney *U* test; $n$ = 6-7).

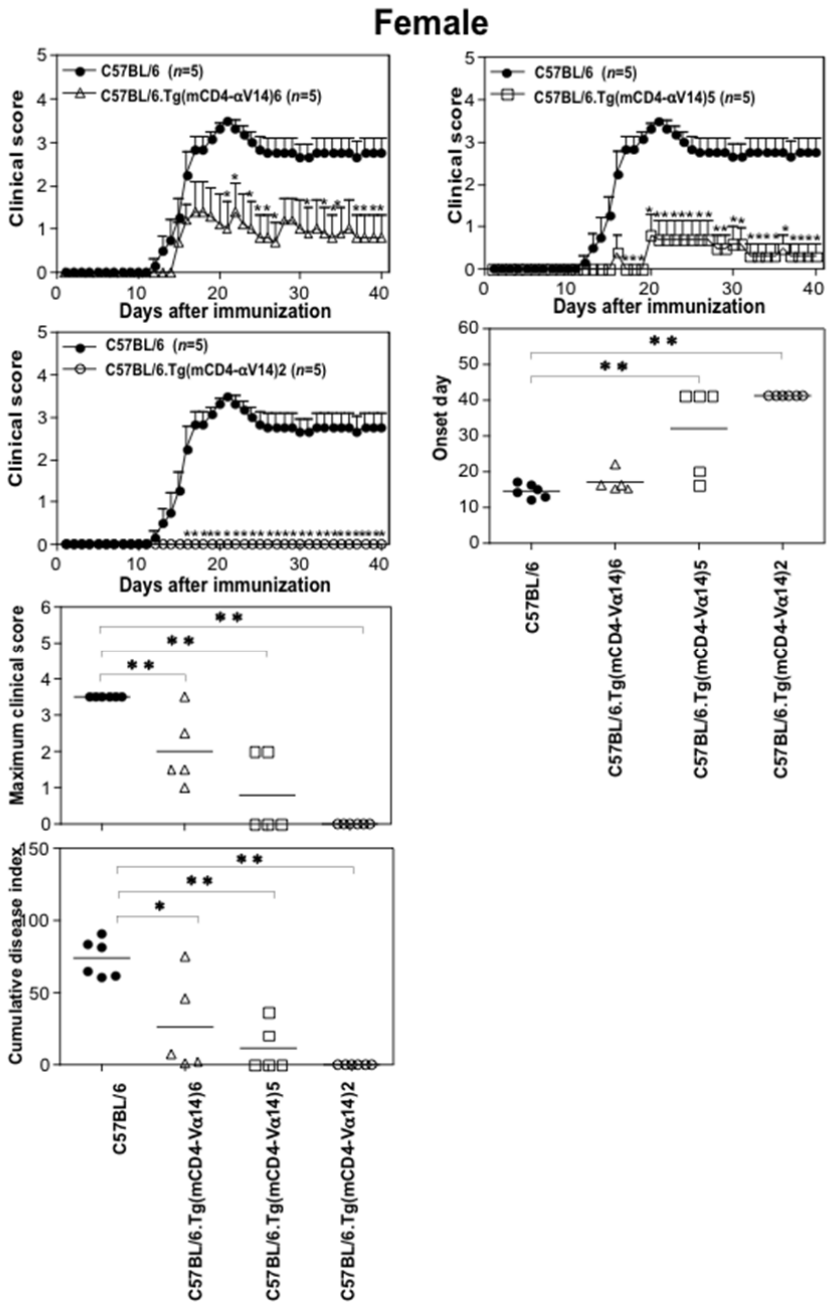


Figure 6.9 Analysis of the clinical course of active $MOG_{35-55}$/CFA + PTX -induced EAE in female C57BL/6 (*closed circles*), C57BL/6.Tg(mCD4-Va14)2 (*upward triangles*), C57BL/6.Tg(mCD4-Va14)5 (*open square*) and C57BL/6.Tg(mCD4-Va14)2 (*open circles*) mice. Significant differences in the clinical score per day between C57BL/6 and C57BL/6.Tg(mCD4-Va14) mice are indicated (*$p < 0.05$). Differences in the onset of disease, maximum clinical score and cumulative disease are indicated (*$p < 0.05$, **$p < 0.01$, ***$p < 0.001$ uncorrected Mann-Whitney *U* test; $n = 5$-6).

## 6.3 Discussion

NKT cells are a group of T cells that express common markers for T and NK cells and are activated by lipids and glycolipids (Godfrey et al., 2004; MacDonald 2002). NKT cells produce IL4/IFNγ/IL17 cytokines and these cytokines play a key role in EAE (Godfrey et al., 2004; Coquet et al., 2008; Lees et al., 2008; Stromnes 2008).

To date, most research about the role of NKT cells in EAE has been focused on the immune response to NKT cells ligation (Jahng et al., 2001; Singh et al., 2001; Furlan et al., 2003). Little research has been done about the NKT cell number in EAE (Novak et al., 2011; Miljković et al., 2011; Yokote et al., 2008). This chapter illustrated the genetic control of NKT cells numbers in the phenotype of EAE.

C57BL/6 mice have higher numbers of NKT cells than NOD/Lt and NOD.*NKrp1b* mice (Jordan et al., 2009; Poulton et al., 2001). NOD/Lt mice develop a mild form of relapsing-remitting EAE and C57BL/6 mice develop a chronic form of EAE (Slavin et al., 1998). NOD.*Nkrp1b* mice carry the B6 alleles at the NKC on Chomosome 6 to express the marker NK1.1 (Esteban et al., 2003). Here, it is shown that the phenotype of EAE is similar between NOD/Lt and NOD.*Nkrp1b* mice, which demonstrates that the B6 alleles at the NKC on Chomosome 6 do not affect the severity of EAE in NOD/Lt

mice. However, deeper studies are necessary to conclusively demonstrate whether NKT cells expressed the NK1.1 marker affect the severity of EAE. NK1.1 marker is express in a small population of NKT cells and in NK cells (Slifka et al., 2004). Fritz et al., (2001) reported that cells expressing the $NK1.1^{+}$ marker, $DX5^{+}$ and $\alpha\beta^{+}$ TCR regulate EAE.

The lack of CD1d decreases dramatically the NKT cell numbers (Mendiratta et al., 1997). The reduced numbers of NKT cells in the absence of *Cd1d* do not affect the clinical course of EAE neither in NOD/Lt mice nor in C57BL/6 mice. Although, Teige et al., (2004) reported that EAE is exacerbated in the absence *Cd1d*, these results support the findings of Mars et al., (2002) and Singh et al., (2001) who found that the severity of EAE is not altered in *Cd1d*-deficient mice. Different results can be associated to different protocols to induce EAE.

The Idd13 locus is located on chromosome 2 and is a strong component of the distinction between NOD and NOR mice (Reifsnyder et al., 2005). NOD.*Idd13* mice have higher NKT cells numbers than NOD/Lt mice (Esteban et al., 2003; Chen et al., 2007). Although, Mayo et al., (2007) reported that NOR/Lt mice decrease the severity of disease in the presence of PTX and, in the absence of PTX NOR/Lt mice are completely resistant to EAE. We are the first group reporting that NOD.*Idd13* mice increase the severity of disease.

NKT cells numbers also increase in NOD.*Nkrp1b.Nkt1,* NOD.*Nkrp1b.Nkt2a,* NOD.*Nkrp1b.Nkt2b* and NOD.*Nkrp1b.Nkt2e* mice (Rocha-Campos et al., 2006; Jordan et al., 2007). However, the development of EAE remains unaltered in these mice. To my knowledge studies of EAE in these mice has not been reported previously.

TCR CD4-Vα14 C57BL/6 transgenic mice are enriched in CD1-restricted NKT cells. Although, previous report in transgenic mice show that TCR Vα14 -Jα281 transgenic NOD mice enriched in CD1d-restricted NKT cells, are protected from EAE (Mars et al., 2002). This study is the first reporting that TCR CD4-Vα14 transgene inserted in three different places decrease the severity of EAE in C57BL/6 mice.

All together, further studies are required to identified whether NKT cells expressing the NK1.1 marker alter the development of EAE. CD1d does not affect the severity of EAE. Idd13 locus affects the severity of EAE but not the *Nkt1, Nkt2a, Nkt2b and Nkt2e* loci. TCR CD4-Vα14 construct affect the severity of EAE. Although the mechanisms affecting the severity of EAE remain to be defined, in this chapter we report that specific genes control NKT cells numbers are able to influence the severity of EAE. It possible that congenic alleles that boost NKT cell numbers may control the

phenotype of EAE and/or influence the immune response because of the specific subsets of NKT cells generated during the disease.

# CHAPTER 7

# CHAPTER 7

# GENERAL DISCUSSION AND CONCLUSIONS

MS is a chronic inflammatory and degenerative disease that affects the CNS. This disease affects mainly young adults and is more common in women than in men; but it is more severe in men than in women. MS is classified as an autoimmune disease because the immune cells attack the CNS' own cells with an unclear cause. Despite the cause is not clear, genetic and environmental factors have been associated with the initiation and progression of MS (Wynn et al., 1990; Duquette et al., 1992; Moldovan et al., 2008).

Both genetics and environmental factors associated with MS are mainly studied in animal models, which reproduce some forms of the disease. EAE is the most commonly used animal model for the study of the pathogenesis and immunoregulation of CNS autoimmunity. Although EAsE has some limitations to replicate the autoimmune inflammation observed in MS, it is a useful model for a deeper understanding of MS biology. In the present study, EAE was used as an animal model to

assess the role of TLRs and NKT cells in gene/environment interactions in CNS-autoimmune inflammation.

MS and EAE are dominated by $CD4^+$ T helper (Th) cells secreting Th1, Th17, Th2 and iTreg cells (Corrale et al., 1995; Lassmann et al., 2001). Th17 and Th1 cells are associated with CNS autoimmune damage while Th2 is associated with CNS autoimmune protection (Link et al., 1994; Maddur et al., 2012). In general, there are two subsets of Th17 cells: 1) Th17 (Th17β) cells, which requires of IL6 and TGFβ for their development, and expresses higher IL10, CCL20, CXCR6, IL17A and IL17F and; 2) Th17 (23) cells that require of IL6, IL23 and IL1 and expresses higher IL22, CCL9 and CXCR3. Th1 cells require of IL12 and IFNγ and produce IFNγ. In contrast, Th2 cells and iTreg cells seem to down regulate autoimmune inflammation in the CNS. Th2 cells require IL4 and produce IL4, IL5, IL10 and IL13. iTreg cells require TGFβ and IL2 to produce TGFβ (review in Kurebayashi et al., 2013).

Th1, Th17, Th2 and iTreg cytokines regulate each other, for example: a) Th17 differentiation is inhibited by the production of IL2, IL4 and IFNγ; b) Th1 differentiation is inhibited by IL4 production; c) Th2 differentiation is inhibited by IFNγ and IL2 and d) Treg is inhibited by IL6 (D'Andrea et al., 1993; Oukka et al., 2007; review in Kurebayashi et al., 2013).

Gene microarray analysis of MS plaques from autopsy of MS patients showed increased levels of IL6, IL17 and IFNγ including altered pathways of these cytokines (Lock et al., 2002). Altered numbers of IL17 and IFNγ have been found in RRMS and SPMS (Frisullo et al., 2008). RRMS patients show altered levels of IL4, IL6, IL12 and IL10 (Link et al., 1994; Chen et al., 2012; Kallaur et al., 2013). TGFβ production is defective and TGFβ signalling is reduced in MS patients (Mokhtarian et al 1994; Meoli et al., 2011). Moreover, evidence of the role of Th1, Th17, Th2 and iTreg cytokines secretion in autoimmune inflammation is also seen in EAE for example; mice are resistant to EAE in the absence of IL23 or IL6, while IL4 and IL10 has anti-inflammatory effect (Eugster et al., 1998; Cua et al., 2003; Hirota et al., 2011; Payne et al., 2012 and Fitzgerald et al., 2007).

TLRs and NKT cells respond to environmental factors by the production and/or expression of Th1, Th17, Th2 and iTreg cytokines; for example: Ligation of TLRs modulates the differentiation of human Th17 cells (Kattah et al., 2008). IL6 is generated in response to ligation of TLR2 and augmented on response to ligation of TLR4 and TLR2/6 heterodimer, (Takeuchi et al., 2000, Thoma-Uszynski et al., 2000, McCurdy et al., 2001, Mu et al., 2001; Jin et al., 2011). TGFβ is produced in response to microflora, which is identified by TLRs (Rakoff-Nahoum et al., 2004; Atarashi et al., 2008; Ivanov et al., 2008; Zeuthen et al., 2008). IL23 and

IL1 are up regulated in response to pathogenic *E. coli* K4 after ligation of TLR2 and TLR4 (Cammarota et al., 2009). IFNγ is produced in response of TLRs such as TLR2 and TLR4 and promotes TLR signalling (Hu et al., 2006; Schroder, et al., 2006; Brüll et al., 2010). IL17, IFNγ and IL4 are produced by different NKT cell subsets, examples include: $CD4^-$ NKT cells and $CD4^-CD8^-$ NKT cells produce IFNγ; $CD4^+$ NKT cells produce IL4; $CD4^-NK1.1^-$ NKT cells produced IL17 (Gumperz et al., 2002; Lee et al., 2002; Michel et al., 2007; Coquet et al., 2008).

This research illustrates part of the phenotype of $MOG_{35-55}$/CFA+PTX induced EAE generated by $CD4^+$ T helper (Th) cytokine production via TLRs and NKT cells. The absence of MyD88 completely protect mice of active $MOG_{35-55}$/CFA+PTX induced EAE as reported before by Prinz et al., (2006); Marta et al., (2008) and Lampropoulou et al., (2008). However, the absence of TLR1 and TLR6 do not alter the clinical course of EAE. The role of TLR1 is reported for the first time in this study and the role of TLR6 is consistent with results previously reported by Marta et al., (2008). However, controversial results have been found in active EAE in the absence of TLR4, TLR2 and TLR9. Our studies rule out a role of TLR4 in the disease while Marta et al (2008) found that TLR4 protects against EAE. This work supports a decrease of clinical course of EAE in the absence of TLR9 (Prinz et al., 2006), although Marta et al (2008) found a mild increase in of the severity of disease. This study also found a decrease in the severity

of active EAE in the absence of TLR2 but Prinz et al (2006) did not find differences. Results from this study are consistent with the effect of *M. tuberculosis* that was used as adjuvant. The difference between these studies and those from of Marta et al (2008) is the autoantigen. Marta used recombinant rat MOG protein and we used $MOG_{35-55}$. Kerfoot et al., (2004) do not mention the sex of the mice used in the experiment. Prinz et al (2006) only used female mice in the experiments. The different protocol of EAE induction, the sex of the animal models and the environment seem to be associated with distinct results. This study reports a partial resolution of this discrepancy when we describe a mild reduction in EAE clinical socores of female, but not male in the absence of TLR2 in C57BL/6 mice. Moreover, this study suggests that microflora or pathogen exposure in different animal facilities contributed to different results.

In order to discard any effect of the adjuvant (CFA, which contains *M. tuberculosis* and; PTX, which signal through TLR4 (Kerfoot et al., 2004)), the roles of TLR2, TLR4 and TLR9 were studied in the passive model of EAE. In this model adoptive transfers were performed by transfer lymphocytes from: WT to TLR2 deficient mice, WT to WT; WT to TLR2 deficient mice; WT to TLR9 deficient mice; TLR2 deficient mice to WT and TLR2 deficient mice to TLR2 deficient mice.

Adoptive transfer of WT lymphocytes into WT recipients resulted in similar clinical signs of active $MOG_{35-55}$/CFA+PTX induced EAE. The severity of passive EAE decreased in TLR4 deficient mice, thus PTX partially signal through TLR4. Clinical signs of passive EAE decreased in the absence of TLR9, nevertheless; the inhibition of disease was similar to that seen in active EAE. The adoptive transfer of TLR2 deficient cells into either WT or TLR2 deficient recipients resulted in ameliorated disease, similar to active EAE in the absence of TLR2 in female mice. In contrast, the transfer of WT cells into TLR2 deficient mice resulted in complete protection in both male and female mice; suggesting that the presence of TLR2 at the induction of disease creates a dependence on TLR2 signalling in the effector phase. Our results were consistent with the findings of Reynolds et al., (2010). Protection in the absence of TLR2 was associated to a decrease of $CD4^+$ T cell infiltration in CNS, a decrease of $CD4^+$ T cell secreting IL17 in the CNS, undetectable levels of circulating IL6 and increase numbers of central ($CD62L^+$) $CD4^+CD25^+Foxp3^+$ regulatory T cells. These results provide a potential mechanism of TLR2 in the development of autoimmune CNS inflammation as IL6 is produced after TLR2 ligation, and IL6 is involved in $CD4^+$ T cell differentiation into Th17 cells, which are inhibited by Treg cells (Takeuchi et al., 2000, Thoma-Uszynski et al., 2000, McCurdy et al., 2001, Mu et al., 2001; Jin et al., 2011; Kurebayashi et al., 2013).

The role of TLRs was further studied in NOD mice. Consistent with the results of Amor et al., (1993) and Slavin et al., (1998), NOD mice

developed a form of relapsing/remitting EAE. In contrast to C57BL/6.*Tlr2*$^{-/-}$ mice, NOD.*Tlr2*$^{-/-}$ mice did not affect the severity of disease. As NOD/Lt mice are susceptible to T1D, we tested whether insulitis associated with T1D development compensated for the lack of TLR2 signalling in these mice.

Because NOD/*Lt* and NOD.*Tlr*$^{-/-}$ developed a mild form of EAE, a better model of EAE was used. Active $MOG_{35-55}$/CFA+PTX induced EAE was induced in in NOD.*H2*$^{d}$ and NOD.*H2*$^{b}$ mice, which are resistant to Type 1 diabetes (T1D) (Pearson et al., 2003; Yoshida et al., 2008). NOD.*H2*$^{d}$ mice developed a chronic form of EAE similar to C57BL/6 mice and NOD.*H2*$^{b}$ mice showed a severe form of relapsing-remitting EAE.

To test the hypothesis that insulitis associated with T1D development in some way compensated for the lack of TLR2 signalling in NOD mice, the B6 MHC, *H2*$^{b}$ was crossed onto the NOD and NOD.*Tlr2*$^{-/-}$ strains. NOD.*H2*$^{b}$.*Tlr2*$^{-/-}$ mice did not show relapses of disease after the initial peak of disease. To my knowledge, this is the first study showing the phenotype of EAE in NOD.*H2*$^{d}$, NOD.*H2*$^{b}$, NOD.*H2*$^{b}$.*Tlr2*$^{-/-}$. These results indicate that the role of TLR2 is particularly important in the effector phase of both chronic and relapsing-remitting $MOG_{35-55}$/CFA+PTX induced EAE. In addition, these data suggest that both TLR2 signalling and immunological

events associated with autoimmunity at a distant site can mediate relapses in CNS autoimmunity.

Finally, NKT cells are also involved in $CD4^+$ T helper (Th) cytokine production. Activation of NKT cells by glycolipids was found to protect the CNS of autoimmune inflammation by the preferential production of IL4, GM-CSF, IL4 and IFNγ (Miyamoto et al., 2001; Parekh et al., 2013). Opposing these results, Quian et al., (2010) found that α-galcer exacerbate EAE by the production of IL17. NKT cells are restricted by CD1d molecule; and enrich in CD1d-restricted NKT cells protect from EAE (Mars et al., 2002; Mars et al., 2008). Protection is associated with CNS NKT cells infiltration and CNS local expression of CD1d (Mars et al., 2002; Mars et al., 2008). It seems that only enrichment of CD1d in CNS provide protection against autoimmune inflammation. Consistent with this statement, our experiments show that the severity of $MOG_{35-55}$/CFA+PTX induced EAE decrease in transgenic mice but not in congenic mice. C57BL/6.Tg(mCD4-Vα14)6 female decreases the clinical signs of disease in female mice but not male mice and in C57BL/6.Tg(mCD4-Vα14)5 female and male mice while C57BL/6.Tg(mCD4-Vα14)2 female were completely protected from the disease. Mars et al., (2002) reported that TCR Vα14-Jα81 transgenic NOD mice are protected from EAE by inhibiting IFNγ production in spleen These results suggest that $CD4^+$Vα14 NKT cells produce preferentially one of the four groups of cytokines that could dictate

the phenotype of $MOG_{35-55}$/CFA + PTX induced EAE; nevertheless if the phenotype of EAE depends on cytokine production by NKT cells or by NKT cell infiltration need to be clarified.

Given the different results in the role of TLR2 and NKT cells, it would be important to understand more fully the mechanisms involved in their participation in CNS autoimmune inflammation before translate this results into therapeutic options for MS. Then it would be important to replicate the results in different animal models, environments and sexes. On the other side the key role of MyD88 in CNS autoimmune inflammation requires the development, validation and testing of MS drugs in several animal models. If results are favorable and consistent in different animal models, they must be translated into therapeutic options for specific individuals.

# REFERENCES

# REFERENCES

Abel B, Thieblemont N, Quesniaux VJ, Brown N, Mpagi J, Miyake K, Bihl F, Ryffel B. Toll-like receptor 4 expression is required to control chronic Mycobacterium tuberculosis infection in mice. *Journal of Immunology*. 2002; 169(6): 3155-3162.

Adachi O, Kawai T, Takeda K, Matsumoto M, Tsutsui H, Sakagami M, Nakanishi K, Akira S. Targeted disruption of the MyD88 gene results in loss of IL-1- and IL-18-mediated function. *Immunity*. 1998; 9(1): 143-150.

Aggarwal S, Yurlova L, Simons M. Central nervous system myelin: structure, synthesis and assembly. *Trends Cell Biology*. 2011; 21(10): 585-593.

Agmon-Levin N, Lian Z, Shoenfeld Y. Explosion of autoimmune diseases and the mosaic of old and novel factors. *Cell & Molecular Immunology*. 2011; 8(3): 189-192.

Aguirre-Cruz L, Flores-Rivera J, De La Cruz-Aguilera DL, Rangel-López E, Corona T. Multiple sclerosis in Caucasians and Latino Americans. *Autoimmunity*. 2011; 44(7): 571-575.

Akira S, Uematsu S, Takeuchi O. Pathogen Recognition and Innate

Immunity. *Cell*. 2006; 124: 783-801.

Alexopoulou L, Holt AC, Medzhitov R, Flavell RA. Recognition of double-stranded RNA and activation of NF-kappaB by Toll-like receptor 3. *Nature*. 2001; 413(6857): 732-738.

Amor S, Baker D, Groome N, Turk JL. Identification of a major encephalitogenic epitope of proteolipid protein (residues 56-70) for the induction of experimental allergic encephalomyelitis in Biozzi AB/H and nonobese diabetic mice. *Journal of Immunology*. 1993; 150(12): 5666-5672.

Anaya JM, Gómez L, Castiblanco J. Is there a common genetic basis for autoimmune diseases? *Clinical & Developmental Immunology*. 2006; 13(2-4): 185-195.

Andersson A, Covacu R, Sunnemark D, Danilov AI, Bianco AD, Khademi M, Wallström E, Lobell A, Brundin L, Lassmann H, Harris RA. Pivotal Advance: HMGB1 expression in active lesions of human and experimental multiple sclerosis. *Journal of Leukocyte Biology*. 2008; 84(5): 1248-1255.

Apetoh L, Ghiringhelli F, Tesniere A, Obeid M, Ortiz C, Criollo A, Mignot G, Maiuri MC, Ullrich E, Saulnier P, Yang H, Amigorena S, Ryffel B, Barrat FJ, Saftig P, Levi F, Lidereau R, Nogues C, Mira JP, Chompret A, Joulin V, Clavel-Chapelon F, Bourhis J, André F,

Delaloge S, Tursz T, Kroemer G, Zitvogel L. Toll-like receptor 4-dependent contribution of the immune system to anticancer chemotherapy and radiotherapy. *Nature Medicine*. 2007; 13(9): 1050-1059.

Araki M, Kondo T, Gumperz JE, Brenner MB, Miyake S, Yamamura T. Th2 bias of CD4+ NKT cells derived from multiple sclerosis in remission. *International Immunology*. 2003; 15(2): 279-288.

Aranami T, Yamamura T. Th17 Cells and autoimmune encephalomyelitis (EAE/MS). *Allergology International: official journal of the Japanese Society of Allergology*. 2008; 57(2): 115-120.

Atarashi K, Nishimura J, Shima T, Umesaki Y, Yamamoto M, Onoue M, Yagita H, Ishii N, Evans R, Honda K, Takeda K. ATP drives lamina propria T(H)17 cell differentiation. *Nature*. 2008; 455(7214): 808-812.

Aung LL, Fitzgerald-Bocarsly P, Dhib-Jalbut S, Balashov K. Plasmacytoid dendritic cells in multiple sclerosis: chemokine and chemokine receptor modulation by interferon-beta. *Journal of Neuroimmunology*. 2010; 226(1-2): 158-164.

Back SA, Tuohy TM, Chen H, Wallingford N, Craig A, Struve J, Luo NL, Banine F, Liu Y, Chang A, Trapp BD, Bebo BF Jr, Rao MS, Sherman LS. Hyaluronan accumulates in demyelinated lesions and

inhibits oligodendrocyte progenitor maturation. *Nature Medicine*. 2005; 11(9): 966-972.

Bafica A, Scanga CA, Feng CG, Leifer C, Cheever A, Sher A. TLR9 regulates Th1 responses and cooperates with TLR2 in mediating optimal resistance to *Mycobacterium tuberculosis*. *The Journal of Experimental Medicine*. 2005; 202(12): 1715-1724.

Baker D, Rosenwasser OA, O'Neill JK, Turk JL. Genetic analysis of experimental allergic encephalomyelitis in mice. *Journal of Immunology*. 1995; 155(8): 4046-4051.

Balashov KE, Aung LL, Vaknin-Dembinsky A, Dhib-Jalbut S, Weiner HL. Interferon-β inhibits toll-like receptor 9 processing in multiple sclerosis. *Annals of Neurology*. 2010; 68(6): 899-906.

Bar-Or A, Fawaz L, Fan B, Darlington PJ, Rieger A, Ghorayeb C, Calabresi PA, Waubant E, Hauser SL, Zhang J, Smith CH. Abnormal B-cell cytokine responses a trigger of T-cell-mediated disease in MS? *Annals of Neurology*. 2010; 67(4): 452-461.

Barcellos LF, Oksenberg JR, Begovich AB, Martin ER, Schmidt S, Vittinghoff E, Goodin DS, Pelletier D, Lincoln RR, Bucher P, Swerdlin A, Pericak-Vance MA, Haines JL, Hauser SL. HLA-DR2 Dose Effect on Susceptibility to Multiple Sclerosis and Influence on Disease Course. *American Journal of Human Genetics*. 2003; 72(3):

710–716.

Baxter AG. The origin and application of experimental autoimmune encephalomyelitis. *Nature Reviews Immunology*. 2007; 7(11): 904-912.

Becher B, Durell BG, Miga AV, Hickey WF, Noelle RJ. The clinical course of experimental autoimmune encephalomyelitis and inflammation is controlled by the expression of CD40 within the central nervous system. *Journal of Experimental Medicine*. 2001; 193(8): 967-974.

Bendelac A, Rivera MN, Park SH, Roark JH. Mouse CD1-specific NK1 T cells: development, specificity, and function. *Annual Review of Immunology*. 1997;15:535-62.

Berer K, Mues M, Koutrolos M, Rasbi ZA, Boziki M, Johner C, Wekerle H, Krishnamoorthy G. Commensal microbiota and myelin autoantigen cooperate to trigger autoimmune demyelination. *Nature*. 2011; 479(7374): 538-541.

Bertrams HJ, Kuwert EK. Association of histocompatibility haplotype HLA-A3-B7 with multiple sclerosis. *Journal of Immunology*. 1976; 117(5 Pt.2): 1906-1912.

Berzins SP, Smyth MJ, Baxter AG. Presumed guilty: natural killer T cell defects and human disease. *Nature Reviews Immunology*. 2011; 11(2): 131-142.

Bettelli E, Pagany M, Weiner HL, Linington C, Sobel RA, Kuchroo VK. Myelin Oligodendrocyte Glycoprotein–specific T Cell Receptor Transgenic Mice Develop Spontaneous Autoimmune Optic Neuritis. *The Journal of Experimental Medicine*. 2003; 197(9): 1073-1081.

Bhigjee AI, Moodley K, Ramkissoon K. Mult Scler. Multiple sclerosis in KwaZulu Natal, South Africa: an epidemiological and clinical study. *Multiple Sclerosis*. 2007; 13(9): 1095-1099.

Billiau A, Matthys P. Modes of action of Freund's adjuvants in experimental models of autoimmune diseases. *Journal of Leukocyte Biology*. 2001; 70(6): 849-860.

Bö L, Geurts JJ, Mörk SJ, van der Valk P. Grey matter pathology in multiple sclerosis. *Acta Neurologica Scandinavica Supplementum*. 2006; 183: 48-50.

Brian A, Thieblemont N, Quesniaux VJF, Brown N, Mpagi J, Miyake K, Bihl F, Ryffel B. Toll-Like Receptor 4 Expression Is Required to Control Chronic Mycobacterium tuberculosis Infection in Mice. *Journal of Immunology*. 2002; 169(6): 3155-3162.

Brightbill HD, Libraty DH, Krutzik SR, Yang RB, Belisle JT, Bleharski JR, Maitland M, Norgard MV, Plevy SE, Smale ST, Brennan PJ, Bloom BR, Godowski PJ, Modlin RL. Host defense mechanisms triggered by microbial lipoproteins through toll-like receptors. *Science*. 1999;

285(5428): 732-736.

Brüll F, Mensink RP, van den Hurk K, Duijvestijn A, Plat J. TLR2 activation is essential to induce a Th1 shift in human peripheral blood mononuclear cells by plant stanols and plant sterols. *The Journal of Biological Chemistry*. 2010; 285(5): 2951-2958.

Bsibsi M, Bajramovic JJ, Vogt MH, van Duijvenvoorden E, Baghat A, Persoon-Deen C, Tielen F, Verbeek R, Huitinga I, Ryffel B, Kros A, Gerritsen WH, Amor S, van Noort JM. The microtubule regulator stathmin is an endogenous protein agonist for TLR3. *Journal of Immunology*. 2010; 184(12): 6929-6937.

Bsibsi M, Persoon-Deen C, Verwer RW, Meeuwsen S, Ravid R, Van Noort JM. Toll-like receptor 3 on adult human astrocytes triggers production of neuroprotective mediators. *Glia*. 2006; 53(7): 688-695.

Bsibsi M, Ravid R, Gveric D, van Noort JM. Broad expression of Toll-like receptors in the human central nervous system. *Journal of Neuropathology and Experimental Neurology*. 2002; 61(11): 1013-1021.

Budd RC, Miescher GC, Howe RC, Lees RK, Bron C, MacDonald HR. Developmentally regulated expression of T cell receptor beta chain variable domains in immature thymocytes. *The Journal of*

*Experimental Medicine*. 1987;166(2): 577-5782.

Cammarota M, De Rosa M, Stellavato A, Lamberti M, Marzaioli I, Giuliano M. *In vitro* evaluation of Lactobacillus plantarum DSMZ 12028 as a probiotic: emphasis on innate immunity. *International Journal of Food Microbiology*. 2009; 135(2): 90-98.

Cantorna MT, Zhao J, Yang L. Vitamin D, invariant natural killer T-cells and experimental autoimmune disease. *The Proceeding of Nutrition Society*. 2012; 71(1): 62-66.

Chen Y, Langrish CL, McKenzie B, Joyce-Shaikh B, Stumhofer JS, McClanahan T, Blumenschein W, Churakovsa T, Low J, Presta L, Hunter CA, Kastelein RA, Cua DJ. Anti-IL-23 therapy inhibits multiple inflammatory pathways and ameliorates autoimmune encephalomyelitis. *The Journal of Clinical Investigation*. 2006; 116(5): 1317-1326.

Chen YC, Yang X, Miao L, Liu ZG, Li W, Zhao ZX, Sun XJ, Jiang GX, Chen SD, Cheng Q. Serum level of interleukin-6 in Chinese patients with multiple sclerosis. *Journal of Neuroimmunology*. 2012; 249(1-2): 109-111.

Chen YG, Driver JP, Silveira PA, Serreze DV. Subcongenic analysis of genetic basis for impaired development of invariant NKT cells in NOD mice. *Immunogenetics*. 2007; 59(9): 705-712.

Clarke TB, Davis KM, Lysenko ES, Zhou AY, Yu Y, Weiser JN. Recognition of peptidoglycan from the microbiota by Nod1 enhances systemic innate immunity. *Nature Medicine*. 2010;16(2): 228-231.

Colombo M, Dono M, Gazzola P, Roncella S, Valetto A, Chiorazzi N, Mancardi GL, Ferrarini M. Accumulation of clonally related B lymphocytes in the cerebrospinal fluid of multiple sclerosis patients. *Journal of Immunology*. 2000; 164(5): 2782-2789.

Contini C, Cultrera R, Seraceni S, Castellazzi M, Granieri E, Fainardi E. Cerebrospinal fluid molecular demonstration of Chlamydia pneumoniae DNA is associated to clinical and brain magnetic resonance imaging activity in a subset of patients with relapsing-remitting multiple sclerosis. *Multiple Sclerosis*. 2004; 10(4): 360-369.

Cooper GS, Bynum ML, Somers EC. Recent insights in the epidemiology of autoimmune diseases: improved prevalence estimates and understanding of clustering of diseases. *Journal of Autoimmunity*. 2009; 33(3-4): 197-207.

Cooper GS, Stroehla BC. The epidemiology of autoimmune diseases. *Autoimmunity Reviews*. 2003; 2(3): 119-125.

Coquet JM, Chakravarti S, Kyparissoudis K, McNab FW, Pitt LA,

McKenzie BS, Berzins SP, Smyth MJ, Godfrey DI. Diverse cytokine production by NKT cell subsets and identification of an IL-17-producing CD4-NK1.1- NKT cell population. *Proceeding of National Academy of Sciences of the United States of America*. 2008; 105(32): 11287-11292.

Coquet JM, Kyparissoudis K, Pellicci DG, Besra G, Berzins SP, Smyth MJ, Godfrey DI. IL-21 is produced by NKT cells and modulates NKT cell activation and cytokine production. *Journal of Immunology*. 2007; 178(5): 2827-2834.

Correale J, Farez M. Helminth antigens modulate immune responses in cells from multiple sclerosis patients through TLR2-dependent mechanisms. *Journal of Immunology*. 2009; 183(9): 5999-6012.

Correale J, Farez M. Monocyte-derived dendritic cells in multiple sclerosis: the effect of bacterial infection. *Journal of Neuroimmunology*. 2007; 190(1-2): 177-189.

Correale J, Fiol M, Gilmore W. The risk of relapses in multiple sclerosis during systemic infections. *Neurology*. 2006; 67(4): 652-659.

Correale J, Gilmore W, McMillan M, Li S, McCarthy K, Le T, Weiner LP. Patterns of cytokine secretion by autoreactive proteolipid protein-specific T cell clones during the course of multiple sclerosis. *Journal of Immunology*. 1995; 154(6): 2959-2968.

Cua DJ, Sherlock J, Chen Y, Murphy CA, Joyce B, Seymour B, Lucian L, To W, Kwan S, Churakova T, Zurawski S, Wiekowski M, Lira SA, Gorman D, Kastelein RA, Sedgwick JD. Interleukin-23 rather than interleukin-12 is the critical cytokine for autoimmune inflammation of the brain. *Nature*. 2003; 421(6924): 744-748.

D'Andrea A, Aste-Amezaga M, Valiante NM, Ma X, Kubin M, Trinchieri G. Interleukin 10 (IL-10) inhibits human lymphocyte interferon gamma-production by suppressing natural killer cell stimulatory factor/IL-12 synthesis in accessory cells. *The Journal of Experimental Medicine*. 1993; 178(3): 1041-1048.

Dal Canto MC, Lipton HL. Multiple sclerosis. Animal model: Theiler's virus infection in mice. *The American Journal of Pathology*. 1977; 88(2): 497-500.

Dalla Libera D, Di Mitri D, Bergami A, Centonze D, Gasperini C, Grasso MG, Galgani S, Martinelli V, Comi G, Avolio C, Martino G, Borsellino G, Sallusto F, Battistini L, Furlan R. T regulatory cells are markers of disease activity in multiple sclerosis patients. *PLoS One*. 2011; 6(6): e21386.

de la Monte SM, Ropper AH, Dickersin GR, Harris NL, Ferry JA, Richardson EP Jr. Relapsing central and peripheral demyelinating diseases. Unusual pathologic features. *Archives Neurology*. 1986; 43(6): 626-629.

Deber CM, Reynolds SJ. Central nervous system myelin: structure, function, and pathology. *Clinical Biochemistry*. 1991; 24(2): 113-134.

Démoulins T, Gachelin G, Bequet D, Dormont D. A biased Valpha24+ T-cell repertoire leads to circulating NKT-cell defects in a multiple sclerosis patient at the onset of his disease. *Immunology Letters*. 2003; 90(2-3): 223-228.

Deng C, Radu C, Diab A, Tsen MF, Hussain R, Cowdery JS, Racke MK, ThomasJA. IL-1 Receptor-Associated Kinase 1 Regulates Susceptibility to Organ-Specific Autoimmunity. *Journal of Immunology*. 2003; 170(6): 2833-2842.

Djelilovic-Vranic J, Alajbegovic A. Role of early viral infections in development of multiple sclerosis. *Medisinski Arhiv*. 2012; 66(3 s1): 37-40.

Du X, Poltorak A, Wei Y, Beutler B. Three novel mammalian toll-like receptors: gene structure, expression, and evolution. European Cytokine Network. 2000; 11(3): 362-71.

Duquette P, Pleines J, Girard M, Charest L, Senecal-Quevillon M, Masse C. The increased susceptibility of women to multiple sclerosis. *The Canadian Journal of Neurological Sciences*. 1992; 19: 466-471.

Ebers GC, Sadovnick AD, Risch NJ. A genetic basis for familial

aggregation in multiple sclerosis. Canadian Collaborative Study Group. *Nature*. 1995; 377(6545): 150-151.

Ebers GC, Sadovnick AD. The geographic distribution of multiple sclerosis: a review. *Neuroepidemiology*. 1993; 12(1): 1-5.

Elian M, Nightingale S, Dean G. Multiple sclerosis among United Kingdom-born children of immigrants from the Indian subcontinent, Africa and the West Indies. *Journal of Neurology, Neurosurgery and, Psychiatry*. 1990; 53(10): 906-911.

Enevold C, Oturai AB, Sørensen PS, Ryder LP, Koch-Henriksen N, Bendtzen K. Polymorphisms of innate pattern recognition receptors, response to interferon-beta and development of neutralizing antibodies in multiple sclerosis patients. *Multiple Sclerosis*. 2010; 16(8): 942-949.

Erridge C, Attina T, Spickett CM, Webb DJ. A high-fat meal induces low-grade endotoxemia: evidence of a novel mechanism of postprandial inflammation. *The American Journal of Clinical Nutrition*. 2007; 86(5): 1286-1292.

Erridge C. Endogenous ligands of TLR2 and TLR4: agonists or assistants? *Journal of Leukocyte Biology*. 2010; 87(6): 989-999.

Esiri MM. Multiple sclerosis: a quantitative and qualitative study of immunoglobulin-containing cells in the central nervous system.

*Neuropathology and Applied Neurobiology*. 1980; 6(1): 9-21.

Esteban LM, Tsoutsman T, Jordan MA, Roach D, Poulton LD, Brooks A, Naidenko OV, Sidobre S, Godfrey DI, Baxter AG. Genetic control of NKT cell numbers maps to major diabetes and lupus loci. *Journal of Immunology*. 2003; 171(6): 2873-2878.

Eugster HP, Frei K, Kopf M, Lassmann H, Fontana A. IL-6-deficient mice resist myelin oligodendrocyte glycoprotein-induced autoimmune encephalomyelitis. *Europen Journal of Immunology*. 1998; 28(7): 2178-2187.

Fang C, Zhang X, Miwa T, Song WC. Complement promotes the development of inflammatory T-helper 17 cells through synergistic interaction with Toll-like receptor signalling and interleukin-6 production. *Blood*. 2009; 114(5): 1005-10015.

Farez MF, Quintana FJ, Gandhi R, Izquierdo G, Lucas M, Weiner HL. Toll-like receptor 2 and poly(ADP-ribose) polymerase 1 promote central nervous system neuroinflammation in progressive EAE. *Nature Immunology*. 2009; 10(9): 958-964. Erratum in: *Natute Immunology*. 2010; 11(1): 97.

Farina C, Krumbholz M, Giese T, Hartmann G, Aloisi F, Meinl E. Preferential expression and function of Toll-like receptor 3 in human astrocytes. *Journal of Neuroimmunology*. 2005; 159(1-2): 12-19.

Fernald GH, Knott S, Pachner A, Caillier SJ, Narayan K, Oksenberg JR, Mousavi P, Baranzini SE. Genome-wide network analysis reveals the global properties of IFN-beta immediate transcriptional effects in humans. *Journal of Immunology*. 2007; 178(8): 5076-5085.

Ferwerda G, Girardin SE, Kullberg BJ, Le Bourhis L, de Jong DJ, Langenberg DM, van Crevel R, Adema GJ, Ottenhoff TH, Van der Meer JW, Netea MG. NOD2 and toll-like receptors are nonredundant recognition systems of Mycobacterium tuberculosis. *PLoS Pathogens*. 2005; 1(3): 279-285.

Fitzgerald DC, Zhang GX, El-Behi M, Fonseca-Kelly Z, Li H, Yu S, Saris CJ, Gran B, Ciric B, Rostami A. Suppression of autoimmune inflammation of the central nervous system by interleukin 10 secreted by interleukin 27-stimulated T cells. *Nature Immunology*. 2007; 8(12): 1372-1379.

Flachenecker P. Epidemiology of neuroimmunological diseases. *Journal of Neurology*. 2006; 253 (s5):V2-8. Review. Erratum in: *Journal of Neurology* 2008; 255(2): 308.

Fletcher JM, Jordan MA, Snelgrove SL, Slattery RM, Dufour FD, Kyparissoudis K, Besra GS, Godfrey DI, Baxter AG. Congenic Analysis of the NKT Cell Control Gene *Nkt2* Implicates the Peroxisomal Protein Pxmp4. *Journal of Immunology*. 2008; 181(5): 3400-3412.

Fowlkes BJ, Kruisbeek AM, Ton-That H, Weston MA, Coligan JE, Schwartz RH, Pardoll DM. A novel population of T-cell receptor alpha beta-bearing thymocytes which predominantly expresses a single V beta gene family. *Nature*. 1987; 329(6136): 251-254.

Fransson M, Burman J, Lindqvist C, Atterby C, Fagius J, Loskog A. T regulatory cells lacking CD25 are increased in MS during relapse. *Autoimmunity*. 2010; 43(8): 590-597.

Frisullo G, Nociti V, Iorio R, Patanella AK, Marti A, Caggiula M, Mirabella M, Tonali PA, Batocchi AP. IL17 and IFNgamma production by peripheral blood mononuclear cells from clinically isolated syndrome to secondary progressive multiple sclerosis. *Cytokine*. 2008; 44(1): 22-25.

Fritz RB, Zhao ML. Regulation of experimental autoimmune encephalomyelitis in the C57BL/6J mouse by NK1.1+, DX5+, alpha beta+ T cells. *Journal of Immunology*. 2001; 166(6): 4209-4215.

Fujita M, Otsuka T, Mizuno M, Tomi C, Yamamura T, Miyake S. Carcinoembryonic antigen-related cell adhesion molecule 1 modulates experimental autoimmune encephalomyelitis via an iNKT cell-dependent mechanism. *The American Journal of Pathology*. 2009; 175(3): 1116-1123.

Fung I, Garrett JP, Shahane A, Kwan M. Do bugs control our fate? The

influence of the microbiome on autoimmunity. *Current Allergy and Asthma Reports*. 2012; 12(6): 511-519.

Furlan R, Bergami A, Cantarella D, Brambilla E, Taniguchi M, Dellabona P, Casorati G, Martino G. Activation of invariant NKT cells by alphaGalCer administration protects mice from MOG35-55-induced EAE: critical roles for administration route and IFN-gamma. *European Journal of Immunology*. 2003; 33(7):1830-1838.

Furlan R, Cuomo C, Martino G. Animal models of multiple sclerosis. *Methods in Molecular Biology*. 2009; 549: 157-173.

Furtado GC, Marcondes MC, Latkowski JA, Tsai J, Wensky A, Lafaille JJ. Swift entry of myelin-specific T lymphocytes into the central nervous system in spontaneous autoimmune encephalomyelitis. *Journal of Immunology*. 2008; 181(7): 4648-4655.

Geier DA, Geier MR. A case-control study of serious autoimmune adverse events following hepatitis B immunization. *Autoimmunity*. 2005; 38(4): 295-301.

Gigli G, Caielli S, Cutuli D, Falcone M. Innate immunity modulates autoimmunity: type 1 interferon-beta treatment in multiple sclerosis promotes growth and function of regulatory invariant natural killer T cells through dendritic cell maturation. *Immunology*. 2007; 122(3): 409-417.

Gijbels K, Van Damme J, Proost P, Put W, Carton H, Billiau A. Interleukin 6 production in the central nervous system during experimental autoimmune encephalomyelitis. *European Journal of Immunology*. 1990; 20(1): 233-235.

Giordano M, D'Alfonso S, Momigliano-Richiardi P. Genetics of multiple sclerosis: linkage and association studies. *American Journal of Pharmacogenomics*. 2002; 2(1): 37-58.

Godfrey DI, Hammond KJ, Poulton LD, Smyth MJ, Baxter AG. NKT cells: facts, functions and fallacies. *Immunology Today*. 2000; 21(11): 573-583.

Godfrey DI, Kronenberg M. Going both ways: Immune regulation via CD1d-dependent NKT cells. *Journal of Clinical Investigation*. 2004; 114: 1379-1388.

Govindaraj RG, Manavalan B, Lee G, Choi S. Molecular modeling-based evaluation of hTLR10 and identification of potential ligands in Toll-like receptor signalling. *PLoS One*. 2010; 5(9): e12713.

Gregersen PK. Discordance for autoimmunity in monozygotic twins. Are "identical" twins really identical? *Arthritis Rheumatism*. 1993; 36(9): 1185-1192.

Grzesiuk AK. Epidemiological profile in multiple sclerosis patients, Uberaba, MG, Brazil. *Arquivos Neuropsiquiatria*. 2011; 69(5): 852.

Gumperz, J. E., S. Miyake, T. Yamamura, M. B. Brenner. Functionally distinct subsets of CD1d-restricted natural killer T cells revealed by CD1d tetramer staining. *The Journal of Experimental Medicine*. 2002; 195: 625–636.

Guo B, Chang EY, Cheng G. The type I IFN induction pathway constrains Th17-mediated autoimmune inflammation in mice. *The Journal of Clinical Investigation*. 2008; 118(5): 1680-1690.

Gutcher I, Urich E, Wolter K, Prinz M, Becher B. Interleukin 18-independent engagement of interleukin 18 receptor-alpha is required for autoimmune inflammation. Nature Immunology. 2006; 7(9): 946-953.

Hafler DA, Slavik JM, Anderson DE, O'Connor KC, De Jager P, Baecher-Allan C. Multiple sclerosis. *Immunological Reviews*. 2005; 204: 208-31.

Haines JL, Terwedow HA , Burgess K , Pericak-Vance MA , Rimmler JB , Martin ER, Oksenberg JR, Lincoln R, Zhang DY, Banatao DR , Gatto N, Goodkin DE, Hauser SL. Linkage of the MHC to familial multiple sclerosis suggests genetic heterogeneity. The Multiple Sclerosis Genetics Group. *Human Molecular Genetics*. 1998; 7: 1229-1234.

Hammann KP, Hopf HC. Monocytes constitute the only peripheral blood

cell population showing an increased burst activity in multiple sclerosis patients. *International Archives of Allergy Applied Immunology*. 1986; 81(3): 230-234.

Hammond KJ, Godfrey DI. NKT cells: potential targets for autoimmune disease therapy? *Tissue Antigens*. 2002; 59(5): 353-363.

Hansen BS, Hussain RZ, Lovett-Racke AE, Thomas JA, Racke MK. Multiple toll-like receptor agonists act as potent adjuvants in the induction of autoimmunity. *Journal of Neuroimmunology*. 2006; 172(1-2): 94-103.

Hansen T, Skytthe A, Stenager E, Petersen HC, Kyvik KO, Brønnum-Hansen H. Risk for multiple sclerosis in dizygotic and monozygotic twins. *Multiple Sclerosis*. 2005; 11(5): 500-503.

Harbo HF, Lie BA, Sawcer S, Celius EG, Dai KZ, Oturai A, Hillert J, Lorentzen AR, Laaksonen M, Myhr KM, Ryder LP, Fredrikson S, Nyland H, Sørensen PS, Sandberg-Wollheim M, Andersen O, Svejgaard A, Edland A, Mellgren SI, Compston A, Vartdal F, Spurkland A. Genes in the HLA class I region may contribute to the HLA class II-associated genetic susceptibility to multiple sclerosis. *Tissue Antigens*. 2004; 63(3): 237-247.

Harrer A, Pilz G, Einhaeupl M, Oppermann K, Hitzl W, Wipfler P, Sellner J, Golaszewski S, Afazel S, Haschke-Becher E, Trinka E, Kraus J.

Lymphocyte subsets show different response patterns to *in vivo* bound natalizumab-A flow cytometric study on patients with multiple sclerosis. *PLoS One*. 2012; 7(2): e31784.

Harrer A, Wipfler P, Einhaeupl M, Pilz G, Oppermann K, Hitzl W, Afazel S, Haschke-Becher E, Strasser P, Trinka E, Kraus J. Natalizumab therapy decreases surface expression of both VLA-heterodimer subunits on peripheral blood mononuclear cells. *Journal of Neuroimmunology*. 2011; 234(1-2): 148-154.

Harrington LE, Hatton RD, Mangan PR, Turner H, Murphy TL, Murphy KM, Weaver CT. Interleukin 17-producing CD4+ effector T cells develop via a lineage distinct from the T helper type 1 and 2 lineages. *Nature Immunology*. 2005; 6(11): 1123-1132.

Hasan U, Chaffois C, Gaillard C, Saulnier V, Merck E, Tancredi S, Guiet C, Brière F, Vlach J, Lebecque S, Trinchieri G, Bates EE. Human TLR10 is a functional receptor, expressed by B cells and plasmacytoid dendritic cells, which activates gene transcription through MyD88. *Journal of Immunology*. 2005; 174(5): 2942-2950.

Hayashi T, Gray CS, Chan M, Tawatao RI, Ronacher L, McGargill MA, Datta SK, Carson DA, Corr M. Prevention of autoimmune disease by induction of tolerance to Toll-like receptor 7. *Proceedings of the National Academy of Sicences of the United States of America*. 2009; 106(8): 2764-2769.

Hecker M, Paap BK, Goertsches RH, Kandulski O, Fatum C, Koczan D, Hartung HP, Thiesen HJ, Zettl UK. Reassessment of blood gene expression markers for the prognosis of relapsing-remitting multiple sclerosis. *PLoS One*. 2011; 6(12): e29648.

Hemmi H, Takeuchi O, Kawai T, Kaisho T, Sato S, Sanjo H, Matsumoto M, Hoshino K, Wagner H, Takeda K. A Toll-like receptor recognizes bacterial DNA. *Nature*. 2000; 408(6813): 740-745.

Hemminki K, Li X, Sundquist J, Hillert J, Sundquist K. Risk for multiple sclerosis in relatives and spouses of patients diagnosed with autoimmune and related conditions. *Neurogenetics*. 2009; 10(1): 5-11.

Hempel K, Freitag A, Freitag B, Endres B, Mai B, Liebaldt G. Unresponsiveness to experimental allergic encephalomyelitis in Lewis rats pretreated with complete Freund's adjuvant. *International Archieves of Allergy and Applied Immunology*. 1985; 76(3): 193-199.

Herrmann I, Kellert M, Schmidt H, Mildner A, Hanisch UK, Brück W, Prinz M, Nau R. Streptococcus pneumoniae Infection aggravates experimental autoimmune encephalomyelitis via Toll-like receptor 2. *Infection and Immunity*. 2006; 74(8): 4841-4848.

Hilliard B, Samoilova EB, Liu TS, Rostami A, Chen Y. Experimental

autoimmune encephalomyelitis in NF-kappa B-deficient mice: roles of NF-kappa B in the activation and differentiation of autoreactive T cells. *Journal of Immunology*. 1999; 163(5): 2937-29343.

Hirota K, Duarte JH, Veldhoen M, Hornsby E, Li Y, Cua DJ, Ahlfors H, Wilhelm C, Tolaini M, Menzel U, Garefalaki A, Potocnik AJ, Stockinger B. Fate mapping of IL-17-producing T cells in inflammatory responses. *Nature Immunology*. 2011; 12(3): 255-263.

Hirotani M, Niino M, Fukazawa T, Kikuchi S, Yabe I, Hamada S, Tajima Y, Sasaki H. Decreased IL-10 production mediated by Toll-like receptor 9 in B cells in multiple sclerosis. *Journal of Neuroimmunology*. 2010; 221(1-2): 95-100.

Hofstetter HH, Ibrahim SM, Koczan D, Kruse N, Weishaupt A, Toyka KV, Gold R. Therapeutic efficacy of IL-17 neutralization in murine experimental autoimmune encephalomyelitis. *Cellular Immunology*. 2005; 237(2): 123-130.

Hofstetter HH, Shive CL, Forsthuber TG. Pertussis Toxin Modulates the Immune Response to Neuroantigens Injected in Incomplete Freund's Adjuvant: Induction of Th1 Cells and Experimental Autoimmune Encephalomyelitis in the Presence of High Frequencies of Th2 Cells. *Journal of Immunology*. 2002; 169(1): 117-125.

Holmøy T. Immunopathogenesis of multiple sclerosis: concepts and

controversies. *Acta Neurologica Scandinavica*. 2007; 115 (s187), 39–45.

Hoshino K, Takeuchi O, Kawai T, Sanjo H, Ogawa T, Takeda Y, Takeda K, Akira S. Cutting edge: Toll-like receptor 4 (TLR4)-deficient mice are hyporesponsive to lipopolysaccharide: evidence for TLR4 as the Lps gene product. *Journal of Immunology*. 1999; 162(7): 3749-3752.

Hsueh CJ, Kao HW, Chen SY, Lo CP, Hsu CC, Liu DW, Hsu WL. Comparison of the 2010 and 2005 versions of the McDonald MRI criteria for dissemination-in-time in Taiwanese patients with classic multiple sclerosis. *Journal of Neurological Sciences*. 2013; 329(1-2): 51-54.

Hu X, Paik PK, Chen J, Yarilina A, Kockeritz L, Lu TT, Woodgett JR, Ivashkiv LB. IFN-gamma suppresses IL-10 production and synergizes with TLR2 by regulating GSK3 and CREB/AP-1 proteins. *Immunity*. 2006; 24(5): 563-574.

Humason GH. Animal Tissue Techniques. *W.H. Freeman & Company, San Franscisco*. 1972; p. 238-239.

Hundeshagen A, Hecker M, Paap BK, Angerstein C, Kandulski O, Fatum C, Hartmann C, Koczan D, Thiesen HJ, Zettl UK. Elevated type I interferon-like activity in a subset of multiple sclerosis patients: molecular basis and clinical relevance. *Journal of*

*Neuroinflammation*. 2012; 9: 140.

Ichikawa HT, Williams LP, Segal BM. Activation of APCs through CD40 or Toll-like receptor 9 overcomes tolerance and precipitates autoimmune disease. *Journal of Immunology*. 2002; 169(5): 2781-2787.

Ichiyama K, Yoshida H, Wakabayashi Y, Chinen T, Saeki K, Nakaya M, Takaesu G, Hori S, Yoshimura A, Kobayashi T. Foxp3 inhibits RORgammat-mediated IL-17A mRNA transcription through direct interaction with RORgammat. *The Journal of Biological Chemistry*. 2008; 283(25): 17003-17008.

Illés Z, Kondo T, Newcombe J, Oka N, Tabira T, Yamamura T. Differential expression of NK T cell V alpha 24J alpha Q invariant TCR chain in the lesions of multiple sclerosis and chronic inflammatory demyelinating polyneuropathy. *Journal of Immunology*. 2000; 164(8): 4375-4381.

Ivanov II, Frutos Rde L, Manel N, Yoshinaga K, Rifkin DB, Sartor RB, Finlay BB, Littman DR. Specific microbiota direct the differentiation of IL-17-producing T-helper cells in the mucosa of the small intestine. *Cell Host & Microbe*. 2008; 4(4): 337-349.

Jack CS, Arbour N, Manusow J, Montgrain V, Blain M, McCrea E, Shapiro A, Antel JP. TLR signalling tailors innate immune responses in

human microglia and astrocytes. *Journal of Immunology*. 2005; 175(7): 4320-4330.

Jahng A, Maricic I, Aguilera C, Cardell S, Halder RC, Kumar V. Prevention of autoimmunity by targeting a distinct, noninvariant CD1d-reactive T cell population reactive to sulfatide. *The Journal of Experimental Medicine*. 2004 199(7): 947-957.

Jahng AW, Maricic I, Pedersen B, Burdin N, Naidenko O, Kronenberg M, Koezuka Y, Kumar V. Activation of natural killer T cells potentiates or prevents experimental autoimmune encephalomyelitis. *The Journal of Experimental Medicine*. 2001; 194(12): 1789-1799.

Janssen WJ, Henson PM. Cellular Regulation of the Inflammatory Response. *Toxicologic Pathology*. 2012; 40(2): 166-173.

Jaskiewicz E. Epitopes on myelin proteins recognized by autoantibodies present in multiple sclerosis patients. *Postepy Higieny Medycyny Doswiadczalnej*. 2004; 58: 472-482.

Jewtoukoff V, Amzazi S, Lebar R, Bach MA, Marche PN. T-cell receptor identification of an oligodendrocyte-specific autoreactive cytotoxic T-cell clone without self restriction. *Scandinavian Journal of Immunology*. 1992, 36(6): 893-898.

Jiang S, Game DS, Davies D, Lombardi G, Lechler RI. Activated CD1d-restricted natural killer T cells secrete IL-2: innate help for

$CD4^+CD25^+$ regulatory T cells? *European Journal of Immunology*. 2005; 35(4): 1193-1200.

Jin J, Samuvel DJ, Zhang X, Li Y, Lu Z, Lopes-Virella MF, Huang Y. Coactivation of TLR4 and TLR2/6 coordinates an additive augmentation on IL-6 gene transcription via p38MAPK pathway in U937 mononuclear cells. *Molecular Immunology*. 2011; 49(3): 423-432.

Jones BW, Means TK, Heldwein KA, Keen MA, Hill PJ, Belisle JT, Fenton MJ. Different Toll-like receptor agonists induce distinct macrophage responses. *Journal of Leukocyte Biology*. 2001; 69(6): 1036-1044.

Jordan MA, Fletcher JM, Pellicci D, Baxter AG. Slamf1, the NKT cell control gene Nkt1. Journal of Immunology. 2007; 178(3): 1618-1627.

Jordan MA, Poulton LD, Fletcher JM, Baxter AG. Allelic variation of Ets1 does not contribute to NK and NKT cell deficiencies in type 1 diabetes susceptible NOD mice. *The Review of Diabetic Studies*. 2009; 6(2): 104-116.

Jordan MA, Poulton LD, Fletcher JM, Baxter AG. Allelic variation of Ets1 does not contribute to NK and NKT cell deficiencies in type 1 diabetes susceptible NOD mice. *The Review of Diabetic Studies*. 2009; 6(2): 104-116.

Kachapati K, Adams D, Bednar K, Ridgway WM. The non-obese diabetic (NOD) mouse as a model of human type 1 diabetes. *Methods in Molecular Biology*. 2012; 933: 3-16.

Kaisho T, Akira S. Toll-like receptor function and signalling. *Journal of Allergy and Clinical Immunology*. 2006; 117 (5): 979-987.

Kallaur AP, Oliveira SR, Colado Simão AN, Delicato de Almeida ER, Kaminami Morimoto H, Lopes J, de Carvalho Jennings Pereira WL, Marques Andrade R, Muliterno Pelegrino L, Donizete Borelli S, Kaimen-Maciel DR, Vissoci Reiche EM. Cytokine profile in relapsing remitting multiple sclerosis patients and the association between progression and activity of the disease. *Molecular Medicine Reports*. 2013; 7(3): 1010-1020.

Karlsson J, Zhao X, Lonskaya I, Neptin M, Holmdahl R, Andersson A. Novel Quantitative Trait Loci Controlling Development of Experimental Autoimmune Encephalomyelitis and Proportion of Lymphocyte Subpopulations. *The Journal of Immunology*. 2003; 170: 1019-1026.

Kastrukoff LF, Morgan NG, Zecchini D, White R, Petkau AJ, Satoh J, Paty DW. A role for natural killer cells in the immunopathogenesis of multiple sclerosis. *Journal of Neuroimmunology*. 1998; 86(2): 123-133.

Kattah MG, Wong MT, Yocum MD, Utz PJ. Cytokines secreted in response to Toll-like receptor ligand stimulation modulate differentiation of human Th17 cells. *Arthritis Rheumatism*. 2008; 58(6): 1619-1629.

Kawai T, Akira S. TLR signalling. *Seminars in Immunology*. 2007; 19(1): 24-32.

Kemppinen A, Sawcer S, Compston A. Genome-wide association studies in multiple sclerosis: lessons and future prospects. *Briefings in Functional Genomics*. 2011; 10(2): 61-70.

Kerfoot SM, Long EM, Hickey MJ, Andonegui G, Lapointe BM, Zanardo RCO, Bonder C, James WG, Robbins SM, Kubes P. TLR4 Contributes to Disease-Inducing Mechanisms Resulting in Central Nervous System Autoimmune Disease. *Journal of Immunology*. 2004; 173(11): 7070-7077.

Kinjo Y, Wu D, Kim G, Xing GW, Poles MA, Ho DD, Tsuji M, Kawahara K, Wong CH, Kronenberg M. Recognition of bacterial glycosphingolipids by natural killer T cells. *Nature*. 2005; 434(7032): 520-525.

Kipp M, Clarner T, Dang J, Copray S, Beyer C. The cuprizone animal model: new insights into an old story. *Acta Neuropathologica*. 2009; 118(6): 723-736.

Komiyama Y, Nakae S, Matsuki T, Nambu A, Ishigame H, Kakuta S, Sudo

K, Iwakura Y. IL-17 plays an important role in the development of experimental autoimmune encephalomyelitis. *Journal of Immunology*. 2006; 177(1): 566–573.

Kouwenhoven M, Ozenci V, Gomes A, Yarilin D, Giedraitis V, Press R, Link H. Multiple sclerosis: elevated expression of matrix metalloproteinases in blood monocytes. *Journal of Autoimmunity*. 2001; 16(4): 463-470.

Krause I, Tomer Y, Elias D, Blank M, Gilburd B, Cohen IR, Shoenfeld Y. Inhibition of diabetes in NOD mice by idiotypic induction of SLE. *Journal of Autoimmunity*. 1999; 13(1): 49-55.

Kroner A, Vogel F, Kolb-Mäurer A, Kruse N, Toyka KV, Hemmer B, Rieckmann P, Mäurer M. Impact of the Asp299Gly polymorphism in the toll-like receptor 4 (tlr-4) gene on disease course of multiple sclerosis. *Journal of Neuroimmunology*. 2005; 165(1-2): 161-165.

Kuchroo VK, Martin CA, Greer JM, Ju ST, Sobel RA, Dorf ME. Cytokines and adhesion molecules contribute to the ability of myelin proteolipid protein-specific T cell clones to mediate experimental allergic encephalomyelitis. *Journal of Immunology*. 1993; 151(8): 4371-4382.

Kumar H, Kawai T, Akira S. Toll-like receptors and innate immunity. *Biochemical and Biophysical Research Communications.* 2009;

388(4): 621-625.

Kurebayashi Y, Nagai S, Ikejiri A, Koyasu S. Recent advances in understanding the molecular mechanisms of the development and function of Th17 cells. *Genes to Cells*. 2013; 4: 247-265.

Kürtüncü M, Tüzün E, Türkoğlu R, Petek-Balcı B, Içöz S, Pehlivan M, Birişik Ö, Ulusoy C, Shugaiv E, Akman-Demir G, Eraksoy M. Effect of short-term interferon-β treatment on cytokines in multiple sclerosis: significant modulation of IL-17 and IL-23. *Cytokine*. 2012; 59(2): 400-4002.

Lafon M, Megret F, Lafage M, Prehaud C. The innate immune facet of brain: human neurons express TLR-3 and sense viral dsRNA. *Journal of Molecular Neurosciences*. 2006, 29(3): 185-194.

Lalor SJ, Dungan LS, Sutton CE, Basdeo SA, Fletcher JM, Mills KH. Caspase-1-processed cytokines IL-1beta and IL-18 promote IL-17 production by gammadelta and CD4 T cells that mediate autoimmunity. *Journal of Immunology*. 2011; 186(10): 5738-5748.

Lampropoulou V, Hoehlig K, Roch T, Neves P, Calderon Gomez E, Sweenie CH, Hao Y, Freitas AA, Steinhoff U, Anderton SM, Fillatreau S. TLR-Activated B Cells Suppress T Cell-Mediated Autoimmunity. *Journal of Immunology*. 2008; 180(7): 4763-4773.

Lassmann H, Brück W, Lucchinetti C. Heterogeneity of multiple sclerosis

pathogenesis: implications for diagnosis and therapy. *Trends in Molecular Medicine*. 2001; 7(3): 115-121.

Lau AW, Biester S, Cornall RJ, Forrester JV. Lipopolysaccharide-activated IL-10-secreting dendritic cells suppress experimental autoimmune uveoretinitis by MHCII-dependent activation of CD62L-expressing regulatory T cells. *Journal of Immunology*. 2008; 180(6): 3889-3899.

Lee K, Hwang S, Paik DJ, Kim WK, Kim JM, Youn J. Bacillus-derived poly-γ-glutamic acid reciprocally regulates the differentiation of T helper 17 and regulatory T cells and attenuates experimental autoimmune encephalomyelitis. *Clinical and Experimental Immunology*. 2012; 170(1): 66-76.

Lee YK, Menezes JS, Umesaki Y, Mazmanian SK. Proinflammatory T-cell responses to gut microbiota promote experimental autoimmune encephalomyelitis. *Procceding of the National Academy of Science of the United States of America*. 2011; 108, s1: 4615-4622.

Lee, P. T., K. Benlagha, L. Teyton, A. Bendelac. Distinct functional lineages of human V(alpha)24 natural killer T cells. *Journal of Experimental Medicine*. 2002; 195(5): 637–641.

Lees JR, Golumbek PT, Sim J, Dorsey D, Russell JH. Regional CNS responses to IFN-gamma determine lesion localization patterns

during EAE pathogenesis. *Journal of Experimental Medicine*. 2008; 205(11): 2633-2642.

Li W, Minohara M, Su JJ, Matsuoka T, Osoegawa M, Ishizu T, Kira J. Helicobacter pylori infection is a potential protective factor against conventional multiple sclerosis in the Japanese population. *Journal of neuroimmunology*. 2007; 184(1-2): 227-231.

Lincoln MR, Ramagopalan SV, Chao MJ, Herrera BM, Deluca GC, Orton SM, Dyment DA, Sadovnick AD, Ebers GC. Epistasis among HLA-DRB1, HLA-DQA1, and HLA-DQB1 loci determines multiple sclerosis susceptibility. *Proceeding of National Academy of Sciences of the United States of America*. 2009; 106(18): 7542-7547.

Lindberg M. [Use of NSAIDs in rheumatoid arthritis should be limited]. *Ugeskr Laeger*. 2013;175(15): 1039-1041.

Lindsey JW. Immunogenetics. Characteristics of initial and reinduced experimental autoimmune encephalomyelitis. *Immunogenetics*. 1996; 44(4): 292-297.

Link J, Söderström M, Olsson T, Höjeberg B, Ljungdahl A, Link H. Increased transforming growth factor-beta, interleukin-4, and interferon-gamma in multiple sclerosis. *Annals of Neurology*. 1994; 36(3): 379-386.

Linthicum DS, Munoz JJ, Blaskett A. Acute experimental autoimmune

encephalomyelitis in mice. I. Adjuvant action of Bordetella pertussis is due to vasoactive amine sensitization and increased vascular permeability of the central nervous system. *Cellular Immunology*. 1982; 73(2): 299-310.

Liu Y, Teige A, Mondoc E, Ibrahim S, Holmdahl R, Issazadeh-Navikas S. Endogenous collagen peptide activation of CD1d-restricted NKT cells ameliorates tissue-specific inflammation in mice. *The Journal of Clinical Investigation*. 2011; 121(1): 249-264.

Liu YJ. IPC: professional type 1 interferon-producing cells and plasmacytoid dendritic cell precursors. *Annual Reviews of Immunology*. 2005; 23: 275-306.

Lock C, Hermans G, Pedotti R, Brendolan A, Schadt E, Garren H, Langer-Gould A, Strober S, Cannella B, Allard J, Klonowski P, Austin A, Lad N, Kaminski N, Galli SJ, Oksenberg JR, Raine CS, Heller R, Steinman L. Gene-microarray analysis of multiple sclerosis lesions yields new targets validated in autoimmune encephalomyelitis. *Nature Medicine*. 2002; 8(5): 500-508.

Lünemann A, Tackenberg B, DeAngelis T, da Silva RB, Messmer B, Vanoaica LD, Miller A, Apatoff B, Lublin FD, Lünemann JD, Münz C. Impaired IFN-γ production and proliferation of NK cells in multiple sclerosis. *International Immunology*. 2011; 23(2): 139-148.

MacDonald HR. Development and selection of NKT cells. *Current Opinion in Immunology*. 2002; 14(2): 250-254.

Macdonald HR. NKT cells: In the beginning... *European Journal of Immunology*. 2007; 37, s1: S111-S115.

Maddur MS, Miossec P, Kaveri SV, Bayry J. Th17 cells: biology, pathogenesis of autoimmune and inflammatory diseases, and therapeutic strategies. *The American Journal of Pathology*. 2012; 181(1): 8-18.

Makino S, Kunimoto K, Muraoka Y, Mizushima Y, Katagiri K, Tochino Y. Breeding of a non-obese, diabetic strain of mice. *Jikken Dobutsu*. 1980; 29 (1): 1-13.

Marrie RA, Yu N, Blanchard J, Leung S, Elliott L. The rising prevalence and changing age distribution of multiple sclerosis in Manitoba. *Neurology*. 2010; 74(6): 465-471. Erratum in: *Neurology*. 2011; 77(11): 1105.

Mars LT, Gautron AS, Novak J, Beaudoin L, Diana J, Liblau RS, Lehuen A. Invariant NKT cells regulate experimental autoimmune encephalomyelitis and infiltrate the central nervous system in a CD1d-independent manner. *Journal of Immunology*. 2008; 181(4): 2321-2329.

Mars LT, Laloux V, Goude K, Desbois S, Saoudi A, Van Kaer L, Lassmann

H, Herbelin A, Lehuen A, Liblau RS. Cutting edge: V alpha 14-J alpha 281 NKT cells naturally regulate experimental autoimmune encephalomyelitis in nonobese diabetic mice. *Journal of Immunology*. 2002; 168(12): 6007-6011.

Marta M, Anderson A, Isaksson M, Kampe O, Lobell A. Unexpected regulatory roles of TLR4 and TLR9 in experimental autoimmune encephalomyelitis. *European Journal of Immunology*. 2008; 38(2): 565-575.

Matsumoto C, Oda T, Yokoyama S, Tominari T, Hirata M, Miyaura C, Inada M. Toll-like receptor 2 heterodimers, TLR2/6 and TLR2/1 induce prostaglandin E production by osteoblasts, osteoclast formation and inflammatory periodontitis. *Biochemical and Biophysical Research Communications*. 2012; 428(1): 110-115.

Matusevicius D, Kivisäkk P, He B, Kostulas N, Ozenci V, Fredrikson S, Link H. Interleukin-17 mRNA expression in blood and CSF mononuclear cells is augmented in multiple sclerosis. *Multiple Sclerosis*. 1999; 5(2): 101-104.

Mayo S, Quinn A. Altered susceptibility to EAE in congenic NOD mice: Altered processing of the encephalitogenic MOG35-55 peptide by NOR/LtJ mice. *Clinical Immunology*. 2007; 122(1): 91-100.

McClelland EE, Smith JM. Gender specific differences in the immune

response to infection. *Archivum Immunologiae et Therapiae Experimentalis (Warsz).* 2011; 59(3): 203-213.

McCurdy JD, Lin TJ, Marshall JS. Toll-like receptor 4-mediated activation of murine mast cells. *Journal of Leukocyte Biology*. 2001; 70(6): 977-984.

McGonagle D, McDermott MF. A Proposed Classification of the Immunological Diseases. *PLoS Medicine*. 2006; 3(8): e297.

McLeod JG, Hammond SR, Kurtzke JF. Migration and multiple sclerosis in immigrants to Australia from United Kingdom and Ireland: a reassessment. I. Risk of MS by age at immigration. *Journal of Neurology*. 2011; 258(6): 1140-1149.

McLeod JG, Hammond SR, Kurtzke JF. Migration and multiple sclerosis in United Kingdom and Ireland immigrants to Australia: a reassessment. II. Characteristics of early (pre-1947) compared to later migrants. *Journal of Neurology*. 2012; 259(4): 684-693.

Means TK, Wang S, Lien E, Yoshimura A, Golenbock DT, Fenton MJ. *Journal of Immunology*. 1999; 163(7): 3920-3927.

Melcon M, Melcon C, Bartoloni L, Cristiano E, Duran J, Grzesiuk A, Fragoso Y, Brooks JB, Díaz V, Romero García K, Cabrera Gomez J, Abad P, Islas MM, Gracia F, Diaz de Bedoya VH, Ruiz MC, Hackembruch J, Oehninger C, Ketzoian C, Soto A; the "Grupo

Colaborativo Multicéntrico para el Estudio de la Esclerosis Multiple en America Latina y el Caribe" (GEEMAL). Towards establishing MS prevalence in Latin America and the Caribbean. *Multiple Sclerosis.* 2013; 19(2): 145-152.

Mendiratta SK, Martin WD, Hong S, Boesteanu A, Joyce S, Van Kaer L. CD1d1 mutant mice are deficient in natural T cells that promptly produce IL-4. *Immunity*. 1997; 6(4): 469-477.

Mendiratta SK, Martin WD, Hong S, Boesteanu A, Joyce S, Van Kaer L. CD1d1 mutant mice are deficient in natural T cells that promptly produce IL-4. *Immunity*. 1997; 6(4): 469-477.

Meoli EM, Oh U, Grant CW, Jacobson S. TGF-β signalling is altered in the peripheral blood of subjects with multiple sclerosis. *Journal of Neuroimmunology*. 2011; 230(1-2): 164-168.

Michel, M.-L., A. C. Keller, C. Paget, M. Fujio, F. Trottein, P. B. Savage, C.-H. Wong, E. Schneider, M. Dy, M. C. Leite-de-Moraes. Identification of an IL-17-producing NK1.1(neg) iNKT cell population involved in airway neutrophilia. *Journal of Experimental Medicine*. 2007; 204(5): 995–1001.

Miljković D, Momčilović M, Stanojević Z, Rašić D, Mostarica-Stojković M. It is still not for the old iron: adjuvant effects of carbonyl iron in experimental autoimmune encephalomyelitis induction. *Journal of*

*Neurochemisty*. 2011; 118(2): 205-214.

Miller SD, Karpus WJ. Experimental autoimmune encephalomyelitis in the mouse. *Current Protocols in Immunology*. 2007; 15.1.

Mills KH. TLR-dependent T cell activation in autoimmunity. *Nature Reviews Immunology*. 2011; 11(12): 807-822.

Milo R, Kahana E. Multiple sclerosis: geoepidemiology, genetics and the environment. *Autoimmunity Reviews*. 2010; 9(5): A387-394.

Miyamoto K, Miyake S, Yamamura T. A synthetic glycolipid prevents autoimmune encephalomyelitis by inducing TH2 bias of natural killer T cells. *Nature*. 2001; 413(6855): 531-534.

Mokhtarian F, Shi Y, Shirazian D, Morgante L, Miller A, Grob D. Defective production of anti-inflammatory cytokine, TGF-beta by T cell lines of patients with active multiple sclerosis. *Journal of Immunology*. 1994; 152(12): 6003-6010.

Moldovan IR, Cotleur AC, Zamor N, Butler RS, Pelfrey CM. Multiple sclerosis patients show sexual dimorphism in cytokine responses to myelin antigens. *Journal of Neuroimmunology*. 2008; 193(1-2): 161-169.

Moroni L, Bianchi I, Lleo A. Geoepidemiology, gender and autoimmune disease. *Autoimmunity Reviews*. 2012; 11(6-7): A386-392.

Mu HH, Sawitzke AD, Cole BC. Presence of Lps(d) mutation influences cytokine regulation *in vivo* by the Mycoplasma arthritidis mitogen superantigen and lethal toxicity in mice infected with M. arthritidis. *Infection and Immunity*. 2001; 69(6): 3837-3844.

Muindi K, Cernadas M, Watts GF, Royle L, Neville DC, Dwek RA, Besra GS, Rudd PM, Butters TD, Brenner MB. Activation state and intracellular trafficking contribute to the repertoire of endogenous glycosphingolipids presented by CD1d [corrected]. *Proceeding of the National Academy of Sciences of the United States of America*. 2010; 107(7): 3052-3057. Erratum in: *Proceeding of the National Academy of Sciences of the United States of America*. 2010; 107(13): 6118.

Munger KL, Zhang SM, O'Reilly E, Hernán MA, Olek MJ, Willett WC, Ascherio A. Vitamin D intake and incidence of multiple sclerosis. *Neurology*. 2004; 62(1): 60-65.

Nagyoszi P, Wilhelm I, Farkas AE, Fazakas C, Dung NT, Haskó J, Krizbai IA. Expression and regulation of toll-like receptors in cerebral endothelial cells. *Neurochemistry International*. 2010; 57(5): 556-564.

Nichols FC, Housley WJ, O'Conor CA, Manning T, Wu S, Clark RB. Unique lipids from a common human bacterium represent a new class of Toll-like receptor 2 ligands capable of enhancing

autoimmunity. *The American Journal of Pathology*. 2009; 175(6): 2430-2438.

Nichols FC, Yao X, Bajrami B, Downes J, Finegold SM, Knee E, Gallagher JJ, Housley WJ, Clark RB. Phosphorylated dihydroceramides from common human bcteria are recovered in human tissues. *PLoS One*. 2011; 6(2): e16771.

Nishida M, Suda R, Nagamatsu Y, Tanabe S, Onohara N, Nakaya M, Kanaho Y, Shibata T, Uchida K, Sumimoto H, Sato Y, Kurose H. Pertussis toxin up-regulates angiotensin type 1 receptors through Toll-like receptor 4-mediated Rac activation. *Journal of Biological Chemistry*. 2010; 285(20): 15268-15277.

Novak J, Lehuen A. Mechanism of regulation of autoimmunity by iNKT cells. *Cytokine*. 2011; 53(3): 263-270.

O'Brien K, Fitzgerald D, Rostami A, Gran B. The TLR7 agonist, imiquimod, increases IFN-beta production and reduces the severity of experimental autoimmune encephalomyelitis. *Journal of Neuroimmunology*. 2010; 221(1-2): 107-111.

O'Brien K, Fitzgerald DC, Naiken K, Alugupalli KR, Rostami AM, Gran B. Role of the innate immune system in autoimmune inflammatory demyelination. *Current medicinal chemistry*. 2008; 15(11): 1105-1115.

O'Keeffe J, Gately CM, Counihan T, Hennessy M, Leahy T, Moran AP, Hogan EL. T-cells expressing natural killer (NK) receptors are altered in multiple sclerosis and responses to alpha-galactosylceramide are impaired. *Journal of the Neurological Sciences*. 2008; 275(1-2): 22-28.

Oh SJ, Chung DH. Invariant NKT cells producing IL-4 or IL-10, but not IFN-gamma, inhibit the Th1 response in experimental autoimmune encephalomyelitis, whereas none of these cells inhibits the Th17 response. *Journal of Immunology*. 2011; 186(12): 6815-6821.

Oldenburg M, Krüger A, Ferstl R, Kaufmann A, Nees G, Sigmund A, Bathke B, Lauterbach H, Suter M, Dreher S, Koedel U, Akira S, Kawai T, Buer J, Wagner H, Bauer S, Hochrein H, Kirschning CJ. TLR13 recognizes bacterial 23S rRNA devoid of erythromycin resistance-forming modification. *Science*. 2012; 337(6098): 1111-1115.

Oukka M. Interplay between pathogenic Th17 and regulatory T cells. *Annals of the Rheumatic Disease*. 2007; 66 (s3): iii87-90.

Pál E, Tabira T, Kawano T, Taniguchi M, Miyake S, Yamamura T. Costimulation-dependent modulation of experimental autoimmune encephalomyelitis by ligand stimulation of V alpha 14 NK T cells. *Journal of Immunology*. 2001; 166(1): 662-668.

Parekh VV, Wu L, Olivares-Villagómez D, Wilson KT, Van Kaer L. Activated Invariant NKT Cells Control Central Nervous System Autoimmunity in a Mechanism That Involves Myeloid-Derived Suppressor Cells. *Journal of Immunology*. 2013; 190(5): 1948-1960.

Park H, Li Z, Yang XO, Chang SH, Nurieva R, Wang YH, Wang Y, Hood L, Zhu Z, Tian Q, Dong C. A distinct lineage of CD4 T cells regulates tissue inflammation by producing interleukin 17. *Nature Immunology*. 2005; 6(11): 1133-1141.

Pasare C, Medzhitov R. Toll pathway-dependent blockade of CD4+CD25+ T cell-mediated suppression by dendritic cells. *Science*. 2003; 299(5609): 1033-1036.

Paulos CM, Wrzesinski C, Kaiser A, Hinrichs CS, Chieppa M, Cassard L, Palmer DC, Boni A, Muranski P, Yu Z, Gattinoni L, Antony PA, Rosenberg SA, Restifo NP. Microbial translocation augments the function of adoptively transferred self/tumor-specific CD8+ T cells via TLR4 signalling. *Journal of Clinical Investigation*. 2007; 117(8): 2197-2204. Erratum in: *The Journal of Clinical Investigation*. 2007; 117(10): 3140.

Payne NL, Dantanarayana A, Sun G, Moussa L, Caine S, McDonald C, Herszfeld D, Bernard CC, Siatskas C. Early intervention with gene-modified mesenchymal stem cells overexpressing interleukin-4 enhances anti-inflammatory responses and functional recovery in

experimental autoimmune demyelination. *Cell Adhesion & Migration*. 2012; 6(3): 179-189.

Pearson T, Markees TG, Serreze DV, Pierce MA, Marron MP, Wicker LS, Peterson LB, Shultz LD, Mordes JP, Rossini AA, Greiner DL. Genetic disassociation of autoimmunity and resistance to costimulation blockade-induced transplantation tolerance in nonobese diabetic mice. *Journal of Immunology*. 2003; 171(1): 185-195.

Pearson T, Markees TG, Wicker LS, Serreze DV, Peterson LB, Mordes JP, Rossini AA, Greiner DL. NOD congenic mice genetically protected from autoimmune diabetes remain resistant to transplantation tolerance induction. *Diabetes*. 2003; 52(2): 321-326.

Pekmezovic T, Drulovic J, Milenkovic M, Jarebinski M, Stojsavljevic N, Mesaros S, Kisic D, Kostic J. Lifestyle factors and multiple sclerosis: A case-control study in Belgrade. *Neuroepidemiology*. 2006; 27(4): 212-216.

Pellicci DG, Hammond KJ, Uldrich AP, Baxter AG, Smyth MJ, Godfrey DI. A natural killer T (NKT) cell developmental pathway iInvolving a thymus-dependent NK1.1(-)CD4(+) CD1d-dependent precursor stage. *The Journal of Experimental Medicine*. 2002; 195(7): 835-844.

Pifer R, Benson A, Sturge CR, Yarovinsky F. UNC93B1 is essential for TLR11 activation and IL-12-dependent host resistance to Toxoplasma gondii. *The Journal of Biological Chemistry*. 2011; 286(5): 3307-3314.

Poppe AY, Wolfson C, Zhu B. Prevalence of multiple sclerosis in Canada: a systematic review. *The Canadian Journal of Neurological Sciences*. 2008; 35(5): 593-601.

Porcelli S, Brenner MB, Greenstein JL, Terhorst C, Balk SP, Bleicher PA. Recognition of Cluster of Differentiation 1 Antigens by Human CD4-CD8- CytolyticT Lymphocyte. Nature. 1989; 341: 447-450. 1989. *Journal of Immunology*. 2010; 184(7): 3306-3309.

Poulton LD, Smyth MJ, Hawke CG, Silveira P, Shepherd D, Naidenko OV, Godfrey DI, Baxter AG. Cytometric and functional analyses of NK and NKT cell deficiencies in NOD mice. *International Immunology*. 2001; 13(7): 887-896.

Préhaud C, Mégret F, Lafage M, Lafon M. Virus infection switches TLR-3-positive human neurons to become strong producers of beta interferon. *Journal of Virology*. 2005; 79(20): 12893-12904.

Prinz M, Garbe F, Schmidt H, Mildner A, Gutcher I, Wolter K, Piesche M, Schroers R, Weiss E, Kirschning CJ, Rochford CD, Brück W, Becher B. Innate immunity mediated by TLR9 modulates

pathogenicity in an animal model of multiple sclerosis. *Journal of Clinical Investigation*. 2006; 116(2): 456-464.

Qian G, Qin X, Zang YQ, Ge B, Guo TB, Wan B, Fang L, Zhang JZ. High doses of alpha-galactosylceramide potentiate experimental autoimmune encephalomyelitis by directly enhancing Th17 response. *Cell Research*. 2010; 20(4): 480-491.

Quesniaux V, Fremond C, Jacobs M, Parida S, Nicolle D, Yeremeev V, Bihl F, Erard F, Botha T, Drennan M, Soler MN, Le Bert M, Schnyder B, Ryffel B. Toll-like receptor pathways in the immune responses to mycobacteria. *Microbes and Infection*. 2004; 6(10): 946-959.

Racke MK, Hu W, Lovett-Racke AE. PTX cruiser: driving autoimmunity via TLR4. *Trends Immunology*. 2005; 26(6): 289-291.

Raddassi K, Kent SC, Yang J, Bourcier K, Bradshaw EM, Seyfert-Margolis V, Nepom GT, Kwok WW, Hafler DA. Increased frequencies of myelin oligodendrocyte glycoprotein/MHC class II-binding CD4 cells in patients with multiple sclerosis. *Journal of Immunology*. 2011; 187(2): 1039-1046.

Ragheb S, Li Y, Simon K, VanHaerents S, Galimberti D, De Riz M, Fenoglio C, Scarpini E, Lisak R. Multiple sclerosis: BAFF and CXCL13 in cerebrospinal fluid. *Multiple Sclerosis*. 2011; 17(7):

819-829.

Rakoff-Nahoum S, Paglino J, Eslami-Varzaneh F, Edberg S, Medzhitov R. Recognition of commensal microflora by toll-like receptors is required for intestinal homeostasis. *Cell*. 2004; 118(2): 229-241.

Ramagopalan SV, Ebers GC. Epistasis: multiple sclerosis and the major histocompatibility complex. *Neurology*. 2009; 72(6): 566-567.

Re F, Strominger JL. Toll-like receptor 2 (TLR2) and TLR4 differentially activate human dendritic cells. *The Journal of Biological Chemistry*. 2001; 276(40): 37692-37699.

Reifsnyder PC, Li R, Silveira PA, Churchill G, Serreze DV, Leiter EH. Conditioning the genome identifies additional diabetes resistance loci in Type I diabetes resistant NOR/Lt mice. *Genes and Immunity*. 2005; 6(6): 528-538. Erratum in: *Genes and Immunity*. 2006; 7(2): 184.

Reindl M, Lutterotti A, Ingram J, Schanda K, Gassner C, Deisenhammer F, Berger T, Lorenz E. Mutations in the gene for toll-like receptor 4 and multiple sclerosis. *Tissue Antigens*. 2003; 61(1): 85-88.

Reynolds JM, Martinez GJ, Chung Y, Dong C. Toll-like receptor 4 signalling in T cells promotes autoimmune inflammation. *Proceedings of the National Academy Sciences of the United Stated of America.* 2012; 109(32): 13064-13069.

Reynolds JM, Pappu BP, Peng J, Martinez GJ, Zhang Y, Chung Y, Ma L, Yang XO, Nurieva RI, Tian Q, Dong C. Toll-like receptor 2 signalling in CD4(+) T lymphocytes promotes T helper 17 responses and regulates the pathogenesis of autoimmune disease. *Immunity*. 2010; 32(5): 692-702.

Rioux JD, Abbas AK. Paths to understanding the genetic basis of autoimmune disease. *Nature*. 2005; 435(7042): 584-589.

Roach JC, Glusman G, Rowen L, Kaur A, Purcell MK, Smith KD, Hood LE, Aderem A. The evolution of vertebrate Toll-like receptors. *Proceeding of the National Academy of Sciences of the United States of America*. 2005; 102(27): 9577-9582.

Robinson CP, Yamachika S, Alford CE, Cooper C, Pichardo EL, Shah N, Peck AB, Humphreys-Beher MG. Elevated levels of cysteine protease activity in saliva and salivary glands of the nonobese diabetic (NOD) mouse model for Sjögren syndrome. *Proceeding of the National Academy of Sciences of the United States of America.* 1997; 94(11): 5767-5771.

Roberts BJ, Moussawi M, Huber SA. Sex differences in TLR2 and TLR4 expression and their effect on coxsackievirus-induced autoimmune myocarditis. *Experimental and Molecular Pathology.* 2013; 94(1): 58-64.

Rocha-Campos AC, Melki R, Zhu R, Deruytter N, Damotte D, Dy M, Herbelin A, Garchon HJ. Genetic and functional analysis of the Nkt1 locus using congenic NOD mice: improved Valpha14-NKT cell performance but failure to protect against type 1 diabetes. *Diabetes*. 2006; 55(4): 1163-1170.

Rosati G. The prevalence of multiple sclerosis in the world: an update. *Neurological Sciences*. 2001; 22(2): 117-139.

Schrijver IA, van Meurs M, Melief MJ, Wim Ang C, Buljevac D, Ravid R, Hazenberg MP, Laman JD. Bacterial peptidoglycan and immune reactivity in the central nervous system in multiple sclerosis. *Brain*. 2001; 124(Pt 8): 1544-1554.

Schroder K, Sweet MJ, Hume DA. Signal integration between IFNgamma and TLR signalling pathways in macrophages. *Immunobiology*. 2006; 211(6-8): 511-524.

Schütz C, Oelke M, Schneck JP, Mackensen A, Fleck M. Killer artificial antigen-presenting cells: the synthetic embodiment of a 'guided missile'. *Immunotherapy*. 2010; 2(4): 539-550.

Segal BM, Chang JT, Shevach EM. CpG oligonucleotides are potent adjuvants for the activation of autoreactive encephalitogenic T cells *in vivo*. Journal of Immunology. 2000; 164(11): 5683-5688.

Seino K, Taniguchi M. Functionally distinct NKT cell subsets and subtypes. *The Journal of Experimental Medicine*. 2005; 19; 202(12): 1623-1626.

Sena A, Pedrosa R, Ferret-Sena V, Cascais MJ, Roque R, Araújo C, Couderc R. Interferon beta therapy increases serum ferritin levels in patients with relapsing-remitting multiple sclerosis. *Multiple Sclerosis.* 2008; 14(6): 857-859.

Shaw PJ, Barr MJ, Lukens JR, McGargill MA, Chi H, Mak TW, Kanneganti TD. Signalling via the RIP2 adaptor protein in central nervous system-infiltrating dendritic cells promotes inflammation and autoimmunity. *Immunity*. 2011; 34(1): 75-84.

Shi FD, Takeda K, Akira S, Sarvetnick N, Ljunggren HG. IL-18 directs autoreactive T cells and promotes autodestruction in the central nervous system via induction of IFN-gamma by NK cells. *Journal of Immunology*. 2000; 165(6): 3099-3104.

Shiozaki M, Tashiro T, Koshino H, Shigeura T, Watarai H, Taniguchi M, Mori K. Synthesis and biological activity of hydroxylated analogues of KRN7000 (α-galactosylceramide). *Carbohydrate Research*. 2013; 370: 46-66.

Silverstein AM. Autoimmunity versus horror autotoxicus: the struggle for recognition. *Nature Immunology*. 2001; 2(4): 279-281.

Singh AK, Wilson MT, Hong S, Olivares-Villagómez D, Du C, Stanic AK, Joyce S, Sriram S, Koezuka Y, Van Kaer L. Natural killer T cell activation protects mice against experimental autoimmune encephalomyelitis. The *Journal of Experimental Medicine*. 2001; 194(12): 1801-1811.

Singh MK, Scott TF, LaFramboise WA, Hu FZ, Post JC, Ehrlich GD. Gene expression changes in peripheral blood mononuclear cells from multiple sclerosis patients undergoing beta-interferon therapy. *Journal of Neurological Sciences*. 2007; 258(1-2): 52-59.

Sirota M, Schaub MA, Batzoglou S, Robinson WH, Butte AJ. Autoimmune Disease Classification by Inverse Association with SNP Alleles. *PLoS Genetics*. 2009; 5(12): e1000792.

Slavin A, Ewing C, Liu J, Ichikawa M, Slavin J, Bernard CC. Induction of a multiple sclerosis-like disease in mice with an immunodominant epitope of myelin oligodendrocyte glycoprotein. *Autoimmunity*. 1998; 28(2): 109-120.

Slifka MK, Pagarigan RR, Whitton JL. NK markers are expressed on a high percentage of virus-specific CD8+ and CD4+ T cells. *Journal of Immunology*. 2000; 164(4): 2009-2015. Erratum in: *Journal of Immunology*. 2000; 164(6): following 3444. *Journal of Immunology*. 2004; 172(11): 7220.

Sloane JA, Batt C, Ma Y, Harris ZM, Trapp B, Vartanian T. Hyaluronan blocks oligodendrocyte progenitor maturation and remyelination through TLR2. *Proceeding of the National Academia of Sciences of United States of America*. 2010; 107(25): 11555-11560.

Smorodchenko A, Wuerfel J, Pohl EE, Vogt J, Tysiak E, Glumm R, Hendrix S, Nitsch R, Zipp F, Infante-Duarte C. CNS-irrelevant T-cells enter the brain, cause blood-brain barrier disruption but no glial pathology. *The European Journal Neuroscience*. 2007; 26(6): 1387-1398.

Sospedra M, Martin R. Immunology of multiple sclerosis. *Annual Review of Immunology*. 2005; 23: 683-747.

Soulika AM, Lee E, McCauley E, Miers L, Bannerman P, Pleasure D. Initiation and progression of axonopathy in experimental autoimmune encephalomyelitis. *The Journal of Neurosciences*. 2009; 29(47): 14965-14979.

Speak AO, Cerundolo V, Platt FM. CD1d presentation of glycolipids. *Immunology and Cell Biology*. 2008; 86(7): 588-597.

Sriram S, Solomon D, Rouse RV, Steinman L. Identification of T cell subsets and B lymphocytes in mouse brain experimental allergic encephalitis lesions. *Journal of Immunology*. 1982, 129(4): 1649-1651.

Stefferl A, Brehm U, Storch M, Lambracht-Washingto D, Bourquin C, Wonigeit K, Lassmann H, Linington C. Myelin Oligodendrocyte Glycoprotein Induces Experimental Autoimmune Encephalomyelitis in the "Resistant" Brown Norway Rat: Disease Susceptibility Is Determined by MHC and MHC-Linked Effects on the B Cell Response. *The Journal of Immunology*. 1999; 163(1): 40-49.

Stromnes IM, Cerretti LM, Liggitt D, Harris RA, Goverman JM. Differential regulation of central nervous system autoimmunity by T(H)1 and T(H)17 cells. *Nature Medicine*. 2008; 14(3): 337-342.

Stromnes IM, Goverman JM. Passive induction of experimental allergic encephalomyelitis. *Nature Protocols*. 2006; 1(4): 1952-1960.

Sutmuller RPM, den Brok MHMGM, Kramer M, Bennink EJ, Toonen LWJ, Kullberg B-J, Joosten LA, Akira S, Netea MG, Adema GJ. Toll-like receptors 2 controls expansion and function of regulatory T cell. *The Journal of Clinical Investigation*. 2006; 116(2): 485-494.

Sutton C, Brereton C, Keogh B, Mills KH, Lavelle EC. A crucial role for interleukin (IL)-1 in the induction of IL-17-producing T cells that mediate autoimmune encephalomyelitis. *The Journal of Experimental Medicine*. 2006; 203(7): 1685-16891.

Sweeney CM, Lonergan R, Basdeo SA, Kinsella K, Dungan LS, Higgins SC, Kelly PJ, Costelloe L, Tubridy N, Mills KH, Fletcher JM. IL-27

mediates the response to IFN-β therapy in multiple sclerosis patients by inhibiting Th17 cells. *Brain Behavior, and Immunity*. 2011; 25(6): 1170-1181.

Szvetko AL, Jones A, Mackenzie J, Tajouri L, Csurhes PA, Greer JM, Pender MP, Griffiths LR. Investigation of the [-/A]8 and C1236T genetic variations within the human Toll-like receptor 3 gene for association with multiple sclerosis. *Neurological Research*. 2010; 32(4): 438-441.

Szvetko AL, Jones A, Mackenzie J, Tajouri L, Csurhes PA, Greer JM, Pender MP, Griffiths LR. An investigation of the C77G and C772T variations within the human protein tyrosine phosphatase receptor type C gene for association with multiple sclerosis in an Australian population. *Brain Research*. 2009; 1255: 148-152.

Tabeta K, Georgel P, Janssen E, Du X, Hoebe K, Crozat K, Mudd S, Shamel L, Sovath S, Goode J, Alexopoulou L, Flavell LA, Beutler B. Toll-like receptors 9 and 3 as essential components of innate immune defense against mouse cytomegalovirus infection. *Proceeding of the National Academy of Sciences of the United States of America*. 2004; 101(10): 3516-3521.

Takeda K, Takeuchi O, Akira S. Recognition of lipopeptides by Toll-like receptors. *Journal of endotoxin research*. 2002; 8(6): 459-463.

Takeuchi O, Akira S. Pattern recognition receptors and inflammation. *Cell*. 2010; 140(6): 805-820.

Takeuchi O, Hoshino K, Akira S. Cutting edge: TLR2-deficient and MyD88-deficient mice are highly susceptible to Staphylococcus aureus infection. *Journal of Immunology*. 2000; 165(10): 5392-5396.

Takeuchi O, Hoshino K, Kawai T, Sanjo H, Takada H, Oagawa T, Takeda K, Akira S. Differential roles of TLR2 and TLR4 in recognition of gram-negative and gram-positive bacteria cell wall components. *Immunity*. 1999; 11(4): 443-451.

Takeuchi O, Kawai T, Mühlradt PF, Morr M, Radolf JD, Zychlinsky A, Takeda K, Akira S. Discrimination of bacterial lipoproteins by Toll-like receptor 6. *International Immunology*. 2001; 13(7): 933-940.

Takeuchi O, Kawai T, Sanjo H, Copeland NG, Gilbert DJ, Jenkins NA, Takeda K, Akira S. TLR6: A novel member of an expanding toll-like receptor family. *Gene*. 1999; 231(1-2): 59-65.

Takeuchi O, Sato S, Horiuchi T, Hoshino K, Takeda K, Dong Z, Modlin RL, Akira S. Cutting edge: role of Toll-like receptor 1 in mediating immune response to microbial lipoproteins. *Journal of Immunology*. 2002; 169(1): 10-14.

Teige A, Teige I, Lavasani S, Bockermann R, Mondoc E, Holmdahl R, Issazadeh-Navikas S. CD1-dependent regulation of chronic central

nervous system inflammation in experimental autoimmune encephalomyelitis. *Journal of Immunology*. 2004; 172(1): 186-194.

Theiler M. Spontaneus Encephalomyelitis of mice, a new virus disease. *The Journal of Experimental Medicine*. 1937; 65(5): 705-719.

Thoma-Uszynski S, Kiertscher SM, Ochoa MT, Bouis DA, Norgard MV, Miyake K, Godowski PJ, Roth MD, Modlin RL. Activation of toll-like receptor 2 on human dendritic cells triggers induction of IL-12, but not IL-10. *Journal of Immunology*. 2000; 165(7): 3804-3810.

Toneatto S, Finco O, van der PH, Abrignani S, Annunziata P. Evidence of blood–brain barrier alteration and activation in HIV-1 gp120 transgenic mice. *AIDS*. 1999; 13(17): 2343–2348.

Touil T, Fitzgerald D, Zhang GX, Rostami A, Gran B. Cutting Edge: TLR3 Stimulation Suppresses Experimental Autoimmune Encephalomyelitis by Inducing Endogenous IFN-beta. *Journal of Immunology*. 2006; 177(11): 7505-7509.

Turrin NP. Central nervous system Toll-like receptor expression in response to Theiler's murine encephalomyelitis virus-induced demyelination disease in resistant and susceptible mouse strains. *Virology Journal*. 2008; 5: 154.

Uematsu S, Akira S. The role of Toll-like receptors in immune disorders. *Expert Opinion on Biological Theraphy*. 2006; 6(3): 203-214.

Urcelay E, Blanco-Kelly F, de Las Heras V, de la Concha EG, Arroyo R, Martínez A. TLR4 haplotypes in multiple sclerosis: a case-control study in the Spanish population. *Journal of Neuroimmunology*. 2007; 192(1-2): 215-218.

Venken K, Hellings N, Hensen K, Rummens JL, Stinissen P. Memory $CD4^{+}CD127$high T cells from patients with multiple sclerosis produce IL-17 in response to myelin antigens. *Journal of Neuroimmunology*. 2010; 226(1-2): 185-191.

Venken K, Hellings N, Thewissen M, Somers V, Hensen K, Rummens JL, Medaer R, Hupperts R, Stinissen P. Compromised $CD4^{+}$ CD25(high) regulatory T-cell function in patients with relapsing-remitting multiple sclerosis is correlated with a reduced frequency of FOXP3-positive cells and reduced FOXP3 expression at the single-cell level. *Immunology*. 2008; 123(1): 79-89.

Viglietta V, Baecher-Allan C, Weiner HL, Hafler DA. Loss of functional suppression by $CD4^{+}CD25^{+}$ regulatory T cells in patients with multiple sclerosis. *Journal of Experimental Medicine*. 2004; 199(7): 971-979.

Visscher BR, Bunnell DH, Detels R. Multiple sclerosis and multiple moves: an etiologic hypothesis. *American Journal of Epidemiology*. 1981; 113(2): 140-143.

Visser L, Jan de Heer H, Boven LA, van Riel D, van Meurs M, Melief MJ, Zähringer U, van Strijp J, Lambrecht BN, Nieuwenhuis EE, Laman JD. Proinflammatory bacterial peptidoglycan as a cofactor for the development of central nervous system autoimmune disease. *Journal of Immunology*. 2005; 174(2): 808-816.

Visser L, Melief MJ, van Riel D, van Meurs M, Sick EA, Inamura S, Bajramovic JJ, Amor S, Hintzen RQ, Boven LA, 't Hart BA, Laman JD. Phagocytes containing a disease-promoting Toll-like receptor/Nod ligand are present in the brain during demyelinating disease in primates. *The American Journal of Pathology*. 2006; 169(5): 1671-1685.

von Budingen HC, Menge T, Hauser SL, Genain CP. Restrictive and diversifying elements of the anti-myelin/oligodendrocyte glycoprotein antibody response in primate experimental allergic encephalomyelitis. *Immunogenetics*. 2006; 58(2-3): 122–128.

Walder H, Collins M, Kuchroo VK. Activation of antigen-presenting cells by microbial products breaks self tolerance and induce autoimmune disease. *The Journal of Clinical Investigation*. 2004; 113(7): 990-997.

Wang T, Town T, Alexopoulou L, Anderson JF, Fikrig E, Flavell RA. Toll-like receptor 3 mediates West Nile virus entry into the brain causing lethal encephalitis. *Nature Medicine*. 2004; 10(12): 1366-1373.

Weber MS, Starck M, Wagenpfeil S, Meinl E, Hohlfeld R, Farina C. Multiple sclerosis: glatiramer acetate inhibits monocyte reactivity *in vitro* and *in vivo*. *Brain.* 2004; 127(Pt 6): 1370-1378.

Werner SR, Saha JK, Broderick CL, Zhen EY, Higgs RE, Duffin KL, Smith RC. Proteomic analysis of demyelinated and remyelinating brain tissue following dietary cuprizone administration. *Journal of Molecular Neurosciences*. 2010; 42(2): 210-225.

Wolf NA, Amouzegar TK, Swanborg RH. Synergistic interaction between Toll-like receptor agonists is required for induction of experimental autoimmune encephalomyelitis in Lewis rats. *Journal of Neuroimmunology*. 2007; 185(1-2): 115-122.

Wootla B, Denic A, Keegan BM, Winters JL, Astapenko D, Warrington AE, Bieber AJ, Rodriguez M. Evidence for the role of B cells and immunoglobulins in the pathogenesis of multiple sclerosis. *Neurology Research International*. 2011; 2011: 780712.

Wynn DR, Rodriguez M, O'Fallon WM, Kurland LT. A reappraisal of the epidemiology of multiple sclerosis in Olmsted County, Minnesota. *Neurology*. 1990; 40(5): 780-786.

Yarovinsky F, Zhang D, Andersen JF, Bannenberg GL, Serhan CN, Hayden MS, Hieny S, Sutterwala FS, Flavell RA, Ghosh S, Sher A. TLR11 activation of dendritic cells by a protozoan profilin-like protein.

*Science*. 2005; 308(5728): 1626-1629.

Yokote H, Miyake S, Croxford JL, Oki S, Mizusawa H, Yamamura T. NKT cell-dependent amelioration of a mouse model of multiple sclerosis by altering gut flora. *The American Journal of Pathology*. 2008; 173(6): 1714-1723.

Yoshida T, Jiang F, Honjo T, Okazaki T. PD-1 deficiency reveals various tissue-specific autoimmunity by H-2b and dose-dependent requirement of H-2g7 for diabetes in NOD mice. *Proceeding of the National Academy Sciences*. 2008; 105(9): 3533-3538.

Zamvil SS, Steinman L. The T Lymphocyte in Experimental Allergic Encephalomyelitis. *Annual Review of Immunology*. 1990; 8: 579-621.

Zekki H, Feinstein DL, Rivest S. The clinical course of experimental autoimmune encephalomyelitis is associated with a profound and sustained transcriptional activation of the genes encoding toll-like receptor 2 and CD14 in the mouse CNS. *Brain Pathology*. 2002; 12(3): 308-319.

Zeuthen LH, Fink LN, Frokiaer H. Epithelial cells prime the immune response to an array of gut-derived commensals towards a tolerogenic phenotype through distinct actions of thymic stromal lymphopoietin and transforming growth factor-beta. *Immunology*.

2008; 123(2): 197-208.

Zhang D, Zhang G, Hayden MS, Greenblatt MB, Bussey C, Flavell RA, Ghosh S. A toll-like receptor that prevents infection by uropathogenic bacteria. *Science*. 2004; 303(5663): 1522-1526.

Zhang FX, Kirschning CJ, Mancinelli R, Xu XP, Jin Y, Faure E, Mantovani A, Rothe M, Muzio M, Arditi M. Bacterial lipopolysaccharide activates nuclear factor-kappaB through interleukin-1 signalling mediators in cultured human dermal endothelial cells and mononuclear phagocytes. *The Journal of Biological Chemistry*. 1999; 274(12): 7611-7614.

Zhang X, Jin J, Tang Y, Speer D, Sujkowska D, Markovic-Plese S. IFN-beta1a inhibits the secretion of Th17-polarizing cytokines in human dendritic cells via TLR7 up-regulation. *Journal of Immunology*. 2009; 182(6): 3928-3936.

Zhou Y, Ye L, Wan Q, Zhou L, Wang X, Li J, Hu S, Zhou D, Ho W. Activation of Toll-like receptors inhibits herpes simplex virus-1 infection of human neuronal cells. *Journal of Neurosciences Research*. 2009; 87(13): 2916-1925.

# APPENDICES

# APPENDIX 1

# LOCALIZATION OF TOLL-LIKE RECEPTORS

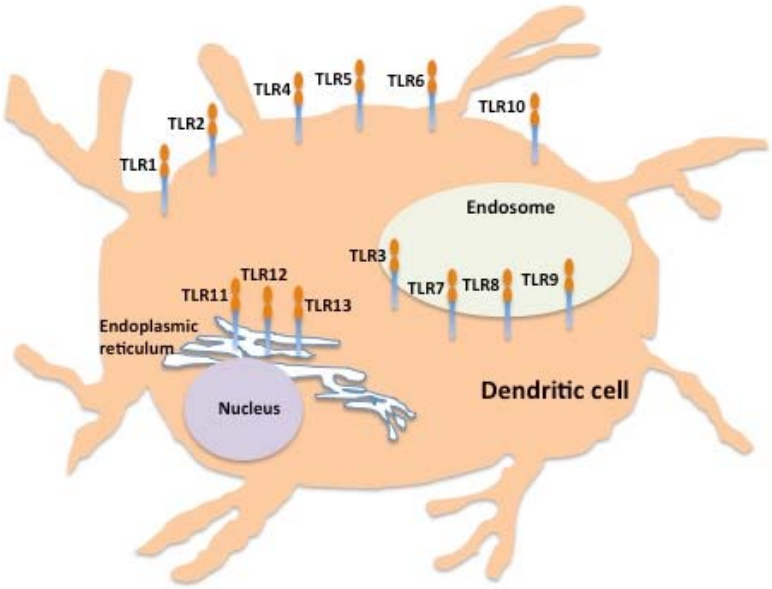


Dendritic cell showing the extracellular and intracellular localization of Toll-like receptors.

# APPENDIX 2

# PRODUCTION OF C57BL/6.*CD1d*$^{-/-}$ MICE

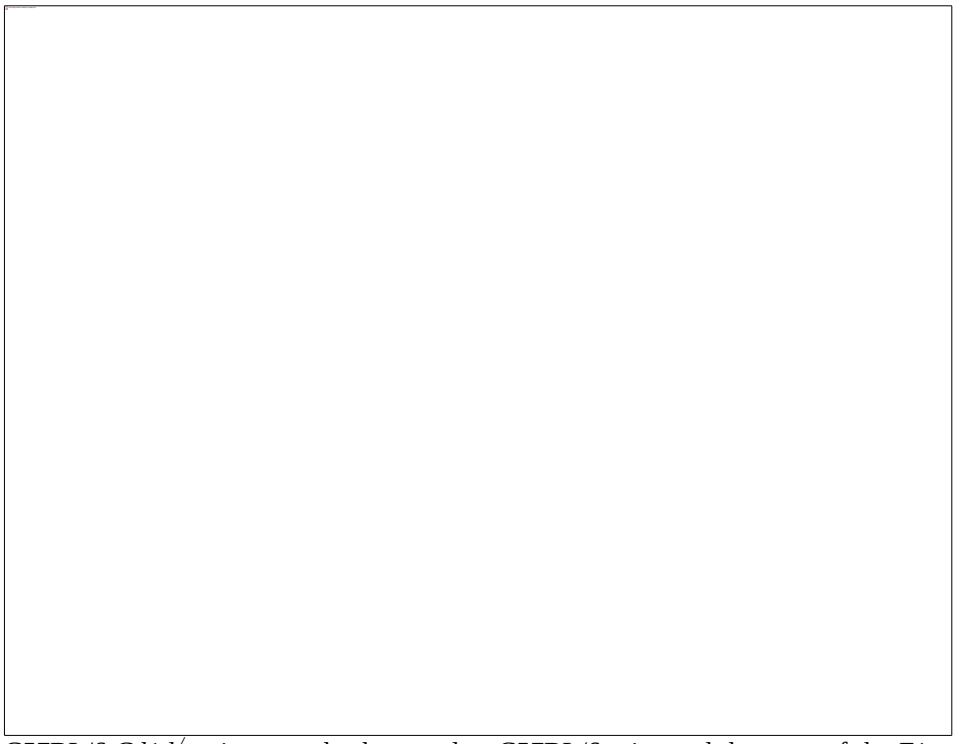

C57BL/6.*Cd1d*$^{-/-}$ mice were backcrossed to C57BL/6 mice and the pups of the F1 generation were intercrossed. F1 pups were genotyping as declared in Chapter 2 Materials and Methods for selection of homozygous mutants. C57BL/6.*Cd1d*$^{-/-}$ homozygous mice were intercrossed to extend the new line of mice.

# APPENDIX 3

# PRODUCTION OF NOD.*H2*$^{b}$.*Tlr2*$^{-/-}$ MICE

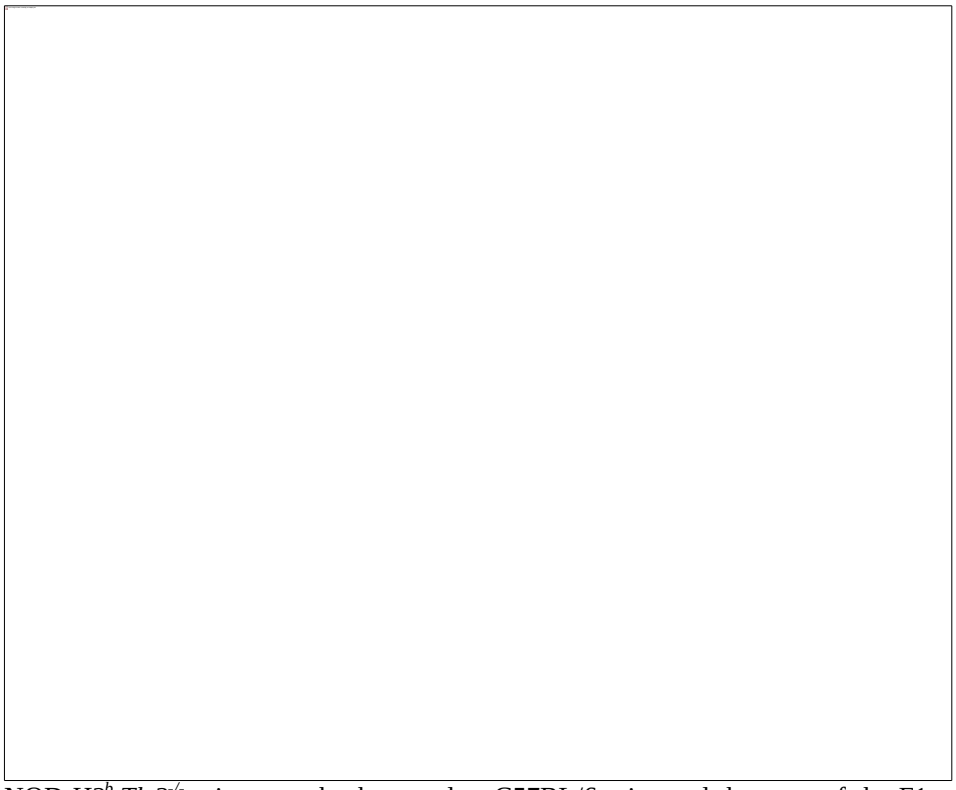

NOD.*H2*$^{b}$.*Tlr2*$^{-/-}$ mice were backcrossed to C57BL/6 mice and the pups of the F1 generation were intercrossed. F1 pups were genotyping as declared in Chapter 2 Materials and Methods for selection of homozygous mutants. NOD.*H2*$^{b}$.*Tlr2*$^{-/-}$ homozygous mice were intercrossed to extend the new line of mice.

# APPENDIX 4

# MOUSE IDENTIFICATION

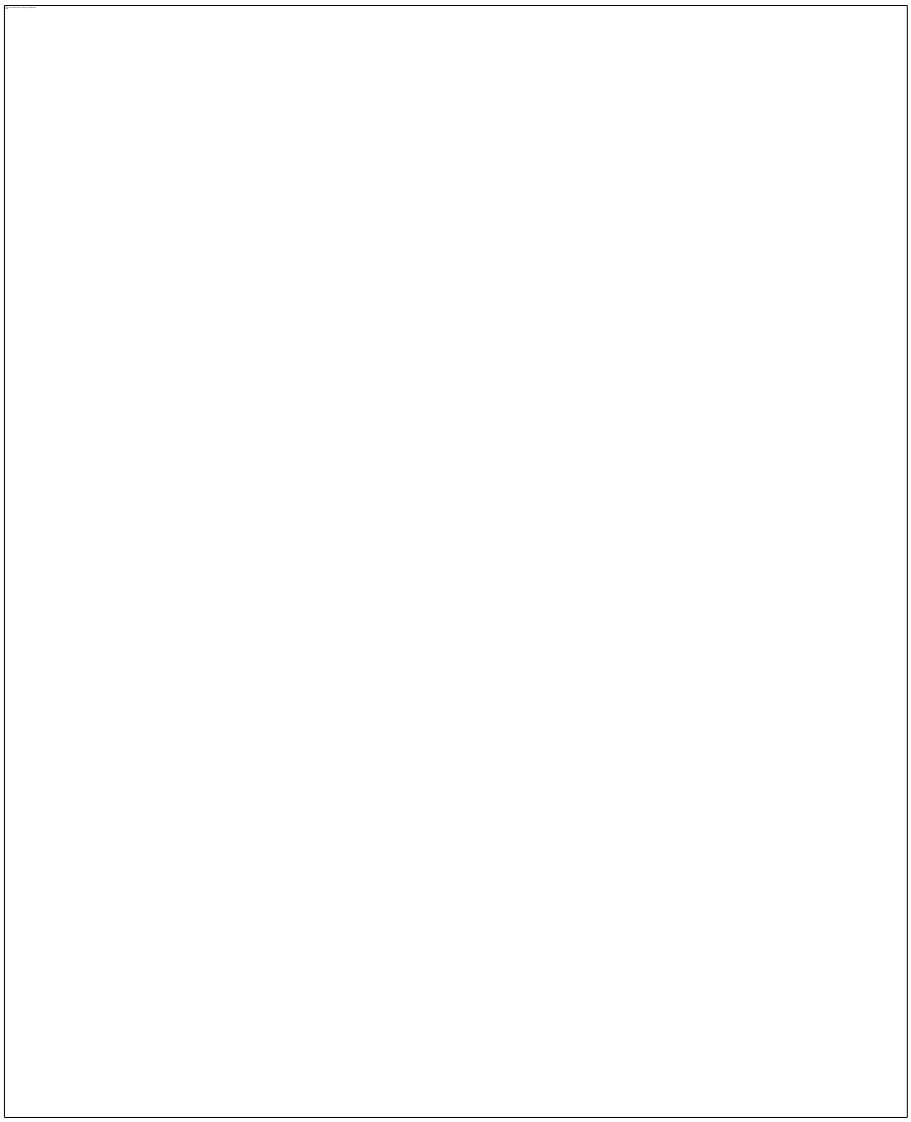

Dorsal view of head mice with ear clipping for identification. Units are marked in the right ear (1, 2, 3, 4, 5, 6, 7, 8, 9). Tens are marked in the left ear (10, 20, 30; 40, 50, 60, 70, 80, 90). This method allowed identifying mice from the number 1 to the number 99 using a combination of units and tens as showed in the example.

# APPENDIX 5

# SEQUENCES OF PRIMERS

| Target DNA construct | Name | Sequence (5' to 3') |
|---|---|---|
| H2b | D17mit 176 (Fw[1]) | GCCTAACTAGACTACAAGCCTTGC |
| H2b | D17mit 176 (Rv[2]) | GTAGGTACATACAACCCACATACAGG |
| TLR2 | A (Rv) | GTTTAGTGCCTGTATCCAGTCAGTGCG |
| TLR2 | B (Fw) | TTGGATAAGTCTGATAGCCTTGCCTCC |
| TLR2 | C (Rv) | ATCGCCTTCTATCGCCTTCTTGACGAG |
| MyD88 | A (Rv) | AGACAGGCTGAGTGCAAACTTGTGCTG |
| MyD88 | B (Fw) | AGCCTCTACACCCTTCTCTTCTCCACA |
| MyD88 | C (Rv) | ATCGCCTTCTATCGCCTTCTTGACGAG |
| Vα14 | Vα14 (Fw) | TGTAGGCTCAGATTCCCAACC |
| Vα14 | Vα14 (Rv) | TGTAGGCTCAGATTCCCAACC |
| GAPDH | GAPDH (Fw) | TGCCGCCTGGAGAAACCTGTATGTATG |
| GAPDH | GAPDH (Rv) | TGGAAGAGTGGGAGTTGCTGTTGAACT |
| Nkrp1b | D6mit135 (Fw) | CCTAACAGTTCAATTTGTCAGCC |
| Nkrp1b | D6mit135 (Rv) | CCAGCCCCCAATTTGATATA |

[1] Fw - Forward
[2] RV - Reverse

# APPENDIX 6

# POLYMERASE CHAIN REACTION (PCR)

| **Targeting DNA constructs** | **$H_2O$ (µl)** | **GoTaq Green (2X)** | **Primer (Fw)** | **Primer (Rv)** | **1µl of DNA** | **Total Volume (µl)** |
|---|---|---|---|---|---|---|
| H2b | 10.5 | (12.5µl) | 0.5µl (10µM) | 0.5µl (10µM) | 20-180 ng/µl | 25 |
| Vα14 | 6.5 | (12.5µl) | 0.5µl (10µM) | 0.5µl (10µM) | 20 ng/µl | 25 |
| Nkrp1b | 9.70 | (12.5µl) | 0.90µl (6.6µM) | 0.90µl (6.6µM) | 20-180 ng/µl | 25 |
| TLR2 + GAPDH | 4.1 | (12.5µl) | 0.7µl (6µM)<br>0.2µl (2µM) | 0.7µl (6µM)<br>0.2µl (2µM) | 20-180 ng/µl | 20 |
| MyD88 + GAPDH | 4.1 | (12.5µl) | 0.7µl (10µM)<br>0.2µl (2µM) | 0.7µl (10µM)<br>0.2µl (2µM) | 20-180 ng/µl | 20 |

# APPENDIX 7

# TERMOCYCLING PROTOCOLS FOR PCR

| Target DNA construct | Initial denaturation | Denaturation | Annealing | Elongation | Final elongation |
|---|---|---|---|---|---|
| H2b | | (32 cycles) | | | |
| Nkrp1b | 95 °C<br>3 minutes | 95 °C<br>30 seconds | 55 °C<br>30 seconds | 72 °C<br>30 seconds | 72 °C<br>7 minutes |
| TLR2 | | (35 cycles) | | | |
| | 95 °C<br>3 minutes | 94 °C<br>30 seconds | 67 °C<br>60 seconds | 74 °C<br>60 seconds | 74 °C<br>10 minutes |
| MyD88 | | (35 cycles) | | | |
| | 95 °C<br>3 minutes | 94 °C<br>30 seconds | 67 °C<br>60 seconds | 74 °C<br>60 seconds | 74 °C<br>10 minutes |
| Vα14 | | (32 cycles) | | | |
| | 95 °C<br>3 minutes | 95 °C<br>60 seconds | 59 °C<br>60 seconds | 72 °C<br>60 seconds | 72 °C<br>7 minutes |

# APPENDIX 8

# ANTIBODIES FOR FLOW CYTOMETRY ANALYSIS

| Specificity | Conjugated to | Host | Isotype | Clone | Catalogue Number | Source |
|---|---|---|---|---|---|---|
| CD45 | Biotin | Rat (LOU) | $IgG_{2b,}$ κ | 30-F11 | 553077 | BD Pharmingen™ (San Diego, CA) |
| CD45.2 | PB | Mouse (SJL) | IgG2a, κ | 104 | 109820 | BioLegend® (San Diego, CA) |
| βTCR | APC | Armenian Hamster | IgG2, λ1 | H57-597 | 553174 | BD Pharmingen™ (San Diego, CA) |
| | FITC | Armenian Hamster | IgG | H57-597 | 11-5961-85 | eBiosciences™ (San Diego, CA) |
| | PerCp-Cy5.5 | Armenian Hamster | IgG2, λ1 | H57-597 | 560657 | BD Pharmingen™ (San Diego, CA) |
| CD1d | PE | Rat | IgG2b, κ | 1B1 | 12-0011-82 | eBiosciences™ (San Diego, CA) |
| CD4 | FITC | Rat (DA) | $IgG_{2a}$, κ | M4-5 | 553046 | BD Pharmingen™ (San Diego, CA) |

| | | | | | | |
|---|---|---|---|---|---|---|
| | PB | Rat (DA) | $IgG_{2a}$, κ | RM4-5 | 558107 | BD Pharmingen™ (San Diego, CA) |
| | PerCp-Cy5.5 | Rat (DA) | $IgG_{2a}$, κ | RM4-5 | 550954 | BD Pharmingen™ (San Diego, CA) |
| | V450 | Rat (DA) | IgG2a, κ | RM4-5 | 560468 | BD Horizon™ (San Diego, CA) |

Continue antibodies for flow cytometry analysis

| | | | | | | |
|---|---|---|---|---|---|---|
| CD8 | APC-Cy7 | Rat (LOU/Ws1/M) | $IgG_{2a}$, κ | 53-6.7 | 557654 | BD Pharmingen™ (San Diego, CA) |
| CD11b | FITC | Rat (DA) | $IgG_{2b}$, κ | M1/70 | 553310 | BD Pharmingen™ (San Diego, CA) |
| | PE-Cy7 | Rat (DA) | $IgG_{2b}$, κ | M1/70 | 552850 | BD Pharmingen™ (San Diego, CA) |
| CD11c | PE | Armenian Hamster | IgG | N418 | 117308 | BioLegend® (San Diego, CA) |
| | PE-Cy7 | Armenian Hamster | IgG1, λ2 | HL3 | 558079 | BD Pharmingen™ (San Diego, CA) |
| Ccr2 | Biotin | Rat | MC-21 | N/A | N/A | Donated by Matthias Mack |
| FoxP3 | FITC | Rat | IgG2a, κ | FJK-16s | 11-5773-82 | eBiosciences™ (San Diego, CA) |
| CD25 | PE | N/A | N/A | Streptavidin | 554061 | BD Pharmingen™ (San Diego, CA) |
| | Biotin | Rat (LEW) | IgM, κ | 7D4 | 553070 | BD Pharmingen™ (San Diego, CA) |
| CD62L | PE-Cy7 | Rat | IgG2a, κ | MEL-14 | 104418 | BioLegend® (San Diego, CA) |
| CD3e | APC | Armenian Hamster | IgG1, κ | 145-2C11 | 553066 | BD Pharmingen™ (San Diego, CA) |
| IFNγ | FITC | Rat | IgG1, κ | XMG1.2 | 11-7311-82 | eBiosciences™ (San Diego, CA) |

| | | | | | | |
|---|---|---|---|---|---|---|
| Ly6C | PerCP-Cy5.5 | Rat | IgM, κ | AL-21 | 560525 | BD Pharmingen™ (San Diego, CA) |
| IL17 | PE | Rat (LEW) | $IgG_1$, κ | TC11-18H10 | 559502 | BD Pharmingen™ (San Diego, CA) |

Continue antibodies for flow cytometry analysis

| | | | | | | |
|---|---|---|---|---|---|---|
| Streptavidin | PO | N/A | N/A | N/A | S32365 | Invitrogen |
| | PE | N/A | N/A | N/A | 554061 | BD Pharmingen™ (San Diego, CA) |
| | Dylight 649 | N/A | N/A | N/A | N/A | Jackson Immunoresearch (West Grove) |

PO - Pacific orange
PB - Pacific blue
APC - Allophycocyanin
FITC - Fluoroscein isothiocyanate
PerCp - Peridinin-chlorophyII Protein Complex
PerCp-Cy5.5 - Peridinin-chlorophyII Protein Complex with cyanine dye (Cy5.5)
V450 - Violet with an Em Max at 450 nm
APC-Cy7 – Allophycocyanin with cyanine dye (Cy7)
PE-Cy7 - Phycoerythrin with cyanine dye (Cy7)
PE – Phycoerythrin
N/A – Non applicable

# APPENDIX 9

# PREPARATION OF SOLUTIONS AND BUFFERS

## 50x TAE (Tris base, acetic acid and Ethylenediaminetetraacetic acid (EDTA)) buffer solution (1L)

A liter of 50x TAE buffer solution was made up of 242g Tris base (AMRESCO; Ohio, USA), 57.1 ml glacial acetic acid (UNIVAR; Asia Pacific Specialty Chemicals Limited), 18.6g EDTA (AMRESCO; Ohio, USA) and 900 ml distilled $H_20$.

## 1x TAE buffer solution

The buffer solution 1x TAE was made by diluting 50x TAE buffer solution in distillated water. Final solute concentrations are 40mM Tris acetate and 1mM EDTA.

## Agarose gel (2% and 3%) for polyacrylamide gel electrophoresis (PAGE)

Each 100ml of agarose gel was made up of 100 ml of 1x TAE buffer solution, 2.0g agarose (2%) or 3g agarose (3%) (Fisher biotec; Western Australia, Australia) and 7.5 µl Gel red (BIOTIUM, Cat. No. 41003; California, United States of America).

## MACS buffer

Macs buffer consist of PBS (Invitrogen; Victoria, Australia) supplemented with 0.4% of 0.5M EDTA (AMRESCO; Ohio, USA) and 0.2% of 10mM Sodium Azide.

## Cell culture medium

RPMI 1640 medium (Invitrogen; Victoria, Australia) was supplemented with 10% (v/v) fetal cow serum (FCS) (Invitrogen; Victoria, Australia), 1mM Sodium pyruvate (Invitrogen; Victoria, Australia), 100U/ml penicillin (Invitrogen; Victoria, Australia), 100µg/ml streptomycin sulfate (Invitrogen;

Victoria, Australia), 2mM L-glutamine (Invitrogen; Victoria, Australia), 2 μM 2-Mercaptoethanol (Invitrogen; Victoria, Australia).

## Luxol fast blue (0.1%)

The solution of 0.1% luxol fast blue was made up of 0.1g luxol fast blue (Sigma; New South Wales, Australia), 100 ml of 95% ethyl alcohol (provided by the Department of Marine and Tropical Biology, James Cook University), 0.5 ml of glacial acetic acid (BDH AnalaR; Victoria, Australia).

## Cresyl echt violet (0.1%) or cresyl violet acetate (0.1%)

Cresyl echt violet 0.1% or cresyl violet acetate 0.1% was made up of 0.1 g of cresyl echt violet (cresyl fast violet) (The british drug houses; Poole, England) or cresyl violet acetate (Sigma; New South Wales, Australia), 100 ml of distilled water and 10 drops of glacial acetic acid (added just before use) (BDH AnalaR; Victoria, Australia).

## Lithium carbonate (0.05%)

The solution of 0.05% of lithium carbonate was made up of 0.05 g of lithium carbonate (provided by the Department of Marine and Tropical Biology, James Cook University) and 100 ml of distilled water.

## Silver Nitrate (10%)

Silver nitrate stock 10% was made up of 5g of silver nitrate (UNILAB; Sydney, Australia) and 50 ml of distilled water.

## Ammonium Hydroxide (1%)

Ammonium hydroxide 1% was made up of 1 ml of ammonium hydroxide (concentrated) (UNIVAR; New South Wales, Australia) and 100 ml of distilled water.

## Developer Stock

The developer stock solution was made up of 20 ml of 37-40% formaldehyde (provided by the Department of Marine and Tropical Biology, James Cook University), 0.5g of citric acid (trisodium dihydrate) (Sigma; Missouri, USA), 2 drops of nitric acid (concentrated) (AnalaR; Victoria, Australia) and 100 ml of distilled water.

## Developer Working

The developer working solution was made up of 8 drops of developer stock solution, 8 drops of ammonium hydroxyide (concentrated) (UNIVAR; New South Wales, Australia) and 50 ml of distilled water.

## Sodium Thiosolfate (HYPO) (5%)

Sodium Thiosolfate (HYPO) 5% was made up of 5g of sodium thiosolfate (Univar,; New South Wales, Australia) and 100 ml of distilled water.

## Enzyme/Collagenase buffer

Enzyme/Collagenase buffer was made up 4 g/L $MgCl_2$ (BDH AnaR; Victoria, Australia), 2.55 g/L $CaCl_2$ (UNILAB; New South Wales, Australia), 3.73 g/L KCl (UNIVAR; New South Wales, Australia), 8.95 g/L NaCl (UNIVAR; New South Wales, Australia), 500U/ml of DNase (Sigma; NSW, Australia) and dd$H_2O$. Ensure pH is between 6 and 7.